Nearly Gaussian Curvature Perturbations in Ekpyrotic Cosmologies

D i s s e r t a t i o n

zur Erlangung des akademischen Grades

d o c t o r r e r u m n a t u r a l i u m

(Dr. rer. nat.)

im Fach Physik

Spezialisierung: Theoretische Physik

eingereicht an der

Mathematisch-Naturwissenschaftlichen Fakultät

der Humboldt-Universität zu Berlin

von

Enno Mallwitz

Präsidentin der Humboldt-Universität zu Berlin:
Prof. Dr. Dr. Sabine Kunst

Dekan der Mathematisch-Naturwissenschaftlichen Fakultät:
Prof. Dr. Elmar Kulke

Gutachter/innen:	1. Prof. Dr. Hermann Nicolai	Humboldt-Universität zu Berlin
	2. Prof. Dr. Jan Plefka	Humboldt-Universität zu Berlin
	3. Prof. Dr. Robert Brandenberger	McGill University

Tag der mündlichen Prüfung: 15.02.2019

ABSTRACT

In this thesis, we study the ekpyrotic scenario, which is a cosmological model of the early universe. In this model the "initial conditions" of the universe are determined by a contracting ekpyrotic phase, which means that the conventional "Big Bang" is replaced by a bounce. The following thesis addresses the tension between ekpyrotic predictions and the observations of the Cosmic Microwave Background radiation by the Planck team. According to the Planck data, the primordial curvature fluctuations are nearly scale-invariant and Gaussian. During ekpyrosis, the self-interactions of the perturbations are generally large, which results in sizable non-Gaussian signatures of the nearly scale-invariant curvature perturbations. In this thesis, we propose two approaches in order to resolve the tension with observations.

In the non-minimal entropic mechanism, nearly scale-invariant entropy perturbations are created due to a non-minimal kinetic coupling between two scalar fields. We will show that the non-Gaussian corrections during ekpyrosis are precisely zero leading to overall small non-Gaussian signatures after the conversion process from entropy perturbations to curvature perturbations.

In the following, we will consider a kinetic conversion phase, which takes place after a non-singular bounce leading to fairly different predictions compared to a kinetic conversion before the bounce, since the entropy perturbations can grow quite substantially during the bounce phase. Due to this growth, the possibly large non-Gaussian corrections created during the ekpyrotic phase become suppressed during the bounce. Consequently, the resulting non-Gaussian signatures of the curvature perturbations depend mostly on the conversion process.

The last part of this thesis addresses a major problem of the inflationary paradigm: Due to large adiabatic fluctuations, slow-roll eternal inflation creates infinitely many physically distinct pocket universes, which challenges the predictability of the inflationary paradigm. We propose a model in the framework of scalar-tensor theories, which conflated ideas of both inflation and ekpyrosis. During conflation, the universe undergoes accelerated expansion like during inflation, but there are no large adiabatic fluctuations like during ekpyrosis resulting in the absence of the runaway behavior in slow-roll eternal inflation.

ZUSAMMENFASSUNG

In dieser Arbeit studieren wir das ekpyrotische Szenario, welches ein kosmologisches Modell des frühen Universums ist. Dieses Modell erklärt mit Hilfe einer kontrahierenden ekpyrotischen Phase die "Anfangsbedingungen" des Universums. Das bedeutet, dass der konventionelle "Urknall" durch einem Rückprall ersetzt wird. In dieser Arbeit versuchen wir die Unstimmigkeiten zwischen den Vorhersagen der ekpyrotischen Modelle und den Messungen der Kosmologischen Hintergrundstrahlung des Planck Satelliten zu lösen. Den Planck Messungen zufolge sind die ursprünglichen adiabatischen Fluktuationen fast skaleninvariant und gaußverteilt. Während der ekpyrotischen Phase sind die Selbstwechselwirkungen der Fluktuationen typischer Weise groß. Dies hat zur Folge, dass die nicht-Gaußschen Korrekturen der adiabatischen Fluktuationen ebenfalls groß sind. Wir schlagen zwei Ansätze vor, um die Unstimmigkeiten zu beheben.

In dem nicht-minimalen entropischen Mechanismus werden fast skaleninvariante entropische Fluktuationen mit Hilfe einer nicht-minimalen kinetischen Kopplung zwischen zwei Skalarfeldern erzeugt. Wir werden zeigen, dass die nicht-Gaußschen Korrekturen während der ekpyrotischen Phase genau Null sind. Dies führt zu insgesamt kleinen nicht-Gaußschen Korrekturen nach der Umwandlung von entropischen zu adiabatischen Fluktuationen.

Im Folgendem werden wir eine kinetische Umwandlung untersuchen, die nach einem nichtsingulären Rückprall stattfindet. Die Resultate weichen deutlich von denen ab, die von einer Umwandlung vor einem Rückprall gewonnen werden, da die entropischen Fluktuationen während des Rückpralls erheblich wachsen können. Dies hat zur Folge, dass die möglichen nicht-Gaußschen Korrekturen, die zur Zeit der ekpyrotischen Phase erzeugt wurden, während des Rückpralls unterdrückt werden. Die resultierenden nicht-Gaußschen Korrekturen der adiabatischen Fluktuationen hängen somit größtenteils von dem Umwandlungsprozess ab.

Im letzten Teil der Arbeit gehen wir ein gravierendes Problem des inflationären Paradigmas an, welches "slow-roll eternal inflation" genannt wird. Aufgrund von großen adiabatischen Fluktuationen werden unendlich viele physikalisch unterschiedliche Universen erzeugt. Dies stellt die Vorhersagbarkeit des inflationären Paradigmas in Frage. Wir schlagen ein auf der Skalar-Tensor-Gravitationstheorie basierendes Modell vor, das Ideen von Inflation und Ekpyrosis verbindet. Während der Konflation expandiert das Universum beschleunigt, ähnlich wie in Modellen der Inflation. Jedoch existieren hier keine großen adiabatischen Fluktuationen, da sich diese wie in ekpyrotischen Modelle verhalten. Somit tritt im konflationärem Modell kein "slow-roll eternal inflation" auf.

ACKNOWLEDGMENTS

I would like to thank my supervisor Jean-Luc Lehners for his guidance and support. I am very happy and grateful that I had the opportunity to be a part of the theoretical cosmology group. Thanks to you I have learned a lot about various aspects of cosmology in the attempt to discover secrets of the early universe.

I would like to thank my official supervisor Hermann Nicolai. I am very grateful that I had the opportunity to work at the Max-Planck-Institute for Gravitational Physics.

I would like to express my gratitude to the examiners of this thesis: Jan Plefka and Robert Brandenberger. I would also like to thank Matthias Staudacher and Alejandro Saenz for being part of the graduation committee.

I would like to thank Stefan Fredenhagen. I enjoyed your inspiring lectures and i am very grateful for your support.

I would like to thank the current and former members of the theoretical cosmology group as well as the frequent visitors of the group: Michael Koehn, Lorenzo Battarra, Rhiannon Gwyn, Angelika Fertig, Esther Kähler, Clemens Hübner-Worseck, George Lavrelashvili, Edward Wilson-Ewing, Sayantan Choudhury, Shane Farnsworth, Alice Di Tucci and Sebastian Bramberger. I really enjoyed the conversations with all of you and I have learned a lot during our weekly group meetings.

Angelika, I enjoyed collaborating with you very much. I am proud of our achievements during our time as PhD students and I wish you all the best for the future. I would like to give special thanks to Sebastian Bramberger for the inspiring and exciting conversations. I enjoyed the company of all former and current PhD students at the institute. In particular I would like to thank Despoina Katsimpouri, Isha Kotecha, Olof Ahlen, Seungjin Lee and Pan Kessel.

I want to dedicate this thesis to my mother. I will be forever grateful for your love, support and encouragement. I would like to thank my brother for being a big part of my life, my family for their unconditional love and my friends for enriching my life. I would like to thank Theresa for being by my side. I am very happy that I have found you in this vast universe.

CONTENTS

LIST OF FIGURES

1. INTRODUCTION

In the last ten to twenty years, measurements of e.g., supernovae, the Large Scale Structure and the Cosmic Microwave Background led to a very profound understanding of the evolution of the universe. The precision to which cosmological parameters have been measured is astonishing. The universe on large scales is remarkably simple; it is spatially nearly flat, homogeneous, and isotropic. This means that the initial conditions of the universe had to be rather special. For example, in an expanding universe, the spatial curvature grows with time, which means that initially, the universe had to be very flat. Moreover, the structure in the universe formed due to small preexisting over- and under-densities, which are imprinted in the temperature anisotropies of the Cosmic Microwave Background radiation. The Planck satellite measured the Cosmic Microwave Background leading to the following observation: the preexisting fluctuations are adiabatic, nearly scale-invariant and nearly Gaussian. The current hot big bang model of our universe, which fits the observations, is the so-called ΛCDM model. The universe starts in a very hot and dense phase and cools down due to the expansion of the universe. The expansion history of the universe is fairly well understood, and we will cover basic cosmological concepts in Chapter 2. However, the initial conditions of the universe cannot be explained by the standard hot big bang model. We have to assume that the universe started spatially nearly flat, homogeneous, and isotropic. Moreover, the small anisotropies in the Cosmic Microwave Background have to be added by hand.
Models of the early universe try to explain the initial conditions, which led to the universe we observe today. The initial conditions of the hot big bang cosmology can be obtained dynamically by introducing a phase prior to the conventional hot "Big Bang". During this primordial phase the universe has to be driven towards homogeneity, isotropy, and flatness, while adiabatic, nearly scale-invariant, and nearly Gaussian fluctuations have to seed the anisotropies is the Cosmic Microwave Background.

The inflationary paradigm tries to explain the initial conditions of the universe by introducing a phase of rapid, accelerated expansion [11–13]. Due to the enormous expansion, any other matter content is diluted, such that the universe becomes spatially flat and homogeneous. Inflation can be modeled by a scalar field minimally coupled to gravity in a flat potential.
Ekpyrosis is an alternative model to inflation, where the initial conditions of the universe are created via a slowly contracting phase preceding the conventional "Big Bang". In this scenario the universe undergoes a transition from contraction to expansion replacing the "Big Bang" with

a bounce. Ekpyrosis was first introduced in [14] and extended to a cyclic model in [4, 15, 16]. These models are based on an embedding in heterotic M-theory, and we will discuss the ekpyrotic scenario, the cyclic model and the braneworld picture of the universe in Chapter 3 B. Ekpyrosis can also be modeled by a scalar field minimally coupled to gravity. However, the ekpyrotic potential is steep and negative.

As already mentioned, an important requirement for early universe models is the explanation of super-horizon, nearly scale-invariant adiabatic/curvature fluctuations. Let us briefly state how these fluctuations can be created during inflation. If we perturb the background, there is one scalar degree of freedom in the case of a single scalar field minimally coupled to gravity. A useful quantity is the so-called comoving curvature perturbation, which describes a small local change in the expansion history. It turns out that to first order in perturbation theory, which describes the free evolution of the quantum fluctuations, the fluctuations get amplified and stretched outside the horizon. The nearly scale-invariant fluctuations become classical and act as seeds of the anisotropies in the Cosmic Microwave Background.
However, the adiabatic perturbations created during ekpyrosis have a deep blue spectrum [17, 18]. Moreover, these adiabatic fluctuations stay quantum and do not become classical [19]. We will review the basics of cosmological perturbation theory to first order in Chapter 4 and calculate the evolution of quantum fluctuations during ekpyrosis in Chapter 4 F. While we introduce the basic concepts of the ekpyrotic scenario, we will also discuss the corresponding concepts of inflation. This allows us to illustrate the similarities and differences of both models.

The fact that curvature perturbations do not become amplified during ekpyrosis led to the "new ekpyrotic scenario" [20, 21], which is a two-field ekpyrotic model. The presence of an unstable direction in the potential creates nearly scale-invariant entropy/isocurvature perturbations via the entropic mechanism [22–24]. Entropy perturbations perturb the transverse direction (in field space) of the background solution. The tachyonic potential can spoil the initial conditions [21] and the duration of the ekpyrotic phase. However, in the context of the cyclic model, this led to the so-called "phoenix" universe [25–27], which provides a selection principle for a successful cyclic model of ekpyrosis. We will cover the new ekpyrotic scenario in Chapter 5.

We will then investigate second order effects – namely non-Gaussian corrections – and the resulting theoretical and observational consequences of early universe models in Chapter 6. The

second order corrections correspond to self-interactions of the perturbations. The inflationary potential is very flat, and thus the self-interactions are small. However, in the ekpyrotic case, the potential is very steep, which typically leads to large self-interactions and consequently large non-Gaussian corrections. The non-Gaussianities are in tension with observations. The challenges for inflationary and ekpyrotic models will be reviewed in Chapter 7.

The resolution of the typically large non-Gaussian signatures [28] in ekpyrotic models is the focus of this thesis. The non-minimal entropic mechanism [29–32] creates nearly scale-invariant entropy perturbations via a non-minimal kinetic coupling between two scalar fields. In collaboration with Angelika Fertig and Jean-Luc Lehners, we have shown in [31] that this model produces overall small non-Gaussian corrections, which will be discussed in detail in Chapter 8. In the non-minimal entropic mechanism, the potential does not depend on the second scalar field. However, the non-Gaussian corrections arise due to self-interactions, which are precisely zero during ekpyrosis, because the potential does not depend on the second scalar field. This has crucial consequences: In contrast to the "new ekpyrotic scenario", the intrinsic non-Gaussian corrections vanish resolving the tensions with observations.

Eventually, the ekpyrotic phase has to come to an end – the universe has to undergo a bounce from a contracting to an expanding phase. The challenges and developments of bouncing cosmologies will be covered in Chapter 9 and Chapter 10. A realization of a non-singular bounce can be obtained via a ghost-condensate [20, 24, 33], which is technically fairly simple and constitutes a healthy effective field theoretical description [8]. This allows us to calculate the evolution of the background as well as the evolution of the adiabatic and entropy perturbations during a non-singular bounce.

An important step for the viability of ekpyrotic models is the conversion phase: Entropy perturbations have to be converted to curvature perturbations in order to explain the structure formation in the universe. We will discuss the cosmological predictions from a conversion phase in detail in Chapter 6 E. In various studies [22, 34, 35], the conversion phase takes place after (or during) the ekpyrotic phase and before the bounce. The findings of [8] suggest that the effective field theoretical description of a ghost-condensate bounce is under better control in the presence of a negative potential. This was the motivation to investigate the conversion process after a non-singular bounce. In Chapter 11 we will calculate the evolution of entropy perturbations dur-

ing a non-singular bounce and the subsequent conversion phase based on our findings in [9] in collaboration with Angelika Fertig, Jean-Luc Lehners and Edward Wilson-Ewing. It turns out that the possibly large non-Gaussian corrections created during ekpyrosis become suppressed during the non-singular bounce phase. This means that the non-Gaussian signatures depend mostly on the conversion process reducing the tension of the entropic mechanism with observations.

Since the very first inflationary models, a vast amount of early universe models have been proposed – based on single scalar fields, multiple scalar fields, generalized scalar fields, single scalar fields minimally and non-minimally coupled to gravity, higher derivative theories,...
Hundreds of different models alone are based on inflation – for a review see, e.g., [36]. However, many conceptual and fundamental problems of the inflationary paradigm remain unresolved (cf. Chapter 7). A severe challenge is (slow-roll) eternal inflation: rare, large adiabatic fluctuations can cause a region in the universe to expand more rapidly since the scalar field moves up in the potential. This can happen over and over leading to an infinite amount of pocket universes – each physically different. With no probability measure, the multiverse challenges the predictability of inflation.

In Chapter 13 we propose an early universe model with a phase of accelerated expansion based on our paper [10] in collaboration with Angelika Fertig and Jean-Luc Lehners. The basic idea is to conflate ideas of inflation and ekpyrosis combining features of both models. During conflation, the universe undergoes accelerated expansion like during inflation, but perturbations behave like during ekpyrosis. Hence (slow-roll) eternal inflation does not occur during conflation since there are no large adiabatic fluctuations. The model belongs to the class of scalar-tensor theories, where the scalar field is non-minimally coupled to gravity. We will cover the physical concepts of scalar-tensor theories before the construction of the conflationary phase in Chapter 12.

The results presented in this thesis based on [9, 10, 31] will be put in context with the theoretical and experimental developments in recent years in Chapter 14. We will review the properties, challenges, open problems, and predictions of these models. Finally, we will discuss how future experiments can falsify or provide evidence for the ekpyrotic scenario as a possible early universe model.

2. COSMOLOGY – AN INTRODUCTION

The following chapter will provide a brief review of the standard model of cosmology. We will discuss the basic concepts of cosmology, important measurements and the resulting cosmological parameters. We will then encounter shortcomings of the standard big bang theory, which are mainly initial condition problems.

A. FLRW Cosmology

Einstein's theory of general relativity answered many philosophical questions about the universe with a physical theory. In the 1920's Albert Einstein [37], Alexander Friedmann [38, 39] and George Lemaître [40, 41] realized that the Einstein equations allow dynamical solutions of the universe. Lemaître was the first who considered that the expanding universe could have a beginning. The idea of an early quantum state, which he called the "primeval atom" later led to the name "Big Bang". In 1929 Edwin Hubble [42] discovered that distant nebulae are actually other galaxies and that the recession velocity of these galaxies increases with distance. This led to the Hubble law and consequently to the discovery that the universe is indeed expanding. In 1964 Penzias and Wilson [43] measured an isotropic background signal: the Cosmic Microwave Background (CMB) radiation. We will cover the CMB in detail in Chapter 2 C. For now, let us state that the existence of such an isotropic background radiation provides strong evidence for the expansion of the universe and for the spatial isotropy and homogeneity on large scales. Isotropy means that there is no preferred direction in space: The universe looks the same in each direction; it is rotation invariant. Another indication for spatial isotropy are the results of large-scale structure measurements. In Fig. 1 the measurement of the 2dF galaxy redshift survey [1] is plotted. On small scales, there are sheets and filaments, while on large scales the galaxy distribution becomes spatially isotropic.

Homogeneity implies that the universe looks the same at each point in space – it is translation invariant. An observer capable of jumping around in space would see the same physics at each point in space if the universe is homogeneous. While we can measure spatial isotropy on large scales, we cannot confirm that the universe is homogeneous. However, our position in the universe is seemingly not special, which means that it is very probable that a distant observer would also see an isotropic distribution of galaxies on larges scales. It the universe is spatially isotropic in multiple points in space, then the universe is also spatially homogeneous. The concept of homogeneity and

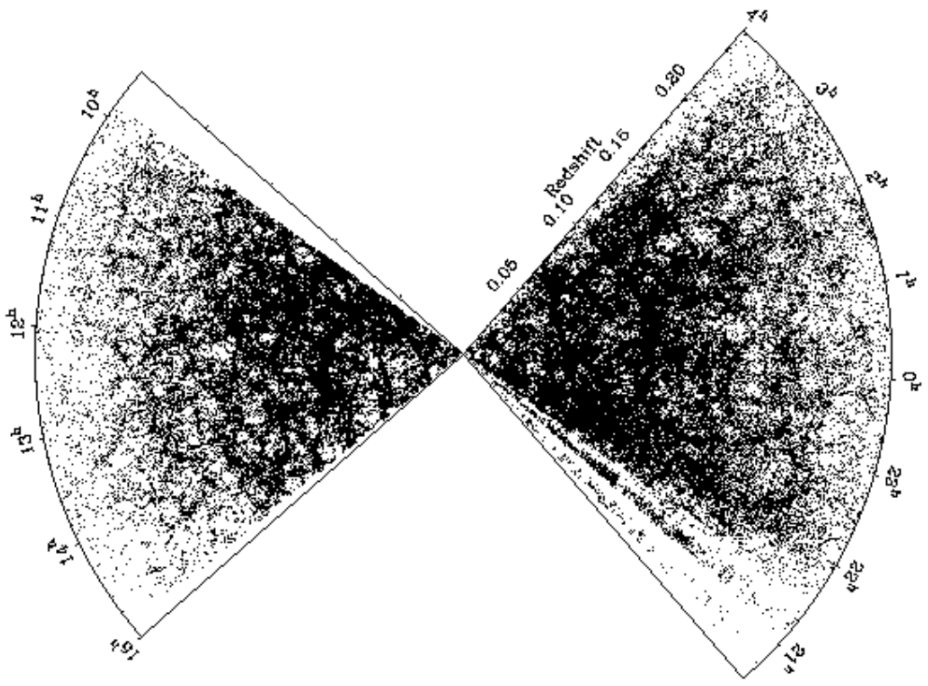

FIG. 1. 2dF galaxy redshift survey shows the position of galaxies for redshifts up to $z = 0.25$. On smaller scales galaxies cluster together, while on large scales the distribution becomes spatially isotropic. Figure from [1].

isotropy in general relativity is called the Cosmological Principle, which is a generalization of the Copernican Principle. The universe is essentially the same at each spatial point. As seen from the large scale structure measurements the Cosmological Principle is valid on large scales. The homogeneity and isotropy allow us to calculate the dynamics of our universe in a simple way. We can foliate the four-dimensional manifold in $\mathbb{R} \times \Sigma$, where $\mathbb{R}$ is the time direction and Σ is a maximally symmetric 3-space. We can chose a metric of the form

$$\mathrm{d}s^2 = -\mathrm{d}t^2 + a^2(t)\gamma_{ij}(\boldsymbol{x})\mathrm{d}x^i\mathrm{d}x^j, \tag{2.1}$$

where $a(t)$ is the scale factor determining the relative size of the spatial hypersurface Σ at times t. We have chosen so-called comoving coordinates, where cross-terms $\mathrm{d}t\,\mathrm{d}x^i$ are absent. The metric with a maximally symmetric surface Σ is the famous Friedmann-Lemaitre-Roberson-Walker (FLRW) metric:

$$\mathrm{d}s^2 = -\mathrm{d}t^2 + a^2(t)\left[\frac{\mathrm{d}r^2}{1-kr^2} + r^2(\mathrm{d}\theta^2 + \sin^2\theta\mathrm{d}\phi^2)\right]. \tag{2.2}$$

The metric is invariant under the following redefinition: $k \to k/|k|\,, r \to r\sqrt{|k|}\,, a \to a/|k|$, such that $k/|k| = \text{sign k}$ is the relevant parameter. This means there are three possible cases: An

open universe with constant negative spatial curvature $k = -1$, a flat universe with zero spatial curvature and a closed universe with constant positive spatial curvature $k = +1$.
Changing the coordinates in (2.2) the three space metric reads $d\sigma^2 = d\chi + r^2 d\Omega^2$, where $r = \sinh\chi$ for $k = -1$, $r = \chi$ for $k = 0$ and $r = \sin\chi$ for $k = 1$.

The Einstein equations are given by:

$$G_{\mu\nu} \equiv R_{\mu\nu} - \frac{1}{2} g_{\mu\nu} R + \Lambda g_{\mu\nu} = T_{\mu\nu}, \tag{2.3}$$

where we have set $8\pi G = M_P^{-2} = 1$. We will use the so-called reduced Planck units and $c = \hbar = 1$ throughout this thesis, if not otherwise stated. Moreover, we will use the metric signature $(-+++)$. In order to calculate the Einstein equations we have to calculate the Christoffel symbols for the FLRW metric:

$$\Gamma^0_{ij} = \frac{\dot{a}}{a} g_{ij} \quad , \quad \Gamma^i_{0j} = \frac{\dot{a}}{a} \delta^i_j \quad , \quad \Gamma^2_{12} = \frac{1}{r} \tag{2.4}$$

$$\Gamma^1_{11} = \frac{kr}{1 - Kr^2} \quad , \quad \Gamma^1_{22} = \Gamma^1_{33} \sin^{-2}\theta = -r(1 - kr^2) \tag{2.5}$$

$$\Gamma^2_{33} = -\sin\theta\cos\theta \quad , \quad \Gamma^3_{23} = \cot\theta \tag{2.6}$$

This leads to the following non-zero components of the Ricci tensor

$$R_{00} = -3\frac{\ddot{a}}{a} \quad , \quad R_{ij} = \left(a\ddot{a} + 2\dot{a}^2 + 2k\right) \gamma_{ij} \tag{2.7}$$

and the Ricci scalar

$$R = \frac{3}{a}\left(a\ddot{a} + 2\dot{a}^2 + k\right). \tag{2.8}$$

Assuming homogeneity and isotropy the most general matter fluid is the perfect fluid. An observer comoving with the fluid would see the universe as isotropic. The energy-momentum tensor of a perfect fluid is given by

$$T^{\mu\nu} = p g^{\mu\nu} + (p + \rho) u^\mu u^\nu, \tag{2.9}$$

where $p(t)$ is the pressure, $\rho(t)$ is the energy density of the fluid and u^ν is the comoving four-velocity satisfying $u^\mu u_m = -1$. For a comoving observer in the rest frame we have

$$T^\mu_\nu = diag(-\rho(t), p(t), p(t), p(t)). \tag{2.10}$$

The equation of state w of the fluid is given by $p = w\rho$. Another parameter representing the equation of state is ϵ, defined via

$$p = \left(\frac{2}{3}\epsilon - 1\right)\rho, \tag{2.11}$$

with the relations $w = \frac{2}{3}\epsilon - 1$ and $\epsilon = \frac{3}{2}(w+1)$. The parameter ϵ in inflationary models is also called the slow-roll parameter, while in ekpyrotic models it is called the fast-roll parameter, as will become apparent in later chapters. It is usually assumed that ϵ is constant or slowly varying.
From the Bianchi identity for the Einstein tensor ($G^{\mu\nu}_{;\nu} = 0$) we find that the energy-momentum tensor is also covariantly conserved: $T^{\mu\nu}_{;\nu} = 0$. This leads to the equation of continuity:

$$\dot{\rho} + 3H(\rho + p) = 0, \tag{2.12}$$

where we have introduced the Hubble parameter

$$H = \frac{\dot{a}}{a} \tag{2.13}$$

For a constant equation of state, we can integrate the equation of continuity yielding

$$\rho \sim \frac{1}{a^{2\epsilon}} \sim \frac{1}{a^{3(w+1)}}. \tag{2.14}$$

The energy density is not conserved in a dynamic universe. From (2.14) we can see how different matter contents scale in an expanding or contracting universe. This is very important in order to understand which matter content is dominant at different stages of the evolution of the universe.

Pressure free matter (dust) has an equation of state $w = 0$ or $\epsilon = \frac{3}{2}$. This matter content includes ordinary baryonic matter (e.g., stars and planets) and also dark matter when averaged over large scales. From (2.14) we see that the energy density scales as $\rho \sim a^{-3}$ – the energy density scales inversely with the volume.

For radiation/relativistic particles the equation of state is given by $w = \frac{1}{3}$ or $\epsilon = 2$. The energy density scales as $\rho \sim a^{-4}$. Thus the energy density of radiation falls off faster than the energy density of dust. From these considerations, we can already deduce that in an expanding universe the universe was dominated by radiation followed by a matter dominated era. The scaling $\rho \sim a^{-4}$ can be understood as follows: the number of e.g. photons scales with the volume as $\sim a^{-3}$. Moreover, the wavelength scales also with the scale factor leading to a frequency or energy scaling of $\sim a^{-1}$ due to the expansion of the universe (redshift).

The cosmological constant has an equation of state $w = -1$ or $\epsilon = 0$. The energy density of the cosmological constant is constant and the pressure is negative. This negative pressure can lead to an accelerated expansion of the universe. However, models of dark energy and inflation usually

replace the cosmological constant by a scalar field in order to obtain a dynamical description allowing for a beginning and ending of such a phase.

As just mentioned another very important matter content is described by one or multiple scalar fields. In this thesis, we will discuss a variety of different scalar field models. For now, we will note that the energy density of a single scalar field with a constant equation of state is also given by

$$\rho \sim \frac{1}{a^{2\epsilon}}. \tag{2.15}$$

We have discussed the matter content and geometry on the basis of the Cosmological Principle. We can now calculate the corresponding Einstein equations: the famous Friedmann equations. Assuming the FLRW metric and matter content described by a perfect fluid, we obtain

$$H^2 + \frac{k}{a^2} = \frac{1}{3}\rho, \tag{2.16}$$

$$\frac{\ddot{a}}{a} = -\frac{1}{6}(\rho + 3p) = -\frac{1}{3}\rho(\epsilon - 1). \tag{2.17}$$

The equations are called the first and second Friedmann equation. The first equation is often simply referred to as the Friedmann equation, while the second equation is called the acceleration equation. ρ and p denote the overall energy density and pressure, which consists of the sum of all the different matter contents.

In the case of a spatially flat universe with $k = 0$, we can find a very useful definition of the equation of state parameter:

$$\epsilon \equiv -\frac{\dot{H}}{H^2}. \tag{2.18}$$

Let us consider a spatially flat ($k = 0$) universe with a constant equation of state ϵ. In this case, the solutions to the Friedmann equations are scaling solutions. Scaling solutions have the property that all terms in the equations of motion scale in the same way with time. This class of solutions will also be very important in the case of inflation and ekpyrosis: Scaling solutions are exact, and one can find approximations for more complicated cases based on the scaling solutions. The scaling solutions for $k = 0$ and $\epsilon = const.$ in an expanding universe ($0 < t < \infty$) are given by

$$a(t) = t^{1/\epsilon} \quad , \quad H = \frac{1}{\epsilon t} \quad , \quad \rho = \frac{3}{\epsilon^2 t^2}, \tag{2.19}$$

while in a contracting universe ($-\infty < t < 0$) we have

$$a(t) = (-t)^{1/\epsilon} \quad , \quad H = \frac{1}{\epsilon t} \quad , \quad \rho = \frac{3}{\epsilon^2 t^2}. \tag{2.20}$$

In an expanding universe the Hubble parameter $H > 0$ and the scale factor a increases with time, while in a contracting universe Hubble parameter $H < 0$ and the scale factor a decreases with time. Comparing the solutions with the Friedmann equation (2.16) we indeed find that each terms scales as t^{-2}.

Let us take a look how the universe behaves when it is dominated by a single matter component in an expanding universe:

In the case of dust the scale factor is given by $a(t) \sim t^{\frac{2}{3}}$ and from the second Friedmann equation we find that the universe is decelerating.
For a radiation dominated universe we find a scale factor of the form $a(t) \sim t^{\frac{1}{2}}$, while the universe is again decelerating.
The cosmological constant yields an exponential expansion $a(t) \sim e^{Ht}$ with $\rho = const.$ and $H = const.$. This solution is the well known de Sitter (dS) phase, which is accelerating. From the acceleration equation we find that the universe is accelerating for $w < -\frac{1}{3}$.

Let us define the critical density

$$\rho_c = 3H^2, \tag{2.21}$$

which corresponds to a spatially flat universe. The critical density today is measured to be approximately [44]:

$$\rho_c = 3H_0^2 \approx \frac{3}{8\pi G}(68\, km\, s^{-1}\, Mpc^{-1}) \approx 10^{-26}\, kg/m^3. \tag{2.22}$$

We can use the current critical density to define a density parameter

$$\Omega = \frac{\rho_0}{3H_0^2} = \frac{\rho_0}{\rho_c} \tag{2.23}$$

and rewrite the Friedmann equation as

$$\Omega - 1 = \frac{k}{a^2 H^2}. \tag{2.24}$$

Thus Ω also describes if the universe is open, flat or closed. We are now interested in the dynamics of the universe in the presence of several matter components. The Friedmann equation reads

$$3H^2 = \frac{\rho_r}{a^4} + \frac{\rho_m}{a^3} - \frac{3k}{a^2} + \Lambda\,. \tag{2.25}$$

We can also define current fractional energy densities $\Omega_i = \rho_i/\rho_0$ for each matter content individually:

$$\Omega_r = \frac{\rho_{r,0}}{3H_0^2} \quad , \quad \Omega_m = \frac{\rho_{m,0}}{3H_0^2} \quad , \quad \Omega_k = -\frac{k}{3H_0^2} \quad , \quad \Omega_\Lambda = \frac{\Lambda}{3H_0^2}, \tag{2.26}$$

leading to a Friedmann equation of the form

$$\left(\frac{H}{H_0}\right)^2 = \frac{\Omega_r}{a^4} + \frac{\Omega_m}{a^3} + \frac{\Omega_k}{a^2} + \Omega_\Lambda \,. \tag{2.27}$$

Note, that one can write the Friedmann equation using today's cosmological parameters as

$$1 = \Omega_r + \Omega_m + \Omega_k + \Omega_\Lambda \,, \tag{2.28}$$

where we have set $a = 1$ and $H = H_0$. The Planck 2015 measurements obtained the following values of the cosmological parameters today (to 1 σ) [44]:

$$\begin{aligned} \Omega_r &= (9.15 \pm 0.34) \times 10^{-5}, \\ \Omega_m &= 0.308 \pm 0.012, \\ \Omega_k &= -0.005 \pm 0.017, \\ \Omega_\Lambda &= 0.692 \pm 0.12, \\ H_0 &= (67.8 \pm 0.9)\, kms^{-1}Mpc^{-1}. \end{aligned} \tag{2.29}$$

The universe today is almost flat and thus we can use a flat FLRW metric with $k = 0$ to describe the evolution of the universe. The fact, that the curvature term is so small is very surprising and one of the puzzles of the standard hot big bang cosmology. This will be addressed in Chapter 2 D. We have just given a very brief introduction to the evolution of our universe. Today the universe undergoes accelerated expansion due to the dark energy domination. The prior phase was dominated by matter, during which the large scale structure was formed. And the preceding phase was dominated by radiation. The currently best fitting model which describes our universe is called the ΛCDM-model , where Λ stands for the cosmological constant and CDM for cold dark matter.

B. Light Propagation and Causal Structure

Due to the expansion of the universe the wavelength of light changes accordingly to

$$\lambda_0 = \lambda_1 \frac{a(t_0)}{a(t_R)} \equiv \lambda_1(1+z), \tag{2.30}$$

where t_R is the time of emission and t_0 corresponds to the time of observation (today). We have introduced the redshift z: in an expanding universe $a(t_0) > a(t_R)$ leading to $z > 0$, which means that light is red shifted (longer wavelength) due to the expansion. While in a contraction universe light is blue shifted.

Conformal time τ is defined via

$$\mathrm{d}\tau = \frac{\mathrm{d}t}{a}. \tag{2.31}$$

We can write the FLRW metric with $k = 0$ in this new time coordinate:

$$\mathrm{d}s^2 = a^2(\tau)\left(-\mathrm{d}\tau^2 + \mathrm{d}r^2 + r^2(\mathrm{d}\theta^2 + \sin^2\theta \mathrm{d}\phi^2)\right) . \tag{2.32}$$

In the case of a flat universe the FLRW metric is conformally equivalent to the Minkowski metric. Light propagates according to $ds^2 = 0$ and assuming a propagation along r leads to

$$\mathrm{d}\tau = \pm \mathrm{d}r\,. \tag{2.33}$$

Let us introduce the notion of the particle horizon. It determines the maximal distance light can travel between the initial time t_i (which is often set to $t_i = 0$) and the final time t_f. Since light propagates on null-lines and nothing travels faster than light, it determines the causal structure.

$$r_f - r_i = \Delta\tau = \int_{\tau(t_i)}^{\tau(t_f)} \mathrm{d}\tau = \int_{t_i}^{t_f} \frac{\mathrm{d}t}{a}. \tag{2.34}$$

Note that the physical distance is then given by $d = a(t)(r_f - r_i)$. We can rewrite (2.34)

$$r_f - r_i = \int_{t_i}^{t_f} \frac{\mathrm{d}t}{a} = \int_{t_i}^{t_f} \frac{\mathrm{d}a}{Ha^2} = \int_{t_i}^{t_f} \frac{\mathrm{d}(\ln a)}{aH}, \tag{2.35}$$

where $(aH)^{-1}$ is called the comoving Hubble radius, while H^{-1} is called the Hubble radius. Let us emphasize the difference between the comoving particle horizon τ and the comoving Hubble radius. Particles separated by more than τ could have *never* been in causal contact with each other, while particles separated by more than $(aH)^{-1}$ cannot communicate *now*.

For $a \sim t^n$ with $n < 1$ we can estimate the physical particle horizon

$$d = a(t) \int_0^t \frac{\mathrm{d}t'}{a(t')} = t^n \int_0^t \mathrm{d}t'\, t^{-n} = \frac{t}{1-n} \sim H^{-1}. \tag{2.36}$$

The Hubble radius H^{-1} determines the causally connected region in the universe. A mode with momentum k redshifts in an expanding universe; the physical momentum is given by $k_{phys} = k/a$. Thus a mode with momentum k is inside the horizon (sub-horizon) if:

$$\frac{k}{aH} \ll 1, \tag{2.37}$$

while a mode with momentum k is outside the horizon (super-horizon) if

$$\frac{k}{aH} \gg 1. \tag{2.38}$$

Note that the $(aH)^{-1}$ is the comoving Hubble radius, which determines if modes are inside or outside the horizon at a given time. In the case of a constant equation of state with $k = 0$ we have calculated the scaling solution (2.19), which can be used to calculate the behavior of the comoving Hubble radius. Using

$$\rho \sim \frac{1}{a^{3(1+w)}} \sim H^2 \quad , \quad a \sim t^{1/\epsilon} \tag{2.39}$$

we find

$$(aH)^{-1} \sim a^{\frac{1}{3}(1+3w)}. \tag{2.40}$$

This implies that the comoving Hubble radius grows monotonically for ordinary matter (dust $w = 0$ and radiation $w = 1/3$) in an expanding universe, which has significant consequences: In the past, the comoving Hubble radius was smaller than today. Regions which are in causal contact today were causally disconnected in the past.

Going back in time also means that the universe becomes smaller, which implies that the universe was much denser and hotter in the past. The energy of a photon is given by $E = \frac{hc}{\lambda} = k_B T$, and we can write the wavelength as

$$\lambda = \frac{hc}{k_B T}\,. \tag{2.41}$$

We have seen that the expansion leads to a redshift of the wavelength $\lambda \sim a$ and thus the temperature scales as $T \sim a^{-1}$. During radiation domination $a \sim t^{1/2}$ leading to $T \sim t^{-1/2}$. This allows us to determine the thermal history of the very early universe. We will focus on a very important observation and evidence for the hot big bang cosmology: the Cosmic Microwave Background radiation.

C. The Cosmic Microwave Background

In 1964 Penszias and Wilson measured an isotropic background signal [43] – the Cosmic Microwave Background (CMB) radiation. In the last 20-30 years, a variety of measurements by e.g. WMAP, COBE and most recently the Planck satellite led to a profound understanding of the universe. The Cosmic Microwave Background is a remnant of the early universe. At around the time of radiation-matter equality, the universe was filled with photons, electrons, protons and helium ions. During that time the universe was opaque. Photons scattered permanently off free electrons via Thomson scattering. At some point, the energy was low enough such that free electrons could bind with free protons and helium ions to form hydrogen and helium. Since photons interact much less with neutral atoms, the universe became transparent. The photons were suddenly able to move freely in all directions in the universe. The radiation emitted has a black body distribution, since photons, electrons, and protons were in thermal equilibrium. The moment when neutral atoms formed and the photons in the universe were released is called "recombination" or moment of last scattering. This happened at around 370 000 years after the "Big Bang" at a temperature of about $3000K$, which is related to a redshift of $z = 1089.94 \pm 0.42$ [44]. This means that the wavelength of the emitted photons increased by a factor of 1090 since then, which corresponds to a temperature of $T = 2.7K$ and a frequency peak of around $\nu = 160$ GHz today. We can calculate the (comoving) distance to the so-called last scattering surface, which marks the maximal radius of the observable universe (via light), from (2.34):

$$d_{ls} = a_0(r_{ls} - r_0) = \int \frac{\mathrm{d}t}{a} = \int_{a_{ls}}^{a_0=1} \frac{\mathrm{d}a}{H_0\sqrt{\Omega_r + \Omega_m a^2 + \Omega_\Lambda a^4}} \approx \frac{3.15}{H_0} \approx 45.3\,\text{billion light years}, \tag{2.42}$$

where we have used $a_0 = 1$, $H^{-1} \approx 14.4$ billion light years, the Friedmann equation (2.16), the cosmological parameters (2.29) obtained by Planck and the fact that $a_{LS} = 1/1090$ at the time of last scattering.

We can also calculate the (comoving) distance to the "Big Bang" surface, where $a_i = 0$ leading to $d_{bb} \approx \frac{3.21}{H_0} \approx 46.2$ billion light years. In Fig. 2 we have drawn the last scattering surface and the "Big Bang" surface. The Hubble radius (which is just the distance between the "Big Bang" surface and the last scattering surface c.f. Eq. (2.36)) at the time of last scattering is also shown in the figure. We see regions, which at the time of last scattering could not have been in causal contact. We can estimate that the causal radius is just about 1° in the sky today using $\sin\theta \approx (d_{bb} - d_{ls})/d_{ls}$. This is very surprising, since the Cosmic Microwave Background radiation is so isotropic. We will come back to this "horizon problem" in the next section.

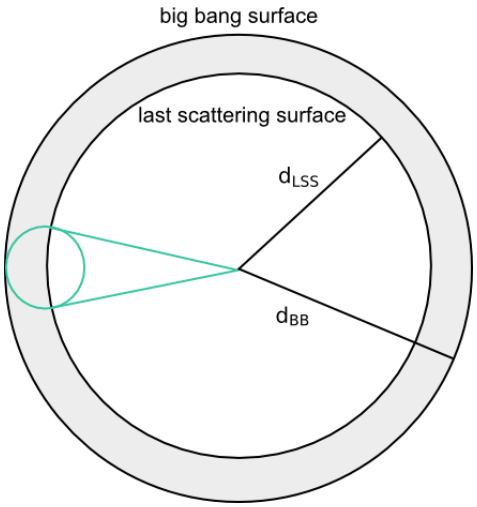

FIG. 2. The Cosmic Microwave Background radiation was emitted at the moment of last scattering. We observe in the middle of the sphere the CMB radiation today, which was emitted at a distance d_{LSS}. The Hubble radius $1/H$ (in turquoise) at the time of last scattering corresponds to just about 1° in the sky today. Figure based on [2].

The isotropy of the Cosmic Microwave Background is one of the most important evidence for the isotropy of the universe. We would like to understand why the universe is so isotropic, which models of the early universe have to address.

It turns out that the CMB is not perfectly isotropic, there are small temperature fluctuations of the order $\sim 10^{-5}$. These density/temperature fluctuations play a vital role in the structure formation in the universe. The small temperature anisotropies in the CMB can be described by an expansion in spherical harmonics Y_l^m on the sky. The monopole corresponds to $l = 0$, the dipole to $l = 1$, the quadrupole to $l = 2$, while m is an integer running from $-l$ to $+l$.

The temperature fluctuations are thus

$$\delta T(\hat{n}) = \sum_{lm} a_{lm} Y_l^m(\hat{n}), \tag{2.43}$$

where $\hat{n}$ denotes the direction in the sky. The temperature anisotropies observed by the Planck satellite are shown in Fig. 3. One can also define rotationally invariant quantities

$$C_l^{TT} = \frac{1}{2l+1} \sum_{lm} \langle a_{lm}^* a_{lm} \rangle \,, \tag{2.44}$$

where $\langle ... \rangle$ denotes an ensemble average. C_l^{TT} is the angular correlation function of the temperature fluctuations. One usually uses the quantity $D_l^{TT} = l(l+1)C_l^{TT}/2\pi$.

In Fig. 4 we see the famous angular power spectrum of the temperature fluctuations of the CMB radiation. The shape can be explained by the dynamics during the radiation-matter phase if nearly

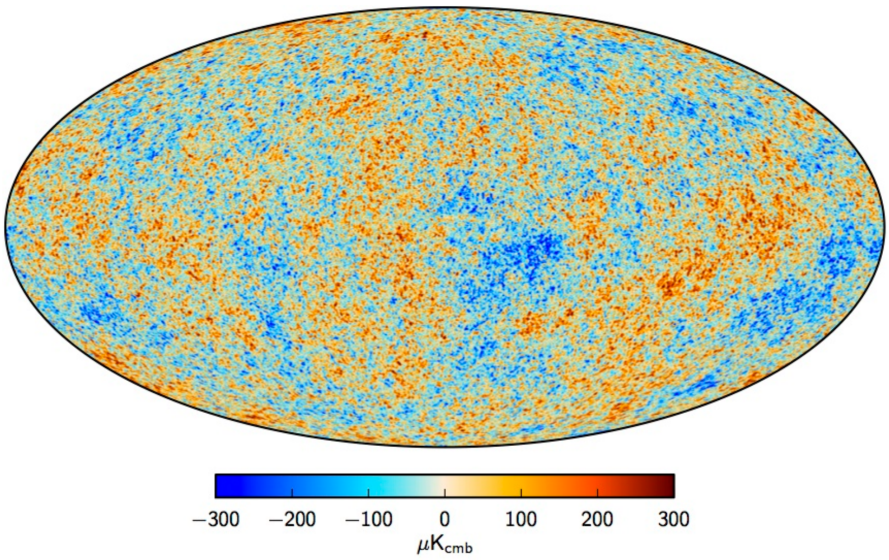

FIG. 3. The figure shows the all-sky map of the Cosmic Microwave Background radiation. In this figure, the galaxy foregrounds and the dipole (corresponding to the relative motion of the solar system to the CMB) have been subtracted. Hot spots are shown in red, while cold spots are shown in blue. Figure taken from[3].

scale-invariant fluctuations were present before this phase. Moreover, the nearly scale-invariant fluctuations had to be super-horizon. In fact, they enter the horizon while it increases with time. The existence of these super-horizon modes has to be explained by a model of the early universe.

For now, we will introduce these perturbations by hand and try to explain their origin in detail throughout this thesis. A very useful quantity to describe these fluctuations is the so-called curvature perturbation $\mathcal{R}(t,x)$. It denotes a local and time-dependent fluctuation in the curvature. This corresponds to a small, local change in the scale factor – a local change of the expansion of the universe. Locally the universe expands a little bit less or more leading to fluctuations in the temperature. Let us write the curvature perturbation in Fourier space as

$$\mathcal{R}_{\mathbf{k}}(t) = \int \mathrm{d}^3x \mathcal{R}(t,\mathbf{x}) e^{-i\mathbf{kx}}. \tag{2.45}$$

We define the power spectrum $P_{\mathcal{R}}$ as the two-point correlation function in Fourier space

$$\langle \mathcal{R}_{\mathbf{k}} \mathcal{R}_{\mathbf{k}'} \rangle \equiv (2\pi)^3 \delta(\mathbf{k}+\mathbf{k}') P_{\mathcal{R}}(k). \tag{2.46}$$

We can relate the power spectrum of the curvature perturbation with the angular power spectrum of the CMB temperature fluctuations via a transfer function $T_l(k)$:

$$C_l^{TT} = \int \frac{\mathrm{d}^3k}{(2\pi^3)} P_{\mathcal{R}} T_l^2(k). \tag{2.47}$$

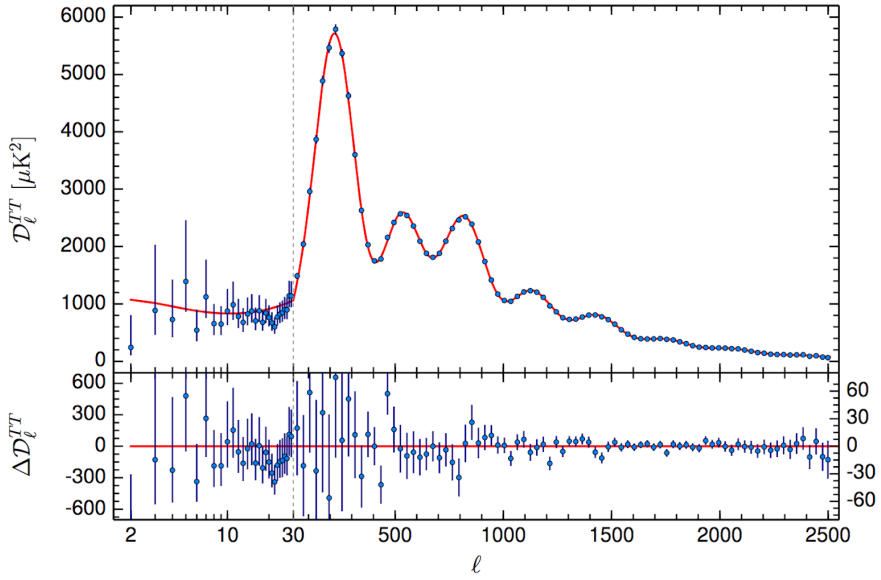

FIG. 4. The figure shows the angular power spectrum of the temperature anisotropies in the Cosmic Microwave Background. Small l correspond to large scales (small k), while large l correspond to small scales. The position and size of the peaks and troughs are well understood in terms of the physics during matter-radiation equality, which allows for the determination of the cosmological parameters of the ΛCDM model – the fit is shown as a red line. Figure taken from [3].

The transfer function $T_l(k)$ (which encodes the evolution) can be calculated and consequently we obtain the power spectrum of the primordial curvature perturbations by measuring the power spectrum of the CMB temperature fluctuations. Let us define the variance $\Delta^2_{\mathcal{R}}$ and the spectral index n_s of the curvature perturbations:

$$\Delta^2_{\mathcal{R}} \equiv \frac{k^3}{2\pi^2} P_{\mathcal{R}} \quad , \quad n_s - 1 \equiv \frac{d\ln\Delta_{\mathcal{R}}}{d\ln k}, \tag{2.48}$$

where $n_s = 1$ corresponds to a scale-invariant spectrum – this means that the power spectrum is independent of the scale k. The real space correlation function is given by

$$\langle \mathcal{R}^2(\mathbf{x})\rangle = \int \frac{\mathrm{d}^3k}{(2\pi)^3} P_{\mathcal{R}}(k) = \int \mathrm{d}\ln k \Delta^2_{\mathcal{R}}, \tag{2.49}$$

where we have used $\mathrm{d}^3k = 4\pi k^2 \mathrm{d}k$. It is customary to write the variance as a power-law in k:

$$\Delta^2_{\mathcal{R}} = A_{\mathcal{R}} \left(\frac{k}{\tilde{k}}\right)^{n_s - 1}, \tag{2.50}$$

where $\tilde{k}$ is a reference scale called the pivot scale. The Planck team used $\tilde{k} = 0.05 Mpc^{-1}$ and obtained the following measurements up to 1σ [6]:

$$A_{\mathcal{R}} = (2.975 \pm 0.056) \times 10^{-9}, \tag{2.51}$$

$$n_s = 0.9649 \pm 0.0042. \tag{2.52}$$

The primordial curvature perturbations have a nearly scale-invariant spectrum. The spectrum is slightly red – there is a bit more power on larger scales (corresponding to smaller k). The measurements of the CMB radiation by WMAP, COBE and most recently by Planck [6, 44, 45] gave us a very precise picture of the early universe and subsequently of the universe today. The precision to which cosmological parameters have been measured is astonishing. We cannot cover all the physics involved in the CMB radiation and the consequential insights we obtained from the recent Planck measurements. For a review on the CMB see e.g. [46, 47].

One very important topic and the central theme of this thesis is the non-Gaussianity of the curvature perturbations and subsequently the temperature fluctuations. If the fluctuations are Gaussian, the two-point correlation function suffices to define all even higher order correlation functions, while the odd correlation functions are zero. We can define the bispectrum as the 3-point correlation function of the curvature perturbations in Fourier space

$$\langle \mathcal{R}_{k_1} \mathcal{R}_{k_2} \mathcal{R}_{k_3} \rangle = (2\pi)^3 \delta(\mathbf{k}_1 + \mathbf{k}_2 + \mathbf{k}_3) B(k_1, k_2, k_3) \tag{2.53}$$

and the trispectrum

$$\langle \mathcal{R}_{k_1} \mathcal{R}_{k_2} \mathcal{R}_{k_3} \mathcal{R}_{k_4} \rangle = (2\pi)^3 \delta(\mathbf{k}_1 + \mathbf{k}_2 + \mathbf{k}_3 + \mathbf{k}_4) T(k_1, k_2, k_3, k_4)\,. \tag{2.54}$$

The amount of non-Gaussianity is parametrized by f_{NL}, while the amplitude of the trispectrum is parametrized by g_{NL}. The Planck team published the following bounds to 1σ [45]:

$$f_{NL}^{local} = 0.8 \pm 5.0, \tag{2.55}$$

$$g_{NL}^{local} = (9.9 \pm 7.7) \times 10^4, \tag{2.56}$$

where $f_{NL} = 0$ corresponds to a purely Gaussian distribution. The primordial curvature perturbations are nearly scale-invariant and nearly Gaussian. A model of the early universe has to describe how such super-horizon curvature perturbations are created. As we will see the ekpyrotic model, which is the early universe model of interest in this thesis, usually produces sizable non-Gaussianities. The main goal of this work is to construct an ekpyrotic model, which describes the initial conditions of the universe we observe today.

Another important aspect of the Cosmic Microwave Background radiation is its polarization, which can be described by an intensity matrix I_{ij} in the plane (perpendicular to the direction of

propagation)

$$I_{ij} = \begin{pmatrix} T+Q & U \\ U & T-Q \end{pmatrix}, \tag{2.57}$$

where U and Q are the Stokes parameters and T denotes the temperature anisotropies. The Stokes parameters can be expanded in spin-2 spherical harmonics

$$(Q \pm iU)(\hat{n}) = \sum_{l,m} a_{\pm 2,lm\pm 2} Y_{lm}(\hat{n}). \tag{2.58}$$

Let us consider the following linear combinations

$$a_{E,lm} = -\frac{1}{2}(a_{2,lm} + a_{-2,lm}), \tag{2.59}$$

$$a_{B,lm} = -\frac{1}{2i}(a_{2,lm} - a_{-2,lm}), \tag{2.60}$$

where the first term corresponds to the so-called E-mode, which is symmetric under parity transformations, and the second term corresponds to the so-called B-mode, which is anti-symmetric under parity. In (2.44) we have defined the temperature-temperature angular correlation function. We can now extend this definition including the E-modes and B-modes

$$C_l^{XY} = \frac{1}{2l+1} \sum_m \langle a^*_{X,lm} a_{Y,lm} \rangle, \tag{2.61}$$

where $X, Y = T, E, B$. We have seen in Eq. (2.47) that the temperature-temperature angular power spectrum C_l^{TT} is related to primordial scalar curvature perturbations. It turns out that these scalar perturbations can only create E-modes, while primordial tensor perturbations (primordial gravitational waves) produce E-modes and B-modes. The primordial tensor fluctuations induce a quadrupole in the radiation field leading to B-mode polarizations via Thomson-scattering. Consequently, a measurement of primordial B-modes in the CMB would correspond to an indirect measurement of primordial gravitational waves. Until now these primordial B-modes have not been measured resulting in a bound on the ratio of the primordial tensor perturbations and primordial scalar perturbations, which is called the tensor-to-scalar ratio r [6]:

$$r < 0.064. \text{ at } 95\% \text{ confidence level.} \tag{2.62}$$

D. Hot Big Bang Puzzles

In the following, we will summarize the more prominent hot big bang puzzles.

The flatness problem:

The universe today is spatially flat with $\Omega_k = -0.005 \pm 0.017$ [45]. We know from the Friedmann equation (2.27), that the curvature term scales as $\sim \Omega_k a^{-2}$, which suggests that the spatial curvature should dominate eventually in an expanding universe. The spatial curvature in the early universe had to be very small, such that its energy density could have never dominated the evolution of the universe. Let us estimate how small the initial curvature had to be.

Using the Friedmann equation (2.24)

$$\Omega - 1 = \frac{k}{a^2 H^2}\,, \tag{2.63}$$

we obtain using $a \sim t^{2/3}$ during matter domination $\Omega - 1 \sim a$, while during radiation domination we find $\Omega - 1 \sim a^2$ with $a \sim t^{1/2}$. We can now compare the curvature at e.g. the electro-weak energy scale ≈ 1 TeV to the curvature at radiation-matter equality ≈ 1 eV assuming radiation domination

$$\frac{|\Omega - 1|_{LS}}{|\Omega - 1|_{EW}} \approx \frac{a_{LS}^2}{a_{EW}^2} \approx \frac{T_{EW}^2}{T_{LS}^2} \approx 10^{24}. \tag{2.64}$$

The curvature grew by a factor of 10^{24} between the electro-weak energy scale and the time of radiation-matter equality. Overall the curvature grew by a factor of 10^{27} between the electro-weak energy scale and today. This growth is even larger if we would go towards higher energy scales, e.g. the grand unified scale of $10^{16} GeV$ leads to a total growth of approximately 10^{53}. This means that the universe had to be very flat in the early universe and this fine-tuning of the initial conditions is called the flatness problem.

The flatness problem arises because of the scaling $(aH)^{-2}$ of the curvature term. We recognize that $(aH)^{-1}$ is the comoving Hubble radius and it always increases with time in a matter or radiation dominated universe. This fact also led to the horizon problem, which we will discuss now.

The horizon problem:

The comoving Hubble radius is growing with time during matter or radiation domination in an expanding universe. Regions of causal contact decrease as we go back in time. The isotropy of the Cosmic Microwave Background radiation is thus very puzzling. We have seen that only a region

of angular size of 1° on the sky today could be in causal contact at the time of recombination. The physical horizon distance – the maximal distance light could have traveled since the "Big Bang"– is given by

$$d_H(t) = a(t) \int_0^t \frac{\mathrm{d}t'}{a(t')} \tag{2.65}$$

with $a(t) \sim t^{1/2}$ during radiation domination and $a(t) \sim t^{2/3}$ during matter domination we find:

$$d_H(t) \sim a(t) \times \begin{cases} a(t) & \text{radiation} \\ a(t)^{1/2} & \text{matter} \end{cases} . \tag{2.66}$$

The causal horizon increases faster than the scale factor: with increasing time the universe contains more regions which were never in causal contact with each other. Let us estimate the number of causally disconnected regions of the CMB radiation in the sky. We compare the volume of the universe today with the volume of the particle horizon at the time of last scattering

$$N(z) \sim \left(\frac{a_0}{d_H(t)}\right)^3 \approx (1+z)^{3/2} \approx 4 \cdot 10^5, \tag{2.67}$$

where we have used $a_0 = 1$ and (2.66) with $d_H \sim a^{3/2} = (1+z)^{-3/2}$. We need a mechanism which explains how $\sim 10^5$ seemingly disconnected patches could have been in causal contact. If the comoving Hubble radius would have evolved differently than the particle horizon in the early universe, then the horizon problem could be solved.

The singularity puzzle:
In the standard hot big bang cosmology the scale factor $a(t) \to 0$ as we approach the "Big Bang" at $t = 0$. Curvature invariants like the Ricci scalar go to infinite as $a(t) \to 0$, since $R \sim t^{-2}$. This singularity is a true singularity, which was first formulated in the famous Penrose-Hawking singularity theorems [48, 49].

The anisotropy puzzle:
In Chapter 2 C we have discussed the Cosmic Microwave Background radiation, which provides important evidence for the isotropy of the universe. The seemingly causally disconnected regions at the time of recombination were related to the horizon problem, which has to be resolved by a model of the early universe. Moreover, the existence of nearly scale-invariant and nearly Gaussian super-horizon curvature perturbations has to be explained. We need a mechanism that can create these super-horizon modes.

3. INFLATION AND EKPYROSIS

A. Inflation

In the previous chapter we have discussed shortcomings of the standard big bang model. We would like to explain the initial conditions of the universe which is spatially flat, homogeneous and isotropic – while small anisotropies seed the structure formation of the universe.
We have noticed that the flatness and horizon problem arose because the comoving Hubble radius grows in an expanding universe with an equation of state $w > \frac{1}{3}$:

$$(aH)^{-1} \sim a^{\frac{1}{3}(1+3w)}. \tag{3.1}$$

Let us consider the following scenario: if the comoving Hubble radius was initially large in the past and decreasing for a sufficiently long time, we could solve the flatness and horizon problem:

$$\frac{d}{dt}\left(\frac{1}{aH}\right) < 0. \tag{3.2}$$

In an expanding universe $H > 0$ and thus with

$$\frac{d}{dt}\left(\frac{1}{\dot{a}}\right) < 0 \tag{3.3}$$

we immediately obtain that the universe expands accelerated

$$\ddot{a} > 0. \tag{3.4}$$

From the acceleration equation

$$\frac{\ddot{a}}{a} = -\frac{1}{6}(\rho + 3p) = -\frac{1}{6}\rho(1 + 3w) \tag{3.5}$$

we find a third equivalent condition:

$$p < -\frac{1}{3}\rho \quad \text{or} \quad w < -\frac{1}{3}, \tag{3.6}$$

which tells us that the pressure has to be sufficiently negative.

The early universe phase of accelerated expansion with an equation of state $w < -\frac{1}{3}$ ($\epsilon < 1$) and a shrinking comoving Hubble radius is called inflation [11–13]. In Fig. 5 we have sketched the evolution of the comoving Hubble radius $(aH)^{-1}$.

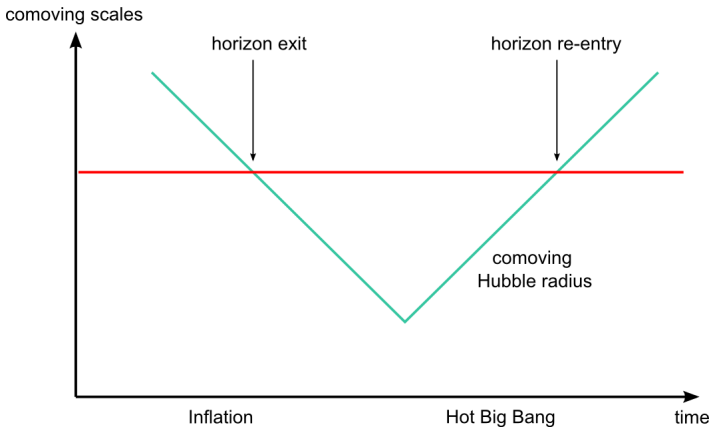

FIG. 5. During inflation the comoving Hubble radius $(aH)^{-1}$ shrinks. Comoving scales k leave the horizon at $aH = k$. In the subsequent hot big bang evolution the comoving Hubble radius increases and the corresponding comoving scale k re-enters the horizon. Figure based on [2].

If inflation lasts long enough the universe is rendered flat, homogeneous and isotropic. Moreover, quantum fluctuations during inflation become amplified and subsequently classical acting as seeds for the CMB anisotropies – this will be discussed in Chapter 4.

Inflation can be described by a wide variety of models – for a review see e.g. [36]. Here we will discuss the dynamics of a single scalar field minimally coupled to gravity in a potential, where the action is given by

$$S = \int d^4x\sqrt{-g}\left(\frac{R}{2} - \frac{1}{2}g^{\mu\nu}\partial_\mu\phi\partial_\nu\phi - V(\phi)\right) \tag{3.7}$$

and the energy-momentum tensor of the scalar field reads

$$T_{\mu\nu} = \frac{-2}{\sqrt{-g}}\frac{\delta S_\phi}{\delta g^{\mu\nu}} = \partial_\mu\phi\partial_\nu\phi - g_{\mu\nu}\left(\frac{1}{2}\partial^\sigma\phi\partial_\sigma\phi + V(\phi)\right). \tag{3.8}$$

The equations of motion can be obtained by varying the action w.r.t the metric and the scalar field leading to:

$$R_{\mu\nu} - \frac{1}{2}g_{\mu\nu}R = T_{\mu\nu}\,, \tag{3.9}$$

$$\Box\phi = V_{,\phi}\,. \tag{3.10}$$

Assuming homogeneity, flatness and isotropy we use the flat FLRW metric. Moreover, the homogeneous scalar field $\phi(\mathbf{x}, t) = \phi(t)$ is described by a perfect fluid with energy density ρ and pressure p:

$$\rho = \frac{1}{2}\dot{\phi}^2 + V(\phi), \tag{3.11}$$

$$p = \frac{1}{2}\dot{\phi}^2 - V(\phi), \tag{3.12}$$

while the equation of state reads

$$w = \frac{p}{\rho} = \frac{\frac{1}{2}\dot{\phi}^2 - V(\phi)}{\frac{1}{2}\dot{\phi}^2 + V(\phi)}. \tag{3.13}$$

The Friedmann equations and the equation of motion for the scalar field are given by

$$3H^2 = \frac{1}{2}\dot{\phi}^2 + V(\phi)\,, \tag{3.14}$$

$$\dot{H} = -\frac{1}{2}\dot{\phi}\,, \tag{3.15}$$

$$0 = \ddot{\phi} + 3H\dot{\phi} + V_{,\phi}\,. \tag{3.16}$$

We can obtain negative pressure and accelerated expansion if the potential energy dominates over the kinetic energy. For a sufficiently flat potential and a slowly rolling field

$$\frac{1}{2}\dot{\phi}^2 \ll V(\phi) \tag{3.17}$$

we find an equation of state $w \approx -1$ or $\epsilon \ll 1$. Note that we have defined the equation of state ϵ in (2.18). In the context of inflation ϵ is also called the slow-roll parameter and we can re-express it in various ways using the background equations of motion

$$\epsilon = -\frac{\dot{H}}{H^2} = \frac{\dot{\phi}^2}{2H^2} \approx \frac{V_{,\phi}^2}{2V^2}, \tag{3.18}$$

where we have used the slow-roll condition (3.17) in the last step. The slow-roll condition and flatness of the potential is indeed characterized by the smallness of the slow-roll parameter $\epsilon \ll 1$, which is of order $\mathcal{O}(10^{-2})$ in most inflationary single scalar field models.

We can define a second slow-roll parameter η:

$$\eta = -\frac{\dot{\epsilon}}{H\epsilon}, \tag{3.19}$$

which satisfies the slow-roll condition $\eta \ll 1$ ensuring that inflation lasts a sufficient long time. Using $\epsilon \ll 1$ we find

$$\eta \approx 2\frac{V_{,\phi\phi}}{V} - 4\epsilon, \tag{3.20}$$

which characterizes the slope of the potential. It is customary to classify single scalar field inflationary models into two types: large field models satisfying $0 < \eta < \epsilon$ and $V'' > 0$ and small field models with $\eta < 0 < \epsilon$ and $V'' < 0$. We will discuss which inflationary models are favored by

observations in Chapter 7.

Using the slow-roll approximation, the Friedmann equation reads

$$H \approx \frac{1}{3} V(\phi) \approx const. \tag{3.21}$$

During inflation the Hubble rate H is approximately constant. The limit $H = const.$ is called the de Sitter limit leading to an exponentially growing scale factor

$$a(t) = e^{Ht}. \tag{3.22}$$

We indeed see that the comoving Hubble radius $(aH)^{-1}$ decreases during inflation due to the exponential, accelerated expansion and a constant Hubble rate. For a more general case, using the definition $\epsilon \equiv -\dot{H}/H^2$ and conformal time $d\tau = dt/a$, we obtain

$$\frac{d}{d\tau}\left(\frac{1}{aH}\right) = \epsilon - 1 \tag{3.23}$$

and thus to first order in slow-roll parameters

$$aH \approx -\frac{1}{\tau}(1+\epsilon). \tag{3.24}$$

The scale factor in the de Sitter limit reads:

$$a(\tau) = -\frac{1}{H\tau}. \tag{3.25}$$

Note that in the de Sitter limit, inflation would never end, since the potential is perfectly flat. Moreover, the de Sitter limit $\epsilon \to 0$ is ill-defined, which becomes apparent when we discuss the behavior of perturbations during inflation. During matter domination $a(\tau) \sim \tau$ and during radiation radiation $a(\tau) \sim \tau^2$, where the initial singularity $a(\tau) = 0$ happens at $\tau = 0$. During inflation the singularity $a(\tau) = 0$ occurs at $\tau \to -\infty$. This means in terms of conformal time there was enough time, such that the previously causally disconnected patches at the time of last scattering were indeed causally connected in the past.

The overall dynamics of inflation can be summarized as follows: For given initial conditions, which we will discuss in Chapter 7, the inflationary phase starts. The inflaton field ϕ rolls slowly on a nearly flat potential leading to accelerated expansion. After a sufficiently long time, the universe is rendered flat and homogeneous setting the initial conditions of the standard hot big bang model. At a certain point the slow-roll condition breaks down, and ϵ becomes $\mathcal{O}(1)$ ending the inflationary phase. Modifications of the inflationary model allow for reheating: In the following, the scalar field decays into standard model particles and reheats the universe leading to the subsequent hot big bang cosmology.

B. Ekypyrosis

In a contracting universe, anisotropies become important, as we will show now. Let us consider an anisotropic universe described by the Kasner-like metric:

$$ds^2 = -dt^2 + a^2(t) \sum_i e^{2\beta_i(t)} (dx^i)^2, \tag{3.26}$$

where β_i parametrizes the anisotropies in the x_i direction satisfying $\sum_i \beta i = 0$. The Einstein equations read

$$\ddot{\beta}_i + 3H\dot{\beta}_i = 0\,, \tag{3.27}$$

$$3H^2 = \sum_i \dot{\beta}_i^2\,. \tag{3.28}$$

From the first equation we obtain $\dot{\beta}_i \sim a^{-3}$, such that the Friedmann equation including anisotropies becomes:

$$3H^2 = \frac{\rho_r}{a^4} + \frac{\rho_m}{a^3} - \frac{3k}{a^2} + \Lambda + \frac{\sigma^2}{a^6} + \frac{\rho_\phi}{a^{3(1+w)}}, \tag{3.29}$$

where σ describes the anisotropic energy density. In an expanding universe, the curvature term becomes dominant, while in a contracting universe anisotropies dominate the evolution. It is a well know result that a contracting universe with anisotropies leads to the so-called BKL (Belinsky, Khalatnikov and Lifshitz)-mixmaster behavior when approaching the big crunch [50, 51]. The universe becomes more and more anisotropic described by a Kasner solution – while two spatial directions shrink the other spatial direction grows. Moreover, the universe jumps from one Kasner-universe to another repeatedly.

In order to avoid the BKL-mixmaster universe we need a matter content that suppresses the anisotropies – namely a matter content with equation of state $w > 1$ or $\epsilon > 3$. This phase with a large equation of state (large pressure) is called ekpyrosis and was first introduced in [14].

Ekpyrosis can be modeled by a scalar field minimally coupled to gravity in a steep negative potential. The equation of state is indeed greater than one if the potential $V(\phi)$ is negative

$$w = \frac{p}{\rho} = \frac{\frac{1}{2}\dot{\phi}^2 - V(\phi)}{\frac{1}{2}\dot{\phi}^2 + V(\phi)} > 1\,. \tag{3.30}$$

The background equations of motion are again given by

$$3H^2 = \frac{1}{2}\dot{\phi}^2 + V(\phi)\,, \tag{3.31}$$

$$\dot{H} = -\frac{1}{2}\dot{\phi}\,, \tag{3.32}$$

$$0 = \ddot{\phi} + 3H\dot{\phi} + V_{,\phi}\,. \tag{3.33}$$

Let us introduce a negative exponential potential

$$V(\phi) = -V_0 e^{-c\phi}\,, \tag{3.34}$$

where V_0 and c are constants – the relation between c and ϵ turns out to be given by $c = \sqrt{2\epsilon}$. There exists a scaling solution similar to the case in (2.20). Each term in the Friedmann equation scales in the same way with time:

$$a(t) = a_0(-t)^{1/\epsilon} \quad , \quad H(t) = \frac{1}{\epsilon t} \quad , \quad \phi(t) = \frac{1}{\sqrt{2\epsilon}} \ln\left(\frac{V_0\epsilon^2}{3-\epsilon}t^2\right) \quad , \quad V(t) = \frac{3-\epsilon}{\epsilon^2 t^2}, \tag{3.35}$$

where a_0 is an integration constant and time runs from $(-\infty < t < 0)$. In the case where $\epsilon \gg 1$ we can use the approximation

$$\phi(t) \approx \frac{1}{\sqrt{2\epsilon}} \ln\left(-\epsilon V_0 t^2\right) = \sqrt{\frac{2}{\epsilon}} \ln\left(-\sqrt{\epsilon V_0}\, t\right) \quad , \quad V(t) \approx -\frac{1}{\epsilon t^2} = \frac{2}{c^2 t^2} \tag{3.36}$$

The universe contracts very slowly during ekpyrosis since $\epsilon > 3$ and ends in a big crunch towards $t \to 0$. The universe has to bounce from a contracting phase to an expanding phase corresponding to the universe we observe today. The bounce is a crucial and theoretically challenging phase, which will be discussed in detail in Chapter 10. The bounce usually takes place during the kinetic dominated phase, which corresponds to the time when the ekpyrotic potential is negligible. A modification of the ekpyrotic potential (3.34) allows for a transition to a kinetic phase, cf. Fig. 6.

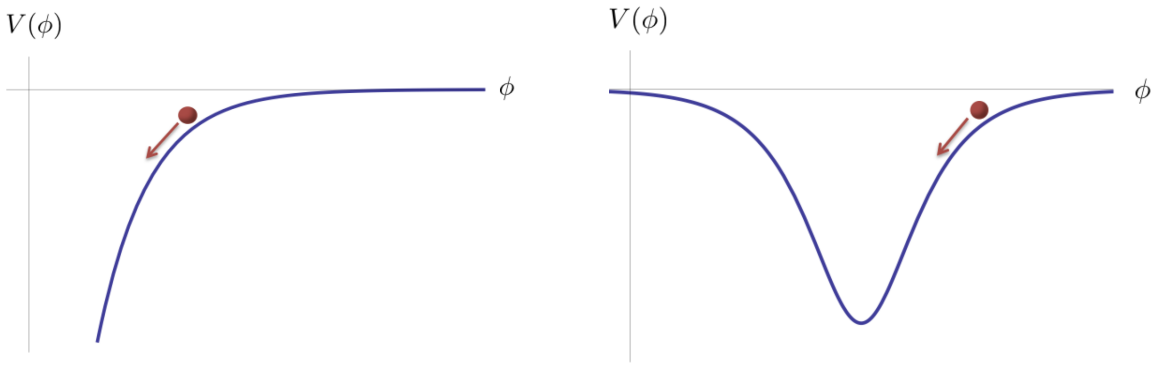

FIG. 6. *Left:* The typical ekpyrotic negative exponential potential is shown. *Right:* A modification allows for a transition from an ekpyrotic phase to a kinetically dominated phase – here we have chosen a symmetric potential. The bounce usually occurs during the kinetic phase; however, it is also possible that the bounce occurs at the bottom of the potential, cf. Chapter 11.

The ekpyrotic scaling solution is an attractor solution [52]. It is stable to conventional matter perturbations, curvature, and shear perturbations. It also means that if the initial conditions before

ekpyrosis are close to the ekpyrotic initial condition, the solution will approach the scaling solution. The fact that ekpyrosis has a global attractor solution is an important result for the robustness of ekpyrosis. We will return to the initial conditions of ekpyrosis in the context of two-field models in Chapter 5.

We have seen that during inflation $H \approx const.$ while the scale factor grows by a large amount. During ekpyrosis, the scale factor is almost constant while $|H|$ grows. The comoving Hubble radius $(aH)^{-1}$ decreases during ekpyrosis, and we will calculate now how long ekpyrosis has to last in order to solve the flatness and horizon problem. From equation (2.64) we have seen that the curvature grows by a factor of 10^{27} (up to 10^{53}) between the electro-weak (or the grand unified scale) and today – this corresponds to a growth of around e^{60} or e^{120} respectively. From $\Omega - 1 = k(aH)^{-2}$ we find that the comoving Hubble radius has to shrink by a factor of e^{30} or e^{60} during ekpyrosis. Using the fact that the scale factor is nearly constant during ekpyrosis and $H \sim t^{-1}$ leads to

$$\frac{t_{ek-beg}}{t_{ek-end}} = e^{60}. \tag{3.37}$$

As we will see in Chapter 5 C, the amplitude of the entropy perturbations, which are created during ekpyrosis, is determined by the depth of the ekpyrotic potential leading to an energy scale around the GUT scale $V_{min} = (10^{-2} M_{Pl})^2$ in order to match observations, cf. Eq. (5.32). Using the scaling solution (3.36) with $c = 15$ we obtain

$$t_{ek-end} \sim 10^3 t_{Pl}. \tag{3.38}$$

Combining (3.37) and (3.38), ekpyrosis has to last at least

$$t_{ek-beg} \geq 10^{30} t_{Pl} \approx 10^{-13} s \tag{3.39}$$

in order to solve the flatness problem.

The ekpyrotic model [14] was extended to a cyclic model in [4, 15, 16]. This model is based on an embedding in heterotic M-theory. In the braneworld picture, our visible three spatial dimensions correspond to one brane. This brane is separated by a hidden dimension across another brane. The distance between the two branes decreases due to an attractive force. When the two branes collide, a bounce occurs creating matter and radiation on the brane. The separated branes attract each other again continuing the cycle. In the effective 4-dimensional description the scalar field corresponds to the distance of the two branes and the evolution is determined by the scalar field in a potential as shown in Fig. 7. Today we are in the dark energy dominated phase, where the scalar

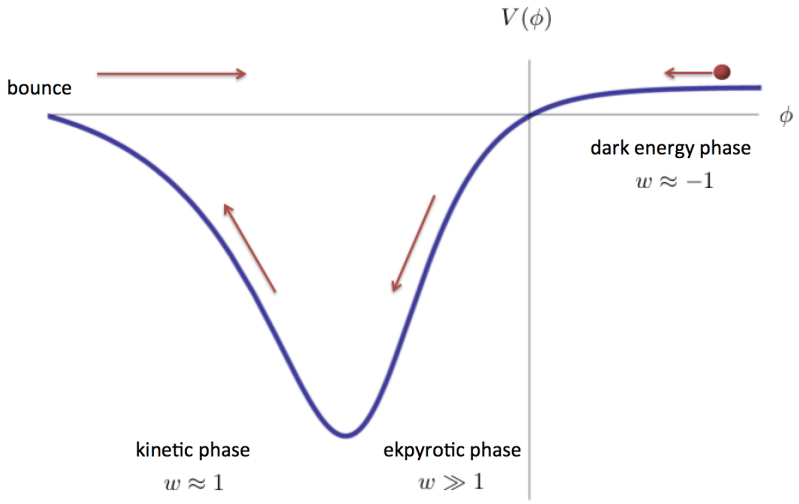

FIG. 7. Here the cyclic evolution is shown. Today we are in the dark energy phase. At some point the scalar field rolls down the steep negative potential leading to a slowly contracting ekpyrotic phase. The universe undergoes a bounce during the kinetically dominated phase leading to a hot big bang cosmology. Figure based on [4].

field ϕ nearly rests on top of the potential. Due to the attractive force between the branes, the scalar field rolls down the steep negative potential leading to a slowly contracting ekpyrotic phase. During that phase, the universe is driven towards spatial homogeneity, isotropy, and flatness. At the end of the subsequent kinetic phase, the universe undergoes a bounce creating matter and radiation leading to a hot big bang cosmology. After the bounce, the universe is kinetically dominated followed by a radiation and matter dominated phase. The scalar field jumps on top of the positive potential, which results in a dark energy phase continuing the cycle.

The cyclic ekpyrotic model incorporates a singular bounce which does not allow to track the evolution of the background and perturbations through the bounce. In this thesis, we will focus on non-singular bounces models, in which we can follow the evolution through the bounce phase, cf. Chapter 10.

4. LINEAR PERTURBATIONS

In the previous chapter, we have discussed how inflation and ekpyrosis render the universe flat, homogeneous, and isotropic. Another important success of these models is the evolution of quantum fluctuations. As we will see, these small perturbations are the seeds of the temperature fluctuations in the Cosmic Microwave Background. The nearly scale-invariant spectrum of these temperature fluctuations can be explained via the primordial evolution of the universe.

This chapter is structured as follows. First, we will review the basics of cosmological perturbation theory based on reviews in, e.g. [2, 53–55]: We will calculate the scalar and tensor degrees of freedom, introduce common gauge choices and discuss the evolution of adiabatic perturbations during ekpyrosis and inflation.

As we will see, during ekpyrosis the adiabatic fluctuations are not amplified, and thus a modification to the single scalar field model has to be made to match with observations. We will then discuss the "new ekpyrotic scenario" in Chapter 5, where an unstable direction in the potential leads to nearly scale-invariant entropy perturbations via the entropic mechanism.

A. Gauge Transformations

The action for a single scalar field minimally coupled to gravity is given by

$$S = \int d^4x\sqrt{-g}\left(\frac{R}{2} - \frac{1}{2}g^{\mu\nu}\partial_\mu\phi\partial_\nu\phi - V(\phi)\right) \tag{4.1}$$

We can split the scalar field into the homogeneous background solution $\bar{\phi}$ and the local perturbation $\delta\phi$:

$$\phi(t,\mathbf{x}) = \bar{\phi}(t) + \delta\phi(t,\mathbf{x}). \tag{4.2}$$

The metric then also reads:

$$g_{\mu\nu}(t,\mathbf{x}) = \bar{g}_{\mu\nu} + \delta g_{\mu\nu}(t,\mathbf{x}). \tag{4.3}$$

This allows us to calculate the perturbed Einstein equations for small perturbations

$$\delta G_{\mu\nu} = \delta T_{\mu\nu}. \tag{4.4}$$

The perturbed FLRW metric can be written in the following way:

$$ds^2 = -(1+2A)\,dt^2 + 2a(t)B_i dx^i dt + a^2(t)\left(\delta_{ij} + h_{ij}\right) dx^i dx^j\,. \tag{4.5}$$

We separate the perturbations into three categories: scalar, vector and tensor perturbations. We can decompose each vector into a longitudinal and a transverse part

$$B_i = B_{Li} + B_{Ti} = \partial_i B + B_{Ti}\,. \tag{4.6}$$

Since the longitudinal part is curl-free, we can express it as a gradient of a scalar field B. The transverse part is divergence free $\partial_i B_T^i = 0$. Thus there is one scalar mode B and two vector modes B_{Ti}. Similarly the symmetric tensor h_{ij} can be decomposed into

$$h_{ij} = 2\psi\delta_{ij} + 2\partial_i\partial_j E + 2_{(}\partial_i E_{j)} + E_{ij}\,, \tag{4.7}$$

where E_{ij} is traceless and transverse $E^{ij}\delta_{ij} = 0, \partial_i E^{ij} = 0$ and E_i is transverse. Thus there are two scalar modes ψ and E, two vector modes E_i and two tensor modes E_{ij}.

To summarize we have the four scalars A, B, ψ, E, the vectors B_{Ti}, E_i and two tensor modes E_{ij}.

In the following, we will see how many physical scalar and tensor degrees there are.
Let us consider a local gauge transformation:

$$x^\alpha \to \tilde{x}^\alpha = x^\alpha + \xi^\alpha\,, \tag{4.8}$$

where ξ can be decomposed into $\xi^\alpha = (\xi^0, \xi^i)$ with $\xi^i = \xi_T^i + \partial^i\xi$. So ξ and ξ^0 are scalars and $\partial_i\xi_T^i = 0$ is a divergent free 3-vector. Under such a gauge transformation we can calculate the transformation-law for scalar and tensor quantities.
For any scalar quantity we have

$$\tilde{\rho}(\tilde{x}) = \rho(x)\,, \tag{4.9}$$

thus to first order we find

$$\rho(x) \to \tilde{\rho}(\tilde{x}) = \tilde{\rho}(x-\xi) = \rho(x) - \rho(x)_{,\alpha}\xi^\alpha. \tag{4.10}$$

Using the fact that the background is homogeneous we obtain the following expression for a scalar quantity under a gauge transformation:

$$\delta\tilde{\rho}(x) = \delta\rho(x) - \xi^0\dot{\rho}. \tag{4.11}$$

For the metric we have the following transformation property to first order in ξ:

$$\tilde{g}^{\mu\nu}(\tilde{x}) = g^{\alpha\beta}(x)\left(\delta^\mu_\alpha + \frac{\partial\xi^\mu}{\partial x^\alpha}\right)\left(\delta^\nu_\beta + \frac{\partial\xi^\nu}{\partial x^\beta}\right) = g^{\mu\nu}(x) + g^{\alpha\nu}(x)\frac{\partial\xi^\mu}{\partial x^\alpha} + g^{\mu\beta}(x)\frac{\partial\xi^\nu}{\partial x^\beta}\,. \tag{4.12}$$

Together with

$$\tilde{g}^{\mu\nu}(\tilde{x}^\alpha) = g^{\mu\nu}(x^\alpha + \xi^\alpha) = g^{\mu\nu}(x^\alpha) + \xi^\rho g^{\mu\nu}(x^\alpha)_{,\rho} \tag{4.13}$$

we find the expression for a tensor quantity under a gauge transformation:

$$\tilde{g}^{\mu\nu}(x) = g^{\mu\nu}(x) - g^{\mu\nu}_{,\rho} + g^{\rho\nu}\xi^\mu_{,\rho} + g^{\mu\rho}\xi^\nu_\rho\,. \tag{4.14}$$

We can now calculate the transformation properties of the scalar quantities in the perturbed metric (4.5) using (4.11) and (4.14)

$$A \to A + \dot{\xi}_0 \tag{4.15}$$

$$B \to B + \frac{1}{a}(-\xi_0 - \dot{\xi} + 2H\xi) \tag{4.16}$$

$$\psi \to \psi + H\xi_0 \tag{4.17}$$

$$E \to E - \frac{1}{a^2}\xi \tag{4.18}$$

The tensor perturbations are left unchanged, they are gauge-invariant. The two tensor degrees of freedom correspond to primordial gravitational waves, which we will discuss at a later stage.
We can also find scalar quantities which are gauge-invariant by combining the above expressions. One well known example are the so-called Bardeen potentials:

$$\Phi = A + \frac{d}{dt}[a(B - a\dot{\psi})]\,, \tag{4.19}$$

$$\Psi = E - H(B - a\dot{\psi})\,. \tag{4.20}$$

So far we have seen, that the scalar perturbations are not necessarily gauge-invariant. In order to determine, which quantities are physical degrees of freedom one has two options. One can work with only gauge-invariant quantities (like the Bardeen potentials) or one fixes a gauge (fix ξ^0 and ξ). In the case of a single scalar field minimally coupled to gravity the perturbed Einstein equations give rise to the condition $\Phi = \Psi$ in the absence of anisotropic stress. This means that there is only one physical scalar degree of freedom.

A prominent and useful gauge is the so-called comoving gauge. In this gauge the scalar field is unperturbed. In the perturbed space-time the surfaces of constant time are also surfaces of the

constant scalar field. The scalar field acts as clock in this gauge. The comoving gauge is defined via

$$\delta\phi_{com} = 0\,. \tag{4.21}$$

Using the transformation property (4.11), the scalar field transforms under a time slicing ($t \to t + \xi^0 = t + \delta t$) as

$$\delta\phi \to \delta\phi - \dot{\phi}\delta t\,. \tag{4.22}$$

Thus we have to fix the gauge, such that

$$\delta t = \frac{\delta\phi}{\dot{\phi}}\,. \tag{4.23}$$

In this gauge the scalar field perturbations are zero, while all the scalar perturbations are only in the metric. Thats why this gauge is very convenient and we will work in this gauge most of the time. Moreover, from (4.17) we have

$$\psi \to \psi + H\delta t \tag{4.24}$$

and thus in comoving gauge

$$\psi \to \psi + H\frac{\delta\phi}{\dot{\phi}} \equiv \mathcal{R}\,. \tag{4.25}$$

This quantity is gauge invariant and in this gauge it is directly related to the fluctuation in the scale factor on constant time (or ϕ) surfaces as can be seen from the perturbed FLRW metric (4.5). Thats why it is called the comoving curvature perturbation $\mathcal{R}$. For a more general matter content it is defined as

$$\mathcal{R} \equiv \psi + \frac{2H}{\rho + p}\delta q\,, \tag{4.26}$$

where δq denotes the off-diagonal part of the perturbed energy-momentum tensor $\delta T^0_i = \partial_i \delta q$. The comoving curvature perturbation is a very important quantity – as it remains constant on super-horizon scales in the case of a single scalar field.

A closely related quantity is the curvature perturbation on uniform energy-density hypersurfaces [56]:

$$-\zeta \equiv \psi + H\frac{\delta\rho}{\dot{\rho}}\,. \tag{4.27}$$

This quantity is gauge invariant, since on constant energy-surfaces $\delta\rho = 0$ and then ζ denotes again fluctuations in the scale factor. These two quantities are related by a gauge transformation via

$$-\zeta = \mathcal{R} + \frac{2\rho}{3(\rho+p)}\left(\frac{k}{aH}\right)^2 \Psi\,. \tag{4.28}$$

On large scales ($k \to 0$), ζ and $\mathcal{R}$ coincide (up to a sign) and are used interchangeably in the literature.

In the spatially flat gauge the curvature ψ_{flat} vanishes: $\psi_{flat} = 0$. The slicing is given by

$$\psi \to \psi_{flat} = \psi + H\delta t = 0 \tag{4.29}$$

leading to the following gauge fixing

$$\delta t = -\frac{\psi}{H}\,. \tag{4.30}$$

Moreover, the scalar field transforms as

$$\delta\phi \to \delta\phi - \dot{\phi}\delta t = \delta\phi + \frac{\dot{\phi}}{H}\psi\,. \tag{4.31}$$

This is the definition of the so-called Mukhanov-Sasaki variable Q:

$$Q = \delta\phi + \frac{\dot{\phi}}{H}\psi = \frac{\dot{\phi}}{H}\mathcal{R}\,. \tag{4.32}$$

In flat gauge the scalar fluctuations are entirely in the scalar field:

$$Q_{flat} = \delta\phi\,. \tag{4.33}$$

B. ADM-Formalism

In the following, we will calculate the second order action of the scalar and tensor perturbations. It is useful to use the Arnowitt-Deser-Misner (ADM)-formalism [57], where we split the metric as follows

$$ds^2 = -N^2dt^2 + h_{ij}(dx^i + N^i dt)(dx^j + N^j dt)\,, \tag{4.34}$$

here N is the lapse function and N_i is the shift vector. h_{ij} denotes the metric on the fixed-time hypersurface and the determinant is given by $\sqrt{-g} = N\sqrt{h}$. Let us plug this metric into the action of a single scalar field (this can be generalized for more complicated actions):

$$S = \int dx^4\sqrt{-g}\left[\frac{1}{2}R - \frac{1}{2}g^{\mu\nu}\partial_\mu\phi\partial_\nu\phi - V(\phi)\right]\,. \tag{4.35}$$

The Ricci scalar R in 4 dimensions is related to the 3-dimensional Ricci scalar $R^{(3)}$ via the contracted Cadazzi equation:

$$R = R^{(3)} + K^{ij}K_{ij} - K^2, \tag{4.36}$$

where K_{ij} is the extrinsic curvature. The rescaled extrinsic curvature

$$E_{ij} = NK_{ij} \tag{4.37}$$

is given by

$$E_{ij} = \frac{1}{2}\dot{h}_{ij} - \nabla_i N_j - \nabla_j N_i = \frac{1}{2}\dot{h}_{ij} - 2\nabla_{(i}N_{j)}\,. \tag{4.38}$$

Plugging (4.34) and (4.36) into the action (4.35) leads to:

$$S = \frac{1}{2}\int \mathrm{d}^4x\sqrt{h}N(R^{(3)} + h^{ij}\partial_i\phi\partial_j\phi - 2V) + \frac{1}{2}\int \mathrm{d}^4x\sqrt{h}N^{-1}(E_{ij}E^{ij} - E^2 + (\dot{\phi} - N^i\partial_i\phi)^2)\,. \tag{4.39}$$

In the following, we chose the comoving gauge, where $\delta\phi = 0$ and the scalar fluctuation are entirely in the metric described by the comoving curvature perturbation $\mathcal{R}$:

$$h_{ij} = a^2\left[(1 + 2\mathcal{R})\delta_{ij} + \gamma_{ij}\right], \tag{4.40}$$

where γ_{ij} denotes the tensor perturbations, which will be discussed later. Varying the action with respect to N and N_i yields the following constraint equations:

$$\frac{\delta\mathcal{L}}{\delta N} = R^{(3)} - N^{-2}(E_{ij}E^{ij} - E^2) - N^{-2}\dot{\phi}^2 - 2V = 0\,, \tag{4.41}$$

$$\frac{\delta\mathcal{L}}{\delta N_i} = \nabla_i[N^{-1}(E^i_j - \delta^i_j E)] = 0\,. \tag{4.42}$$

The solution to first order are given by

$$N = 1 + \frac{\dot{\mathcal{R}}}{H}\,, \tag{4.43}$$

$$N_i = \frac{1}{H}\partial_i\mathcal{R} + a^2\frac{\dot{\phi}^2}{2H^2}\partial_i\left((\partial_j\partial^j)^{-1}\dot{\mathcal{R}}\right)\,, \tag{4.44}$$

where ∂^{-2} is defined such that $\partial^{-2}\partial^2\mathcal{R} = \mathcal{R}$. We can now plug the solutions (4.43) and (4.44) into the action (4.39). Moreover, we use (4.38) and (4.40) to rewrite everything in terms of the comoving curvature perturbation $\mathcal{R}$.

This leads to a lengthy expression, which can be expanded in powers of $\mathcal{R}$. Schematically the action can be written as

$$S = \int \mathrm{d}^4x\mathcal{L}[\mathcal{R}(x)] = \int \mathrm{d}^4x\left(\mathcal{L}_0 + \mathcal{L}^{(2)}[\mathcal{R}(x)] + \mathcal{L}^{(3)}[\mathcal{R}(x)] + ...\right)\,, \tag{4.45}$$

where the zeroth order $\mathcal{L}_0$ is the background action, $\mathcal{L}^{(2)}$ describes the free propagation of the scalar perturbations and $\mathcal{L}^{(3)}$ describes the self-interaction of the scalar perturbations. A non-zero $\mathcal{L}^{(3)}$ corresponds to non-Gaussian corrections. Non-Gaussianities are an important feature to distinguish different models of the early universe and it is the central theme of this thesis.
For now we are interested in the linear perturbations and thus we will only consider the second order action $\mathcal{L}^{(2)}$.

C. Evolution of Curvature Perturbations for a Single Scalar Field

In the following, we will calculate the behavior of scalar and tensor fluctuations during inflation and ekpyrosis. This is a well established treatment developed by [56, 58–62] in the context of inflation and by [17, 18] in the ekpyrotic case. Most of the results will refer to the above citations within this chapter.
We expand the action up to second order in perturbations and after many integrations by parts we end up with the following action:

$$S^{(2)} = -\int \mathrm{d}^4x\sqrt{-g}\epsilon g^{\mu\nu}\partial_\mu\mathcal{R}\partial_\nu\mathcal{R} = \int \mathrm{d}^3x\mathrm{d}t\epsilon[a^3\dot{\mathcal{R}}^2 - a(\partial_i\mathcal{R})^2]\,, \tag{4.46}$$

where $\epsilon = \frac{\dot{\phi}^2}{2H^2}$. We introduce the so-called Mukhanov-Sasaki variable

$$v = z\mathcal{R} \quad \text{with} \quad z^2 = 2a^2\epsilon\,, \tag{4.47}$$

which allows us to canonically normalize the action. Switching to conformal time leads to

$$S^{(2)} = \frac{1}{2}\int \mathrm{d}^3x\mathrm{d}\tau\left[(v')^2 - (\partial_i v)^2 + \frac{z''}{z}v^2\right]\,, \tag{4.48}$$

where a prime $'$ denotes a derivative w.r.t. conformal time $d\tau = dt/a$. We expand the perturbations into Fourier modes

$$v(\tau,\mathbf{x}) = \int \frac{\mathrm{d}^3k}{(2\pi)^3}v_{\mathbf{k}}(\tau)e^{i\mathbf{kx}}\,. \tag{4.49}$$

The equation of motion is also known as Mukhanov-Sasaki equation:

$$v_{\mathbf{k}}'' + \left(k^2 - \frac{z''}{z}\right)v_{\mathbf{k}} = 0\,. \tag{4.50}$$

Each mode with momentum $\mathbf{k}$ evolves independently – in other words there is no mixing of modes at the linear level. Equation (4.50) is the equation of motion of an harmonic oscillator with a time-dependent mass $m^2 = (k^2 - z''/z)$. The second term is due to the presence of gravity and

it will have important consequences for the evolution of the quantum fluctuations in the early universe. We will encounter (4.50) and variations of this equations various times in this thesis. We will review the standard treatment in dealing with this equation in the following.

D. Quantization

We quantize the field by promoting the mode functions to operators

$$\hat{v}_{\mathbf{k}}(\tau) = v_k(\tau)\hat{a}_{\mathbf{k}} + v_k(\tau)^* \hat{a}^\dagger_{-\mathbf{k}}, \tag{4.51}$$

where $v(\tau)$ are the complex solutions to equation (4.50) and $\hat{a}^\dagger_{-\mathbf{k}}$ and $\hat{a}_{\mathbf{k}}$ are the creation and annihilation operators satisfying

$$[\hat{a}_{\mathbf{k}}, \hat{a}^\dagger_{-\mathbf{k}'}] = (2\pi)^2 \delta(\mathbf{k} - \mathbf{k}'). \tag{4.52}$$

The field operator and its conjugate momentum $\hat{\pi} = \hat{v}'$ satisfy the usual equal time commutator relation

$$[\hat{v}(\tau, \mathbf{x}), \hat{\pi}(\tau, \mathbf{y})] = i\delta(\mathbf{x} - \mathbf{y}), \tag{4.53}$$

while

$$[\hat{v}(\tau, \mathbf{x}), \hat{v}(\tau, \mathbf{y})] = [\hat{\pi}(\tau, \mathbf{x}), \hat{\pi}(\tau, \mathbf{y})] = 0. \tag{4.54}$$

The Wronskian is a constant of motion

$$W[v_k, v_k] \equiv v_k^* v_k' - v_k^{*\prime} v_k = i\,, \tag{4.55}$$

where the r.h.s has to be chosen such that (4.52) is satisfied. In other words, the Wronskian normalizes the mode function acting as a boundary condition for the modes. We chose the vacuum state for the fluctuations

$$a_{\mathbf{k}} \left|0\right\rangle = 0\,, \tag{4.56}$$

which corresponds to the second boundary condition of the modes. The standard choice is the so-called Bunch-Davies vacuum, where the modes satisfy

$$\lim_{|k\tau|\to\infty} v_k = \frac{1}{\sqrt{2k}} e^{-ik\tau}\,. \tag{4.57}$$

The modes on small scales or/and very early times correspond to the Minkowski vacuum with positive frequency solution. The very small scale modes do not "feel" the curvature and thus

behave like in Minkowski space. We can immediatly see that (4.57) is a solution of (4.50) if $z''/z \ll k^2$.

Moreover, the time-dependent mass term can lead to an instability. For example in the case of the de Sitter limit during inflation we had $a(\tau) = -(H\tau)^{-1}$, see (3.24), obtaining

$$\frac{z''}{z} = \frac{2}{\tau^2}\,. \tag{4.58}$$

In this case, the Mukhanov-Sasaki equation reads

$$v_k'' + \left(k^2 - \frac{2}{\tau^2}\right) v_k = 0\,. \tag{4.59}$$

The negative sign leads to an instability and consequently to an amplification of the mode function with solution

$$v_k = \frac{1}{\sqrt{2k}} e^{-ik\tau} \left(1 - \frac{i}{k\tau}\right)\,, \tag{4.60}$$

where we have used the Bunch-Davies vacuum as initial condition. In the late time/large scale limit $|k\tau| \to 0$ we obtain

$$\lim_{|k\tau|\to 0} v_k \sim \tau^{-1}\,. \tag{4.61}$$

The modes v_k grow during inflation and leave the horizon at $k = aH$. Let us investigate the behavior of the (physical) modes – the comoving curvature perturbation $\mathcal{R}_k$. We should note that the de Sitter limit is actually ill-defined here. Taking the limit $\epsilon \to 0$ corresponds to $z \to 0$, which is defined via $z^2 = 2a^2\epsilon$ as the prefactor in the second order action (4.46). In the next chapter we will calculate the evolution in a more general setting and will use the so-called quasi de Sitter limit in the inflationary case. Using $a(\tau) = -(H\tau)^{-1}$ we obtain

$$z = -\frac{\sqrt{2\epsilon}}{\tau H}\,. \tag{4.62}$$

Thus the comoving curvature perturbation $\mathcal{R}_k = v_k/z$ in the de Sitter limit is given by

$$\mathcal{R}_k = \frac{iH}{\sqrt{4k^3\epsilon}} e^{-ik\tau} \left(1 + ik\tau\right)\,. \tag{4.63}$$

The comoving curvature perturbation becomes constant on large scales:

$$\lim_{|k\tau|\to 0} \mathcal{R}_k = const. \tag{4.64}$$

This is an important result. The comoving curvature perturbations grow and become super-horizon. After horizon exit the perturbations freeze – they become constant. We will denote the

moment of horizon crossing via the subscript $_*$. We will now introduce important quantities to describe the perturbations and make contact with observations.

The two-point correlation function reads:

$$\begin{aligned}\langle \hat{v}_{\mathbf{k}}, \hat{v}_{\mathbf{k}'} \rangle &= \langle 0 | \hat{v}_{\mathbf{k}}, \hat{v}_{\mathbf{k}'} | 0 \rangle \\ &= v_k v^*_{k'} \langle 0 | [\hat{a}_{\mathbf{k}}, \hat{a}^\dagger_{-\mathbf{k}'}] | 0 \rangle \\ &= (2\pi)^3 |v_k|^2 \delta(\vec{k} + \vec{k}') \\ &\equiv (2\pi)^3 P_v(k) \delta(\vec{k} + \vec{k}') \,,\end{aligned} \tag{4.65}$$

where we have used the general solution (4.51) and the commutation relation (4.52) of the creation and annihilation operators. $P_v(k)$ is the power spectrum, which we introduced in (2.46) in the context of the temperature fluctuations in Cosmic Microwave Background. Equivalently, in terms of the comoving curvature perturbation $\mathcal{R}$ we obtain

$$\begin{aligned}\langle \hat{\mathcal{R}}_{\mathbf{k}}, \hat{\mathcal{R}}_{\mathbf{k}'} \rangle &= (2\pi)^3 |\mathcal{R}_k|^2 \delta(\mathbf{k} + \mathbf{k}') \\ &\equiv (2\pi)^3 P_{\mathcal{R}}(k) \delta(\mathbf{k} + \mathbf{k}') \,.\end{aligned} \tag{4.66}$$

The variance $\Delta^2_{\mathcal{R}}$ is given by

$$\Delta^2_{\mathcal{R}} = \frac{k^3}{2\pi^2} P_{\mathcal{R}} \tag{4.67}$$

and the spectral index reads:

$$n_s - 1 \equiv \frac{d \ln \Delta^2_{\mathcal{R}}}{d \ln k}. \tag{4.68}$$

It is useful to write the variance in a power-law form

$$\Delta^2_{\mathcal{R}} = A_{\mathcal{R}} \left(\frac{k}{\tilde{k}} \right)^{n_s - 1} , \tag{4.69}$$

where $\tilde{k}$ is a reference scale also called pivot scale and $A_{\mathcal{R}}$ is the amplitude. Note that $n_s = 1$ leads to a scale-invariant spectrum, while $n_s < 1$ corresponds to a red spectrum and $n_s > 1$ to a blue spectrum.

Using (4.63) the power spectrum of the comoving curvature perturbation $\mathcal{R}$ in the de Sitter limit reads:

$$P_{\mathcal{R}} = \frac{H^2_*}{4k^3 \epsilon} \,, \tag{4.70}$$

while the variance is given by

$$\Delta^2_{\mathcal{R}} = \frac{H_*^2}{8\pi^2\epsilon} \tag{4.71}$$

leading to a perfect scale-invariant spectrum $n_s = 1$. Note that in the literature one often uses the terminology power spectrum instead of the variance $\Delta^2_{\mathcal{R}}$ – in this case $\tilde{P}_{\mathcal{R}}$ is in fact the rescaled power spectrum corresponding to the variance. During inflation in the de Sitter limit, the curvature perturbations $\mathcal{R}$ become amplified and super-horizon with a scale-invariant spectrum. The amplitude depends on the ratio of the squared Hubble parameter at horizon crossing and the slow-roll parameter ϵ. The de Sitter limit $\epsilon \to 0$ corresponds to a perfectly flat potential, which means that inflation would never end. As we will see in a more realistic inflationary scenario, where ϵ is small but non-zero, the comoving curvature perturbations obtain a nearly scale-invariant spectrum, since modes exit the horizon at different times.

E. General solutions

Let us solve the equation of motion in a more general setting. Depending on the background dynamics the term z''/z can be complicated, such that there only exist approximate analytic (or numerical) solutions. However, we can find analytic solutions, if we can rewrite (4.50) in the following form

$$v_k + \left[k^2 + \frac{1}{\tau^2}\left(\frac{1}{4} - \nu^2\right)\right] v_k = 0, \tag{4.72}$$

which is a Bessel equation and the general solution is given in terms of Hankel functions

$$v_k(\tau) = \sqrt{-k\tau}\left(\alpha_k H_\nu^{(1)}(-k\tau) + \beta_k H_\nu^{(2)}(-k\tau)\right), \tag{4.73}$$

where ν is the Hankel index, which is constant (or approximately constant) and given by:

$$\nu = \sqrt{\frac{z''}{z}\tau^2 + \frac{1}{4}}\,. \tag{4.74}$$

The Hankel functions are given in terms of Bessel functions

$$H_\nu^{(1,2)}(x) = J_\nu(x) \pm iY_\nu(x). \tag{4.75}$$

To leading order the Hankel functions have the following asymptotic behavior for large arguments ($x \to \infty$), corresponding to early times/small scales:

$$H^{(1,2)}(x) = \sqrt{\frac{2}{\pi x}} \exp\left(\pm i(x - \frac{\nu x}{2} - \frac{\pi}{4})\right), \tag{4.76}$$

while for small arguments ($x \to 0$), corresponding to late times/large scales we find

$$H^{(1,2)}(x) = \mp \frac{i}{\pi}\Gamma(\nu)\left(\frac{x}{2}\right)^{-\nu} . \tag{4.77}$$

At early times $\tau \to -\infty$, the modes are deep inside the horizon and the Bunch-Davies solution is given by:

$$v_k = \frac{1}{\sqrt{2k}} e^{-k\tau} . \tag{4.78}$$

Comparing this solution to the large argument behavior (corresponding to early times/small scales) of the Hankel function fixes the two constants in equation (4.73)

$$\alpha_k = \sqrt{\frac{\pi}{4k}} e^{i\pi(2\nu+1)/4} \quad , \quad \beta_k = 0 \tag{4.79}$$

yielding the following solution in terms of the Hankel function of the first kind:

$$v_k = \sqrt{\frac{\pi}{4}}\sqrt{-\tau} H_\nu^{(1)}(-k\tau) , \tag{4.80}$$

where we have neglected the unimportant phase factor. This is an important expression and we will use it numerous times in this thesis.

Now we can use the small argument behavior of the Hankel function $H_\nu^{(1)}$ to find the late time/large scale $|k\tau| \to 0$ solution of the modes:

$$v_k = \frac{2^\nu \Gamma(\nu)}{\sqrt{4\pi k}} (-k\tau)^{-\nu+\frac{1}{2}} , \tag{4.81}$$

which corresponds to the following scale-dependence in terms of ν

$$v_k \sim k^{-\nu} . \tag{4.82}$$

The comoving curvature perturbation is related to the canonically normalized Mukhanov-Sasaki variable via $\mathcal{R} = v/z$. Depending on the background dynamics parametrized by z (and ν) we can determine the power spectrum, the time dependence and scale dependence of the comoving curvature perturbation $\mathcal{R}$.

From (4.81) we obtain the following scale-dependence of the comoving curvature perturbations in the large scale limit:

$$\mathcal{R}_k \sim k^{-\nu} . \tag{4.83}$$

The variance, cf. Eq. (4.67), is thus given by

$$\Delta^2_{\mathcal{R}} \sim k^{-2\nu+3} \tag{4.84}$$

and the spectral index, cf Eq. (4.68), reads:

$$n_s - 1 = 3 - 2\nu\,. \tag{4.85}$$

Let us summarize the results of this chapter: The solution of the Mukhanov-Sasaki equation (4.72) is given in terms of the Hankel function of the first kind

$$v_k = \sqrt{\frac{\pi}{4}}\sqrt{-\tau}H_\nu^{(1)}(-k\tau)\,, \tag{4.86}$$

where the Hankel index ν reads

$$\nu = \sqrt{\frac{z''}{z}\tau^2 + \frac{1}{4}}\,, \tag{4.87}$$

which determines the large scale limit of the modes

$$v_k = \frac{2^\nu \Gamma(\nu)}{\sqrt{4\pi k}}\,(-k\tau)^{-\nu+\frac{1}{2}} \tag{4.88}$$

leading to a spectral index of the comoving curvature perturbations $\mathcal{R}$

$$n_s - 1 = 3 - 2\nu\,. \tag{4.89}$$

1. *Adiabatic Scalar Perturbations during Inflation*

In the following, we want to calculate the behavior of the curvature perturbations $\mathcal{R}$ during inflation in the slow-roll approximation $\epsilon \ll 1$, which we have discussed in (3 A).

We can expand $z = a\sqrt{2\epsilon}$ in terms of the slow-roll parameters ϵ and η to first order yielding

$$\frac{z''}{z} \approx a^2H^2\left(2 - \epsilon + \frac{3}{2}\eta\right)\,. \tag{4.90}$$

Using

$$aH \approx -\frac{1}{\tau}(1+\epsilon)\,, \tag{4.91}$$

which we have obtained in equation (3.24), the Hankel index ν in the slow-roll approximation to first order in slow-roll parameters reads

$$\nu = \sqrt{\frac{z''}{z}\tau^2 + \frac{1}{4}} \approx \frac{3}{2} + \epsilon + \frac{\eta}{2}\,. \tag{4.92}$$

Using the large scale limit

$$v_k = \frac{2^\nu \Gamma(\nu)}{\sqrt{4\pi k}}\,(-k\tau)^{-\nu+\frac{1}{2}} \tag{4.93}$$

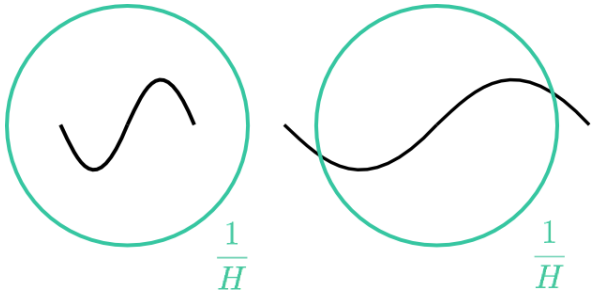

FIG. 8. During inflation the Hubble radius H^{-1} is nearly constant. The physical wavelength $\lambda_{phys} = a\lambda$ becomes super-horizon due to the accelerated expansion. The horizon crossing happens at $k = aH$ and the comoving curvature perturbation $\mathcal{R}$ becomes constant.

we obtain the spectral index of the comoving curvature perturbations $\mathcal{R}$

$$n_s - 1 = -2\epsilon - \eta\,. \tag{4.94}$$

The Planck team measured the spectral index $n_s = 0.9677 \pm 0.0060$ corresponding to a red tilt [44]. This fact constraints the value of η: small field models with convex potentials belong to the class of models characterized by a negative η, which makes the spectrum blue while the first term in Eq. (4.94) makes the spectrum red. In the next chapter we will calculate the evolution of tensor perturbations (primordial gravitational waves) during inflation. The combination of the spectral index n_s and the tensor-to-scalar ratio r allows for a comparison of inflationary models with observations, which will be covered in Chapter 7.

Let us summarize the behavior of the scalar fluctuations during inflation: On small scales the modes oscillate like in Minkowski space. At some point the modes become amplified due to the negative mass term. Moreover, the comoving curvature perturbation $\mathcal{R}$ becomes constant on very large scales – the modes freeze outside the horizon. The physical wavelength $\lambda_{phys} = a/k$ grows, while the physical horizon is nearly constant given by $1/H$ – this behavior is shown in Fig 8. In other words the horizon exit is given by $|k\tau| = 1$ or equivalently $k = aH$. The moment of horizon crossing is denoted by $k_* = a_* H_*$.

2. Tensor Perturbations during Inflation

Now we consider the evolution of tensor perturbations (gravitational waves) during inflation. At linear order the scalar and tensor perturbations evolve independently. Using the ADM-decomposition, we obtain the second order action of the tensor perturbations analogous to the scalar perturbations. The resulting second order action is given by

$$S^{(2)} = -\frac{1}{8}\int \mathrm{d}^4x\sqrt{-g}g^{\mu\nu}\partial_\mu\gamma_{ij}\partial_\nu\gamma_{ij}\,. \tag{4.95}$$

The tensor perturbation has two components denoted by $\lambda = (+,\times)$. Going to Fourier space we have the following decomposition

$$\gamma_{ij}(\vec{k}) = \sum_\lambda \left[\hat{a}(\vec{k},\lambda)u_k + \hat{a}^\dagger(-\vec{k},\lambda)u_k^*\right] e_{ij}(\vec{k},\lambda)/a\,, \tag{4.96}$$

where $e_{ij}(\vec{k},\lambda)$ is the polarization tensor and u_k is the canonically normalized variable given by $u_k = \frac{a}{2}\gamma_k$. The variation of the action w.r.t. u_k yields the mode equation:

$$u_{\mathbf{k}}'' + \left(k^2 - \frac{a''}{a}\right)u_{\mathbf{k}} = 0\,. \tag{4.97}$$

Note that in the case of $\epsilon = const.$, this equation of motion is exactly the same as the equation of motion of the scalar modes (4.50), since $z''/z = a''/a$ for $\epsilon = const.$ This means that the spectrum of the adiabatic scalar fluctuations and the tensor fluctuations are the same.
We can thus adopt the previous calculations. We quantize the field

$$\hat{u}_{\mathbf{k}} = u_k(\tau)\hat{a}_{\mathbf{k}} + u_k^*(\tau)a^\dagger_{-\mathbf{k}} \tag{4.98}$$

using the quantization condition

$$[\hat{a}_{\mathbf{k}}, \hat{a}^\dagger_{-\mathbf{k}'}] = (2\pi)^2\delta(\mathbf{k}-\mathbf{k}')\,, \tag{4.99}$$

as well as the Wronskian

$$W[u_k, u_k] \equiv u_k^* u_k' - u_k^{*\prime}u_k = i\,, \tag{4.100}$$

The equation of motion in the de Sitter limit reads

$$u_k'' + \left(k^2 - \frac{2}{\tau^2}\right)u_k = 0\,, \tag{4.101}$$

leading to the solution

$$u_k = \frac{1}{\sqrt{2k}}e^{-ik\tau}\left(1 - \frac{i}{k\tau}\right)\,. \tag{4.102}$$

At late times we obtain

$$\lim_{|k\tau|\to 0} u_k = -\frac{1}{\sqrt{2k}}\frac{i}{k\tau}\,. \tag{4.103}$$

Using $u_k = \frac{a}{2}\gamma_k$ with $a = -(H\tau)^{-1}$ and defining the power spectrum as the sum of the power spectra of both polarizations leads to

$$P_T = 2\,|\gamma_k|^2 = 2\left|\frac{2u_k}{a}\right|^2 = \frac{4H_*^2}{k^3}\,, \tag{4.104}$$

while the variance is given by

$$\Delta_T^2 = \frac{k^3}{2\pi^2}P_T = \frac{2H_*^2}{\pi^2} \equiv A_T\left(\frac{k}{k_*}\right)^{n_T}\,. \tag{4.105}$$

Note that a scale-invariant spectrum of the tensor perturbations corresponds to $n_T = 0$ by definition, while in the case of the scalar spectral index $n_s = 1$ corresponds to a scale-invariant spectrum. In the de Sitter limit, the tensor perturbations have a scale-invariant spectrum. Also, note that the tensor amplitude depends only on the Hubble parameter H and not on ϵ. This is in contrast to the scalar field amplitude in Eq. (4.71). Let us define the tensor-to-scalar ratio

$$r = \frac{\Delta_T^2}{\Delta_{\mathcal{R}}^2} = 16\epsilon, \tag{4.106}$$

where we have used (4.71) and (4.105). In 2014 the BICEP2 team [63] announced a measurement of primordial gravitational waves. However, it turned out that dust foregrounds were subtracted incorrectly. Until today primordial gravitational waves have not been detected and the current bound on the tensor-to-scalar ratio is given by $r < 0.11$ [44]. A variety of inflationary models are in tension with a small tensor-to-scalar ratio r and we will discuss the challenges of inflationary and ekpyrotic models in Chapter 7.

F. Adiabatic Scalar Perturbations and Tensor Perturbations during Ekpyrosis

Let us investigate the behavior of adiabatic fluctuation during ekpyrosis. In the previous chapter we have calculated the behavior of adiabatic/curvature perturbations in the case of a single scalar field minimally coupled to gravity. We have reviewed the quantization procedure, the Mukhanov-Sasaki equation and its general solutions, and finally we have calculated the power-spectrum and the spectral index.

We can thus easily determine the behavior of curvature and tensor perturbations during ekpyrosis. The background scaling solution (3.35) in a steep negative potential is given by

$$a(t) = \tilde{a}_0 (t)^{1/\epsilon} \,, \tag{4.107}$$

where $\tilde{a}_0$ is a constant. Using $d\tau = dt/a$ we find

$$\tau = -\frac{\epsilon}{1-\epsilon} t^{-(1-\epsilon)/\epsilon} \,, \tag{4.108}$$

and thus we can write the scale factor in terms of conformal time

$$a(\tau) = a_0 (-\tau)^{1/(1-\epsilon)} \,. \tag{4.109}$$

Keeping in mind the definition $z^2 = 2a^2\epsilon$ we see that

$$\frac{z''}{z} = \frac{a''}{a} = \frac{2-\epsilon}{(1-\epsilon)^2}\frac{1}{\tau^2} \quad \text{for } \epsilon = const. \tag{4.110}$$

This leads to the following mode equation (4.50):

$$v_k'' + \left(k^2 - \frac{2-\epsilon}{(1-\epsilon)^2}\frac{1}{\tau^2} \right) v_k = 0 \,, \tag{4.111}$$

where τ runs from large negative values towards zero and $\epsilon > 3$ is the equation of state, which is constant during ekpyrosis. We have already discussed this equation of motion in Chapter 4 D. Assuming that at small scales the modes behave like in Minkowski space, corresponding to the Bunch-Davies vacuum, the solution is given in terms of the Hankel function of the first kind up to a phase (4.80)

$$v_k = \sqrt{\frac{\pi}{4}} \sqrt{-\tau} H_\nu^{(1)}(-k\tau) \,, \tag{4.112}$$

with the Hankel index (4.87)

$$\nu = \frac{1}{2}\frac{3-\epsilon}{(1-\epsilon)} \,. \tag{4.113}$$

Since $\epsilon > 3$ the Hankel index $0 < \nu < 1/2$ and thus the spectral index

$$n_s - 1 = 3 - 2\nu = 2 - \frac{\epsilon - 3}{\epsilon - 1} \tag{4.114}$$

is highly blue, $3 < n_s < 4$. The adiabatic/curvature perturbations during ekpyrosis have a highly blue spectrum [17, 18] and cannot act as the seeds of the structure formation. Moreover, the adiabatic fluctuations stay quantum: there is no quantum to classical transition in contrast to the inflationary case [19]. This is an important difference between inflation and ekpyrosis and the motivation for the model of conflation, which we will discuss in Chapter 13.

Moreover, the tensor perturbations also have a blue spectrum and stay quantum, since the equations of motion are the same for scalar and tensor fluctuations in the case of a single scalar field minimally coupled to gravity with a constant equation of state, cf. Chapter 4 E 2. From Eq. (4.111)

$$u_k'' + \left(k^2 - \frac{2-\epsilon}{(1-\epsilon)^2}\frac{1}{\tau^2}\right) u_k = 0 \tag{4.115}$$

we immediately find the tensor spectral index

$$n_T = 3 - 2\nu = 3 - \frac{\epsilon - 3}{\epsilon - 1} = -\frac{2\epsilon}{1-\epsilon}\,, \tag{4.116}$$

which is highly blue. During ekpyrosis, there is no amplification of tensor modes, and consequently, the tensor-to-scalar ratio is zero. Note, that at second order in perturbations the tensor and scalar curvature fluctuations interact, which can lead to a non-zero tensor-to-scalar ratio [64]. However, this effect is small and does not change the fact that ekpyrotic models predict an absence of primordial gravitational waves. It is possible that gravitational waves could have been produced at another stage, but until now such models have not been investigated.

This is an important distinction between inflationary and ekpyrotic models. Typically, inflationary models predict a sizable scalar-to-tensor ratio – depending on the energy scale of inflation – while ekpyrotic models predict no primordial gravitational waves. Consequently, a measurement of primordial gravitational waves would rule out the current ekpyrotic models.

In order to create nearly scale-invariant adiabatic perturbations in an ekpyrotic scenario, we have to modify the single-scalar field ekpyrotic model introduced in Chapter 3 B.

5. EKPYROSIS AS A TWO-FIELD-MODEL: THE NEW EKPYROTIC SCENARIO

In the previous chapter, we have investigated the behavior of adiabatic perturbations during ekpyrosis. In contrast to inflation, the adiabatic quantum fluctuations during ekpyrosis have a deep blue spectrum and stay quantum – the fluctuations do not become amplified and squeezed. In order to obtain large scale curvature perturbations, which become the seeds of structure formation, one has to modify the ekpyrotic model described in Chapter 3 B. In the "new ekpyrotic scenario" [20] a second scalar field is introduced.

We will see in the following that the scalar perturbations perpendicular to the background evolution (in field space) – in the so-called entropy direction – obtain a nearly scale-invariant spectrum due to the presence of an unstable transverse direction in the potential. This process is called entropic mechanism, and we will discuss the evolution of entropy perturbations in Chapter 5 C. These entropy perturbations have to be converted into curvature perturbations. We will give a brief introduction to the conversion process at the end of this chapter and discuss the conversion in detail in Chapter 6 E and Chapter 11 C.

A. Background

Let us consider the following two-field model

$$S = \int \mathrm{d}^4x\sqrt{-g}\left[\frac{R}{2} - \frac{1}{2}g^{\mu\nu}\partial_\mu\phi_1\partial_\mu\phi_1 - \frac{1}{2}g^{\mu\nu}\partial_\mu\phi_2\partial_\mu\phi_2 - V(\phi_1,\phi_2)\right], \tag{5.1}$$

where both fields have a steep negative potential of the form

$$V(\phi_1,\phi_2) = -V_1e^{-c_1\phi_1} - V_2e^{-c_2\phi_2}, \tag{5.2}$$

where $c_1(\phi_1)$ and $c_2(\phi_2)$ are usually set to be constant, if not stated otherwise. This model is called the new ekpyrotic scenario [20]. We will perform a field redefinition such that the adiabatic field σ represents the path along the background trajectory:

$$\dot\sigma^2 = \dot\phi_1^2 + \dot\phi_2^2. \tag{5.3}$$

Introducing an angle θ between the background trajectory and ϕ_1 we obtain

$$\dot\sigma = \dot\phi_1\cos\theta + \dot\phi_2\sin\theta, \tag{5.4}$$

where

$$\cos\theta = \frac{\dot\phi_1}{\dot\sigma} = \frac{\dot\phi_1}{\sqrt{\dot\phi_1^2+\dot\phi_2^2}} \quad , \quad \sin\theta = \frac{\dot\phi_2}{\dot\sigma} = \frac{\dot\phi_2}{\sqrt{\dot\phi_1^2+\dot\phi_2^2}}. \tag{5.5}$$

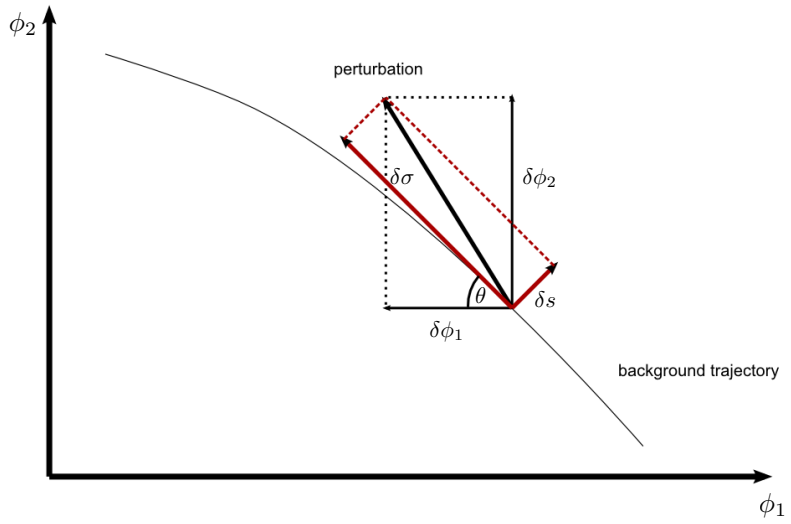

FIG. 9. The adiabatic perturbations $\delta\sigma$ perturb the background along the background trajectory, while entropy perturbations δs perturb the transverse direction of the background trajectory. Figure based on [5].

In Fig 9 we have drawn a general field space trajectory. The adiabatic field σ evolves along the background trajectory while there is (per definition) no evolution in the perpendicular direction of the adiabatic field. Only the perturbations in the transverse direction will evolve – these are the so-called entropy perturbations δs.

The adiabatic field σ in terms of ϕ_1 and ϕ_2 is given by

$$\sigma = \frac{\dot{\phi}_1\phi_1 + \dot{\phi}_2\phi_2}{\dot{\sigma}}\,. \tag{5.6}$$

We can easily define the adiabatic and entropy perturbations cf. Fig 9

$$\delta\sigma = \delta\phi_1\cos\theta + \delta\phi_2\sin\theta\,, \tag{5.7}$$

$$\delta s = \delta\phi_1\sin\theta + \delta\phi_2\cos\theta\,. \tag{5.8}$$

The adiabatic field is not gauge invariant, as we have already seen in the single scalar field case. However, it is related to the comoving curvature perturbation $\mathcal{R}$ via:

$$\mathcal{R} = \psi + \frac{H}{\dot{\phi}}\delta\sigma\,. \tag{5.9}$$

Note that we can chose the comoving gauge where $\delta\sigma = 0$ and the scalar degree of freedom is the comoving curvature perturbation $\mathcal{R}$. Moreover, in flat gauge $\psi = 0$ and we obtain $\mathcal{R} = \frac{H}{\dot{\phi}}\delta\sigma$.

Let us first consider the background solution. The ekpyrotic two-field potential (5.2) can be expressed in the new variables in the following way:

$$V(\sigma, s) = -V_0 e^{-\sqrt{2\epsilon}\sigma}\left(1 + \frac{1}{2}\epsilon s^2 + \frac{\kappa_3}{3!}\epsilon^{3/2}s^3 + ...\right), \tag{5.10}$$

where the parameter κ_3 is given by

$$\kappa_3 = 2\sqrt{2}\frac{c_1^2 - c_2^2}{|c_1 c_2|}, \tag{5.11}$$

which vanishes for a symmetric potential with $c_1 = c_2$. The ekpyrotic scaling solution in the two-field case reads:

$$\sigma = -\sqrt{\frac{2}{\epsilon}}\ln\left(\sqrt{V_0\epsilon}t\right) \quad , \quad a \sim (-t)^{1/\epsilon} \quad , \quad s = 0 \quad , \quad \theta = const. \tag{5.12}$$

where we have assumed that $\epsilon = \frac{c_1^2}{2} + \frac{c_2^2}{2}$ is large, cf. Chapter 3 B. The field rolls along the ridge of the potential with the same scaling solution as in single scalar field case; s is strictly speaking not a field, since $s = 0$, by definition, along the background trajectory – s denotes the transverse direction, which is also often denoted as χ. However, there is an unstable direction perpendicular to the background direction. The presence of this tachyonic direction has various physical implications.

Due to the entropy perturbations, the field may fall off the ridge during the ekpyrotic phase. Consequently, ekpyrosis could not last long enough in order to render the universe flat and isotropic. This also means that the initial conditions in the new ekpyrotic scenario are harder to fulfill. The evolution of the adiabatic field σ is shown in Fig, 10. In the "phoenix universe" [25–27] – the embedding of the new ekpyrotic scenario in a cyclic model – suitable initial conditions are selected naturally.

B. Adiabatic and Entropy Perturbations

In this chapter, we will discuss the splitting into adiabatic and entropy perturbations in detail. Moreover, we will calculate the evolution of curvature perturbations and entropy perturbations in the new ekpyrotic scenario. Let us briefly review a general definition of adiabatic and entropy perturbations. Adiabatic or curvature perturbations perturb the solution along the background solution. This means that the perturbation in any scalar quantity X is described by (see e.g. [53])

$$H\delta t = \frac{\delta X}{\dot{X}}. \tag{5.13}$$

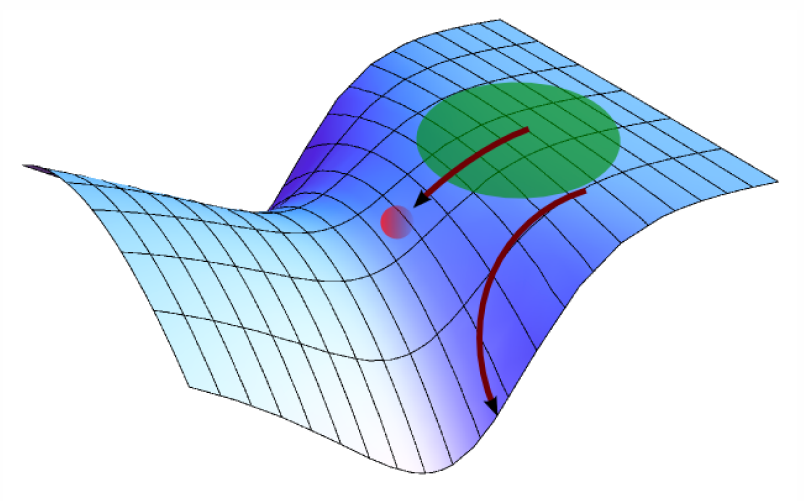

FIG. 10. The adiabatic field σ rolls along the ridge in the presence of an unstable direction for suitable initial conditions. However, the adiabatic field σ can fall off the ridge due to unsuitable initial conditions or due to entropy perturbations transverse to the background trajectory.

An example is the energy density and the pressure

$$\frac{\delta\rho}{\dot{\rho}} = \frac{\delta p}{\dot{p}}. \tag{5.14}$$

A time displacement δt results in a relative change of all quantities.

The general definition of the entropy perturbation between any two matter quantities X and Y is given by [5]:

$$S_{xy} = H\left(\frac{\delta X}{\dot{X}} - \frac{\delta Y}{\dot{Y}}\right). \tag{5.15}$$

We have defined the adiabatic and entropy perturbations in terms of $\delta\phi_1$ and $\delta\phi_1$ in Eq. (5.7) and Eq. (5.8) respectively. The splitting into adiabatic and entropy perturbations was first considered by [5] at the linear level, and later extended by various authors [65–67]. Let us define the adiabatic and entropic unit vector

$$e^I_\sigma \equiv \frac{1}{\sqrt{\dot{\phi}_1^2 + \dot{\phi}_2^2}}\left(\dot{\phi}_1, \dot{\phi}_2\right), \qquad e^I_s \equiv \frac{1}{\sqrt{\dot{\phi}_1^2 + \dot{\phi}_2^2}}\left(-\dot{\phi}_2, \dot{\phi}_1\right), \tag{5.16}$$

which can be written, using the angle θ in field space, as

$$e^I_\sigma = (\cos\theta, \sin\theta), \qquad e^I_s = (-\sin\theta, \cos\theta). \tag{5.17}$$

At linear order the adiabatic and entropy perturbations are then defined to be

$$\delta\sigma^{(1)} = e_{\sigma I}\delta\phi^I, \qquad \delta s^{(1)} = e_{sI}\delta\phi^I, \tag{5.18}$$

which coincides with our previous result in (5.7) and (5.8). The advantage of this notation will become apparent when dealing with higher order perturbations and/or generalized multi-field models. It also allows us to calculate the derivative w.r.t to the adiabatic or entropic direction in a simple way – for example $V_\sigma \equiv e^I_\sigma V_{,I}$, $V_s \equiv e^I_s V_{,I}$, $V_{ss} \equiv e^I_s e^J_s V_{,IJ}$. A useful relation is $V_s = -\dot{\sigma}\dot{\theta}$, which will be used throughout this thesis.

We can imagine that in general the evolution of adiabatic and entropy perturbations can become complicated. If the trajectory in field space bends ($\dot{\theta} \neq 0$) the adiabatic and entropy perturbations interact – they source each other. However, during ekpyrosis there is no bending in field space: the adiabatic field rolls along the ridge of the potential.

Consequently, during ekpyrosis the evolution of the adiabatic and entropy perturbations to first order is fairly simple, since $\dot{\theta} = 0$. The field rolls down the adiabatic direction and the curvature perturbations to first order behave like in the single scalar field case. This means that in the new ekpyrotic scenario the spectrum of the comoving curvature perturbation $\mathcal{R}$ and of the tensor perturbation is highly blue, cf. Chapter 4 F.

Because of the simplicity of this two-field model, we will skip the general derivation of the equations of motion to first order in perturbations in the case of multiple fields, which can be found in e.g. [5]. The equation of motion for the entropy perturbations to first order are given by [5]:

$$\ddot{\delta s} + 3H\dot{\delta s} + \left(\frac{k^2}{a^2} + V_{ss} + 3\dot{\theta}^2\right)\delta s = \frac{\dot{\theta}}{\dot{\sigma}}\frac{k^2}{2\pi G a^2}\Psi\,. \tag{5.19}$$

On large scales or for $\dot{\theta} = 0$ the source term on the r.h.s is negligible and the evolution of δs decouples from the adiabatic evolution.

As discussed, if the field space bends the entropy perturbations can source the curvature perturbations. On large scales the evolution of the comoving curvature perturbation $\mathcal{R}$ to first order is determined by [5]:

$$\dot{\mathcal{R}} = -\frac{2H}{\dot{\sigma}}\dot{\theta}\delta s = \sqrt{\frac{2}{\epsilon}}\dot{\theta}\delta s\,. \tag{5.20}$$

This is in contrast to the single scalar field case where the comoving curvature perturbations become constant on large scales, which can be easily confirmed by using (5.20); in the single scalar field case $\delta s = 0$ and thus $\dot{\mathcal{R}} = 0$ on large scales.

We will derive a more general evolution equation in Chapter 6 E and we will discuss the conversion process in detail throughout this thesis.

C. The Entropic Mechanism

We will now calculate the evolution of the entropy perturbations δs to first order during ekpyrosis. Using $\dot{\theta} = 0$, the equation of motion (5.19) reads

$$\ddot{\delta s} + 3H\dot{\delta s} + \left(\frac{k^2}{a^2} + V_{ss}\right)\delta s = 0. \tag{5.21}$$

We first rewrite the equation in terms of conformal time $d\tau = dt/a$ and the re-scaled variable $\delta S = a\delta s$:

$$\delta S'' + \left(k^2 - \frac{a''}{a} + a^2 V_{ss}\right)\delta S = 0\,, \tag{5.22}$$

where $'$ denotes the derivative w.r.t. conformal time. It is important to note that the ekpyrotic phase has to come to an end eventually. Meaning that the ekpyrotic potential has to flatten out leading to a kinetic phase. Since the ekpyrotic potential is parametrized by the fast-roll parameter ϵ, we will introduce a time dependence of ϵ. We chose a time-dependence in terms of e-folding time (scale-factor time) $dN \equiv d\ln a$, which corresponds to $\frac{d}{dt} = H\frac{d}{dN}$. Requiring a slow change in ϵ and $\epsilon \gg 1$, we will keep only linear term in $d\epsilon/dN$.

Differentiating $\epsilon = \frac{\dot{\sigma}^2}{2H^2}$ twice, using the background equation of motion for σ and $V_{ss} = V_{\sigma\sigma}$ leads to the following expressions [22]:

$$\frac{a''}{a} = H^2a^2(2-\epsilon)\,, \tag{5.23}$$

$$V_{ss} = H^2(6\epsilon - 2\epsilon^2 + \frac{5}{2}\epsilon_{,N})\,, \tag{5.24}$$

$$aH = \frac{1}{\epsilon\tau}\left(1 + \frac{1}{\epsilon} + \frac{\epsilon_{,N}}{\epsilon^2}\right)\,. \tag{5.25}$$

The equation of motion (5.22) becomes:

$$\delta S'' + \left[k^2 - \frac{2}{\tau^2}\left(1 - \frac{3}{2\epsilon} + \frac{3\epsilon_{,N}}{4\epsilon^2}\right)\right]\delta S = 0\,. \tag{5.26}$$

It is now straightforward to calculate the solution in analogy to the single scalar field case. Setting the Bunch-Davies vacuum as initial conditions in the far past leads to the following solution (up to a phase)

$$\delta S = \frac{\sqrt{-k\tau}}{2}H_\nu^{(1)}(-k\tau)\,, \tag{5.27}$$

where the Hankel index ν is given by:

$$\nu = \frac{3}{2}\left(1 - \frac{2}{3\epsilon} + \frac{\epsilon_{,N}}{3\epsilon^2}\right)\,. \tag{5.28}$$

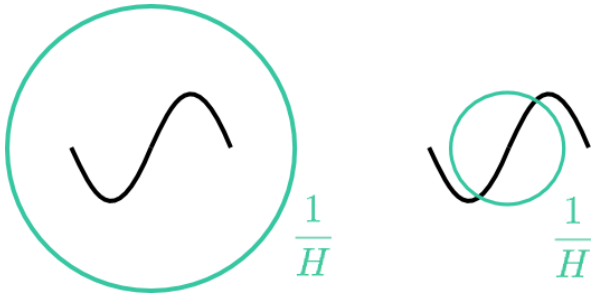

FIG. 11. The modes start deep inside the Hubble radius H^{-1}. Since $H^{-1} \sim t$ the Hubble radius shrinks as t goes from large negative values towards zero. The entropy perturbations become super-horizon.

Thus the spectral index of the entropy perturbations reads

$$n_s - 1 = \frac{2}{\epsilon} - \frac{\epsilon_{,N}}{\epsilon^2} \,. \tag{5.29}$$

The first term – the gravitational contribution – makes the spectrum blue. The second term leads to a red tilt, since ϵ is decreasing in order to end the ekpyrotic phase while N is negative in a contracting universe. In order to estimate the spectral index we can rewrite the above expression in terms of $\mathcal{N} = d\ln(aH)$ – the number of e-folds before ekpyrosis ends. Assuming a power-law dependence $\epsilon \approx \mathcal{N}^\alpha$ leads to [22]

$$n_s - 1 = \frac{2}{\epsilon} - \frac{d\ln\epsilon}{d\mathcal{N}} \approx \frac{2}{\mathcal{N}^\alpha} - \frac{\alpha}{\mathcal{N}} \,. \tag{5.30}$$

The overall sign of the spectral index is sensitive to α. For example $\alpha \approx 2$ leads to $n_s \approx 0.97$, which is in good agreement with the Planck data [44, 68].

In the late time limit ($-k\tau \to 0$), the solution is given by:

$$\delta S = \frac{1}{\sqrt{2}(-\tau)k^\nu} \,. \tag{5.31}$$

The entropy perturbations become amplified. In the inflationary case the modes exit the horizon, since the scale factor a stretches the modes while the Hubble radius $H^{-1} \approx const.$. In the ekpyrotic scenario the scale factor $a \approx const.$, while the Hubble radius H^{-1} shrinks by a large amount. We have drawn the corresponding diagram in Fig 11. Using the scaling solution, we find an estimate for the amplitude of δs at the end of ekpyrosis:

$$\delta s(t_{ek-end}) \approx \frac{|\epsilon V_{ek-end}|^{1/2}}{\sqrt{2}k^\nu} \,. \tag{5.32}$$

As already mentioned, an important step is the conversion of entropy perturbations to curvature perturbations, which are the seeds of the temperature fluctuations in the Cosmic Microwave Background radiation. We will discuss the conversion mechanism in detail in Chapter 6 E. For now we

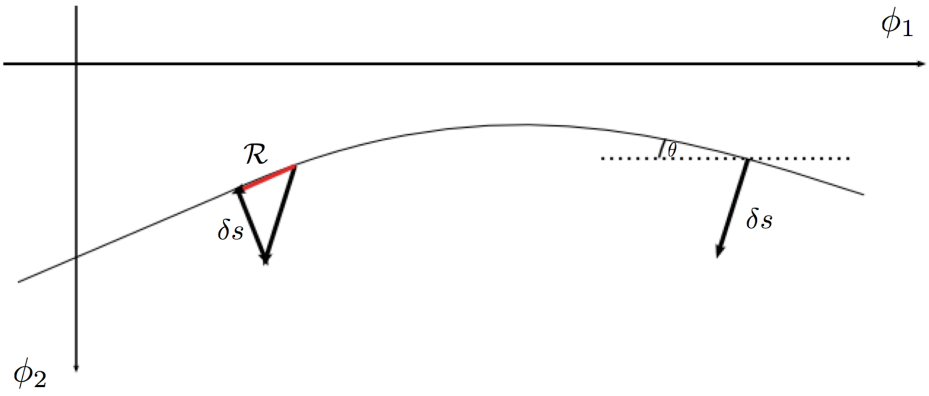

FIG. 12. Entropy perturbations are converted to curvature perturbations via a bending in field space. The amount of conversion depends on the efficiency of the conversion process.

will give a brief overview in order to estimate the conversion process to first order in perturbations. One possibility is the so-called kinetic conversion, which takes place during the kinetic phase after ekpyrosis and before the bounce. During the kinetic phase the ekpyrotic potential can be neglected leading to the following background solution

$$H = \frac{1}{3t} \quad , \quad \dot{\sigma} = -\sqrt{\frac{2}{3}}\frac{1}{t} \tag{5.33}$$

and the entropy perturbations are described by

$$\ddot{\delta s} + 3H\dot{\delta s} = 0\,, \tag{5.34}$$

which means that the entropy perturbations grow logarithmically – we will neglect his small growth for now. In order to convert entropy perturbations to curvature perturbations the background trajectory has to bend

$$\dot{\mathcal{R}} = -\frac{2H}{\dot{\sigma}}\dot{\theta}\delta s = \sqrt{\frac{2}{\epsilon}}\dot{\theta}\delta s\,. \tag{5.35}$$

In Fig. 12 a typical conversion process is shown, where the field space trajectory bends due to a repulsive potential at $\phi_2 = 0$. Let us estimate the resulting conversion: assuming that δs is approximately constant during the conversion process and assuming a total bending angle of order unity yields [69]:

$$\mathcal{R}_{conv-end} \approx \frac{1}{5}\delta s_{ek-end}\,, \tag{5.36}$$

where δs_{ek-end} is the value of the entropy perturbation at the end of ekpyrosis. Thus we find:

$$\langle \mathcal{R}^2_{conv-end}\rangle = \int \frac{\mathrm{d}k}{k}\Delta^2_{\mathcal{R}} \approx \frac{\mathrm{d}^3k}{(2\pi)^3}\frac{1}{25}(\delta s_{ek-end})^2 \approx \frac{\mathrm{d}k}{k}\frac{\epsilon V_{ek-end}}{100\pi^2}k^{n_s-1}\,, \tag{5.37}$$

where we have used (5.32) in the last step. This means that the energy scale of the ekpyrotic potential at the end of ekpyrosis has to reach approximately the grand unified scale $V_{ek-end} \approx (10^{-2} M_{PL})^4$ in order to be in agreement with the observed amplitude $\Delta^2_{\mathcal{R}} \approx 3 \times 10^{-9}$ [6].

6. NON-GAUSSIANITY

A. Overview

Large self-interactions of the scalar field give rise to large non-Gaussian contributions. Before the Planck measurements in the year 2013, a variety of inflationary models were developed in order to produce sizable non-Gaussianities. The amount and the specific type, e.g. local or equilateral (see below), of non-Gaussian contributions is an important feature of any model of the primordial universe.

Before we discuss the Planck measurements and the implications for inflationary and ekpyrotic models, we will review the treatment of cosmological perturbations theory up to third order. The bispectrum is defined in an analogous fashion as the power spectrum; it is the Fourier transform of the three-point function:

$$\langle \mathcal{R}_{k_1} \mathcal{R}_{k_2} \mathcal{R}_{k_3} \rangle = (2\pi)^3 B(k_1, k_2, k_3) \delta(\mathbf{k}_1 + \mathbf{k}_2 + \mathbf{k}_3) \tag{6.1}$$

and the trispectrum is the Fourier transform of the four-point function:

$$\langle \mathcal{R}_{k_1} \mathcal{R}_{k_2} \mathcal{R}_{k_3} \mathcal{R}_{k_4} \rangle = (2\pi)^3 T(k_1, k_2, k_3, k_4) \delta(\mathbf{k}_1 + \mathbf{k}_2 + \mathbf{k}_3 + \mathbf{k}_4)\,. \tag{6.2}$$

In the following, we will focus on the second order corrections. However, we will also state important results regarding the trispectrum in order to compare the ekpyrotic predictions with observations.

The non-Gaussianities can be characterized by the amount (also called size) and the shape. The shape is determined by the configuration of the momenta k_i. Because of momentum conservation the momenta form a triangle and it is customary to distinguish three special cases:

The equilateral shape is defined by the condition $k_1 \approx k_2 \approx k_3$, such that the triangle is equilateral, the squeezed (also called local) shape is defined via $k_1 \approx k_2 \gg k_3$ and finally the folded shape is defined by $k_1 \approx 2k_2 \approx 2k_3$. Fig. 13 shows the different configurations.

Non-Gaussianities of the equilateral shape can arise in models with non-standard (higher derivative) kinetic terms, e.g., DBI inflation. In this case, the non-Gaussianities are produced when the

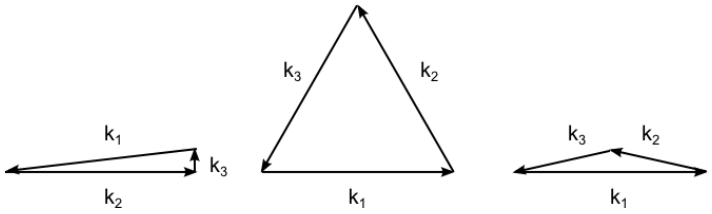

FIG. 13. The figure shows three configurations of the three momenta k_i : the local, equilateral and folded shape respectively.

three modes leave the horizon at the same time since they have the same size. A large equilateral non-Gaussian contribution is caused by a small speed of sound of the perturbations.
The local shape is the most important one in this thesis. It arises naturally in single field models of inflation, but also in two-field models of ekpyrosis. The squeezed or local shape defined by $k_1 \approx k_2 \gg k_3$ can be understood as follows: The mode with small momentum k_3 leaves the horizon first since the wavelength λ_3 is large. The perturbation associated with the momentum k_3 freezes after horizon exit: this results in a modulation of the other two momenta – when leaving the horizon they underlie a changed background.

Local non-Gaussianities can be parametrized by this simple form:

$$\mathcal{R}(x) = \mathcal{R}_L(x) + \frac{3}{5} f_{NL} \left(\mathcal{R}_L(x)\right)^2 + \frac{9}{5} g_{NL} \left(\mathcal{R}_L(x)\right)^3 , \tag{6.3}$$

where $\mathcal{R}_L(x)$ is the linear and Gaussian curvature perturbation. Since $\mathcal{R}_L(x)$ is defined locally in real space it is called local non-Gaussianity. The higher order perturbations are just defined by the linear (Gaussian) fluctuations. The amount of non-Gaussianity is parametrized by f_{NL} (and g_{NL}). In the case of local non-Gaussianities we can already find an expression for the bispectrum. Using the definition of the power-spectrum

$$\langle \mathcal{R}_{k_1} \mathcal{R}_{k_2} \rangle = (2\pi)^3 P_{\mathcal{R}}(k_1) \delta(k_1 + k_2) \tag{6.4}$$

and the definition of the bispectrum (6.1) together with the local expansion (6.3) we find:

$$B(k_1, k_2, k_3) = \frac{6}{5} f_{NL} \left(P_{\mathcal{R}}(k_1) P_{\mathcal{R}}(k_2) + P_{\mathcal{R}}(k_1) P_{\mathcal{R}}(k_3) + P_{\mathcal{R}}(k_2) P_{\mathcal{R}}(k_3) \right) . \tag{6.5}$$

Similarly we obtain for the trispectrum:

$$\begin{aligned} T(k_1, k_2, k_3, k_4) = {} & \tau_{NL} \left(P_{\mathcal{R}}(k_{13}) P_{\mathcal{R}}(k_3) P_{\mathcal{R}}(k_4) + 11 \text{ permutations} \right) \\ & + \frac{54}{25} g_{NL} \left(P_{\mathcal{R}}(k_2) P_{\mathcal{R}}(k_3) P_{\mathcal{R}}(k_4) + 3 \text{ permutations} \right) , \end{aligned} \tag{6.6}$$

where $k_{ij} = |\mathbf{k}_i + \mathbf{k}_j|$. Let us introduce a very useful way of calculating the local non-Gaussianity parameter f_{NL}, which we will use throughout this thesis. From (6.3) we find

$$f_{NL} = \frac{5}{3}\frac{\int_{beg}^{end}\mathcal{R}^{(2)\prime}}{\left(\int_{beg}^{end}\mathcal{R}^{(1)\prime}\right)^2} \quad , \quad g_{NL} = \frac{25}{9}\frac{\int_{beg}^{end}\mathcal{R}^{(3)\prime}}{\left(\int_{beg}^{end}\mathcal{R}^{(1)\prime}\right)^3}, \tag{6.7}$$

where we integrate the evolution equation up to second order in perturbations from the beginning of the evolution until $\mathcal{R}$ becomes constant. As it turns out this is a very easy way of calculating the resulting non-Gaussian signatures of the comoving curvature perturbations in the context of ekpyrosis.

Before we discuss the resulting non-Gaussianities of inflationary and ekpyrotic models let us review the measurements by the Planck team (to 1σ) [45]:

$$f_{NL}^{local} = 0.8 \pm 5.0, \tag{6.8}$$

$$g_{NL}^{local} = (9.9 \pm 7.7) \times 10^4. \tag{6.9}$$

This means that the comoving curvature perturbations are nearly Gaussian and any model of the early universe has to fit these measurements.

B. Calculation of Non-Gaussianities

In Chapter 4 B we have calculated the quadratic action for the scalar perturbation $\mathcal{R}$ in the case of a single field minimally coupled to gravity. We have used the ADM - decomposition and expanded the action of the scalar perturbations up to second oder.

Now we expand the action up to third order, which is the self-interaction of the curvature perturbations in the case of a single scalar field minimally coupled to gravity. We will follow the formalism by Maldacena [70] (see also [71]).

The third order Lagrangian is given by [70]

$$\mathcal{L}^{(3)} = \epsilon^2\mathcal{R}\dot{\mathcal{R}}^2 + \epsilon^2\mathcal{R}(\partial\mathcal{R})^2 - 2\epsilon\dot{\mathcal{R}}(\partial\mathcal{R})(\partial\chi) + 2f(\mathcal{R})\frac{\delta L_2}{\delta\mathcal{R}} + \mathcal{O}(\epsilon^3), \tag{6.10}$$

where

$$f(\mathcal{R}) \equiv \eta/4\mathcal{R} + ... \tag{6.11}$$

and $\frac{\delta L_2}{\delta\mathcal{R}}$ is the variation of the second order action with respect to $\mathcal{R}$. The additional terms in $f(\mathcal{R})$ vanish outside the horizon and thus do not contribute to the non-Gaussian corrections. The term proportional to $f(\mathcal{R})$ can be removed by a field redefinition of the form

$$\mathcal{R} \to \mathcal{R}_n + f(\mathcal{R}_n). \tag{6.12}$$

This redefinition leads to the following change in the bispectrum

$$\langle \mathcal{R}_{k_1}\mathcal{R}_{k_2}\mathcal{R}_{k_3}\rangle = \langle \mathcal{R}_n(\mathbf{k}_1)\mathcal{R}_n(\mathbf{k}_2)\mathcal{R}_n(\mathbf{k}_3)\rangle + \frac{\eta}{4}(\langle \mathcal{R}_n(\mathbf{k}_1)\mathcal{R}_n(\mathbf{k}_2)\mathcal{R}_n(\mathbf{k}_3)\rangle + 2 \text{ perm.}) + ... \quad (6.13)$$

In order to calculate this expectation value, we use the so-called in-in formalism [70]. In particle physics, the S-matrix describes the transition probability for a state in the far past $|\psi\rangle$ to become a state $\langle\psi'|$ in the far future

$$\langle\psi'|\psi\rangle = \langle\psi'(\infty)|\psi(-\infty)\rangle\,, \quad (6.14)$$

where the states in the far past and future do not interact corresponding to two asymptotic conditions.

However, in cosmology we evaluate expectation values of products of fields at fixed times. There is only one asymptotic condition at very early times when the modes are deep inside the horizon corresponding to the Bunch-Davies vacuum. The expectation value of a product of fields reads

$$\langle W(t)\rangle = \langle in|W(t)|in\rangle\,, \quad (6.15)$$

where $|in\rangle$ describes the vacuum in the interacting theory at some early time t' and $t > t'$ corresponds to some later time at e.g. horizon crossing. The idea is now to evolve/project the $|in\rangle$ and $\langle in|$ states to the vacuum states $\langle 0|$ and $|0\rangle$. We will skip the derivation presented in [70] and state the result:

$$\langle W(t)\rangle = -i\int_{-\infty}^{t} dt'\,\langle 0|[W^I(t), H^I_{int}(t')]|0\rangle \quad (6.16)$$

$$= 2\text{Re}\left(-i\int_{-\infty(1-i\epsilon)}^{t} dt'\,\langle 0|W^I(t)H^I_{int}(t')|0\rangle\right)\,, \quad (6.17)$$

where I denotes the interaction picture operators and H^I_{int} is the interacting Hamiltonian which is given by $H^I_{int} = -L^{(3)}$ from equation (6.10) in the case of a single scalar field.

C. Non-Gaussianities Signatures during Inflation

We have expanded the action of the comoving curvature perturbation up to third order and reviewed how we can calculate expectation values in cosmology using the in-in formalism. Now we will use this formalism in order to obtain the non-Gaussian corrections during inflation in the case of a single scalar field minimally coupled to gravity. We expand and quantize the comoving

curvature perturbation as usual

$$\hat{\mathcal{R}}(\tau,\mathbf{x}) = \int \frac{\mathrm{d}^3k}{(2\pi)^3}\hat{\mathcal{R}}(\tau,\mathbf{k})e^{i\mathbf{kx}} \tag{6.18}$$

with

$$\hat{\mathcal{R}}(\tau,\mathbf{k}) \equiv \hat{\mathcal{R}}_k(\tau) = u_k\hat{a}_{\mathbf{k}} + u^*_{-k}\hat{a}^\dagger_{-\mathbf{k}}, \tag{6.19}$$

where u_k are solutions to the Mukhanov-Sasaki equation, which we have obtained in the de Sitter limit (4.63)

$$u_k = \frac{iH}{\sqrt{4\epsilon k^3}}e^{-ik\tau}\left(1+ik\tau\right). \tag{6.20}$$

We can now calculate each term individually using equation (6.17) and the third order Lagrangian (6.10). The first term reads

$$H_{int} = \int \mathrm{d}^3x a^3\epsilon^2\mathcal{R}\dot{\mathcal{R}}^2, \tag{6.21}$$

such that the first term of the 3-point function in fourier space is given by:

$$\begin{aligned}&\langle\mathcal{R}(\mathbf{k}_1,0)\mathcal{R}(\mathbf{k}_2,0)\mathcal{R}(\mathbf{k}_3,0)\rangle = \\ &\mathrm{Re}\left\langle -2i\int\frac{\mathrm{d}^3q_1}{(2\pi)^3}\frac{\mathrm{d}^3q_2}{(2\pi)^3}\frac{\mathrm{d}^3q_3}{(2\pi)^3}\int\mathrm{d}\tau\mathrm{d}^3x a^2\epsilon^2 e^{i(\mathbf{q}_1+\mathbf{q}_2+\mathbf{q}_3)\mathbf{x}}\mathcal{R}_{k_1}\mathcal{R}_{k_2}\mathcal{R}_{k_3}\mathcal{R}_{q_1}\mathcal{R}'_{q_2}\mathcal{R}'_{q_3}\right\rangle .\end{aligned} \tag{6.22}$$

Using Wick's theorem we have to add all possible non-zero contractions. Moreover, we perform the integrals leading to δ-functions and plug in the solutions (6.20). The time integral has the following form

$$\int_{-\infty(1-i\epsilon)}^{0}\mathrm{d}\tau(1-ik_1\tau)e^{iK\tau} = -\frac{ik_1}{K^2}-\frac{i}{K} \tag{6.23}$$

with $K = k_1+k_2+k_3$. The final results reads

$$\langle\mathcal{R}(\mathbf{k}_1,0)\mathcal{R}(\mathbf{k}_2,0)\mathcal{R}(\mathbf{k}_3,0)\rangle = (2\pi)^3\delta^{(3)}(\mathbf{k}_1+\mathbf{k}_2+\mathbf{k}_3)\frac{H^4}{16\epsilon}\frac{1}{k_1^3k_2^3k_3^3}k_2^2k_3^2\left(\frac{1}{K}+\frac{k_1}{K^2}+\text{perm.}\right). \tag{6.24}$$

We repeat the above calculation for all the other terms of the Lagrangian (6.10) and end up with the final result:

$$\langle\mathcal{R}_{k_1}\mathcal{R}_{k_2}\mathcal{R}_{k_3}\rangle = S(k_1,k_2,k_3)\frac{1}{(k_1k_2k_3)^2}\tilde{P}^2_{\mathcal{R}}(2\pi)^7\delta^{(3)}(\mathbf{k}_1+\mathbf{k}_2+\mathbf{k}_3), \tag{6.25}$$

where $\tilde{P}_{\mathcal{R}} = \frac{H^2}{8\pi^2\epsilon}$ is the rescaled power spectrum (or variance), cf. Eq. (4.71), and S is the shape function given by [70, 71]:

$$S = \frac{1}{8k_1k_2k_3}\left((3\epsilon-\eta)\sum_i k_i^3 + \epsilon\sum_{i\neq j}k_i^2k_j^2 + \frac{8\epsilon}{K}\sum_{i>j}k_i^2k_j^2\right). \tag{6.26}$$

The shape function peaks in the squeezed/local limit for $k_3 \to 0$. The non-Gaussianities produced during inflation modeled by a single scalar field minimally coupled to gravity in a potential are of the local form. Comparing the result with (6.5) we obtain in the local limit $\langle \mathcal{R}^3 \rangle \sim f_{NL} \tilde{P}_{\mathcal{R}}^2$, which means that the non-Gaussianity parameter $f_{NL} \sim \epsilon$, which is small of $\mathcal{O}(0.01)$ during inflation. This was expected, since the inflationary potential is very flat leading to small self-interactions.

D. Non-Gaussian Signatures during Ekpyrosis

In the minimal entropic mechanism entropy perturbations are created in the presence of an unstable potential. The potential can be parametrized via:

$$V = -V_0 e^{\sqrt{2\epsilon}\sigma} \left[1 + \epsilon s^2 + \frac{\kappa_3}{3!} \epsilon^{3/2} s^2 + \frac{\kappa_4}{4!} \epsilon^2 s^4 + ... \right] , \tag{6.27}$$

where κ_3 and κ_4 are $\mathcal{O}(1)$. For an exact exponential potential we find $\kappa_3 = 2\sqrt{2}(c_1^2 - c_2^2)/|c_1 c_2|$ and $\kappa_4 = 4\sqrt{2}(c_1^6 - c_2^6)/c_1^2 c_2^2 (c_1^2 + c_2^2)$.

We can use the in-in formalism to calculate the 3-point correlation function of the entropy perturbations [24, 28]

$$\langle (\delta s)^3 \rangle = 2\mathrm{Re} \left(-i \int_{-\infty(1-i\epsilon)}^{t} \mathrm{d}t' \, \langle 0 | \delta s_{\mathbf{k}_1} \delta s_{\mathbf{k}_2} \delta s_{\mathbf{k}_3} H_{int}(t') | 0 \rangle \right) , \tag{6.28}$$

with $H_{int}(t') = V_{sss}(\delta s)^3/3! = -\sqrt{\epsilon}\kappa_3/(3! t'^2)(\delta s)^3$, where we have used the scaling solution during ekpyrosis. We find after some steps analogous to the previous discussion

$$\langle (\delta s)^3 \rangle = (2\pi)^3 2\mathrm{Re} \left(-i \int_{\infty}^{t} \mathrm{d}t' \delta s_{\mathbf{k}_1}(t) \delta s_{\mathbf{k}_2}(t) \delta s_{\mathbf{k}_3}(t) \frac{(-\sqrt{\epsilon}\kappa_3)}{t'^2} \delta s_{\mathbf{k}_1}(t') \delta s_{\mathbf{k}_2}(t') \delta s_{\mathbf{k}_3}(t') \right) . \tag{6.29}$$

Instead of using the mode function obtained in (5.27) we use an approximation to simplify the calculation. For very large ϵ (which corresponds here to neglecting gravity) we obtain the following first order equations of motion:

$$\ddot{\delta s} + \left(k^2 + V_{,ss} \right) \delta s = 0 \tag{6.30}$$

with $V_{,ss} = -2/t^2$. We find the following solution

$$\delta s_k = \frac{1}{\sqrt{2k}} \left(1 - \frac{i}{kt} \right) e^{-ikt} . \tag{6.31}$$

Here we see again that the $V_{,ss}$ term indeed acts like a de Sitter background for the entropy perturbations. Using the solution (6.31) we obtain the 3-point correlation function of the entropy

perturbations

$$\langle(\delta s)^3\rangle = (2\pi)^3\delta^{(3)}(\mathbf{k}_1+\mathbf{k}_2+\mathbf{k}_3)\frac{\sqrt{\epsilon}\kappa_3}{6t^4}\frac{\sum_i k_i^3}{\Pi_i k_i^3}. \tag{6.32}$$

Non-Gaussianities of the entropy perturbations produced via the entropic mechanism are of the local form. Moreover, the bispectrum becomes large for $|k_i t| \ll 1$, which corresponds to large scales – the dominant contribution arises on super-horizon scales. This means we can use the large scale limit when calculating the evolution of these perturbations.

The equation of motion of entropy perturbations to second order on large scales (neglecting gradients) is given by [72]

$$\begin{aligned}\ddot{\delta s} + 3H\dot{\delta s} + \left(V_{ss} + 3\dot{\theta}^2\right)\delta s = \\ -\frac{\dot\theta}{\dot\sigma}(\dot{\delta s})^2 - \frac{2}{\dot\sigma}\left(\ddot\theta + V_\sigma\frac{\dot\theta}{\dot\sigma} - \frac{3}{2}H\dot\theta\right)\delta s\dot{\delta s} + \left(-\frac{1}{2}V_{sss} + 5V_{ss}\frac{\dot\theta}{\dot\sigma} + 9\frac{\dot\theta^3}{\dot\sigma}\right)(\delta s)^2\,.\end{aligned} \tag{6.33}$$

During ekpyrosis the background evolves accordingly to the scaling solution (5.12), which yields:

$$\dot\sigma = -\frac{\sqrt{2}}{\sqrt{\epsilon}t} \quad , \quad V = -\frac{1}{\epsilon t^2} \quad , \quad V_{,\sigma} = -\frac{\sqrt{2}}{\sqrt{\epsilon}t^2} \quad , \quad V_{,\sigma\sigma} = -\frac{2}{t^2}, \tag{6.34}$$

$$V_{,s\sigma} = 0 \quad , \quad V_{,s\sigma} = 0 \quad , \quad V_{,ss} = -\frac{2}{t^2} \quad , \quad V_{,sss} = -\frac{\kappa_3\sqrt{\epsilon}}{t^2}\,. \tag{6.35}$$

Since the non-Gaussianities are of the local form, we can write the entropy perturbations as an expansion of the linear and Gaussian entropy perturbation δs_L. Using the fact that there is no bending in field space during ekpyrosis ($\dot\theta = 0$), the solution of (6.33) during ekpyrosis to leading order in $1/\epsilon$ is given by:

$$\delta s = \delta s_L + \frac{\kappa_3\sqrt{\epsilon}}{8}\delta s_L^2 \tag{6.36}$$

with $\delta s_L \sim \frac{1}{t}$. For completeness let us state the result up to third order

$$\delta s = \delta s_L + \frac{\kappa_3\sqrt{\epsilon}}{8}\delta s_L^2 + \epsilon\left(\frac{\kappa_4}{60} + \frac{\kappa_3^2}{80} - \frac{2}{5}\right)\delta s_L^3\,, \tag{6.37}$$

which corresponds to the solution of the equation of motion (6.33) expanded up to third order in perturbations, cf. [72]. This solution will be useful when calculating the further behavior of entropy perturbations after ekpyrosis – we can use (6.37) as initial conditions before the conversion. Moreover, we see that the intrinsic non-Gaussian contribution of the entropy perturbations depends on $\sqrt{\epsilon}$, which is generally large. This is in contrast to the ekpyrotic model, where the slow-roll parameter is small. This was expected, since the self-interactions are large for steep potentials. The intrinsic non-Gaussianity of the entropy perturbations can be small if the two-field potential is

very symmetric leading to $\kappa_3 \approx 0$. However, as we have already discussed, we need to convert the entropy perturbations to curvature perturbations. In the following chapter, we will describe the conversion process to higher order in perturbations and calculate the corresponding non-Gaussian contribution of the comoving curvature perturbations.

E. Conversion

The conversion of entropy perturbations to curvature perturbations is an important and vital process for the viability of ekpyrotic models. In the following chapter, we will discuss possible conversion processes and their consequences to observational signatures.
In order to convert entropy perturbations to curvature perturbations a bending in field space has to occur. In Chapter 5 C we have already estimated the effect of a kinetic conversion at the linear level in perturbations.

The two main results of the upcoming discussion can be summarized as follows:

- An effective conversion, where a large portion of entropy perturbations are converted to curvature perturbations, leads to more structure formation and generally small non-Gaussian corrections. While non-smooth, rapid and ineffective conversions lead to less structure formation and large non-Gaussianities, which are incompatible with observations.
- There are basically four possibilities for when and how the conversion takes place. During ekpyrosis [28, 34, 73, 74], shortly after the bounce due to modulated preheating [75], after ekpyrosis during the kinetic phase (before the bounce) [22, 35, 69] or during the kinetic phase after the bounce [9]. While the first three possibilities were studied extensively in previous works, the conversion process after a non-singular bounce yielded very interesting results, which are the main subject of this thesis based on [9]. We will cover the findings of our paper in Chapter 10.

For now, we will cover the ekpyrotic conversion and kinetic conversion before the bounce.

In order to calculate the conversion process from entropy to curvature perturbations, we will derive a simple and very useful form of the evolution equation on large scales [69, 73, 76]. Choosing the comoving gauge and using a FLRW metric as the background, the perturbed metric on large scales

(or, more precisely, when spatial gradients can be neglected) can we written as

$$ds^2 = -dt^2 + a(t)^2 e^{2\mathcal{R}(t,x^i)} dx^i dx_i \,. \tag{6.38}$$

The stress-energy tensor of a perfect fluid has the form

$$T^\mu_\nu = \begin{pmatrix} -\rho & 0 \\ 0 & p\,\delta^i_j \end{pmatrix}, \tag{6.39}$$

where ρ is the scalar matter density and p the pressure.
The equation of continuity is given by

$$\dot{\rho} + 3(H + \dot{\mathcal{R}})(\rho + p) = 0\,, \tag{6.40}$$

with the background (denoted by overbars) satisfying

$$\dot{\bar{\rho}} + 3\bar{H}(\bar{\rho} + \bar{p}) = 0\,. \tag{6.41}$$

On comoving hypersurfaces the energy density is uniform, $\rho = \bar{\rho}$ (and hence also $H = \bar{H}$ because of the Friedmann equation). We then obtain

$$\dot{\mathcal{R}} = -\bar{H}\frac{\delta p}{\bar{\rho} + \bar{p} + \delta p}\,, \tag{6.42}$$

where $\delta p \equiv p(t, x^i) - \bar{p}(t)$. On these hypersurfaces $\delta\rho = 0$ and thus we can write the pressure perturbation in terms of a perturbation in the potential, $\delta p = -2\delta V|_{\delta\rho=0}$. Using this relation, we obtain a compact expression for the evolution of the comoving curvature perturbation on large scales:

$$\dot{\mathcal{R}} = \frac{2\bar{H}\delta V}{\dot{\bar{\sigma}}^2 - 2\delta V}\,, \tag{6.43}$$

where $\delta V = V(t, x^i) - \bar{V}(t)$. Note that this equation is valid to all orders in perturbation theory. In concrete applications, one has to expand it to the desired order, and express δV in terms of the adiabatic and entropic fluctuations at that order.

Expanding (6.43) up to second order yields:

$$\dot{\mathcal{R}} = -\frac{2H}{\dot{\sigma}}\dot{\theta}\,\delta s + \frac{H}{\dot{\sigma}^2}\left(V_{ss} + 4\dot{\theta}^2\right)(\delta s)^2 - \frac{V_\sigma}{\dot{\sigma}}\delta s\dot{\delta s}\,, \tag{6.44}$$

where we have dropped the indices $^{(1)}$ and $^{(2)}$. It should be clear to which order these quantities are expanded: e.g. $\dot{\mathcal{R}} = \mathcal{R}^{(1)} + \mathcal{R}^{(2)}$, while the last term reads $\delta s\dot{\delta s} = \delta s^{(1)}\dot{\delta s^{(1)}}$. As we can see the

linear part of the first term coincides with equation (5.20). Moreover, at second order there is a sourcing of curvature perturbations from entropy perturbations without a bending in field space. This means that there is already a sourcing during ekpyrosis due to non-linear effects.

We can use analytic estimates in order to calculate the conversion process to second order in the case of an ekpyrotic conversion and a kinetic conversion. Due to the complexity of Eq. (6.44) we also obtain the non-Gaussian contributions numerically. In the case of local non-Gaussianities the comoving curvature perturbation can be written as (6.3):

$$\mathcal{R}(x) = \mathcal{R}_L(x) + \frac{3}{5} f_{NL} \left(\mathcal{R}_L(x)\right)^2 , \tag{6.45}$$

where $\mathcal{R}_L(x)$ is the linear and Gaussian curvature perturbation. This leads to the non-Gaussianity parameter

$$f_{NL} = \frac{5}{3} \frac{\int_{beg}^{end} \mathcal{R}^{(2)\prime}}{\left(\int_{beg}^{end} \mathcal{R}^{(1)\prime}\right)^2} . \tag{6.46}$$

In order to calculate f_{NL} we have to solve the equation of motion (6.33) of the entropy perturbations on larges scales

$$\begin{aligned} \ddot{\delta s} + 3H\dot{\delta s} + \left(V_{ss} + 3\dot{\theta}^2\right)\delta s = \\ -\frac{\dot{\theta}}{\dot{\sigma}}(\dot{\delta s})^2 - \frac{2}{\dot{\sigma}}\left(\ddot{\theta} + V_\sigma \frac{\dot{\theta}}{\dot{\sigma}} - \frac{3}{2}H\dot{\theta}\right)\delta s\dot{\delta s} + \left(-\frac{1}{2}V_{sss} + 5V_{ss}\frac{\dot{\theta}}{\dot{\sigma}} + 9\frac{\dot{\theta}^3}{\dot{\sigma}}\right)(\delta s)^2, \end{aligned} \tag{6.47}$$

and use the expansion obtained in (6.37)

$$\delta s = \delta s_L + \frac{\kappa_3\sqrt{\epsilon}}{8}\delta s_L^2 , \tag{6.48}$$

which determines the initial conditions before the conversion. Finally we have to integrate (6.46) from the beginning of ekpyrosis to the end of the conversion phase.

In the new ekpyrotic scenario the potential has an unstable direction. This instability leads to the production of nearly scale-invariant entropy perturbations and intrinsic non-Gaussian signatures of the local type via the entropic mechanism, cf. Eq. (6.48).

Let us consider the "ekpyrotic conversion" [20, 34, 74], which takes place during the ekpyrotic phase. The conversion occurs when the scalar field falls off the ridge of the unstable potential, which suggests that this conversion process is very abrupt due to the steepness of the potential. The resulting non-Gaussian parameter due to an ekpyrotic conversion was found to be [28, 72, 73]:

$$f_{NL} = -\frac{5}{12}c_1^2 . \tag{6.49}$$

For completeness we will also include corrections to third order in perturbations, which correspond to the amplitude of the trispectrum:

$$\tau_{NL} = \frac{1}{4} c_1^4 \,, \tag{6.50}$$

$$g_{NL} = \frac{25}{108} c_1^4 \,. \tag{6.51}$$

Since we require $c_1 > 10$ in order to obtain a red spectrum, cf. (5.30), we find that the non-Gaussianities produced during an ekpyrotic conversion are in disagreement with the Planck measurements [45].

In a cyclic embedding of the new ekpyrotic scenario the "phoenix universe" can explain the initial conditions of our universe dynamically [25–27]. Only regions with the right initial conditions for a stable ekpyrotic evolution will undergo a successful cycle, cf. Fig. 10 in Chapter 10, while other regions can end up in a big crunch. Regions where the scalar field rolls off the ridge too early produce less structure and large non-Gaussianities incompatible with observations.

Let us consider the kinetic conversion which we have introduced in Chapter 5 C. In Chapter 3 B we have discussed the cyclic ekpyrotic model which is based on the braneworld picture of the universe [4, 15, 16, 77]. The attractive force between the two branes causes the two branes to approach each other. This attractive force leads to the ekpyrotic potential. At the end of ekpyrosis the potential turns off and the universe is kinetically dominated. In the higher dimensional description the second scalar field describes the size of the internal manifold, while the first scalar field describes the distance between the two branes. Thus the line $\phi_2 = 0$ describes a boundary in field space. Moreover, the presence of matter on the negative tension brane gives rise to a repulsive potential near $\phi_2 = 0$. Thus, during the kinetic phase the field space trajectory automatically bends. This conversion is called "kinetic conversion". It is clear that the amount of conversion is highly model-dependent – as it is determined by the repulsive potential in field space.

The evolution equations (6.47) and (6.44), which describe the evolution of the entropy perturbations and the conversion process are quite complicated. However, a variety of analytic estimates and various numerical simulations led to a very good understanding of the kinetic conversion process [22, 35, 69, 78]. Let us try to get a better understanding of the conversion process to second order in perturbations. The first term in Eq. (6.44) converts the intrinsic non-Gaussian contribution directly to the curvature perturbation due to the bending in field space. This con-

tribution would be zero if there are no intrinsic non-Gaussian corrections during ekpyrosis. The remaining terms are present due to the non-linear relationship between the second order curvature perturbations $\mathcal{R}^{(2)}$ and the first order entropy perturbations. And thus these terms contribute to the final non-Gaussian corrections even if the intrinsic non-Gaussianities are zero. During ekpyrosis ($\dot{\theta} = 0$) there is already a sourcing of entropy to curvature perturbations, which is called integrated non-Gaussianity. The integrated non-Gaussianity parameter, using Eq. (6.46), is given by

$$f_{NL}^{integrated} = \frac{5}{12\mathcal{R}_L^2} \left(\delta s^{(1)}(t_{end})\right)^2 , \tag{6.52}$$

where $\mathcal{R}_L$ is the linear comoving curvature perturbation at the end of the conversion phase and $\delta s^{(1)}(t_{end})$ is the entropy perturbation at the end of ekpyrosis. It turns out that the integrated contribution $f_{NL}^{integrated} \approx 5$, which can be neglected for now, since it is small compared to the contributions during the conversion phase – the other contributions in Eq. (6.46) are typical large, but mostly cancel each other out [69, 78].

Following [69, 78] we will provide an intuitive and easy derivation of the resulting non-Gaussian contributions during the conversion phase, which match the numerical and approximate analytic solutions very well – as we will see below.

During the kinetic phase the potential is not important leading to a logarithmic growth of the entropy perturbations, cf. (5.34). We will neglect this growth in the following. During the conversion phase the repulsive potential leads to a sinusoidal evolution of the entropy perturbations independently of the precise form of the potential:

$$\delta s \approx \cos\left(\omega(t - t_c)\right) \delta s(t_c) , \tag{6.53}$$

where t_c denotes the beginning of the conversion phase, $\omega \approx 5/2\Delta t$ and Δt is the duration of the conversion. The final amplitude of $\mathcal{R}$ after the conversion is smaller than δs, which allows us to assume that the repulsive potential depends only on δs. Moreover, the repulsive potential should not change the background evolution too much, such that $\delta V \ll \dot{\sigma}^2$. From (6.43) we obtain

$$\dot{\mathcal{R}} = \frac{2\bar{H}\delta V}{\dot{\bar{\sigma}}^2 - 2\delta V} \approx \frac{2\bar{H}}{\dot{\bar{\sigma}}^2}\delta V \approx \frac{2\bar{H}}{\dot{\bar{\sigma}}^2}\delta s . \tag{6.54}$$

Using the relation $\dot{\theta} = \frac{V_{,s}}{\dot{\sigma}} \approx \Delta t$ and Eq. (6.53), we can calculate the final comoving curvature perturbation at linear order

$$\mathcal{R}_L = \int \frac{2\bar{H}}{\dot{\bar{\sigma}}^2} \delta s_L \tag{6.55}$$

$$\approx \sqrt{\frac{2}{3}} \frac{\dot{\theta}}{\omega} \sin(\omega \Delta t) \delta s(t_c) \tag{6.56}$$

$$\approx \frac{1}{5} \delta s(t_c) \,. \tag{6.57}$$

Moreover, Eq. (6.54) holds true to all order in perturbation theory. And thus we immediately find the resulting comoving curvature perturbations after the conversion:

$$\mathcal{R}^{(2)} \approx \frac{\kappa_3 \sqrt{\epsilon}}{40} \delta s_L^2 \,, \tag{6.58}$$

$$\mathcal{R}^{(3)} \approx \frac{1}{5} \epsilon \left(\frac{\kappa_4}{60} + \frac{\kappa_3^2}{80} - \frac{2}{5} \right) \delta_L^3 \,, \tag{6.59}$$

where we have used the expansion in Eq. (6.48). The final non-Gaussianity parameters are

$$f_{NL} = \frac{5}{3} \frac{\mathcal{R}^{(2)}}{\mathcal{R}_L^2} \approx \kappa_3 \sqrt{\epsilon} \,, \tag{6.60}$$

$$g_{NL} = \frac{5}{3} \frac{\mathcal{R}^{(3)}}{\mathcal{R}_L^3} \approx 70 \epsilon \left(\frac{\kappa_4}{60} + \frac{\kappa_3^2}{80} - \frac{2}{5} \right) \,. \tag{6.61}$$

Using the above approximations we were able to calculate the final non-Gaussian corrections after a kinetic conversion in a fairly simple way. Moreover, these approximations are very close to the numerical and analytic estimates in [22, 35, 69, 78], which are given by the phenomenological expressions

$$f_{NL} = \frac{3}{2} \sqrt{\epsilon} \kappa_3 + 5 \,, \tag{6.62}$$

$$g_{NL} = 100 \left(\frac{\kappa_4}{60} + \frac{\kappa_3^2}{80} - \frac{2}{5} \right) \epsilon \,. \tag{6.63}$$

In this chapter, we have studied the conversion process up to third order in perturbations. During an ekpyrotic conversion, large non-Gaussianities are produced which are not compatible with observations. The kinetic conversion due to a repulsive potential during the kinetic phase before the bounce produces non-zero non-Gaussian corrections. Even though the conversion process is model-dependent we have obtained fairly general results. A smooth and effective conversion leads to larger $\mathcal{R}_L$ and non-zero non-Gaussianities depending on the steepness and symmetry of the ekpyrotic two-field potential.

7. CHALLENGES FOR INFLATIONARY AND EKPYROTIC MODELS

In this chapter we will review some of the challenges for inflationary and ekpyrotic models. We will face problems which arise from tensions with the Planck measurements as well as fundamental/theoretical problems of the models.

From the Planck measurements we know, that the primordial curvature perturbations are nearly scale-invariant and nearly Gaussian. Moreover, primordial gravitational waves have not been detected yet. Let us briefly summarize the Planck measurements/bounds which have to be predicted by the models of the early universe [6, 44, 45]:

$$A_{\mathcal{R}} = (2.975 \pm 0.056) \times 10^{-9}, \tag{7.1}$$

$$n_s = 0.9649 \pm 0.0042\,, \tag{7.2}$$

$$r < 0.064 \text{ at } 95\% \text{ confidence level}\,, \tag{7.3}$$

$$f_{NL}^{local} = 0.8 \pm 5.0\,, \tag{7.4}$$

$$g_{NL}^{local} = (9.9 \pm 7.7) \times 10^4\,, \tag{7.5}$$

where $A_{\mathcal{R}}$ is the amplitude, n_s is the spectrum of the curvature perturbation $\mathcal{R}$, r is the tensor-to-scalar ratio, f_{NL}^{local} is the non-Gaussianity parameter and g_{NL}^{local} parametrizes the size of the trispectrum (up to 1 σ).

A. Inflation

Let us first look at which inflationary models are in agreement with the Planck data. In Fig. 14 we have plotted the $n_s - r$ – plane published by the Planck team [44]. The simplest models - namely the exponential potential (power-law inflation) as well as the $m^2\phi^2$ - potential (chaotic inflation) – are ruled out. These models of inflation had the advantage of being simple and fairly robust in terms of initial conditions. The smallness of the tensor-to-scalar ratio disfavors a variety of inflationary models. As it turns out the very idea of inflation to provide initial conditions for the universe is challenged by the fact, that inflation itself needs fairly strong initial conditions [79].

Other considerations further challenge the initial conditions for inflation. Entropic arguments suggest that inflation is exponentially unlikely compared to a universe without inflation [80]. Quantum arguments also suggest that it is exponentially unlikely that inflation starts [81].

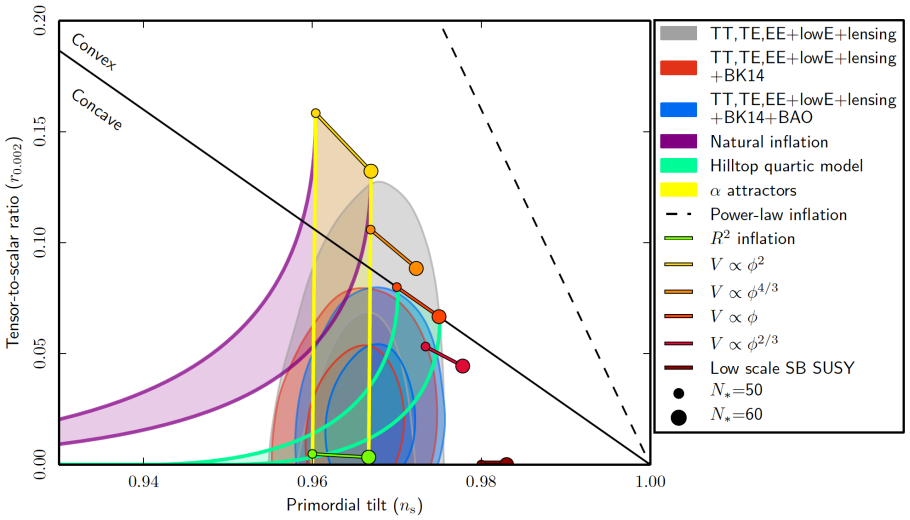

FIG. 14. The figure shows the $n_s - r$ – plane. Observations disfavor a variety of inflationary due to the fact that the tensor-to-scalar ratio r is small. The currently best fitting model is R^2 - inflation, which is a plateau-model of inflation. Figure taken from [6].

Models in agreement with observations belong mostly to the class of plateau models. In these models, the inflaton starts on a plateau and rolls slowly towards the local minimum of the potential. These models are challenged by the unlikeliness problem [79], which states that inflation is more likely to occur around the local minimum of the potential compared to an evolution on top of the plateau. The currently best fitting model is R^2 - inflation, where the spectral index and tensor-to-scalar ratio in terms of e-folds to lowest order are given by [82, 83]

$$n_s - 1 \simeq -\frac{2}{N} \quad , \quad r \simeq \frac{12}{N^2} \, . \tag{7.6}$$

The initial velocity and gradient of the scalar field have to be small in the first place, which is harder to achieve for plateau models compared to chaotic potentials [79, 84]. Moreover, smoothness over more than one Hubble radius is required to initiate inflation, which is again a condition inflation should provide on its own [79].

Inflation cannot yield a complete history of the early universe since the initial singularity is not resolved [85].

Another problem is the trans-Planckian problem of the quantum fluctuations. If inflation lasts only slightly longer than needed in order to solve the big bang puzzles, then the wavelengths of interest today originate from sub-Planckian values [86, 87]. This means we cannot trust the calculations of inflationary models without an embedding in a consistent quantum theory.

The major challenge is eternal inflation [88–90], which occurs in two different scenarios: eternal inflation from false vacuum decay and slow-roll eternal inflation. The idea of slow-roll eternal inflation is as follows: The scalar field rolls slowly down the near flat potential, while small quantum fluctuations seed the temperature fluctuation in the Cosmic Microwave Background. However, there exist rare, large quantum fluctuations which can move the inflaton back up in the potential. This region expands more rapidly since the Hubble rate is larger in this region ($3H^2 \approx V(\phi)$ in the slow-roll approximation). This effect will prolong and dominate the expansion history. Moreover, the large quantum jumps can occur over and over leading to an infinite amount of pocket universes – which means that inflation never ends globally. Since every pocket universe has a different expansion history, an infinite amount of physically distinct universes are created – all possible values of e.g. n_s, A_s, r, f_{NL} can occur: "Anything that can happen will happen; in fact, it will happen infinitely many times" [90]. This famous quote by Alan Guth is troublesome for a theory, which wants to predict the initial conditions of our universe. With no probability measure, the multiverse challenges the predictability of the inflationary paradigm [91–95].

Slow-roll eternal inflation occurs due to large adiabatic quantum fluctuations. In Chapter 13 we will introduce a new model based on our paper [10], which incorporates ideas of both inflation and ekpyrosis. We will construct an accelerated expanding phase – the conflationary phase – which does not suffer from slow-roll eternal inflation.

B. Ekpyrosis

A main challenge for any model with a contracting phase is the transition from contraction to expansion: the bounce. The realization of a healthy bouncing cosmology is a hard task. However, in the last 10 to 20 years a variety of models and ideas led to a better understanding of the bounce phase. We will discuss the developments and challenges of cosmic bounces in detail in Chapter 10. Even though effective field theoretical models like the Galileon bounce and the ghost condensate bounce are fairly well understood, it remains an open question whether such models can arise in a consistent theory of quantum gravity.

In Chapter 5 and Chapter 6 D we have reviewed the entropic mechanism. In this two-field model, nearly scale-invariant entropy perturbations are created in the presence of an unstable potential.

The initial conditions of ekpyrosis can be harder to fulfill, because of the tachyonic transverse direction. The addition of another matter content is one way to solve the initial condition problem [21]. The embedding in a cyclic model leads to a selection principle in the "phoenix universe" [27].

A major drawback of the entropic mechanism is the production of typically large non-Gaussian signatures. The constraints on non-Gaussianities by the Planck measurements challenges ekpyrosis. We have calculated the second order curvature perturbations $\mathcal{R}^{(2)}$, which were produced via a kinetic conversion phase before the bounce. We have obtained the non-Gaussian parameter

$$f_{NL} = \frac{3}{2}\kappa_3\sqrt{\epsilon} + 5, \tag{7.7}$$

where κ_3 parametrizes the symmetry of the two-field potential and ϵ is the fast roll parameter. Since $\epsilon \gg 3$ we require a symmetric potential in order to be in agreement with observations.
The entropic mechanism naturally predicts large non-Gaussianities and this very fact needs to be addressed in order to obtain a viable ekpyrotic model.

In this thesis, we will present two ways to improve the ekpyrotic scenario:

The non-minimal entropic mechanism [29–32] introduces a non-minimal kinetic coupling between two scalar fields. Due to this coupling, nearly scale-invariant entropy perturbations are produced. We have shown in [31] that in this model the intrinsic non-Gaussianities are precisely zero, which leads to overall small non-Gaussian corrections in agreement with the Planck measurements. The mechanism was also generalized for a larger class of non-minimal kinetic couplings [32] and it was shown that there are no initial condition problems in this mechanism [96]. We will discuss the non-minimal entropic mechanism and the results obtained in our paper [31] in the next chapter.

The conversion phase is an important step for a viable ekpyrotic model. We have discussed the kinetic conversion which takes place during the kinetic phase between ekpyrosis and the bounce. In Chapter 11 we will present the findings of our paper [9], which incorporates a kinetic conversion after the bounce. We will show that the value of the non-Gaussianity parameter f_{NL} is mainly determined by the conversion process after the bounce, while the intrinsic non-Gaussian contributions during ekpyrosis are suppressed. This means, that the typically large intrinsic non-Gaussianities produced via the entropic mechanism are not necessary in conflict with observations.

8. NON-MINIMAL ENTROPIC MECHANISM

In this chapter we will discuss an interesting alternative to the entropic mechanism. The drawback of an unstable potential and the inherent restrictions on the initial conditions are absent in this model [96]. The potential is independent of the second scalar field. In the non-minimal entropic mechanism a non-minimal coupling in the kinetic term of the second scalar field is introduced. This mechanism was first introduced by [29, 30] and the action takes the following form:

$$S = \int \mathrm{d}^4x\sqrt{-g}\left[\frac{R}{2} - \frac{1}{2}\partial_\mu\phi\partial^\mu\phi - \frac{1}{2}e^{-b\phi}\partial_\mu\chi\partial^\mu\chi + V_0e^{-c\phi}\right], \tag{8.1}$$

where b, c and V_0 are the parameters of this model. As we will see the non-minimal kinetic coupling provides a de Sitter-like background for the entropy perturbations leading to a nearly scale-invariant spectrum. The non-minimal entropic mechanism was also generalized for a larger class of non-minimal kinetic couplings in [32]. This mechanism is very similar to the pseudo-conformal mechanism [97, 98] and Galilean Genesis [99], where a non-minimal coupling in the kinetic term of a spectator field leads to nearly scale-invariant perturbations.

In the following, we will discuss the background evolution, which is essentially an ekpyrotic phase driven by a single scalar field ϕ with a constant spectator field χ. Afterwards we will calculate the behavior of the entropy perturbations to first order in perturbation theory.

In Chapter 8 C we will calculate the non-Gaussian corrections in the non-minimal entropic mechanism based on our paper [31]. The intrinsic non-Gaussianities are precisely zero leading to overall small non-Gaussian corrections in agreement with the Planck measurements. The following discussion is based on [31].

A. Background

The background equations of motion obtained from the action (8.1) in a flat FLRW universe are given by

$$\ddot{\phi} + 3H\dot{\phi} + cV_0e^{-c\phi} = -\frac{1}{2}be^{-b\phi}\dot{\chi}^2, \tag{8.2}$$

$$\ddot{\chi} + \left(3H - b\dot{\phi}\right)\dot{\chi} + e^{b\phi}V_{,\chi} = 0, \tag{8.3}$$

$$H^2 = \frac{1}{6}\left(\dot{\phi}^2 + e^{-b\phi}\dot{\chi}^2 - 2V_0e^{-c\phi}\right), \tag{8.4}$$

$$\dot{H} = -\frac{1}{2}\left(\dot{\phi}^2 + e^{-b\phi}\dot{\chi}^2\right). \tag{8.5}$$

Since the potential $V(\phi)$ is independent of χ, there is a solution with $\chi = const.$ and we chose coordinates such that

$$\chi = 0. \tag{8.6}$$

Thus the background evolution is described by a single scalar field in an ekpyrotic potential with the scaling solution , cf. (3.35):

$$a(t) \propto (-t)^{1/\epsilon}, \qquad \phi = \sqrt{\frac{2}{\epsilon}} \ln\left[-\left(\frac{V_0\epsilon^2}{(\epsilon-3)}\right)^{\frac{1}{2}} t\right], \qquad \epsilon = \frac{c^2}{2}. \tag{8.7}$$

Note that here we have not used the approximation that ϵ is large. This will become clear at a later stage. In order to solve the flatness problem we require $w > 1$ or $\epsilon > 3$ (i.e. $c^2 > 6$), where the equation of state was defined via $w = \epsilon/3 - 1$.

B. Linear Perturbations

In this chapter we will investigate the behavior of entropy perturbations in the non-minimal entropic model. The equations of motion to first order were calculated e.g. in [29, 30, 100] . A very useful approach is the so-called covariant cosmological perturbation theory [67, 101, 102], which will be used when calculating perturbations to higher order. For now we will just introduce a useful definition of the gauge-invariant entropy perturbation

$$\delta s = e^{-\frac{b}{2}\phi}\delta\chi, \tag{8.8}$$

where the additional factor $e^{-\frac{b}{2}\phi}$ is due to the non-minimal kinetic coupling.
We chose the longitudinal gauge, where the metric is given by

$$\mathrm{d}s^2 = -(1+2\Phi)\mathrm{d}t^2 + a^2(1-2\Phi)\mathrm{d}\mathbf{x}^2, \tag{8.9}$$

where Φ denotes the Bardeen potential and where we have assumed no anisotropic stress, as anisotropies are suppressed during ekpyrosis, leading to ($\Phi = \Psi$).
The equations of motion for χ to linear order reads [29, 30, 100]

$$\begin{aligned} &\ddot{\delta\chi} + (3H - b\dot{\phi})\dot{\delta\chi} + \left[\frac{k^2}{a^2} + e^{b\phi}V_{,\chi\chi}\right]\delta\chi - b\dot{\chi}\dot{\delta\phi} \\ &+ e^{b\phi}\left[V_{,\chi\phi} + bV_{,\chi}\right]\delta\phi = 4\dot{\chi}\dot{\Phi} - 2e^{b\phi}V_{,\chi}\Phi. \end{aligned} \tag{8.10}$$

Using the background solution the equation for χ becomes a closed equation. With $\dot{\chi} = 0$ and $V_{,\chi} = V_{,\phi\chi} = V_{,\chi\chi} = 0$ we obtain the equation of motion for the entropy perturbations δs to first order [100]:

$$\ddot{\delta s} + 3H\dot{\delta s} + \left[\frac{k^2}{a^2} - \frac{b^2}{4}\dot{\phi}^2 - \frac{b}{2}V_{,\phi}\right]\delta s = 0. \tag{8.11}$$

We again change to conformal time $\mathrm{d}t = a\mathrm{d}\tau$, and we chose the canonically normalized entropy perturbation $v_s \equiv a\delta s$, leading to

$$v_s'' + \left[k^2 - \frac{a''}{a} - \frac{b^2}{4}\phi'^2 - \frac{b}{2}a^2V_{,\phi}\right]v_s = 0, \tag{8.12}$$

where a prime denotes the derivative w.r.t conformal time τ. The last two terms in (8.12) are present due to the non-minimal coupling. We can make use of the background solution in order to calculate the different terms.

We have calculated the second term already in (4.110): Using $a(\tau) \propto (-\tau)^{1/(\epsilon-1)}$, we obtain

$$\frac{a''}{a} = -\frac{(\epsilon-2)}{(\epsilon-1)^2\tau^2}. \tag{8.13}$$

The velocity ϕ' in terms of the "fast-roll" parameter ϵ is given by

$$\phi' = \sqrt{2\epsilon}\mathcal{H} = \frac{\sqrt{2\epsilon}}{(\epsilon-1)\tau}. \tag{8.14}$$

In order to evaluate the last term, we can make use of $a^2V_{,\phi} = -\sqrt{2\epsilon}a^2V$ and the first Friedmann equation in conformal time:

$$a^2V = -a^2V_0e^{-c\phi} = 3\mathcal{H}^2 - \frac{1}{2}\phi'^2 = -\frac{(\epsilon-3)}{(\epsilon-1)^2\tau^2}\,. \tag{8.15}$$

Combining the above equations we obtain the equation of motion for the entropy perturbations to first order

$$v_s'' + \left[k^2 - \frac{1}{(\epsilon-1)^2\tau^2}\left(-\epsilon + 2 + \frac{b}{c}(\epsilon^2-3\epsilon) + \frac{b^2}{c^2}\epsilon^2\right)\right]v_s = 0\,, \tag{8.16}$$

where $\epsilon = c^2/2$. It is useful to define a new parameter Δ, which quantifies the difference of the two coefficients b and c

$$\frac{b}{c} \equiv 1 + \Delta\,. \tag{8.17}$$

The equation of motion can now be solved in terms of Hankel functions. Imposing Bunch-Davies vacuum initial conditions, we obtain (up to a phase)

$$v_s = \sqrt{\frac{\pi}{4}}\sqrt{-\tau}H_\nu^{(1)}(-k\tau)\,, \tag{8.18}$$

where the Hankel index ν is given by

$$\nu^2 = \frac{9}{4}\left(1 + \frac{2}{3}\frac{\Delta\epsilon}{(\epsilon-1)}\right)^2 \quad \rightarrow \quad \nu = \frac{3}{2} + \frac{\Delta\epsilon}{(\epsilon-1)}\,. \tag{8.19}$$

Remarkably, no approximation for ν had to be made, since the expression for ν^2 combines to a perfect square. The second solution $\nu = -\frac{3}{2} - \frac{\Delta\epsilon}{(\epsilon-1)}$ corresponds to an unstable solution and will not be considered further.

Making use of the late time behavior $|k\tau| \rightarrow 0$ of the Hankel function we obtain

$$v_s \propto k^{-\nu}(-\tau)^{1/2-\nu} \qquad (|k\tau| \ll 1), \tag{8.20}$$

while the spectral index is given by [29–31]

$$n_s = 4 - 2\nu = 1 - 2\Delta\frac{\epsilon}{(\epsilon-1)}. \tag{8.21}$$

In the case of $b = c$ we obtain an exactly scale-invariant spectrum. We can estimate the possible deviation from scale-invariance: since $\epsilon > 3$ we see that $n_s - 1$ is always between -3Δ and -2Δ. If b is about two percent larger than c we obtain a red spectrum with $n_s = 0.96$ in agreement with the Planck measurements [6]. It is important to note, that in the non-minimal entropic mechanism $\epsilon > 3$ in comparison to the entropic mechanism, in which $\epsilon \gg 1$. Consequently, the requirements on the steepness of the ekpyrotic potential is relaxed in the non-minimal entropic mechanism.

As already discussed in the case of the entropic mechanism in Chapter 5 C, the ekpyrotic potential should eventually flatten out – which corresponds to a diminishing c. We will use the analogous approach by introducing a slowly varying time-dependence of the parameter c.

Until now we have not made any approximations. In order to introduce a time-dependence we will use the limit $\epsilon \gg 1$ like in the minimal entropic mechanism. Using the e-folding time $dN = d\ln a$ we obtain the relations:

$$\mathcal{H} \approx (\epsilon\tau)^{-1}\left(1 + \frac{1}{\epsilon} + \frac{\epsilon_{,N}}{\epsilon^2}\right), \quad -\frac{a''}{a} = \mathcal{H}^2(\epsilon - 2) \approx \tau^{-2}\left(\frac{1}{\epsilon} - \frac{4}{\epsilon^3} + \frac{2\epsilon_{,N}}{\epsilon^3}\right), \tag{8.22}$$

and

$$\phi' = \sqrt{2\epsilon}\,\mathcal{H} \approx \tau^{-1}\sqrt{\frac{2}{\epsilon}}\left(1 + \frac{1}{\epsilon} + \frac{\epsilon_{,N}}{\epsilon^2}\right), \quad a^2 V_{,\phi} = \tau^{-2}\frac{1}{\sqrt{2\epsilon}}\left(2 - \frac{2}{\epsilon} + 3\frac{\epsilon_{,N}}{\epsilon^2}\right). \tag{8.23}$$

Plugging the expressions into the equations of motion (8.12) yields the following spectral index of the entropy perturbations [31]

$$n_s - 1 = -2\Delta - \frac{7}{3}\frac{\epsilon_{,N}}{\epsilon^2} \qquad (\epsilon \gg 1). \tag{8.24}$$

In analogy with a diminishing equation of state ϵ in the entropic mechanism we obtain a red spectrum. Note that $\epsilon_N > 0$, since N and ϵ decrease with time. This means the entropy perturbations are nearly scale-invariant with a red tilt due to the flattening of the potential and/or $b \neq c$.

Let us address the stability of the perturbative solution. We can find the solution of the original scalar field fluctuation $\delta\chi$ by making use of the late-time/large-scale expression for the mode functions (8.20) with ν given in (8.19) and the expression for the potential (8.15). We obtain

$$\delta\chi = e^{\frac{b}{2}\phi}\frac{v_s}{a} \propto (-a\tau)^{\frac{b}{c}}(-\tau)^{\frac{1}{2}-\nu}\frac{1}{a} = constant. \tag{8.25}$$

The original scalar field fluctuation $\delta\chi$ is constant – independent of ϵ and irrespective of whether $b = c$ or not. Thus this solution is stable and the fact that $\delta\chi$ is precisely constant will also have important implications for non-Gaussian corrections as we will see in the next chapter.

In this chapter we have seen how nearly scale-invariant entropy perturbations are created via a non-minimal kinetic coupling between the two fields. Let us try to understand how this mechanism works from another perspective. As already mentioned this mechanism is reminiscent of the pseudo-conformal mechanism [97, 98] and Galilean Genesis [99]. The second order action of the field fluctuation $\delta\chi$ reads

$$S^{(2)} = \int \mathrm{d}^4x\sqrt{-g}\,\Omega^2(\phi)\partial_\mu\delta\chi\partial^\mu\delta\chi \tag{8.26}$$

$$= \int \mathrm{d}^3x\mathrm{d}\tau a^2\,\Omega^2(\phi)\left((\delta\chi')^2 - (\partial_i\delta\chi)^2\right) \tag{8.27}$$

where in this model the non-minimal kinetic coupling reads $\Omega^2(\phi) = e^{b\phi}$, cf. (8.1). Using the scaling solution during ekpyrosis, using Eq. (8.15) and restricting to the case $c = b$, we find that $a^2\Omega^2(\phi) \sim \tau^{-2}$. The non-minimal kinetic coupling $\Omega^2(\phi)$ acts effectively as a de Sitter background for the fluctuations. This mechanism works, since the ekpyrotic potential $V(\phi) = V_0e^{-c\phi}$ scales in the same way as the non-minimal kinetic coupling. We can now generalize this mechanism: suppose we change the potential slightly leading to a slight change in the ekpyrotic scaling solution. We can then find a non-minimal kinetic coupling, such that $a^2\Omega^2(\phi) \sim \tau^{-2}$. This generalization was first considered in [32] and allows for various pairs of $(V(\phi), \Omega(\phi))$.

We have shown that the variance Δ_s^2 has a slight scale dependence, if the potential flattens out or/and if $b \neq$ c (note that $\Delta_s^2 = \frac{k^3}{2\pi^2}P_s$, which should not be confused with the definition $\frac{b}{c} \equiv 1 + \Delta$ determining the difference between b and c). It could also be possible that the spectral index depends on the scale – this is called the running of the spectral index.

The spectral index is defined via

$$n_s - 1 \equiv \frac{d\ln\Delta_s^2}{d\ln k} = -\frac{d\ln\Delta_s^2}{d\mathcal{N}}, \tag{8.28}$$

while the running is defined via

$$\alpha_s \equiv \frac{dn_s}{d\ln k} = -\frac{dn_s}{d\mathcal{N}}. \tag{8.29}$$

It has been shown in [103], that the running α_s in the non-minimal entropic mechanism is $\alpha_s \approx -10^{-2}$ to -10^{-3}. The running is fairly large, if the generation of the red spectrum is entirely due to the diminishing ϵ (the second term in Eq. (8.24)), while the running is smaller if $b \neq c$ causes the red spectrum. In both cases the running α_s is larger compared to most inflationary models and the new ekpyrotic scenario [103], which could provide an important distinction in future observations.

C. Non-Gaussian Corrections

In the following, we will calculate the non-Gaussian corrections for the non-minimal entropic mechanism based on our findings in [31] . The evolution equations for the second order curvature and entropy perturbations will be derived and discussed. The action for this model was given by:

$$S = \int \mathrm{d}^4x\sqrt{-g}\left[\frac{R}{2} - \frac{1}{2}\partial_\mu\phi\partial^\mu\phi - \frac{1}{2}e^{-b\phi}\partial_\mu\chi\partial^\mu\chi + V_0e^{-c\phi}\right]. \tag{8.30}$$

The kinetic terms of the scalar fields can be written in the form

$$-\frac{1}{2}(\partial\phi)^2 - \frac{1}{2}e^{-b\phi}(\partial\chi)^2 \equiv -\frac{1}{2}G_{IJ}\partial^\mu\phi^I\partial_\mu\phi^J, \tag{8.31}$$

where now $\phi^I = (\phi, \chi)$ and I, J can take the values $1, 2$. Here we have introduced a field space metric; the field space metric and its inverse are given by

$$G_{IJ} = \begin{pmatrix} 1 & 0 \\ 0 & e^{-b\phi} \end{pmatrix}, \quad \text{and} \quad G^{IJ} = \begin{pmatrix} 1 & 0 \\ 0 & e^{b\phi} \end{pmatrix}. \tag{8.32}$$

The field space metric leads to non-trivial connections given by

$$\Gamma^1_{22} = \Gamma^\phi_{\chi\chi} = \frac{b}{2}e^{-b\phi}, \quad \Gamma^2_{12} = \Gamma^\chi_{\phi\chi} = -\frac{b}{2}, \tag{8.33}$$

while the only non-trivial component (up to those related by symmetry) of the Riemann tensor is

$$R^1{}_{212} = R^\phi{}_{\chi\phi\chi} = -\frac{b^2}{4}e^{-b\phi}. \tag{8.34}$$

We can also define the zweibeine

$$e_\sigma^I = (-1, 0), \quad e_s^I = (0, e^{\frac{b}{2}\phi}), \tag{8.35}$$

which allow us to rotate the field fluctuations at linear order into the adiabatic and entropy fluctuations

$$\delta\sigma \equiv e_{\sigma I}\, \delta\phi^I = -\delta\phi \qquad \text{and} \qquad \delta s \equiv e_{sI}\, \delta\phi^I = e^{-\frac{b}{2}\phi}\delta\chi. \tag{8.36}$$

Here we recognize the definition of the entropy perturbations to first order in the previous chapter. Note that within this setup we must take $e_\sigma{}^1 = -1$; this is because σ is defined to increase along the background trajectory [101] and thus also $\dot\sigma = -\dot\phi$ is the velocity of the background trajectory in the constant χ backgrounds that we are interested in. We can also define inverse zweibeine via

$$\delta\phi^I = e_\alpha{}^I\, \delta\sigma^\alpha, \tag{8.37}$$

where $\delta\sigma^\alpha = (\delta\sigma, \delta s)$ to linear order.

As shown in [101] we can define the adiabatic and entropic perturbations at second order

$$\delta\sigma^{(2)} \equiv e_{\sigma I}\, \delta^{(2)}\phi^I + \frac{1}{2} e_{\sigma J}\Gamma^J_{LK}(e_\alpha{}^K e_\beta{}^L \delta\sigma^\alpha\delta\sigma^\beta) + \frac{1}{2\dot\sigma}\delta s\dot{\delta s}\,, \tag{8.38}$$

$$\delta s^{(2)} \equiv e_{sI}\, \delta^{(2)}\phi^I + \frac{1}{2} e_{sJ}\,\Gamma^J_{LK}(e_\alpha{}^K e_\beta{}^L \delta\sigma^\alpha\delta\sigma^\beta) - \frac{\delta\sigma}{\dot\sigma}(\dot{\delta s} - \frac{V_{,s}}{2\dot\sigma})\,. \tag{8.39}$$

In our model this yields

$$\delta\sigma^{(2)} = -\delta\phi^{(2)} + \frac{\delta s}{2}\left(\frac{\dot{\delta s}}{\dot\sigma} - \frac{b}{2}\delta s\right), \tag{8.40}$$

$$\delta s^{(2)} = e^{-\frac{b}{2}\phi}\delta\chi^{(2)} + \delta\sigma\left(\frac{b}{4}\delta s - \frac{\dot{\delta s}}{\dot\sigma} + \frac{V_{,s}}{2\dot\sigma^2}\delta\sigma\right). \tag{8.41}$$

The fact that the potential does not depend on the second scalar field χ has crucial consequences on the non-Gaussian corrections. If we expand the action up to third order, no cubic terms in $\delta\chi$ can arise. But these terms are precisely the interaction-terms, which give rise to non-Gaussianities as shown in Chapter 6. Hence there are no intrinsic non-Gaussian corrections in the non-minimal entropic mechanism:

$$\delta\chi^{(2)} = \delta s^{(2)} = 0 \tag{8.42}$$

Let us verify this statement by inspecting the second order equations of motion. Since the potential does not depend on χ, and the background solution satisfies $\dot\chi = 0$, it is immediately clear that the perturbed equation of motion will be identical to that at first order:

$$\frac{\mathrm{d}^2}{\mathrm{d}t^2}(\delta\chi^{(1)} + \delta\chi^{(2)}) + (3H - b\dot\phi)\frac{\mathrm{d}}{\mathrm{d}t}(\delta\chi^{(1)} + \delta\chi^{(2)}) + \frac{k^2}{a^2}(\delta\chi^{(1)} + \delta\chi^{(2)}) = 0. \tag{8.43}$$

There is no source term for $\delta\chi^{(2)}$ in the equation of motion (since there is no cubic term in the action). Equivalently there is no source term for $\delta s^{(2)}$ in the corresponding equation for the entropy perturbations at second order:

$$\ddot{\delta s}^{(2)} + 3H\dot{\delta s}^{(2)} + \left[\frac{k^2}{a^2} - \frac{b^2}{4}\dot{\phi}^2 - \frac{b}{2}V_{,\phi}\right]\delta s^{(2)} = 0, \tag{8.44}$$

where we have used the definition of the second order entropy perturbations (8.40) in the comoving gauge $\delta\sigma = \delta\sigma^{(2)} = 0$. Since there is no source term, the solution is indeed given by

$$\delta\chi^{(2)} = \delta s^{(2)} = 0. \tag{8.45}$$

Note that the linear solution $\delta\chi = const.$ is non-zero due to the quantization of the perturbations, which obey the Heisenberg uncertainty relations.

The intrinsic non-Gaussian corrections vanish in the non-minimal entropic mechanism, which is in direct contrast to the sizable intrinsic non-Gaussianities produced in the entropic mechanism, cf. Chapter 6 D. However, it is still possible that first order entropy perturbations could source second order curvature perturbations during ekpyrosis due to non-linear effects, as discussed in Chapter 6 E. In order to calculate the evolution of the comoving curvature perturbation to second order we have to expand the general evolution equation (6.43), namely

$$\dot{\mathcal{R}} = \frac{2H\delta V}{\dot{\sigma}^2 - 2\delta V}\,, \tag{8.46}$$

up to second order in perturbations.

Let us start by expanding the potential up to second order:

$$\delta V = V_I\,\delta\phi^I + V_I\,\delta^{(2)}\phi^I + \frac{1}{2}V_{,IJ}\delta\phi^I\delta\phi^J. \tag{8.47}$$

Making use of the identities

$$\delta_I^M = e_{\sigma I}\,e_\sigma{}^M + e_{sI}\,e_s{}^M, \tag{8.48}$$

and

$$1 = e_{\sigma I}\,e_\sigma{}^I = e_{sI}\,e_s{}^I, \tag{8.49}$$

we obtain

$$\begin{aligned}
\delta V &= V_I\,e_\alpha{}^I\,\delta\sigma^\alpha + V_I\,e_\sigma{}^I\left[\delta\sigma^{(2)} - \frac{1}{2}e_{\sigma J}\,\Gamma^J_{LK}(e_\alpha{}^K e_\beta{}^L\delta\sigma^\alpha\delta\sigma^\beta) - \frac{1}{2\dot{\sigma}}\delta s\dot{\delta s}\right] \\
&\quad + V_I\,e_s{}^I\left[\delta s^{(2)} - \frac{1}{2}e_{sJ}\,\Gamma^J_{LK}(e_\alpha{}^K e_\beta{}^L\delta\sigma^\alpha\delta\sigma^\beta) + \frac{\delta\sigma}{\dot{\sigma}}(\dot{\delta s} - \frac{V_{,s}}{2\dot{\sigma}})\right] + \frac{1}{2}V_{,IJ}\,e_\alpha{}^I\,e_\beta{}^J\,\delta\sigma^\alpha\,\delta\sigma^\beta \\
&= V_I\,e_\alpha{}^I\,\delta\sigma^\alpha + V_I\,e_\sigma{}^I\left[\delta\sigma^{(2)} - \frac{1}{2\dot{\sigma}}\delta s\dot{\delta s}\right] \\
&\quad + V_I\,e_s{}^I\left[\delta s^{(2)} + \frac{\delta\sigma}{\dot{\sigma}}(\dot{\delta s} - \frac{V_{,s}}{2\dot{\sigma}})\right] + \frac{1}{2}V_{;IJ}\,e_\alpha{}^I\,e_\beta{}^J\,\delta\sigma^\alpha\,\delta\sigma^\beta,
\end{aligned} \tag{8.50}$$

where we have defined $V_{;IJ} = V_{,IJ} - \Gamma^K_{IJ} V_{,K}$. In comoving gauge $\delta\sigma = \delta\sigma^{(2)} = 0$ and hence

$$\delta V = V_{,s}\left(\delta s + \delta s^{(2)}\right) - \frac{V_{,\sigma}}{2\dot\sigma}\delta s\dot{\delta s} + \frac{1}{2}V_{;ss}\,\delta s^2. \tag{8.51}$$

The evolution of the comoving curvature perturbation (8.46) up to second order then becomes

$$\begin{aligned}\dot{\mathcal{R}}^{(1)} + \dot{\mathcal{R}}^{(2)} &= \frac{2H\delta V}{\dot\sigma^2 - 2\delta V} \\ &\approx \frac{2H}{\dot\sigma^2}\delta V[1 + 2\dot\sigma^{-2}\delta V] \\ &= \frac{2H}{\dot\sigma^2}\left[V_{,s}\left(\delta s + \delta s^{(2)}\right) - \frac{V_{,\sigma}}{2\dot\sigma}\delta s\dot{\delta s} + \left(\frac{1}{2}V_{;ss} + 2\frac{V_{,s}^2}{\dot\sigma^2}\right)\delta s^2\right].\end{aligned} \tag{8.52}$$

Such an expansion is justified when $|\delta V/\dot\sigma^2| \ll 1$. In realistic cases, assuming the conversion process lasts longer than 10^{-3} or so e-folds ($\Delta N > 10^{-3}$), this is easily satisfied as at linear order we must obtain

$$\mathcal{R}^{(1)} = \int \frac{2H\delta V}{\dot\sigma^2}\mathrm{d}t = \int \frac{2\delta V}{\dot\sigma^2}\mathrm{d}N \sim \frac{\delta V}{\dot\sigma^2}\Delta N \sim 10^{-5} \tag{8.53}$$

in order to match observations.

We need to look at equation (8.52) both during the ekpyrotic phase and during the conversion phase. In fact, at second order some conversion can already happen during the ekpyrotic phase, where at the linearized level the entropy and curvature modes are entirely decoupled. During the ekpyrotic phase, equation (8.52) reduces to

$$\begin{aligned}\dot{\mathcal{R}}^{(2)} &= \frac{H}{\dot\sigma^2}\left[V_{,\sigma}\left(-\frac{1}{\dot\sigma}\delta s^{(1)}\dot{\delta s^{(1)}}\right) + V_{;ss}\,\delta s^{(1)2}\right] \\ &= \frac{H}{\dot\sigma^2}\left[\frac{V_{,\phi}}{\dot\sigma}\delta s^{(1)}\dot{\delta s^{(1)}} - e_s{}^\chi\, e_s{}^\chi\, \Gamma^\phi_{\chi\chi}\, V_{,\phi}\,\delta s^{(1)2}\right] \\ &= \frac{HV_{,\phi}}{\dot\sigma^2}\delta s^{(1)}\left(\frac{\dot{\delta s^{(1)}}}{\dot\sigma} - \frac{b}{2}\delta s^{(1)}\right),\end{aligned} \tag{8.54}$$

or, in conformal time

$$\mathcal{R}^{(2)\prime} = \frac{\mathcal{H}a^2 V_{,\phi}}{\sigma'^2}\delta s^{(1)}\left(\frac{\delta s^{(1)\prime}}{\sigma'} - \frac{b}{2}\delta s^{(1)}\right). \tag{8.55}$$

Using the late-time/large-scale expression for the entropy mode functions during the ekpyrotic phase (8.20), we obtain

$$\begin{aligned}\frac{\delta s^{(1)\prime}}{\sigma'} - \frac{b}{2}\delta s^{(1)} &= \frac{1}{a}\left[\frac{v_s'}{\sigma'} - \frac{\mathcal{H}v_s}{\sigma'} - \frac{b}{2}v_s\right] \\ &= \frac{v_s}{a}\left[(-1 - \frac{\Delta\epsilon}{\epsilon - 1})(-\frac{\epsilon - 1}{\sqrt{2\epsilon}}) - \frac{1}{\epsilon - 1}(-\frac{\epsilon - 1}{\sqrt{2\epsilon}}) - \frac{b}{2}\right] \\ &= 0\,.\end{aligned} \tag{8.56}$$

Thus, amazingly enough, no second-order curvature perturbations are generated during the ekpyrotic phase when c is a constant. This can be understood from the fact that the linearized solution is given by $\delta\chi^{(1)} = constant$, cf. Eq. (8.25), and thus the linearized solution behaves exactly like the background. If one thinks of the perturbation in the potential $\delta V^{(2)}$ at second order (in Eq. (8.46)) as a linear perturbation around the linearized solution, then it is clear that this vanishes in the same way as the linear perturbation vanishes around the constant χ background solution. In summary, we are finding that the ekpyrotic phase produces no local non-Gaussianity at all, both for the entropy and the curvature fluctuations, when the equation of state is constant.

The above results also hold true for the generalized non-minimal entropic mechanism [32]. Let us review a simple argument that the intrinsic non-Gaussian contributions also vanish in this case. From the second order action, cf. (8.26),

$$S^{(2)} = \int \mathrm{d}^4x\sqrt{-g}\,\Omega^2(\phi)\partial_\mu\delta\chi\partial^\mu\delta\chi \tag{8.57}$$

we obtain the equations of motion

$$\nabla^\nu\left(\Omega^2\partial_\nu(\delta\chi)\right) = 0, \tag{8.58}$$

where ∇^ν denotes the covariant derivative. Using the definition $\delta s = \Omega\delta\chi$ and the solution to the equations of motion $\delta\chi = const.$, we find $\delta s \sim \Omega$. The evolution equation for the comoving curvature perturbations up to second order with a generalized kinetic coupling reads [32]

$$\mathcal{R}^{(2)\prime} = \frac{\mathcal{H}a^2V_{,\phi}}{\sigma'^2}\delta s^{(1)}\left(\frac{\Omega_{,\phi}}{\Omega}\delta s^{(1)} - \frac{\delta s^{(1)\prime}}{\phi'}\right). \tag{8.59}$$

Now using the fact that $\delta s \sim \Omega$, we obtain

$$\frac{(\delta s)'}{\delta s} = \frac{\Omega'}{\Omega} = \frac{\Omega_{,\phi}}{\Omega}\phi', \tag{8.60}$$

which leads to $\mathcal{R}^{(2)\prime} = 0$, and thus the intrinsic non-Gaussian corrections also vanish in the generalized non-minimal entropic mechanism.

In Chapter 8 B, we argued that a natural extension is to allow the equation of state (or fast-roll) parameter ϵ to be a slowly varying function of time. In that case the time-dependence of the entropic mode functions is sightly modified, and we obtain

$$\frac{\delta s^{(1)\prime}}{\sigma'} - \frac{b}{2}\delta s^{(1)} = \frac{1}{6}\frac{v_s}{a}\sqrt{\frac{\epsilon}{2}}\frac{\epsilon_{,N}}{\epsilon^2}. \tag{8.61}$$

Then there exists a small source term for the second-order curvature perturbation during the ekpyrotic phase, with

$$\begin{aligned}\mathcal{R}^{(2)\prime} &= -\frac{\mathcal{H}}{\sigma'^2}a^2 V_{,\sigma}\delta s^{(1)}\left[\frac{\delta s^{(1)\prime}}{\sigma'} - \frac{b}{2}\delta s^{(1)}\right] \\ &= -\frac{1}{12}\frac{v_s^2}{a^2}\frac{1}{(-\tau)}\frac{\epsilon_{,N}}{\epsilon^2}\,.\end{aligned} \tag{8.62}$$

If we approximate the time dependence of the fluctuation modes $v_s/a \propto 1/\tau$ then we can easily perform the integral, obtaining [31]

$$\mathcal{R}^{(2)}_{ek} = -\frac{1}{24}(\delta s_{ek-end})^2\frac{\epsilon_{,N}}{\epsilon^2}\,. \tag{8.63}$$

We can see that the coefficient of $(\delta s_{ek-end})^2$ is tiny, of $\mathcal{O}(10^{-3})$ at most for realistic cases. Thus, the non-minimal entropic mechanism generates almost perfectly Gaussian entropy perturbations over the course of the ekpyrotic phase.

D. Discussion

In this chapter, we have discussed a very promising ekpyrotic model. The background is stable, and the ekpyrotic solution is an attractor [96]. The non-minimal entropic mechanism produces nearly scale-invariant entropy perturbations. The intrinsic non-Gaussianities of these perturbations vanish exactly, and the sourcing due to non-linear effects during ekpyrosis is very small – this also holds true for the generalized non-minimal entropic mechanism in [32]. Moreover, it has been shown in [104] that the intrinsic non-Gaussianities to third order also vanish.

An important step is the conversion phase, which we have discussed in detail in Chapter 6 E. The conversion in the case of a non-minimal kinetic coupling up to third order in perturbations was studied in [104]: The analysis suggests that the non-minimal kinetic coupling has to turn off before the conversion phase. Different scenarios were studied, and the results are in agreement with the kinetic conversion covered in Chapter 6 E. The recently proposed Swampland conjecture [105–108] could also apply to the non-minimal entropic mechanism. The Swampland conjecture constrains the effective field theories which are consistent with a quantum theory of gravity. In particular, effective field theories are only viable in a field space range up to $\Delta\phi \sim \mathcal{O}(1)$. This means that the ekpyrotic phase, the bounce phase, and the conversion phase should be described by different effective field theories. One has to see which implications the String Swampland will have on the development of effective field theory models and consequently on cosmology.

We have obtained the expansion of the entropy perturbations during ekpyrosis in the presence of an unstable potential in (6.37)

$$\delta s = \delta s_L + \frac{\kappa_3 \sqrt{\epsilon}}{8} \delta s_L^2 \,, \tag{8.64}$$

which defines the initial conditions after the ekpyrotic phase, where $\delta s_L \sim \frac{1}{t}$. In the case of the non-minimal entropic mechanism, the second order entropy perturbations vanish:

$$\delta s_L \sim \frac{1}{t} \quad , \quad \delta s^{(2)} = 0 \,. \tag{8.65}$$

In the case of the non-minimal entropic mechanism we can use the expansion (8.64) by choosing $\kappa_3 = 0$. Thus we immediately obtain an estimate for the non-Gaussianity parameter analogous to the discussion in Chapter 6 E:

$$f_{NL}^{local} = \pm 5 \,. \tag{8.66}$$

For a more detailed analysis of the conversion process up to third order see [104]; in this work, the trispectrum was calculated:

$$g_{NL} \sim \mathcal{O}(-10^2) \quad \text{to} \quad \mathcal{O}(-10^3) \,, \tag{8.67}$$

which is negative. Moreover, it has been shown that the running of the spectral index n_s is larger than in single field inflationary models [103]:

$$\alpha_s \sim \mathcal{O}(-10^{-3}) \quad \text{to} \quad \mathcal{O}(-10^{-2}) \,. \tag{8.68}$$

The non-minimal entropic mechanism leads to distinct predictions. However, there is one crucial step left: the transition from contraction to expansion via a cosmological bounce. If we cannot track the evolution of the background and the perturbations through the bouncing phase, then the predictability of the ekpyrotic scenario is lost. In the following chapters, we will discuss the challenges and developments of bouncing cosmologies.

9. GALILEON THEORY

In this chapter, we will discuss Galileon theory, which is a higher derivative theory including a variety of known theories. As we will see the Galileon theory allows for non-singular bounce solutions, which we will cover in detail in Chapter 10.

A. Introduction

Galileon theory was first introduced in [109] in flat space and later generalized in [110–112]. Generalized Galileon theory describes the most general single scalar field Lagrangian (containing higher time derivatives), which yields second order equations of motion. It turned out that Galileon theory is equivalent to Horndenski theory [113], which was formulated more than 30 years earlier. The generalized Galileon action for a single scalar field coupled to gravity is given by [112]:

$$S = \sum_{i=2}^{5} \int \mathrm{d}^4 \sqrt{-g} \mathcal{L}_i, \tag{9.1}$$

with

$$\mathcal{L}_2 = K(X, \phi)\,, \tag{9.2}$$

$$\mathcal{L}_3 = -G_3(X, \phi)\Box\phi\,, \tag{9.3}$$

$$\mathcal{L}_4 = G_4(X, \phi)R + G_{4X}\left[(\Box\phi)^2 - (\nabla_\mu\nabla_\nu\phi)^2\right]\,, \tag{9.4}$$

$$\mathcal{L}_5 = G_5(X, \phi)G_{\mu\nu}\nabla^\mu\nabla^\nu\phi + \frac{G_{5X}}{6}\left[(\Box\phi)^3 - 3\Box\phi(\nabla_\mu\nabla_\nu\phi)^2 + 2(\nabla_\mu\nabla_\nu\phi)^3\right]\,. \tag{9.5}$$

Here $X = -\frac{1}{2}g^{\mu\nu}\partial_\mu\partial_\nu$ is the standard kinetic term, R is the Ricci scalar, $G_{\mu\nu}$ is the Einstein tensor, $(\nabla_\mu\nabla_\nu\phi)^2 = \nabla_\mu\nabla_\nu\phi\nabla^\mu\nabla^\nu\phi$ and $G_{iX} = \frac{\partial G_i}{\partial X}$.

The Galileon action contains a variety of known theories:

- For $G_3 = G_5 = 0$, $G_4 = \frac{1}{2}$ and $K(X, \phi) = X - V(\phi)$ we recover the action for a scalar field minimally coupled to gravity in a potential.
- For $G_3 = G_5 = 0$, $G_4 = \frac{1}{2}$ and $K(X, \phi)$ the theory describes a scalar field with a non-standard kinetic term. Prominent examples are k-essence models of dark energy [114] (or inflation), the Dirac-Born-Infeld action [115] and the ghost condensate [20, 24, 116–118].

- For $G_4 = \frac{1}{2}F(\phi)$ the scalar field is non-minimally coupled to gravity. The well known Brans-Dicke theory [119] is an example of such a scalar-tensor theory. In Chapter 13 we will construct a model where the scalar field is non-minimally coupled to gravity

- For non-zero G_3 the Galileon term is present. In the decoupling limit of the Dvali-Gabadaze-Poratti brane model [120] there is a specific cubic self-interaction term present: the Galileon term. This term was later generalized in the Galileon model [111].

- The term $G_5 \neq 0$ arises for example in Kaluza-Klein compactification of higher-dimensional Lovelock gravity [121]. Another example is covariant Galileon theory [110] which is obtained by the choosing $G_3 = X$, $G_4 = X^2$ and $G_5 = X^2$. We will omit this term from now on, since we will not consider such models.

B. Background Equations

In the following, we will derive the equations of motion obtained from (9.1). An easy way to obtain the equations of motion is to substitute $\phi = \phi(t)$ and $\mathrm{d}s^2 = -N^2\mathrm{d}t^2 + a^2(t)\mathrm{d}\mathbf{x}^2$ into the action (9.1) and then vary the action w.r.t $N(t)$, a(t) and $\phi(t)$. The variation w.r.t $N(t)$ gives the Friedmann equation [112]

$$\sum_{i=2}^{5} \varepsilon_i = 0, \tag{9.6}$$

where

$$\varepsilon_2 = 2XK_X - K\,, \tag{9.7}$$

$$\varepsilon_3 = 6X\dot{\phi}HG_{3X} - 2XG_{3\phi}\,, \tag{9.8}$$

$$\varepsilon_4 = -6H^2G_4 + 24H^2X\left(G_{4X} + XG_{4XX}\right) - 12HX\dot{\phi}G_{4\phi X} - 6H\dot{\phi}G_{4\phi}\,. \tag{9.9}$$

The variation w.r.t $a(t)$ leads to the evolution equation [112]

$$\sum_{i=2}^{5} \mathcal{P}_i = 0, \tag{9.10}$$

where

$$\mathcal{P}_2 = K\,, \tag{9.11}$$

$$\mathcal{P}_3 = -2X\left(G_{3\phi} + \ddot{\phi}G_{3X}\right)\,, \tag{9.12}$$

$$\mathcal{P}_4 = 2\left(3H^2 + 2\dot{H}\right)G_4 + 2\left(\ddot{\phi} + 2H\dot{\phi}\right)G_{4\phi} + 4XG_{4\phi\phi} + \tag{9.13}$$

$$+ 4X\left(\ddot{\phi} - 2H\dot{\phi}\right) G_{4\phi X} - 12H^2 X G_{4X} - 4H\dot{X}G_{4X} - 8\dot{H}XG_{4X} - 8HX\dot{X}G_{4XX}\,. \quad (9.14)$$

And finally the variation w.r.t $\phi(t)$ yields the scalar field equation of motion [112]

$$\frac{1}{a^3}\frac{d}{dt}\left(a^3 J\right) = P_\phi, \quad (9.15)$$

where

$$J = \dot{\phi}K_X - 2\dot{\phi}G_{3\phi} + 6HXG_{3X} + 6H^2\dot{\phi}\left(G_{4X} + 2XG_{4XX}\right) - 12HXG_{\phi X}\,, \quad (9.16)$$

$$P_\phi = K_\phi + 6\left(2H^2 + \dot{H}\right)G_{4\phi} - 2X\left(G_{3\phi\phi} + \ddot{\phi}G_{3\phiX}\right) + 6H\left(\dot{X} + 2HX\right)G_{4\phi X}\,. \quad (9.17)$$

C. Ostrogradski Theorem

Higher derivative scalar theories arise naturally in effective field theories and give rise to a variety of cosmological models. Higher derivative theories allow for non-singular bounce solutions as we will see in Chapter 10. Before we proceed we will discuss the so-called Ostrogradski Theorem, see e.g. [122].

The Ostrogradski Theorem states, that if a Lagrangian depends nondegenerately on second order (or higher) time derivatives, there exists a linear instability in the Hamiltonian. Non-degenerately means that the higher time derivatives cannot be eliminated by partial integration. It also means that one can invert the equation for the canonical momentum, as we will see below.

Thus Lagrangians with higher derivatives are unstable unless these higher derivatives can be eliminated or canceled, such that the equations of motions are 2nd order in time derivatives. This is precisely why Galileon/Horndenski theory does not suffer from the Ostrogradski instability: generalized Galileon theory is the most general scalar field theory coupled to gravity, which admits 2nd order equations of motions.

Here we will briefly show how the Ostrogradski theorem arises following [122]. Consider the Lagrangian $L = L(q, \dot{q}, \ddot{q})$, which depends nondegenerately on $\ddot{q}$. The Euler-Lagrange equation is given by

$$\frac{\partial L}{\partial q} - \frac{d}{dt}\frac{\partial L}{\partial \dot{q}} + \frac{d^2}{dt^2}\frac{\partial L}{\partial \ddot{q}} = 0\,. \quad (9.18)$$

Because of the non-degeneracy $\frac{\partial L}{\partial \ddot{q}}$ depends on $\ddot{q}$ leading to an equation of motion of the form: $q^{(4)} = F(q, \dot{q}, \ddot{q}, q^{(3)})$ and a solution of the form:

$$q(t) = Q\left(t, q_0, \dot{q}_0, \ddot{q}_0, q_0^{(3)}\right)\,, \quad (9.19)$$

where $q^{(3)}$ and $q^{(4)}$ are the third and forth time derivative of q respectively. We need four initial conditions thus there are four canonical variables. We choose:

$$Q_1 \equiv q \quad , \quad P_1 \equiv \frac{\partial L}{\partial \dot{q}} + \frac{d}{dt}\frac{\partial L}{\partial \ddot{q}} \tag{9.20}$$

$$Q_2 \equiv \dot{q} \quad , \quad P_2 \equiv \frac{\partial L}{\partial \ddot{q}} \,. \tag{9.21}$$

The non-degeneracy allows to invert the above equation, such that we can write $\ddot{q}$ in terms of Q_1,Q_2 and P_2, which means there exists a function $a(Q_1, Q_2, P_2)$ such that

$$\frac{\partial L}{\partial \ddot{q}}|_{q=Q_1,\dot{q}=Q_2,\ddot{q}=a} = P_2 \,. \tag{9.22}$$

If the Lagrangian is degenerate, then this inversion is not possible and thus the instability can be avoided. The Hamiltonian is obtained by a Legendre transformation with $\dot{q} = q^{(1)}$ and $\ddot{q} = q^{(2)}$:

$$H(Q_1, Q_2, P_1, P_2) \equiv \sum_{i=1}^{2} P_i q^{(i)} - L \tag{9.23}$$

$$= P_1 Q_2 + P_2 a(Q_1, Q_2, P_2) - L(Q_1, Q_2, a(Q_1, Q_2, P_2)) \,. \tag{9.24}$$

The Hamiltonian (9.23) depends linearly on the canonical momentum P_1. The system is not bound from below or above – P_1 can have any values filling the whole phase space direction.

The linear instability has severe consequences. Let us consider an interacting theory: nothing forbids the system to decay into a waste collection of positive and negative energy particles.

In the case of Galileon theory the Ostrogradski instability is absent, since the equations of motion are second order in time derivatives. For example the term proportional to G_{4X} in (9.4) is chosen such that the higher derivatives are canceled out in the equations of motion.

D. Perturbations for Generalized Galileon Theory

In order to calculate the tensor and scalar perturbations in generalized Galileon theories it is customary to use the ADM-decomposition [57] in the comoving gauge with $\delta\phi = 0$.

We have already calculated the second order action in the case of a single scalar field minimally coupled to gravity in Chapter 4 B . We can follow an analogous calculation using the generalized Galileon action (9.1). We write the perturbed metric as

$$\mathrm{d}s^2 = -N^2 \mathrm{d}t^2 + \gamma_{ij}(\mathrm{d}x^i + N^i \mathrm{d}t)(\mathrm{d}x^j + N^j \mathrm{d}t) \,, \tag{9.25}$$

where N is the lapse function and N_i is the shift vector

$$N = 1 + \alpha \quad , \quad N_i = \partial_i \beta \quad , \quad \gamma_{ij} = a^2(t) e^{2\mathcal{R}} \left(\delta_{ij} + h_{ij} + \frac{1}{2} h_{ik} h_{kj} \right) . \tag{9.26}$$

α, β and $\mathcal{R}$ are the scalar perturbations and h_{ij} is the tensor perturbation. In order to calculate the quadratic action for the scalar and tensor perturbations, we proceed analogously to the standard single scalar field case. We plug the above expressions into the action, and after varying the action w.r.t α and β, we obtain two constraint equations. Using the constraint equations, we can eliminate α and β from the action and obtain the tensor perturbation h_{ij} and one physical scalar degree of freedom: the comoving curvature perturbation $\mathcal{R}$.

1. Tensor Perturbations

The quadratic action for the tensor perturbations reads [112]

$$S = \frac{1}{8}\int \mathrm{d}t\mathrm{d}^3x a^3 \left(\mathcal{G}_T \dot{h}_{ij}^2 - \frac{\mathcal{F}_T}{a^2}(\vec{\nabla} h_{ij})^2\right) , \tag{9.27}$$

where

$$\mathcal{G}_T := 2G_4 \,, \tag{9.28}$$

$$\mathcal{F}_T := 2G_4 - 4XG_{4X} \,. \tag{9.29}$$

The sound speed of the tensor perturbations is given by

$$c_s^2 = \frac{\mathcal{F}_T}{\mathcal{G}_T} \,. \tag{9.30}$$

Thus in scalar-tensor theories and Galileon theories with $G_{4X} = 0$ the sound speed is $c_s^2 = 1$ (as we will see this is not the case for scalar perturbations). As a side note: the detection of gravitational waves from a binary black hole merger by LIGO in 2016 [123] constrains dark energy models based on modified gravity. Galileon dark energy models with non-minimal derivative coupling to gravity are in tension with observations, because the sound speed is measured to be close to one.

From the action (9.27) ghost and gradient instabilities are avoided if

$$\mathcal{G}_T > 0 \quad , \quad \mathcal{F}_T > 0. \tag{9.31}$$

We will discuss ghost and gradient instabilities for tensor and scalar perturbations in Galileon theories in the next chapter.

As usual it is customary to canonically normalize the perturbations, introducing

$$\mathrm{d}y_T := \frac{c_T}{a}\mathrm{d}t \,, \tag{9.32}$$

$$z_T := \frac{a}{2}(\mathcal{F}_T\mathcal{G}_T)^{1/4}\,, \tag{9.33}$$

$$v_{ij} := z_T h_{ij}\,, \tag{9.34}$$

leads to the quadratic action for the canonically normalized tensor modes

$$S = \frac{1}{2}\int \mathrm{d}y_T \mathrm{d}^3x \left(v_{ij}'^2 - (\vec{\nabla}v_{ij})^2 + \frac{z_T''}{z_T}v_{ij}^2\right)\,, \tag{9.35}$$

where a prime denotes a differentiation w.r.t y_T. The action reduces to the standard single scalar field case for $\mathcal{F}_T = \mathcal{G}_T = \frac{1}{2}$.

2. *Scalar Perturbations*

The quadratic action for the scalar perturbation $\mathcal{R}$ is given by [112]

$$S = \int \mathrm{d}t\mathrm{d}^3x a^3 \left(\mathcal{G}_S\dot{\mathcal{R}}^2 - \frac{\mathcal{F}_S}{a^2}(\vec{\nabla}\mathcal{R})^2\right)\,, \tag{9.36}$$

where

$$\mathcal{G}_S := \frac{\Sigma}{\Theta^2}\mathcal{G}_T^2 + 3\mathcal{G}_T\,, \tag{9.37}$$

$$\mathcal{F}_S := \frac{1}{a}\frac{d}{dt}\left(\frac{a}{\Theta}\mathcal{G}_T^2\right) - \mathcal{F}_T\,, \tag{9.38}$$

and

$$\Sigma := XK_X + 2X^2K_{XX} + 12H\dot{\phi}XG_{3X} + 6H\dot{\phi}X^2G_{3XX} - 2XG_{3\phi} - 2X^2G_{3\phi X} \tag{9.39}$$

$$-6H^2G_4 + 6[H^2\left(7XG_{4X} + 16X^2G_{4XX} + 4X^3G_{4XXX}\right) \tag{9.40}$$

$$-H\dot{\phi}\left(G_{4\phi} + 5XG_{4\phi X} + 2X^2G_{4\phi XX}\right)]\,, \tag{9.41}$$

$$\Theta := -\dot{\phi}XG_{3X} + 2HG_4 - 8HXG_{4X} - 8HX^2G_{4XX} + \dot{\phi}G_{4\phi} + 2X\dot{\phi}G_{4\phi X}\,. \tag{9.42}$$

The sound speed is given by $c_s^2 = \mathcal{F}_S/\mathcal{G}_S$. Ghost and gradient instabilities are avoided, if

$$\mathcal{G}_S > 0 \quad , \quad \mathcal{F}_S > 0. \tag{9.43}$$

We canonically normalize the scalar perturbations via

$$\mathrm{d}y_S := \frac{c_S}{a}\mathrm{d}t\,, \tag{9.44}$$

$$z_T := \frac{a}{\sqrt{2}}(\mathcal{F}_S\mathcal{G}_S)^{1/4}\,, \tag{9.45}$$

$$v := z_S\mathcal{R}\,, \tag{9.46}$$

leading to the quadratic action for the canonically normalized scalar field

$$S = \frac{1}{2}\int \mathrm{d}y_S \mathrm{d}^3x \left(v'^2 - (\vec{\nabla} v)^2 + \frac{z_S''}{z_S} v^2 \right) , \tag{9.47}$$

where a prime denotes a differentiation w.r.t y_S.

After reviewing the scalar and tensor perturbations for generalized Galileon theories we can now discuss general properties of the perturbations in Galileon theories. In the following chapter, we will analyze the stability conditions (9.31) and (9.43).

E. No-Go Theorem for Generalized Cubic Galileon Theory

Before we discuss the development, properties and problems of various singular and non-singular bouncing cosmologies, we will review the recently proposed no-go theorem for the generalized cubic Galileon theory in [124, 125], which states that gradient instabilities cannot be avoided during a non-singular bounce.

In order to avoid ghost and gradient instabilities, we require

$$\mathcal{G}_T > 0 \quad , \quad \mathcal{F}_T > 0 \quad \text{and} \quad \mathcal{G}_S > 0 \quad , \quad \mathcal{F}_S > 0. \tag{9.48}$$

We have seen that for $G_4 = \frac{1}{2}$ the functions $\mathcal{F}_T = \mathcal{G}_T = 1$. The time evolution of the functions $\mathcal{F}_T$ and $\mathcal{G}_T$ is caused by the non-minimal coupling to gravity. Moreover, only for a non-zero derivative coupling $G_{4X} \neq 0$ the functions $\mathcal{F}_T \neq \mathcal{G}_T$. From the definition of $\mathcal{F}_S$ in (9.38) we have:

$$\mathcal{F}_S = \frac{1}{a}\frac{d\xi}{dt} - \mathcal{F}_T \tag{9.49}$$

with $\xi = \frac{a\mathcal{G}_T^2}{\Theta}$. From (9.42) we see that Θ is a function of ϕ and H and thus it should be a smooth function of time. Thats why ξ should only vanish at the singularity $a = 0$. The condition $\mathcal{F}_S > 0$ reads:

$$\frac{1}{a}\frac{d\xi}{dt} > \mathcal{F}_T > 0. \tag{9.50}$$

Integrating the above equation from t_i to t_f leads to:

$$\xi_f - \xi_i > \int_{t_i}^{t_f} a\mathcal{F}_T \mathrm{d}t \, . \tag{9.51}$$

This is the important equation resulting in the no-go theorems discussed in [124, 125].

Consider a non-singular universe with scale factor $a \neq 0$ from $t \to -\infty$ to $t \to \infty$. Since $a \neq 0$ the

r.h.s. of (9.51) does generally not converge – only if $\mathcal{F}_T$ converges sufficiently fast towards zero in the asymptotic past and future. We suppose that $\xi_i < 0$ in the case where the integral does not converge:

$$-\xi_f < |\xi_i| - \int_{t_i}^{t_f} a\mathcal{F}_T \mathrm{d}t\,. \tag{9.52}$$

The integral grows for large t_f, since a grows – the r.h.s. eventually becomes negative leading to $\xi_f > 0$. Thus the function ξ has to cross zero which is not possible in a non-singular universe. Suppose now that ξ is always positive:

$$-\xi_i < -\xi_f + \int_{t_i}^{t_f} a\mathcal{F}_T \mathrm{d}t\,. \tag{9.53}$$

For $t_i \to -\infty$ the r.h.s. becomes positive leading to $\xi_i < 0$. This contradicts the assumption that $\xi > 0$. The inequality cannot be fulfilled if the integral does not converge. This is the main result of the no-go theorems [124, 125]. In the case of a non-singular bounce the gradient instability cannot be removed, if the integral does not converge.

Small scale perturbations can grow dramatically during a non-singular bounce due to the gradient instabilities. However, in the presence of the Galileon term $-G_3(X,\phi)\Box\phi$, the small scale perturbations are under better control in comparison to other non-singular bounce models. The dynamics can be modeled such that the gradient instabilities become only important shorty before or after the bounce – during the bounce phase, gradient instabilities are absent [126]. However, this does not really solve the problems associated with the gradient instability.

Maybe we just have to accept that gradient instabilities are present for a large class of non-singular bouncing models. It is important to note that the theories we discuss are just effective field theories. The theory is only valid up to a certain energy scale. It has been shown that in the case of a non-singular bounce via a ghost condensate, the small scale modes of interest lie outside of the validity of the effective field theoretical description [8]. Even though the model has gradient instabilities, the effective field theoretical model is well behaved, and we can calculate the background dynamics and the perturbations around the background. We will discuss the ghost condensate model in detail in Chapter 10 B and will use it in various scenarios in the course of this thesis.

Let us consider the case where we can circumvent the no-go theorem following [127]: $\mathcal{F}_T$ converges sufficiently fast to zero in the far past and future. For example if in the far past $a \sim |t|^p$,

then we need $\mathcal{F}_\mathcal{T} \sim |t|^{-p+1}$. We also need that ξ in equation (9.51) remains finite – suppose that $\Theta \sim |t|^q$, then $\mathcal{G}_\mathcal{T} \sim |t|^{q-p/2}$. This means that $\mathcal{F}_\mathcal{T}$ and $\mathcal{G}_\mathcal{T}$ have to scale differently. Keeping in mind the definition of the two functions from the equations (9.28), this is only possible if there is a non-minimal derivative coupling to gravity in the form of $G_4(X,\phi)R$ with $G(X,\phi)_{4X} \neq 0$. As already stated, non-singular bouncing models without this non-minimal derivative coupling are plagued by gradient instabilities.

The fact that the functions $\mathcal{F}_\mathcal{T}$ and $\mathcal{G}_\mathcal{T}$ have to fall off in the past and future is by no means a desirable property. These functions are the prefactors of the perturbations in the action suggesting a break down of the perturbative description. It was argued in [127], that such a bounce model is fully stable – we have to see if such bounces can be incorporated in viable early universe models in the future.

We should note that after the publication of the no-go theorems [124, 125], a variety of models were proposed, which try to circumvent the no-go theorem. The above discussed model beyond the cubic Galileon – namely the non-minimal derivative coupling $G_4(X,\phi)$ is one example. Other possibilities are, e.g. theories beyond Horndenski [128] and non-singular bounces in the framework of effective field theories of cosmological perturbations [129, 130].

10. COSMIC BOUNCES

A. Introduction

During ekpyrosis, the universe is driven towards homogeneity, isotropy, and flatness in a contracting universe. Eventually, the universe has to undergo a bounce from contraction to expansion. In the previous Chapter 9 E we have discussed a no-go theorem and the resulting gradient instabilities during a non-singular bounce for the Cubic Galileon theory. In the following, we will review a variety of different bouncing cosmologies.

Bouncing cosmologies can be divided into two classes: singular bounces, where the scale factor a in the 4-dimensional description becomes zero and non-singular bounces, where the universe transitions from contraction to expansion at a non-zero value of the scale factor a. In Chapter 3 B we have discussed the cyclic model, which incorporates a singular bounce.

1. *Singular Bounces*

A singular bounce in the braneworld description

The cyclic ekpyrotic model is based on colliding branes in M-theory [15]. While the scale factor becomes zero in the 4-dimensional description when the branes collide, the 5-dimensional scale factor is non-zero. However, this description is only valid up to a Planck time before or after the collision. The lack of a non-perturbative description challenges the predictions of the ekpyrotic models. There has been a lot of discussions about how perturbations evolve during such a singular bounce, and different matching conditions have been proposed [131].

A singular anti-gravity bounce

In [132, 133] a scalar field theory minimally coupled to gravity was lifted to a Weyl-invariant theory, which allowed to trace the cosmological evolution through a big-crunch/big-bang transition.
In this setup, the universe undergoes a brief anti-gravity phase. Analytic solutions were found, and it was shown that this model is geodesically complete. It was argued in [134] that the singularity is not resolved since Weyl-invariant curvature terms diverge. In response it was shown that a sufficient number of conserved quantities exist, such that the theory is geodesically complete [133].

2. Non-Singular Bounces

The ambitious attempt to resolve the initial cosmological singularity of the universe is a hard task [87, 135]. In the following, we will discuss how non-singular bounce solutions can be obtained and review the advances and developments of non-singular bounce models.

Let us consider a single scalar field minimally coupled to gravity. We obtain from the Friedmann equations

$$\dot{H} = -\frac{1}{2}(\rho + p) = -\dot{\phi}^2 \,. \tag{10.1}$$

It is not possible to transition from contraction ($H < 0$) to expansion ($H > 0$) in this framework.

However, the violation of the null energy condition (NEC)

$$\rho + p > 0 \tag{10.2}$$

allows the universe to undergo a bounce from contraction to expansion; in the covariant form the NEC reads $T_{\mu\nu}n^\mu n^\nu \geq 0$ for any null vector n^μ, satisfying $g_{\mu\nu}n^\mu n^\nu = 0$. A NEC violation can be obtained by adding an exotic matter content. As a first try let us consider a ghost field – a scalar field with the wrong kinetic sign. The negative sign in the kinetic term causes a violation of the NEC leading to $\dot{H} = -\frac{1}{2}(\rho + p) = \dot{\phi}^2$. But this naive first try introduces ghosts: the energy of the theory is unbounded from below. The vacuum $\langle\phi\rangle = 0$ is unstable, and nothing prevents the vacuum to decay.
In the case of a tachyon – a scalar field with a negative mass – one can introduce higher order correction terms which stabilize the vacuum. This is the so-called tachyon condensation. For example in the case of a potential of the following form

$$V(\phi) = -\frac{1}{2}m^2\phi^2 + \frac{1}{4}\lambda\phi^4 + ... \tag{10.3}$$

with $\lambda > 0$ the vacuum is stable where $\langle\phi\rangle \neq 0$. A similar idea can be used in the case of the ghost field: higher order derivative terms like $(\partial\phi)^4$ can stabilize the ghost field leading to a ghost condensate. We will cover the ghost condensate in detail in the next chapters. Various non-singular bounce models have been proposed in recent years, and we will give a brief overview in the following.

In the previous chapter, we have reviewed the generalized Galileon theory, which includes a variety of known scalar field models. Non-singular Galileon bounce models have been studied intensively in the literature, e.g. [116, 118, 136–139]. Even if gradient instabilities are unavoidable in the generalized cubic Galileon theory due to the no-go theorem discussed in the previous chapter, the small scale perturbations are under better control due to the presence of the Galileon term, cf. (9.1), namely $\mathcal{L}_3 = -G_3(X,\phi)\Box\phi$. We have to see if perfectly stable non-singular Galileon bounces can be obtained in the future, which circumvent the no-go theorems.

Non-singular bounces can also be obtained via a modification of gravity: For example in Horava-Lifshitz gravity [140, 141], $F(R)$ theories [142] and Gauss-Bonnet gravity [143].

Non-singular bounces have also been constructed in string theory and loop quantum cosmology. One approach in string theory is the so-called s-brane bounce [144, 145]. As the universe contracts, the temperature increases reaching a critical temperature. At this moment a tower of massive string states become massless, which have to be included in the low energy effective action. This results in a so-called s-brane, which can violate the null energy condition leading to a non-singular bounce.

Loop quantum cosmology uses the quantization techniques of loop quantum gravity in a homogeneous and isotropic universe. The leading order quantum gravity corrections lead to loop quantum cosmology effective equations of the classical equations. The effective Friedmann equation reads [146]

$$H^2 = \frac{1}{3}\rho\left(1 - \frac{\rho}{\rho_c}\right) , \tag{10.4}$$

where ρ_c is the critical energy density. The classical Friedmann equation is obtained in the limit $\rho_c \to \infty$. Due to the presence of the correction term, the universe naturally bounces [147, 148].

B. The Ghost Condensate

1. *Pure Ghost Condensate*

In the following, we will discuss the basic conceptions and properties of the ghost condensate [20, 24, 33]. A modification of the pure ghost condensate model enables us to implement a non-singular bounce after the ekpyrotic phase. We will cover important studies and advances regarding the non-singular ghost condensate bounce, which justifies its use throughout this thesis.

In order to stabilize the non-singular bounce phase, we will include higher derivative terms in the Lagrangian. The standard kinetic term becomes a generalized kinetic term of the form $P(X)$ – or more general $P(X, \phi)$.

Let us consider a scalar field minimally coupled to gravity with a non-standard kinetic term

$$S = \int d^4x\sqrt{-g}\left(\frac{1}{2}R + P(X)\right) , \tag{10.5}$$

with

$$P(X) = -X + X^2 . \tag{10.6}$$

The energy density and the pressure are given by

$$\rho = 2XP_X - P , \tag{10.7}$$

$$p = P , \tag{10.8}$$

such that the null energy condition reads $\rho + p > 2XP_X$. The theory admits a shift symmetry $\phi \to \phi + const.$ and the equation of motion of the scalar field reads

$$\frac{d}{dt}(a^3 P_X \dot{\phi}) = 0 . \tag{10.9}$$

There exists a solution at the minimum of P with $P_X = 0$. This solution breaks the shift symmetry and the time translation symmetry down to an unbroken diagonal shift symmetry. The scalar field develops a time-dependent vacuum expectation value which grows linearly in time

$$\langle\phi\rangle = ct , \tag{10.10}$$

where c is a constant. The perturbed second order Lagrangian around this vacuum expectation value is proportional to [20, 33]

$$\mathcal{L} \sim (P_X + 2XP_{XX})\,(\dot{\delta\phi})^2 - P_X(\nabla\delta\phi)^2. \tag{10.11}$$

At the ghost condensate point the equation of state $w = -1$, since $P_X = 0$. The ghost condensate has the same equation of state as the cosmological constant, which led to the development of ghost condensate models with accelerated expansion, e.g. [116]. Moreover, the perturbations (10.11) around the ghost condensate point $P_X = 0$ are ghost free. When P_X becomes zero the speed of sound c_s also becomes zero. In order to obtain a non-zero gradient term one can add higher order corrections [20]

$$\mathcal{L} \sim -\frac{1}{M^2}(\nabla^2\delta\phi)^2, \tag{10.12}$$

which leads to a dispersion relation of the form $\omega^2 \sim k^4/M^2$ – note there is no k^2 term. At the ghost-condensate point Lorentz-invariance is broken; fluctuations with small momentum move slower than fluctuations with large momentum.

At the ghost condensate point the NEC is not violated yet. However, small deviations from the ghost condensate point $P_X = 0$ can lead to a NEC violation when $P_X < 0$. Consequently, the universe undergoes a ghost-free non-singular bounce. We should note that gradient instabilities are present when $P_X < 0$, which can be seen from (10.11). This is an expected result, since the ghost-condensate described by a generalized kinetic term $P(X)$ is part of Galileon theory. The no-go theorem discussed in the previous chapter states, that gradient instabilities during such a non-singular bounce are unavoidable. The consequences of these gradient instabilities will be covered in the next chapter.

2. Ghost Condensate $P(X, \phi)$

We are interested in a cosmological scenario where the universe starts in an ekpyrotic phase with a proceeding non-singular bounce. Here we take ϕ to be the field driving the bounce, while χ is assumed to be transverse (in field space) to the background trajectory during the bounce phase. The transition to the ghost-condensate phase occurs via a sign change of the kinetic term in a ghost-free manner due the presence of higher derivate terms.

We are interested in models of gravity minimally coupled to two scalar fields ϕ, χ with an action of the form

$$S = \int \mathrm{d}^4x\sqrt{-g}\left[\frac{R}{2} + P(X,\phi) - \frac{1}{2}(\partial\chi)^2 - V(\phi,\chi)\right], \tag{10.13}$$

where $X \equiv -\frac{1}{2}g^{\mu\nu}\partial_\mu\phi\partial_\nu\phi = -\frac{1}{2}(\partial\phi)^2$ and $V(\phi,\chi)$ is a potential which we will describe in much more detail later. The kinetic term is given by

$$P(X,\phi) = K(\phi)X + Q(\phi)X^2\,. \tag{10.14}$$

In a flat Robertson-Walker background with the metric

$$\mathrm{d}s^2 = -\mathrm{d}t^2 + a(t)^2\delta_{ij}\mathrm{d}x^i\mathrm{d}x^j\,, \tag{10.15}$$

the background equations of motion are

$$3H^2 = \frac{1}{2}K(\phi)\dot{\phi}^2 + \frac{3}{4}Q(\phi)\dot{\phi}^4 + \frac{1}{2}\dot{\chi}^2 + V(\phi,\chi)\,, \tag{10.16}$$

$$\dot{H} = -\frac{1}{2}K(\phi)\dot{\phi}^2 - \frac{1}{2}Q(\phi)\dot{\phi}^4 - \frac{1}{2}\dot{\chi}^2\,, \tag{10.17}$$

$$0 = P_{,\phi} - V_{,\phi} - P_X(\ddot{\phi} + 3H\dot{\phi}) - P_{XX}\ddot{\phi}\dot{\phi}^2 - P_{X\phi}\dot{\phi}^2\,, \tag{10.18}$$

$$0 = \ddot{\chi} + 3H\dot{\chi} + V_{,\chi}\,. \tag{10.19}$$

During the bounce phase, χ is taken to be constant, and will thus not contribute to the dynamics of the background (but we will be highly interested in the perturbations of χ). During ekpyrosis the functions $K(X,\phi) = 1$ and $Q(X,\phi) = 0$, while the ekpyrotic potential V depends on the specific model; we will cover the entropic mechanism and the non-minimal entropic mechanism.

Eventually, the ekpyrotic phase has to end – if the potential flattens out, the kinetic energy comes to dominate leading to a kinetic phase.

At a certain point the function $Q(X,\phi)$ turns on and $K(X,\phi)$ changes the sign to $K(X,\phi) = -1$ allowing for a ghost-free NEC violation inducing a non-singular ghost condensate bounce.

A non-singular bounce can occur during the kinetic phase while the scalar field rolls up the potential or at the bottom of the potential. We will see that the presence of a potential during the non-singular bounce phase can have important consequences regarding the validity of the effective field theoretical description.

Various parameterizations of the functions $Q(X,\phi)$ and $K(X,\phi)$ are possible. Here we choose the following symmetric form following [149]:

$$K(\phi) = 1 - \frac{2}{\left(1 + \frac{1}{2}\phi^2\right)^2}\,, \tag{10.20}$$

$$Q(\phi) = \frac{q}{\left(1 + \frac{1}{2}\phi^2\right)^2}\,. \tag{10.21}$$

As already stated these functions can turn on during the kinetic phase when the ekpyrotic potential is negligible leading to a pure ghost condensate phase or during the ekpyrotic phase. In the latter case we consider the symmetric potential given by a regularised version of an ekpyrotic potential [8]

$$V(\phi) = -\frac{2V_o}{e^{-\sqrt{2\epsilon}\phi} + e^{\sqrt{2\epsilon}\phi}}\,, \tag{10.22}$$

where V_o and ϵ are constants. Away from the bounce, there will be additional contributions to the potential, which depend on the specific model during ekpyrosis and during the conversion phase. Neglecting the potential, for now, the kinetic term at the ghost condensate point at $\phi = 0$ reads

$$P = -X + qX^2, \tag{10.23}$$

which is just the form of the pure ghost condensate. From $P_X = 0$ we obtain $X = 1/2q$ confirming again that ϕ grows linearly with time. Moreover the energy density $\rho = 2XP_X - P$ reads

$$\rho\,|_{P_X=0} = \frac{1}{4q}, \tag{10.24}$$

which can be interpreted as the energy density of the pure ghost condensate. Restoring the mass dimensions in the Lagrange density (10.14) we see that q has mass dimension -4. The ratio between the horizon length at the bounce and the reduced Planck length is $\sim M_P\, q^{1/4}$. For a sufficient classical horizon length we require a ratio of at least [8]

$$M_P\, q^{1/4} \geq 10^2, \tag{10.25}$$

corresponding to an energy scale of two orders of magnitude below the reduced Planck mass and thus an horizon mass of at most 10^{16} GeV. For $M_P\, q^{1/4} = 10^2$ we obtain, returning to natural units

$$q = 10^8. \tag{10.26}$$

In the presence of a potential the energy density at the ghost condensate point reads:

$$\rho\,|_{P_X=0} = \frac{1}{4q} + V(\phi), \tag{10.27}$$

which leads, using the symmetric potential (10.22), to

$$\rho\,|_{P_X=0} = \frac{1}{4q} - V_0. \tag{10.28}$$

For now we have seen how a ghost-condensate phase can violate the NEC inducing a non-singular bounce. The addition of the functions $K(X,\phi)$ and $Q(X,\phi)$ allows for a dynamical description of an ekpyrotic phase followed by a bounce phase.

Before we continue the discussion of this specific bounce model let us cover important results and developments regarding the ghost condensate model. Aside from the absence of ghosts [33] detailed studies of the perturbative [8] and semi-classical stability [150] properties have been completed. These models (even including a cubic Galileon term) were successfully constructed in $\mathcal{N} = 1$ supergravity [149], which is a very important step in the embedding of such models in a fundamental theory. This "super-bounce" model is considered as one of the more robust non-singular bounce models, see, e.g. [135] for a comparison of different bouncing cosmologies. In the next chapter, we will return to the unavoidable presence of gradient instabilities and argue that all fluctuations which are within the regime of validity of the effective theory remain under control.

3. *Adiabatic Perturbations through the Bounce*

The evolution of the curvature perturbations through a non-singular bounce has been studied in detail in [7]. Here we summarize the main results taken from our review in [9].

In conformal time, the linearized equation of motion for the comoving curvature perturbation $\mathcal{R}$ is given by

$$\frac{d^2\mathcal{R}}{d\tau^2} + \frac{2}{z}\frac{dz}{d\tau}\frac{d\mathcal{R}}{d\tau} + c_s^2 k^2 \mathcal{R} = 0 \ , \tag{10.29}$$

where

$$z^2 = a^2 \frac{P_X X + 2P_{XX}X^2}{H^2} \ , \tag{10.30}$$

$$c_s^2 = \frac{P_X}{P_X + 2P_{XX}X} \ . \tag{10.31}$$

Then, near the bounce (taken to occur at $\tau = 0$) this equation is solved by the series

$$\mathcal{R} = \alpha \left(1 - \frac{1}{2}\bar{c}_s^2 k^2 \tau^2 + \dots\right) + \beta\tau^3 \ , \tag{10.32}$$

where α, β are constants. Here the value of the speed of sound at the bounce is approximated by $\bar{c}_s^2 \approx -1/3$. Thus, for perturbations which have a wavelength that is long compared to the scale of the bounce ($k/a \ll q^{1/4}$), we expect the solution to be approximately constant across the bounce. This is confirmed by numerically solving the equation of motion, see Fig. 15. In the figure, the purple and red lines correspond approximately to the scale of the bounce, and here some evolution of the curvature perturbation is shown. However, for longer-wavelength perturbations (all curves that are above the red line) there is essentially no evolution at the bounce. Modes of potential interest for cosmological observations have a wavelength many orders of magnitude larger still, and such modes remain conserved across the bounce to very high precision. (As an aside, note that the Mukhanov-Sasaki perturbation variable $v = z\mathcal{R}$ blows up across the bounce, as noticed in [151], but this is due to z diverging at the bounce point. The perturbation of physical interest, $\mathcal{R}$, remains frozen on large scales during the bounce.)

We should add one comment regarding the adiabatic modes: as one can see both from the series solution above and the figure, short-wavelength modes are affected by the gradient instability that is caused by the speed of sound squared going negative during the bounce phase. This instability is in fact ever stronger for ever shorter modes. It is thus of importance to know the cut-off of our effective field theory, in order to assess whether the background bounce solution is really

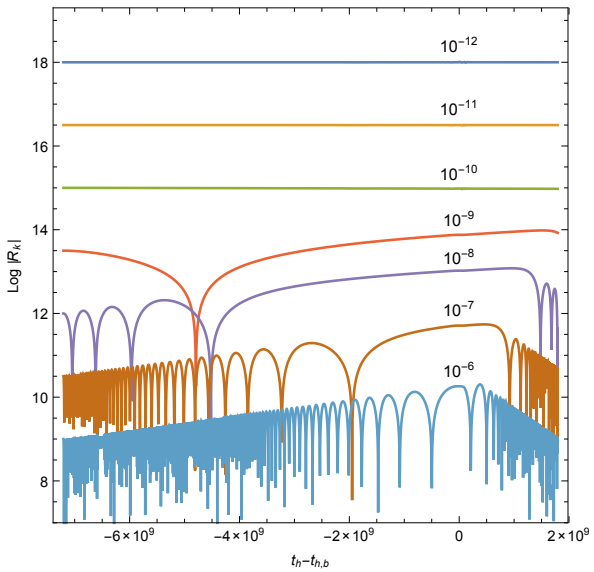

FIG. 15. Evolution of the curvature perturbations (here denoted by $\mathcal{R}_k$) across a flat non-singular ghost condensate bounce, for different wavenumbers k. We are interested in long-wavelength modes which are conserved with high accuracy. The numerical plot here shows the evolution of the curvature perturbation modes in terms of harmonic time t_h, defined as $\mathrm{d}t_h = a^2\mathrm{d}\tau = a^3\mathrm{d}t$. The time interval plotted above is much longer than the period of violation of the null energy condition; see [7, 8] for more details. Figure taken from [8].

trustworthy or not. The cut-off scale Λ_{strong} was calculated in [8] and it was found that it must be evaluated at the moment when $P_X = 0$, with the result that

$$\Lambda^4_{strong} = \frac{2}{q}\,, \qquad \rho\,|_{P_X=0} = \frac{1}{4q} + V(\phi)\,, \tag{10.33}$$

where we have also listed the energy scale of the background (10.28) for comparison. As one can see, in the absence of a potential the cut-off is a factor of 8 above the energy density of the background, and this separation of scales is larger when a negative potential is present, as we have assumed here (in our specific example these two scales are separated by a factor of about 40). Meanwhile, the cut-off is not too far above the energy scale of the background, implying that the most dangerous very short/high frequency perturbation modes indeed lie outside the regime of validity of the theory. Thus, from an effective field theory point of view, this bounce model is reliable. The presence of a negative potential during the bounce phase then suggests that the conversion of entropy into curvature perturbations ought to occur after the bounce, and not before [8]. We will discuss the evolution of entropy perturbations through a non-singular bounce and the proceeding conversion phase in the expanding phase in the following chapter.

11. ENTROPY PERTURBATIONS THROUGH A NON-SINGULAR BOUNCE

We have discussed how the ekpyrotic scenario renders the universe flat, homogeneous, and isotropic. We have covered the evolution of entropy perturbations in the entropic mechanism and non-minimal entropic mechanism during ekpyrosis and the subsequent conversion process during a kinetic phase before the bounce. Moreover, a non-singular bounce phase via a ghost condensate was presented, which is healthy in the effective field theoretical description. The large scale comoving curvature perturbations, which were sourced by entropy perturbations, stay frozen through the non-singular bounce phase, such that the obtained predictions do not change in the proceeding, expanding phase.
In the previous chapter we have argued that the presence of an ekpyrotic potential during the non-singular ghost condensate bounce increases the separation of the cut-off scale Λ_{strong} and the energy scale of the background. This suggests that the conversion could occur after the non-singular bounce.

In the following, we will calculate the evolution of entropy perturbations through a non-singular bounce and the subsequent conversion phase based on our paper [9], which we will follow closely in this chapter. We show that such a scenario offers interesting new possibilities, due to a possible non-trivial evolution of entropy perturbations during the bounce phase joining the contracting and expanding phases together. In particular, we will show with the example of a specific bounce model that entropy perturbations can grow significantly during the bounce phase, with the consequence that these enhanced entropy perturbations can easily provide the dominant contribution to the final post-bounce amplitude of the curvature perturbations leading to the following results:

- The amplitude of the final curvature perturbations tends to be significantly enhanced. Conversely, this means that the entropy perturbations at the end of the ekpyrotic phase can be smaller than currently assumed in this model. In other words, the energy scale of the contraction phase can be smaller.

- The enhancement of the amplitude of the entropy perturbations implies that the importance of its intrinsic non-Gaussianity is reduced. This is because the most important contribution to the non-Gaussianity of the final curvature perturbation comes from the non-linearity of the conversion process, and not from the intrinsic non-Gaussianity that can already be present in the entropy perturbations.

We would like to note that cosmological bounces can also be caused by quantum gravity effects, for example in loop quantum cosmology [146]. Interestingly, at least in the case that the bounce is dominated by an ekpyrotic-like field, the qualitative predictions concerning the scalar and tensor power spectra do not appear to depend significantly on the exact mechanism of the bounce [148, 152] and therefore the qualitative results obtained in the following chapters may also hold in other cases where the bounce occurs due to different physical effects, including quantum gravity effects.

In the following, we will use the specific ghost condensate model introduced in Chapter 10 B 2, where the two-field action (10.13) is given by

$$S = \int \mathrm{d}^4x\sqrt{-g}\left[\frac{R}{2} + P(X,\phi) - \frac{1}{2}(\partial\chi)^2 - V(\phi,\chi)\right], \tag{11.1}$$

with the kinetic term

$$P(X,\phi) = K(\phi)X + Q(\phi)X^2\,, \tag{11.2}$$

where the functions $K(\phi)$ and $Q(\phi)$ are given by (10.20) and (10.21) respectively. In the presence of a potential during the bounce phase we will use the symmetric regularised ekpyrotic potential in Eq. (10.22). A numerical solution of the equations of motion (10.16) - (10.19) near the bounce is shown in Fig. 16. Here the parameters of the model are chosen to be

$$\epsilon = 10\,, \qquad V_o = 2\times 10^{-8}\,, \qquad q = 10^8\,, \tag{11.3}$$

where q, with mass dimension of -4, determines the energy scale of the bounce. In the present case the energy scale is $(10^{-2}M_{Pl})^4$, two orders of magnitude below the reduced Planck mass. This scale also determines the duration of the bounce, i.e. the time period over which the null energy condition is violated, $t \in (-\sqrt{q},\sqrt{q}) = (-10^4, 10^4)$, as is verified in the right panel of Fig. 16 which plots the sum of energy density and pressure. The initial conditions for the bounce solution were chosen such that the bounce occurs at $t = 0$ with

$$\phi(0) = 0\,, \qquad a(0) = 1\,, \qquad \chi(0) = 0\,, \qquad \dot{\chi}(0) = 0\,. \tag{11.4}$$

From the first Friedmann equation with $\rho = 0$, we obtain $\dot{\phi}(0) \approx 9.7\times 10^{-5}$, where we have chosen ϕ to roll from negative to positive values as time progresses. Note that we have chosen $\phi(0) = 0$ at the bounce time since this is the centre of the region where the scalar field ϕ can violate the null energy condition and cause the bounce.

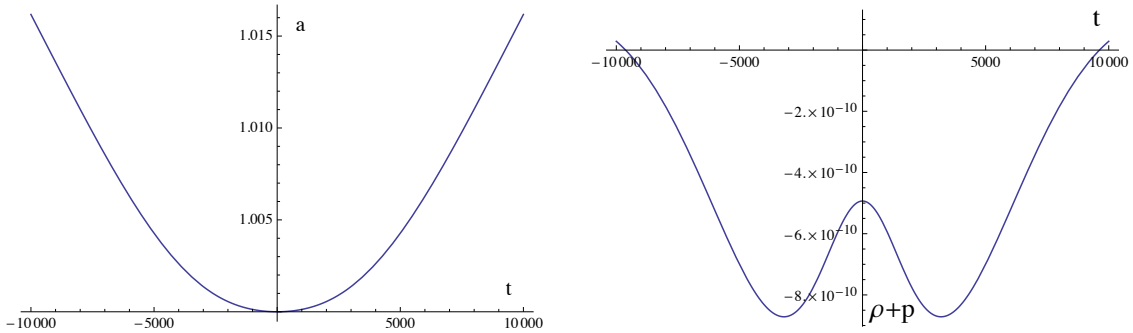

FIG. 16. A numerical solution around the time of the non-singular bounce. The left panel shows the evolution of the scale factor a, while the right panel plots the sum of energy density ρ and pressure p. When this last sum is negative, the null energy condition is violated, which is a necessary condition in order to obtain a non-singular bounce in a flat Robertson-Walker universe. Figure taken from [9].

The bounce is symmetric around $t = 0$ due to the symmetric form of $K(\phi)$ and $Q(\phi)$ (the form of the potential does not affect this since ϕ is kinetic-dominated during the bounce); we made these choices for the sake of simplicity. An asymmetric bounce is also possible (see, e.g., [7]), but the evolution of the long-wavelength perturbations (those of observational interest) is not significantly affected by the details of the bounce since the bounce time is much shorter than the wavelength of these perturbations. One may also approximate the numerical solution analytically near the bounce. Note that at the bounce itself the Hubble rate is zero by definition, $H = 0$, and thus the Friedmann equation implies that the energy density vanishes too. Combining this result with the equation of motion for the scale factor (10.17) and neglecting the potential at the bounce then gives

$$a(t) \approx e^{t^2/(18q)}\,, \tag{11.5}$$

$$\phi(t) \approx \sqrt{\frac{2}{3q}}\,t\,. \tag{11.6}$$

The scalar field ϕ evolves linearly in time near the bounce, which is the characteristic time evolution of a ghost condensate.

The bounce is followed (and, depending on the model, perhaps also preceded) by a phase of kinetic energy domination, during which the kinetic term for ϕ is to a good approximation canonical, and with equation of state $w = 1$. The background equations then reduce to the simple form

$$3H^2 \approx \frac{1}{2}\dot{\phi}^2 \approx -\dot{H}, \qquad \ddot{\phi} + 3H\dot{\phi} \approx 0\,, \tag{11.7}$$

and the solution is given by

$$a \approx \bar{a}_o(\pm t)^{1/3}, \qquad \phi \approx \sqrt{\frac{2}{3}}\ln(\pm t) + \bar{\phi}_o, \tag{11.8}$$

for some constants $\bar{a}_o, \bar{\phi}_o$, and where a positive (negative) sign corresponds to an expanding (contracting) kinetic phase. The energy density scales as $\rho \propto a^{-6}$, since

$$\dot{\phi} \approx \sqrt{\frac{2}{3}}\frac{\bar{a}_o^3}{a^3}\,. \tag{11.9}$$

We are now ready to turn our attention to the behavior of fluctuations in this background.

A. Evolution of Entropy Perturbations

An important simplification of the background we are studying is that only one of the scalar fields, namely ϕ, evolves at the background level. This has the consequence that during the bounce phase, the perturbations of ϕ (which in their gauge-invariant form correspond to curvature perturbations $\mathcal{R}$) and the perturbations of χ (which correspond to entropy perturbations) evolve independently, and we can study them separately. The evolution of the curvature perturbations was already discussed in Chapter 10 B 3. We have shown that the curvature perturbations evolve through the non-singular bounce basically unaffected.

Now we can start to analyze the evolution of the entropy perturbations. We have covered the decomposition of perturbations into adiabatic and entropy modes in Chapter 5 C and Chapter 8 C based on the developments in [5, 65–67]. At linear and second order, the adiabatic and entropy perturbations are then defined to be

$$\delta\sigma^{(1)} = e_{\sigma I}\delta\phi^I\,, \qquad \delta s^{(1)} = e_{sI}\delta\phi^I\,, \tag{11.10}$$

$$\delta\sigma^{(2)} = e_{\sigma I}\delta\phi^{I(2)} + \frac{1}{\dot{\sigma}}\delta s\dot{\delta s}\,, \qquad \delta s^{(2)} = e_{sI}\delta\phi^{I(2)} - \frac{\delta\sigma}{\dot{\sigma}}\left(\dot{\delta s} + \frac{\dot{\theta}}{2}\delta\sigma\right)\,. \tag{11.11}$$

Up to second order and on large scales, they obey the equation of motion

$$\begin{aligned}\ddot{\delta s} + 3H\dot{\delta s} + \left(V_{ss} + 3\dot{\theta}^2\right)\delta s = \\ -\frac{\dot{\theta}}{\dot{\sigma}}(\dot{\delta s})^2 - \frac{2}{\dot{\sigma}}\left(\ddot{\theta} + V_\sigma\frac{\dot{\theta}}{\dot{\sigma}} - \frac{3}{2}H\dot{\theta}\right)\delta s\dot{\delta s} + \left(-\frac{1}{2}V_{sss} + 5V_{ss}\frac{\dot{\theta}}{\dot{\sigma}} + 9\frac{\dot{\theta}^3}{\dot{\sigma}}\right)(\delta s)^2,\end{aligned} \tag{11.12}$$

where $V_\sigma \equiv e^I_\sigma V_{,I}$, $V_s \equiv e^I_s V_{,I}$, $V_{ss} \equiv e^I_s e^J_s V_{,IJ}$, etc. (a useful additional relation is $V_s = -\dot{\sigma}\dot{\theta}$), and where $\delta s = \delta s^{(1)} + \delta s^{(2)}$. Also, at large scales the spatial gradient terms are negligible and have been dropped in the above expression.

B. Entropy Perturbations through the Non-Singular Bounce

During the bounce phase, the field space trajectory is straight ($\dot{\theta} = 0$), and the equation (11.12) thus simplifies to

$$\ddot{\delta s} + 3H\dot{\delta s} + V_{ss}\delta s + \frac{1}{2}V_{sss}(\delta s)^2 = 0\,. \tag{11.13}$$

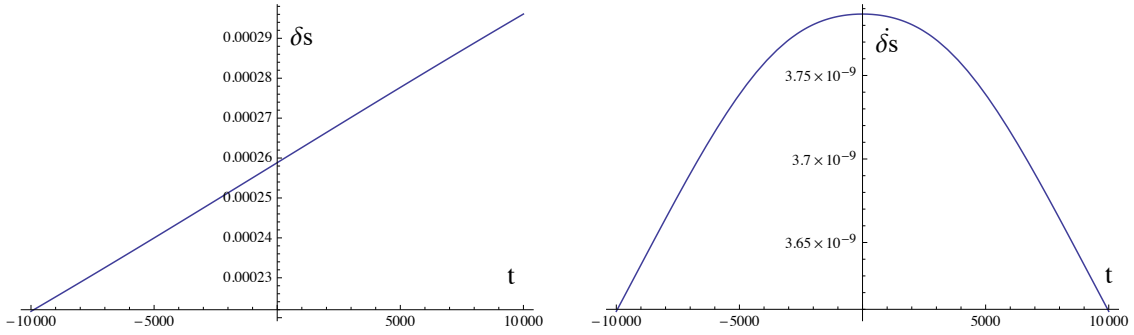

FIG. 17. A plot of the entropy perturbation and its time derivative during the period where the null energy condition is violated, and where the bounce occurs. The parameters are those of Eq. (11.3). In this example, the transverse potential (i.e. the potential in the entropic direction) is flat, and there is a modest growth of the perturbation across the bounce. Figure taken from [9].

Let us first analyze the case where the transverse potential is flat, $V_{ss} = V_{sss} = 0$. In that limit, $\dot{\delta s} = A\,a(t)^{-3}$, which, given (11.5), is easily integrated,

$$\delta s = A\sqrt{\frac{3\pi q}{2}}\,\mathrm{Erf}\left(\frac{t}{\sqrt{6q}}\right) + B, \tag{11.14}$$

where A and B are integration constants determined by the values of δs and $\dot{\delta s}$ at the beginning of the bounce phase. During the bounce period, the entropy perturbation thus changes by an amount

$$\Delta\delta s = A\int_{-t_b=-q^{1/2}}^{t_b=q^{1/2}} e^{-\frac{1}{6q}t^2}dt = A\sqrt{6\pi q}\,\mathrm{Erf}(1/\sqrt{6}) \approx 1.9 \times A\sqrt{q}\,. \tag{11.15}$$

In cosmological models such as those that we consider, the entropy perturbation before the bounce typically reaches a scale not much smaller than the scale of the bounce, i.e. one would expect that the amplitude of the entropy perturbations is of the order of $q^{-1/2}$, and that therefore $Aq^{1/2} \sim \mathcal{O}(1)$. In this case, there is a modest growth of the entropy perturbation during the period of NEC violation. A numerical example confirming this estimate is provided in Fig. 17, where the initial entropy perturbation was taken to be $\delta s_{pre-bounce} = 10^{-5}$. The small growth of the entropy perturbations across a non-singular bounce was previously noted in [151].

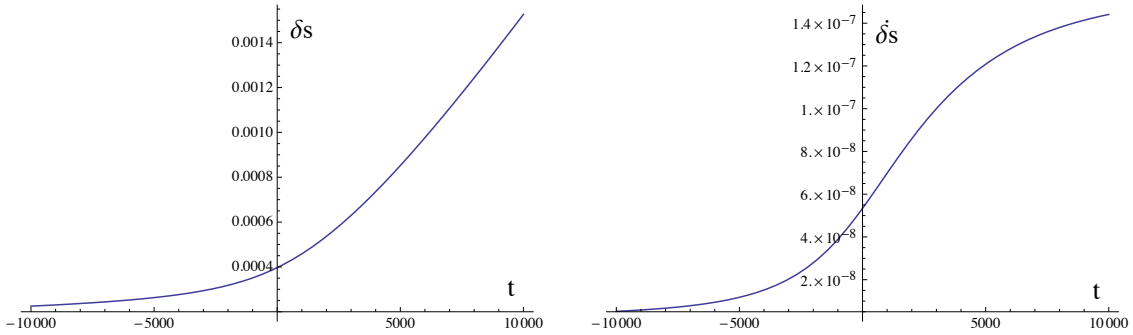

FIG. 18. A plot of the entropy perturbation and its time derivative during the period where the null energy conditions is violated and the bounce occurs. The parameters are again those of Eq. (11.3), but in this example the transverse potential is unstable, see Eq. (11.16). The instability causes an additional growth in the entropy perturbation across the bounce. Figure taken from [9].

An important point here is that in the case that $V_{ss} = V_{sss} = 0$ during the bounce, for this amplification to occur it is essential that the entropy perturbations never freeze. If the entropy perturbations are frozen – i.e. if $\dot{\delta s} = 0$ – at the onset of the bounce phase, then the constant solution $\delta s = B$ is singled out and no amplification will occur during the bounce. So, a necessary condition for the entropy perturbations to be amplified during the bounce is that their time evolution remains non-trivial at all times leading up to the bounce.

We can now also look at the case where a transverse, unstable potential is present during the bounce phase, cf. Chapter 5:

$$V(\phi) = -\frac{2V_o}{e^{-\sqrt{2\epsilon}\phi} + e^{\sqrt{2\epsilon}\phi}} \left(1 + \frac{1}{2}\epsilon\chi^2 + \cdots\right) , \tag{11.16}$$

implying that

$$V_{ss} = -\frac{2V_o\epsilon}{e^{-\sqrt{2\epsilon}\phi} + e^{\sqrt{2\epsilon}\phi}} . \tag{11.17}$$

During the bounce ϕ grows linearly in time, $\phi = \sqrt{2/(3q)}\, t$ leading to

$$V_{ss} = -\frac{2V_o\epsilon}{e^{-\sqrt{4\epsilon/(3q)}t} + e^{\sqrt{4\epsilon/(3q)}t}} = -\frac{V_o\epsilon}{\cosh(\sqrt{4\epsilon/(3q)}t)} \tag{11.18}$$

This unstable potential leads to an additional amplification of the entropy perturbations. A typical example is shown in Fig. 18, where we have chosen the same parameters as in Eq. (11.3). In this example, there is a total growth by a factor of about 7 across the bounce. The growth does depend on the parameters of the model, in particular on ϵ which sets the scale of the instability. However, provided that the overall scale of the potential changes in proportion to the change of scale of

the bounce, i.e. provided $V_o \propto q^{-1}$, then the total growth is independent of the bounce energy scale $q^{-1/4}$. Note that this additional growth in the amplitude of the entropy perturbations will be scale-invariant (i.e. independent of the Fourier wavenumber) since all of the Fourier modes of observational interest are in a regime where the gradient terms in their equations of motion are entirely negligible during the bounce. Hence an unstable transverse potential leads to an additional growth, but at the expense of requiring more special initial conditions since now only trajectories lying very close to the ridge in the potential will make it through the bounce.

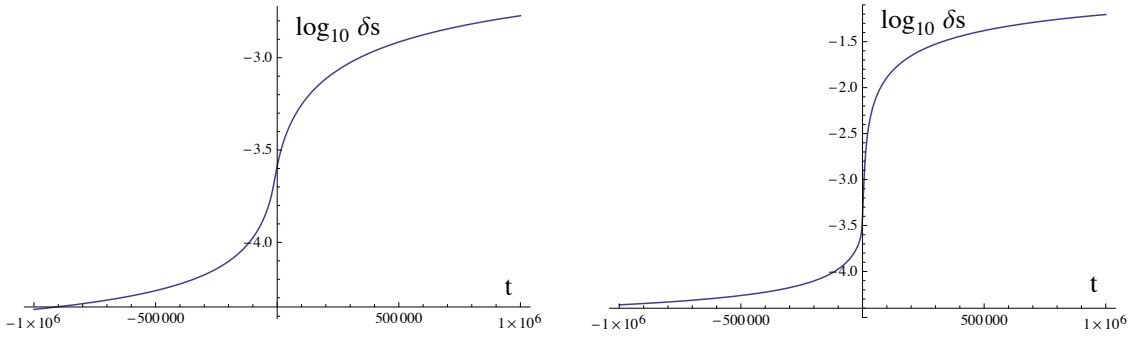

FIG. 19. The growth of the entropy perturbations across the kinetic and bounce phases (where the period of null energy violation is confined to the interval $-10^4 < t < 10^4$). The left panel shows the case where the potential is flat in the entropic direction, while in the right panel this transverse potential is unstable. The combined effect of the kinetic and bounce phases leads to a significant overall amplification of the entropy perturbations. Figure taken from [9].

The bounce is followed (and, if the potential is less important just before the bounce, also preceded) by a phase of kinetic energy domination. During these phases $H = 1/(3t)$ and the potential is subdominant, such that the entropy perturbations obeys the approximate equation $\ddot{\delta s} + (1/t) \times \dot{\delta s} \approx 0$ and consequently grows approximately logarithmically,

$$\delta s = C \ln(t/t_k) + D \tag{11.19}$$

for some integration constants C, D, t_k. Once again, this growth is conditional upon the entropy perturbations not being frozen, i.e. that $\dot{\delta s} \neq 0$ — otherwise $\delta s = D$ and no growth will occur. Even for $C \neq 0$, the growth is rather slow, but the cumulative effect over the two (bounce–expanding kinetic) or three (contracting kinetic–bounce–expanding kinetic) phases can be substantial. We have illustrated this in Fig. 19, where the left panel corresponds to having a flat transverse potential and the right panel shows the case of an unstable transverse potential. Even without an instability, the entropy perturbations tend to grow by 1.5 to 2 orders of magnitude, depending on how long the kinetic phases last. As we will see in detail in the following sections, this growth implies

that a conversion of entropy perturbations into curvature perturbations after the bounce phase easily provides the dominant contribution to the final amplitude of the curvature perturbations, keeping in mind that any curvature perturbations that might be present before the bounce remain constant across that phase. The right panel in Fig. 19 then shows the amplification of the entropy perturbations for the case where the potential in the entropic direction is unstable. In that case, the growth is further enhanced, and in our numerical example, the entropy perturbations reach an overall growth of 3 orders of magnitude. Note that the bounce has the effect of not just amplifying the entropy perturbations, but also its time derivative $\dot{\delta s}$ grows during the bounce, thus bringing with it an even stronger growth during the expanding kinetic phase.

C. Conversion after the Bounce

We have just calculated the evolution of entropy perturbations through a non-singular ghost condensate bounce. We have discussed how these entropy perturbations are created during ekpyrosis via the entropic mechanism in Chapter 5 and Chapter 6 D or via the non-minimal entropic mechanism in Chapter 8.

These perturbations will pass through the bounce as described in Chapter 11 B. At some point, the entropy perturbations need to be converted into curvature perturbations. We will now describe the evolution of the perturbations from the end of ekpyrosis to the end of the conversion process, assuming that the bounce occurs in between these phases. In Fig. 20 we have sketched the overall background evolution. As we have seen, at the end of the ekpyrotic phase the curvature perturbations are negligible, while the entropy perturbations take the form c.f. Eq. (6.37) and Eq. (8.64):

$$\delta s^{(1)} = \delta s_{ek}\,, \qquad \dot{\delta s}^{(1)} = -\frac{\delta s_{ek}}{t_{ek}} \tag{11.20}$$

$$\delta s^{(2)} = \frac{\kappa_3\sqrt{\epsilon}}{8}\delta s_{ek}^2\,, \qquad \dot{\delta s}^{(2)} = -\frac{\kappa_3\sqrt{\epsilon}}{4}\frac{\delta s_{ek}^2}{t_{ek}} \tag{11.21}$$

For our numerical evaluations we choose $\delta s_{ek} = 10^{-5}$. Note that the non-minimally coupled models simply correspond to specifying $\kappa_3 = 0$.

We have reviewed the conversion process in detail in Chapter 6 E. The conversion is described by the evolution equation on large scales, cf. Eq. (6.44):

$$\dot{\mathcal{R}} = -\frac{2H}{\dot\sigma}\dot\theta\,\delta s + \frac{H}{\dot\sigma^2}\left(V_{ss} + 4\dot\theta^2\right)(\delta s)^2 - \frac{V_\sigma}{\dot\sigma}\delta s\dot{\delta s}. \tag{11.22}$$

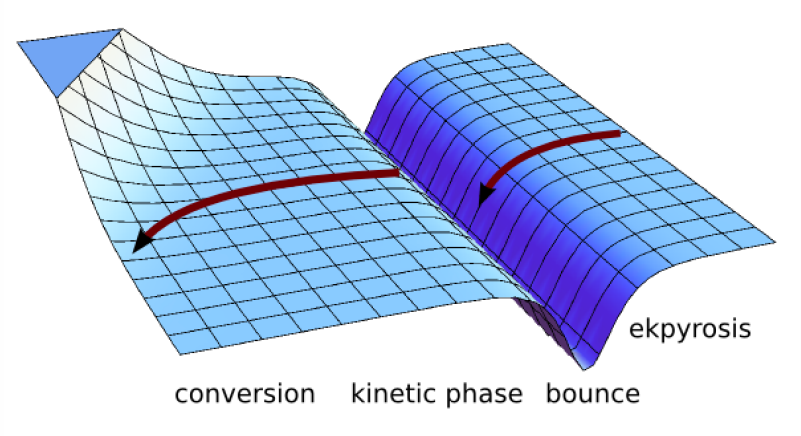

FIG. 20. During the ekpyrotic phase the field rolls down the ekpyrotic potential. Here we have chosen a stable transverse direction corresponding to the non-minimal entropic case. The bounce occurs at the bottom of the ekpyrotic potential. During the expanding kinetic phase the conversion takes place due to the presence of a repulsive potential.

The comoving curvature perturbations can be expanded as, cf. Eq. (6.45):

$$\mathcal{R}(x) = \mathcal{R}_L(x) + \frac{3}{5} f_{NL} \left(\mathcal{R}_L(x)\right)^2 , \tag{11.23}$$

which allows us to calculate the non-Gaussian parameter f_{NL}.

In order to model the conversion, we will add a term to the potential, which will induce a bending of the background trajectory. In a more fundamental context such a term is in principle calculable (see, e.g. the heterotic M-theory embedding of the cyclic universe [153]). Here we will choose our total potential to be given by

$$V(\phi) = -\frac{2V_o}{e^{-\sqrt{2\epsilon}\phi} + e^{\sqrt{2\epsilon}\phi}} \left(1 + \frac{1}{2}\epsilon\chi^2 + \frac{1}{3!}\epsilon^{3/2}\kappa_3\chi^3\right) + V_{rep} \tag{11.24}$$

with

$$V_{rep} = 10^{-4}\, V_o \times e^{-5[\sin(\pi/10)\phi - \cos(\pi/10)\chi - 2]^2} . \tag{11.25}$$

Note that the repulsive potential is simply a smooth (Gaussian-shaped) barrier oriented at an angle to the background trajectory. The bounce occurs at $\phi = 0$ and the conversion process begins at around $\phi = -2$. We should comment on the overall scale that we chose for the repulsive part of the potential: As has been discussed in previous works [78, 154], the most important aspect of the conversion process is the overall efficiency of the conversion, i.e. how much of the initial entropy perturbations is converted into curvature perturbations, c.f. Chapter 6 E. Inefficient conversions

lead to little structure formation and a very wide range of predictions for non-Gaussian corrections. By contrast, the predictions narrow to a much smaller range for efficient conversions, and moreover, they lead to greater structure formation. The amplitude of the entropy perturbation generated via ekpyrosis depends crucially on the energy scale reached by the potential. This energy scale must be rather large (i.e. not too far below the Planck scale) in order for the perturbations to obtain an amplitude in agreement with observations. Hence the conversion process must indeed be efficient, as one cannot assume that the potential reaches even larger energy scales (at which point the effective description used here would certainly break down). For these reasons, we will focus on efficient conversions, and this translates into our choice for the overall scale of the repulsive potential. An important open problem is to justify this assumption in a more fundamental context.

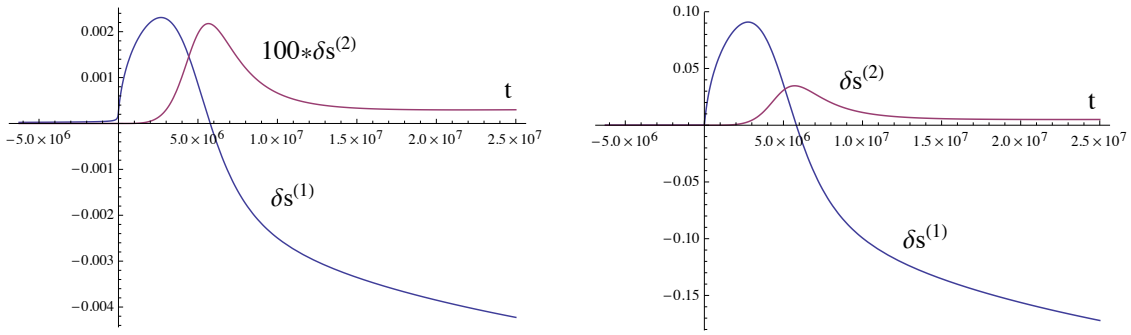

FIG. 21. The evolution of the linear and second order entropy perturbations from after the bounce through the conversion phase. Here we have taken $\kappa_3 = 0$. The left panel corresponds to having a stable potential (11.26) during the bounce (i.e. a flat transverse direction), while the right panel shows the case of the unstable potential (11.24). Figure taken from [9].

We have performed a series of numerical simulations, following the entropy and curvature perturbations through the kinetic and bounce phases until after the conversion period. In these simulations, we have chosen different repulsive potentials in combination with stable and unstable ekpyrotic potentials during the bounce. We will simply show a few typical examples. Fig. 21 shows the evolution of the linear and second order entropy perturbations from after the bounce through the conversion phase. The left panel corresponds to having a stable potential during the bounce (i.e. a flat transverse direction)

$$V(\phi) = -\frac{2V_o}{e^{-\sqrt{2\epsilon}\phi} + e^{\sqrt{2\epsilon}\phi}} + V_{rep}, \tag{11.26}$$

while the right panel shows the case of the unstable potential (11.24), where we have used the background parameters given by (11.3), namely $\epsilon = 10, V_o = 2 \times 10^{-8}$. The linear entropy per-

turbation grows significantly during the bounce phase and starts oscillating during the conversion. The second order perturbation grows as a consequence of the growth of the linear perturbation since the linear perturbation acts as its source. As a result, the growth of the second order perturbation lags a little behind the growth of the linear perturbation, but the overall growth is very significant, as shown in more detail in Fig. 22.

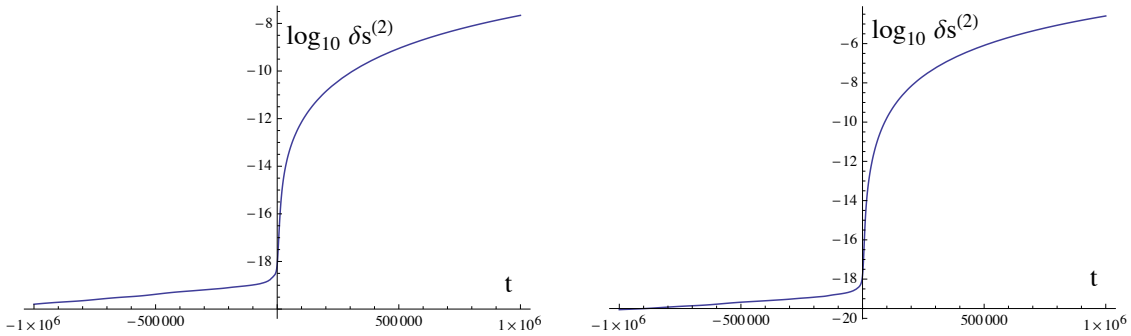

FIG. 22. The left panel shows the logarithm of the second order entropy perturbation for a bounce with the stable potential (11.26) and a preceding kinetic phase. The right panel shows the analogous plot for a bounce with the unstable potential (11.24). The logarithm shows more clearly the overall amplification through the kinetic and bounce phases. Figure taken from [9].

The curvature perturbations at linear and second order are plotted in Fig. 23, where one clearly sees the period of the conversion. At late times, the field space trajectory bends less and less, and the curvature perturbations approach constant values, as expected.

For the specific example shown in the left panels of Figs. 21–23, the potential during the bounce is stable. In this example, the final value of the curvature perturbation $\mathcal{R}$, its ratio to the entropy

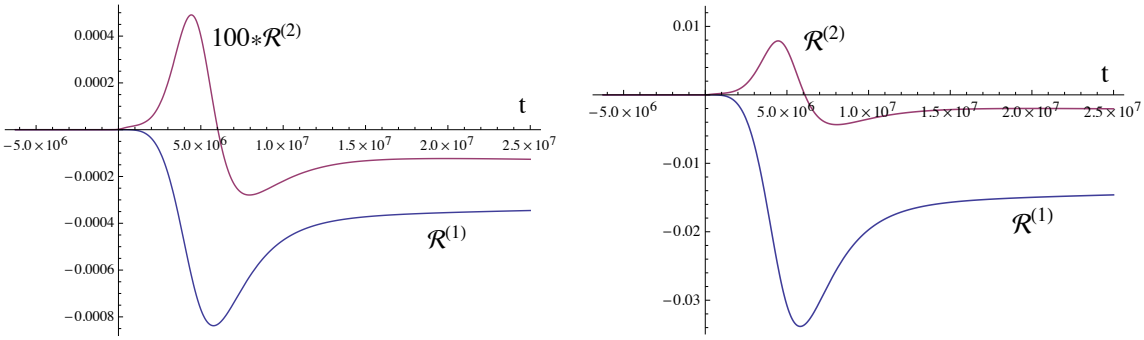

FIG. 23. The evolution of the linear and second order curvature perturbations from after the end of ekpyrosis through the conversion phase. Here we have again taken $\kappa_3 = 0$. The left panel corresponds to having a stable potential (11.26) during the bounce (i.e. a flat transverse direction), while the right panel shows the case of the unstable potential (11.24). Figure taken from [9].

perturbation at the beginning of the conversion phase (i.e. the time at which the trajectory starts bending significantly) and the value of the final non-Gaussianity parameter f_{NL} are given by

$$\mathcal{R}_{final} = -3.5 \times 10^{-4}\,, \tag{11.27}$$

$$\frac{\mathcal{R}_{final}}{\delta s_{conv-beg}} = -0.18\,, \tag{11.28}$$

$$f_{NL} = -4.0\,. \tag{11.29}$$

For the time interval from $t_1 = 1.45 \times 10^6$ to $t_2 = 10.5 \times 10^6$ the background evolves by one e-fold, i.e. aH changes by a factor of e, and during this time 95% of the total conversion takes place. Hence this is clearly a very efficient, yet smooth, conversion. The analogous example for the case with an unstable potential during the bounce phase is shown in the right panels of Figs. 21–23. Here we obtain the values

$$\mathcal{R}_{final} = -1.5 \times 10^{-2}\,, \tag{11.30}$$

$$\frac{\mathcal{R}_{final}}{\delta s_{conv-beg}} = -0.20\,, \tag{11.31}$$

$$f_{NL} = -3.6\,. \tag{11.32}$$

The conversion period is the same as above, and this is an equally efficient conversion. As expected, the final curvature perturbation is however much larger, by almost two orders of magnitude in the present case. Nevertheless, the value of the non-Gaussianity parameter f_{NL} remains of the same order, as the second order perturbation has been amplified correspondingly.

In the examples discussed so far, the entropy perturbation was perfectly Gaussian before the conversion process. This is the relevant case for the non-minimally coupled ekpyrotic models. However, in ekpyrotic models with an unstable potential, there can already be a significant intrinsic non-Gaussianity in the entropy perturbation, parameterized by κ_3 and depending on the tilt of the potential (6.27). The dependence of the final value of f_{NL} on κ_3 is shown in Fig. 24, for the example where the bounce is stable. Interestingly, the dependence on κ_3 is very weak, as the change in f_{NL} is smaller than 2 for $-1 < \kappa_3 < +1$. This may be understood as follows: as the entropy perturbations grow during the bounce phase, the second order part is sourced more and more strongly by the terms quadratic in the linear perturbation. Thus, even though the intrinsic second order term is also amplified (roughly like the linear term), its relative importance compared to the square of the linear term is lessened. Thus, for these models where the conversion takes place after the bounce, the main contribution to the non-Gaussianity comes from the non-linearity of the conversion process itself, and not from a possible intrinsic non-Gaussianity generated during the contraction phase. This is precisely the opposite situation to that described in [69], where

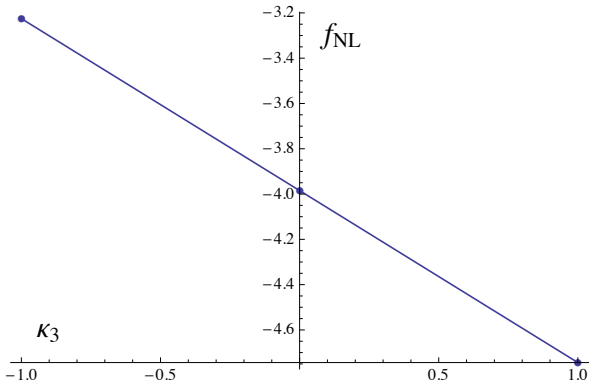

FIG. 24. The dependence of f_{NL} on the intrinsic non-Gaussianity (parameterized by κ_3) is seen to be surprisingly small when converting after the bounce. The example shown here has a stable potential during the bounce. Figure taken from [9].

the conversion process was analyzed for large intrinsic non-Gaussianity and neglecting the non-linearities of the conversion process. Thus, converting after the bounce rather than before brings with it a significant change in the implications of the conversion process.

D. Conversion before the Bounce

It may be useful to contrast the new results that we just described with the old case of having the conversion occur during the phase of kinetic contraction before the bounce, which we covered in detail in Chapter 6 E. Following [104], we take the repulsive potential to be

$$V_{rep} = \frac{12 \times 10^{-9}}{[\sin(\pi/6)\phi + \cos(\pi/6)\chi + 2]^2}\,, \tag{11.33}$$

and the initial conditions for the numerical evolution are given by

$$t_o = -1000 \quad , \quad a_o = 1 \tag{11.34}$$

$$\phi_o = -\sqrt{\frac{2}{3}} - 4.5 \quad , \quad \dot{\phi}_o = \sqrt{\frac{2}{3}}\,\frac{1}{|t_o|} \tag{11.35}$$

$$\delta s_o = 10^{-5} \quad , \quad \dot{\delta s}_o = \frac{10^{-5}}{|t_o|}\,. \tag{11.36}$$

Then we find

$$\mathcal{R}_{final} = 2.3 \times 10^{-6}\,, \tag{11.37}$$

$$\frac{\mathcal{R}_{final}}{\delta s_{conv-beg}} = 0.14\,, \tag{11.38}$$

$$f_{NL} = 6.7\,. \tag{11.39}$$

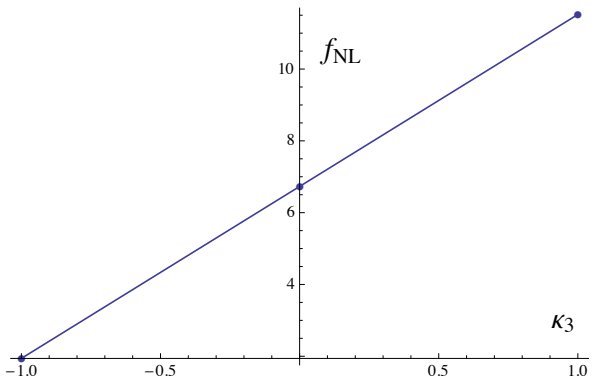

FIG. 25. The dependence of f_{NL} on the intrinsic non-Gaussianity (parameterised by κ_3) for a model of conversion before the bounce. Note that the slope has the opposite sign compared to the case when converting after the bounce: this is due to the fact that here the universe contracts whereas it expands in the other case. Figure taken from [9].

For this example, 87% of the conversion take place over one e-fold of evolution from around $t_1 = -440$ to $t_2 = -70$; thus for this particular example the conversion is slightly less efficient than it was in the examples above, but nevertheless comparable. Due to this difference in efficiency, the value of f_{NL} is slightly higher. The dependence of f_{NL} on κ_3 is shown in Fig. 25. Note that this dependence, which is well parameterised by the phenomenological formula $f_{NL} \approx \frac{3}{2}\sqrt{\epsilon}\kappa_3 + 5$ [35], is vastly more significant in the present case than when converting after the bounce and therefore a wider range of values is obtained.

E. Implications for Models and Observations

The main implication of having a conversion phase during the expansion phase after the bounce, rather than before the bounce, is that the final amplitude of the curvature perturbation is significantly enhanced. As we saw with the help of specific examples, for the case of a bounce with a stable potential the curvature perturbation is approximately two orders of magnitude larger than when the conversion takes place before the bounce. For an unstable potential, the growth is even more significant, by almost four orders of magnitude in the example shown around Eq. (11.30). It is useful to recall from Eq. (5.32) that at the end of the ekpyrotic phase the Fourier mode of the entropy perturbation reaches a value

$$\delta s_k(t_{ek-end}) \approx \frac{|\epsilon V_{ek-end}|^{1/2}}{\sqrt{2}k^{\nu}}\,. \tag{11.40}$$

For the case where the conversion takes place during the contraction phase before the bounce, this leads to the following root mean square value for the curvature perturbation (where we have used the approximation $\mathcal{R} \approx \frac{1}{5}\delta s_{ek-end}$, c.f. Eq. (5.37) and [69]),

$$\langle \mathcal{R}^2 \rangle \approx \int \frac{\mathrm{d}^3 k}{(2\pi)^3} \frac{\epsilon V_{ek-end}}{50 k^{2\nu}} = \int \frac{\mathrm{d}k}{k} \frac{\epsilon V_{ek-end}}{100\pi^2} k^{n_s - 1} \,. \tag{11.41}$$

Matching to the observed value of $\Delta^2_{\mathcal{R}} \approx 3 \times 10^{-9}$ [6] leads to an estimated depth of the potential of $|V_{ek-end}| \approx (10^{-2} M_{Pl})^4$, around the grand unified scale. For conversion after the bounce, we obtain an enhancement of the curvature perturbation by approximately two to four orders of magnitude. This would mean that the potential does not have to become quite so deep, and the energy scale that the potential must reach is around 10^{-4} or 10^{-3} in reduced Planck units.

Despite the fact that the amplitude of the curvature perturbation is significantly enhanced by the conversion process, the level of non-Gaussianity remains similar (though as we have seen the value of the local non-Gaussianity parameter f_{NL} is now mostly determined by the conversion process and not by the intrinsic level of non-Gaussianity produced during the ekpyrotic phase). Our numerical examples suggest that for efficient conversion processes typical values lie in the range

$$-5 \lesssim f_{NL} \lesssim +5 \,, \tag{11.42}$$

while a little less efficient conversions lead to values of $\mathcal{O}(10)$. This is a very interesting range of values, consistent with current bounds on f_{NL}, which are $f_{NL} = 0.8 \pm 10.0$ at the 2σ level [44], but within the reach of not-too-distant future experiments. In particular, the Square Kilometer Array is expecting to reduce the error on local non-Gaussianities to $\sigma(f_{NL}) \approx 1$, cf. [155, 156], at which point one would expect to measure the presently discussed values.

12. SCALAR-TENSOR-THEORIES

In Chapter 9 we have discussed the most general scalar field Lagrangian which yields second order equations of motion: the Galileon (or Horndeski) Lagrangian. We have constructed a bounce via a ghost-condensate phase and extended the discussion to Galileon bounces. In this chapter, we will investigate another subclass of Galileon theory which is called scalar-tensor-theory. In scalar-tensor-theories the scalar and tensor degrees of freedom are mixed. Newtons gravitational constant is no longer constant but a function of the scalar field Φ. The first and very prominant example of a scalar-tensor theory is Brans-Dicke theory [119]. Brans and Dicke considered a modification of general relativity of the following form:

$$S_{BD} = \frac{1}{2}\int d^4x\sqrt{-g}\left[\Phi R - \frac{\omega}{\Phi}g^{\mu\nu}\nabla_\mu\Phi\nabla_\nu\Phi - V(\Phi)\right] + S^{(m)}, \tag{12.1}$$

where $S^{(m)}$ is the action of ordinary matter which is coupled minimally to the metric $g_{\mu\nu}$:

$$S^{(m)} = \int d^4x\sqrt{-g}\mathcal{L}^{(m)}. \tag{12.2}$$

In this theory, matter does not couple directly to the scalar field. However, Φ couples directly to the Ricci scalar. Thus the gravitational field is described by the scalar field Φ and the metric tensor $g_{\mu\nu}$. This leads to a Φ-dependent effective gravitational constant

$$G_{eff} = \frac{1}{8\pi\Phi}, \tag{12.3}$$

here we have not set $8\pi G = 1$. $\Phi > 0$ guarantees the positivity of the gravitational coupling corresponding to attractive and ghost-free gravity. ω is a dimensionless free parameter, which is constrained by Solar System experiments, e.g., $\omega > 40\,000$ by the Cassini probe in 2003 [157]. The natural value for ω of order unity is not in agreement with measurements; Brans-Dicke gravity has to be very close to general relativity in today's cosmology. Note that theories with modified gravity describing the dark energy phase today usually make use of a screening mechanism. Most of the time these theories want to describe large scale modifications and thus use screening mechanisms on low scales in order to match solar system observations [158–160]. However, early universe models incorporating modified gravity can work differently, since these models can dynamically become a theory of general relativity. In the case of a scalar-tensor-theory, this corresponds to a constant field Φ.

In the following, we will look at the generalization of the Brans-Dicke theory, including more general couplings to the Ricci scalar and more general kinetic terms. As already mentioned this is a subclass of Galileon theory of Chapter 9 where $G_3 = G_{4X} = G_5 = 0$. The action is given by

$$S = \int \mathrm{d}^4x\sqrt{-g}\,[F(\Phi)R - P(X,\Phi)] + S^{(m)}. \tag{12.4}$$

A. Einstein Equations for Scalar-Tensor-Theories

We have already obtained the equations of motion of generalized Galileon theory in Chapter 9. We will briefly highlight the effect of the non-minimal coupling to gravity compared to the derivation of the Einstein equations in the case of a minimal coupling to gravity.

The Palatini identity relates the variation of the Ricci tensor $\delta R_{\mu\nu}$ to the variation of the Christoffel symbol $\delta\Gamma^\lambda_{\mu\nu}$:

$$\delta R_{\mu\nu} = \nabla_\lambda \delta\Gamma^\lambda_{\mu\nu} - \nabla_\nu \delta\Gamma^\lambda_{\mu\lambda}\,. \tag{12.5}$$

The variation of the Ricci scalar R reads:

$$\begin{aligned}
\delta R &= R_{\mu\nu}\delta g^{\mu\nu} + g^{\mu\nu}\delta R_{\mu\nu} && (12.6)\\
&= R_{\mu\nu}\delta g^{\mu\nu} + g^{\mu\nu}\left(\nabla_\lambda \delta\Gamma^\lambda_{\mu\nu} - \nabla_\nu \delta\Gamma^\lambda_{\mu\lambda}\right) && (12.7)\\
&= R_{\mu\nu}\delta g^{\mu\nu} - \nabla_\mu\nabla_\nu \delta g^{\mu\nu} + g_{\mu\nu}\Box\delta g^{\mu\nu}\,. && (12.8)
\end{aligned}$$

The last terms normally contribute as a total derivative in the action. However, this will no longer be the case due to the presence of the non-minimal coupling to gravity $F(\Phi)R$. In the case of a flat FLRW metric we obtain the equations of motion for the scalar-tensor theory, which coincides with the equation of motion for the generalized Galileon theory in Chapter 9 B (for $G_3 = G_{4X} = G_5 = 0$):

$$\begin{aligned}
\nabla_\mu\left(P_X\nabla^\mu\Phi\right) &= P_{,\Phi} + \frac{1}{2}RF_{,\Phi}\,, && (12.9)\\
3FH^2 + 3H\dot{F} &= \rho\,, && (12.10)\\
\rho + p + 2F\dot{H} - H\dot{F} + \ddot{F} &= 0\,. && (12.11)
\end{aligned}$$

with the effective energy density $\rho = 2XP_X - P$ and effective pressure $p = P$. As we can see due to the non-minimal coupling the equations of motion become more complicated. However, this also leads to interesting new cosmological solutions.

From now on we will restrict to the case $P(X,\Phi) = K(\Phi)X - V(\Phi)$ (until we discuss non-singular bounces):

$$S = \int \mathrm{d}^4x\sqrt{-g}\left[F(\Phi)R - \frac{1}{2}K(\Phi)g^{\mu\nu}\nabla_\mu\Phi\nabla_\nu\Phi - V(\Phi)\right] + S^{(m)}. \tag{12.12}$$

B. Conformal Transformation

The scalar-tensor-theory action given in equation (12.12) is written in the so-called Jordan frame. In Jordan frame, the scalar field is non-minimally coupled to gravity, while matter is only minimally coupled – there is no direct coupling between the scalar field Φ and ordinary matter. The Jordan frame can be transferred into the so-called Einstein frame via a conformal transformation. In Einstein frame, the scalar field is minimally coupled to gravity, while ordinary matter couples directly to the scalar field. Because of the complexity of the equations of motion (12.9) it is often useful to transform the theory to the Einstein frame, where the equations of motion are generally easier to solve. Since both frames are physically equivalent, the solution can then be transformed back to the Jordan frame. We will examine in the following how a change of frame via a conformal transformation can be obtained. For a review of scalar-tensor-theories and detailed derivations see, e.g. [161, 162].

One can always find a suitable conformal transformation from Jordan frame to Einstein frame if the non-minimally coupling is $F(\Phi) > 0$ (and if there is no derivative coupling $F(\Phi, X)_X = 0$. $F(\Phi, X)_X \neq 0$ does not belong to the class of scalar-tensor theories, cf. Chapter 9).
In the following, we will use the subscript "J" to indicate Jordan frame quantities and no subscript to indicate Einstein frame quantities. Moreover, we use Φ in Jordan frame and ϕ in Einstein frame. The connection between the field-redefinition of the scalar field will be discussed in the upcoming chapter.
In the following, we will transform the scalar-tensor-theory action (12.12) in Jordan frame to the Einstein frame.

$$S_J = \int d^4x\sqrt{-g_J}\left[\frac{1}{2}F(\Phi)R_J - \frac{1}{2}K(\Phi)g_J^{\mu\nu}\nabla_\mu\Phi\nabla_\nu\Phi - V_J(\Phi)\right] + S_J^{(m)}\,, \tag{12.13}$$

where again the matter action is given by

$$S_J^{(m)} = \int \mathrm{d}^4x\sqrt{-g_J}\mathcal{L}^{(m)}\,. \tag{12.14}$$

We perform a point-dependent rescaling of the metric tensor

$$g_{J\mu\nu} \to g_{\mu\nu} = \Omega(x)^2 g_{J\mu\nu}\,. \tag{12.15}$$

Ω is the conformal factor, which is a regular nowhere vanishing function. The transformation is called a Weyl or conformal transformation. Due to the rescaling of the metric, length scales are

changed. However, null vectors and null intervals remain null, leading to the same light-cones in both frames: the causal structure is the same in both frames. Conformal transformations are a very important tool in studying causal structures (e.g., Penrose diagrams).

Inspecting (12.15), the transformation of the 00-component of the metric can be absorbed into the time coordinate interval via:

$$\mathrm{d}t = \Omega \mathrm{d}t_J. \tag{12.16}$$

Using the flat FLRW metric, we obtain for the transformation of the ij-component of the metric

$$a = \Omega a_J. \tag{12.17}$$

We have absorbed the conformal factor Ω in the definition of the time interval dt and the scale factor a. This means that we have two different frames which are related via a conformal transformation. We will discuss the consequences of such a change of frame throughout this chapter.

In order to transform the action (12.13) into the Einstein frame, we need to know how the Ricci scalar R_J transforms under a conformal transformation. From the conformal transformation (12.15) we obtain for the inverse metric and the determinant:

$$g_{\mu\nu} = \Omega(x)^2 g_{J\mu\nu} \quad , \quad g^{\mu\nu} = \Omega(x)^{-2} g^{J\mu\nu} \quad , \quad g = \Omega(x)^8 g_J \, . \tag{12.18}$$

Using the above relations we find for the Christoffel symbols:

$$\Gamma^\alpha_{\mu\nu} = \Gamma^\alpha_{J\mu\nu} + \Omega^{-1} \left(\delta^\alpha_\mu \nabla_\nu \Omega + \delta^\alpha_\nu \nabla_\mu \Omega - g_{J\mu\nu} \nabla^\alpha \Omega \right) . \tag{12.19}$$

This allows us to calculate how the Ricci scalar R_J transforms under the conformal transformation (12.15) [163]:

$$R_J = \Omega^2 \left[R + 6\Box \ln \Omega + 6 g^{\mu\nu} \nabla_\mu \left(\ln \Omega \right) \nabla_\nu \left(\ln \Omega \right) \right] . \tag{12.20}$$

The above equation can be easily inverted using (12.18)

$$R = \Omega^{-2} \left[R_J - 6\Box_J \ln \Omega - 6 g^{\mu\nu}_J \nabla_\mu \left(\ln \Omega \right) \nabla_\nu \left(\ln \Omega \right) \right] , \tag{12.21}$$

where $\Box_J = g^{\mu\nu}_J \nabla_\mu \nabla_\nu$. The second term in both equations contributes as a total derivative in the action.

Plugging the transformed Ricci scalar (12.20) and the transformed metric (12.18) into the action (12.13) yields:

$$S = \int \mathrm{d}^4x\sqrt{-g}\,\Omega^{-4}\left[\frac{1}{2}F(\Phi)\Omega^2\left(R + 6g^{\mu\nu}\nabla_\mu\left(\ln\Omega\right)\nabla_\nu\left(\ln\Omega\right)\right) - \frac{1}{2}K(\Phi)\Omega^2 g^{\mu\nu}\nabla_\mu\Phi\nabla_\nu\Phi - V_J(\Phi)\right] + S^{(m)}\,. \tag{12.22}$$

The scalar field is non-minimally coupled to gravity if

$$\Omega = \sqrt{F}. \tag{12.23}$$

The conformal transformation which changes the Jordan frame action to the Einstein frame action (where the coupling to gravity is minimal) reads

$$g_{\mu\nu} = F g_{J\mu\nu}\,. \tag{12.24}$$

Moreover, we can canonically normalize the scalar field via a field redefinition. Using

$$\partial_\mu \ln\sqrt{F} = \frac{1}{2F}\partial_\mu F = \frac{F_{,\Phi}}{2F}\partial_\mu\Phi \tag{12.25}$$

we obtain

$$S = \int \mathrm{d}^4x\sqrt{-g}\left[\frac{R}{2} - \left(\frac{K(\Phi) - \frac{3}{2}F(\Phi)^2_{,\Phi}}{F(\Phi)}\right)\frac{1}{2}g^{\mu\nu}\nabla_\mu\Phi\nabla_\nu\Phi - \frac{V_J(\Phi)}{F(\Phi)^2}\right] + S^{(m)}. \tag{12.26}$$

Let us introduce the field redefinition:

$$\mathrm{d}\phi = \mathrm{d}\Phi\left(\frac{K(\Phi) - \frac{3}{2}F(\Phi)^2_{,\Phi}}{F(\Phi)}\right)^{1/2}. \tag{12.27}$$

We can also "invert" (12.27) by writing the functions in terms of ϕ, which is necessary when transforming from Einstein frame to Jordan frame. We obtain

$$\sqrt{K(\Phi)}\mathrm{d}\Phi = \mathrm{d}\phi\left(F(\phi) - \frac{3}{2}\frac{F(\phi)^2_{,\phi}}{F(\phi)}\right)^{1/2}. \tag{12.28}$$

Defining the Einstein frame potential

$$V(\phi) = \frac{V_J(\Phi)}{F(\Phi)^2} \tag{12.29}$$

and using the field redefinition yields the final Einstein frame action:

$$S = \int \mathrm{d}^4x\sqrt{-g}\left[\frac{R}{2} - \frac{1}{2}g^{\mu\nu}\nabla_\mu\phi\nabla_\nu\phi - V(\phi)\right] + S^{(m)}. \tag{12.30}$$

It is important to note that this action is generally not equivalent to general relativity. This is due to the matter coupling $S^{(m)}$. We assumed here, that in Jordan frame ordinary matter does

not couple directly to the scalar field. Ordinary matter in Jordan frame only couples minimally to gravity. But this means, that a transformation from Jordan frame

$$S_J^{(m)} = \int \mathrm{d}^4x\sqrt{-g_J}\mathcal{L}^{(m)} \tag{12.31}$$

to the Einstein frame

$$S^{(m)} = \int \mathrm{d}^4x\sqrt{-g}F(\phi)^{-2}\mathcal{L}^{(m)} \tag{12.32}$$

results in a ϕ-dependent matter coupling – the coupling constants are ϕ-dependent. This can give rise to so-called 5th force effects – a violation of the equivalence principle. Geodesics in this frame are different to the ones in general relativity. The fact that the Einstein frame is generally not equivalent to general relativity due to the non-minimal matter coupling causes often confusion or is sometimes just ignored. Only if the scalar field ϕ becomes constant the Einstein frame theory is (classically) equivalent to general relativity.

As a final remark let us state that in conformal field theories the Weyl/conformal transformation

$$g_{\mu\nu} \to \tilde{g}_{\mu\nu} = \Omega(x)^2 g_{\mu\nu} \tag{12.33}$$

resulting in a rescaling

$$x \to \tilde{x} = \Omega x \tag{12.34}$$

is used for the same space-time. There is no change of frame: the conformal factor is not absorbed into the time and space coordinates in contrast to the case we have discussed here cf. (12.16). This leads to the well known conformal transformation properties, e.g., under rescaling the scalar field transforms as

$$\phi(x) \to \phi(\tilde{x}) = \phi(\Omega x) = \Omega^{-\Delta}\phi(x), \tag{12.35}$$

where $\Delta = \frac{D-2}{4}$ is the conformal dimension.

13. CONFLATION

A. Introduction

In the previous chapter, we have discussed the properties of scalar-tensor theories. A non-minimal coupling to gravity allows for a variety of cosmological solutions. It is possible to change from one frame to another via a conformal transformation and we have determined the transformation properties of various quantities. Both frames are physically equivalent since they are related via a conformal transformation. Moreover, as we will see, the scalar and tensor perturbations in both frames are the same.

Scalar-tensor theories of gravity allow for very interesting cosmological solutions e.g. [164–167]. Let us examine shortly possible new features of these scalar-tensor theories (or generalized Galileon theories) in an example. We have reviewed the evolution equation of curvature perturbations $\mathcal{R}$ in generalized Galileon theories in Chapter 9. The action (9.36) can be written in conformal time as

$$S = \int \mathrm{d}\tau \mathrm{d}^3x a^2 \mathcal{G}_S \left(\mathcal{R}'^2 - c_s^2 (\vec{\nabla}\mathcal{R})^2 \right) , \tag{13.1}$$

where we have used $c_S^2 = \frac{\mathcal{F}_S}{\mathcal{G}_S}$. The corresponding equations of motion for the canonically normalized variable $v = z_S \mathcal{R}$ with $z_S = a^2 \mathcal{G}_S$ in momentum space reads

$$v'' + \left(c_s^2 k^2 - \frac{z_S''}{z_S} \right) = 0 \, . \tag{13.2}$$

The spectrum of the comoving curvature perturbations $\mathcal{R}$ is scale-invariant if

$$z = a^2 \mathcal{G}_S \sim \tau^2 \quad \text{or} \quad z = a^2 \mathcal{G}_S \sim \tau^{-2} \, , \tag{13.3}$$

since the equations of motion using (13.3) becomes

$$v'' + (k^2 - \frac{2}{\tau^2}) = 0 \, . \tag{13.4}$$

As a reminder: This is the same equation as in the standard single scalar field case in the de Sitter limit during inflation (4.59). Note, the second solution in (13.3) is used in the matter-dominated contraction models in the standard single scalar field case [168, 169].

Due to the non-trivial $\mathcal{G}_S$ - term in scalar-tensor theories (or generalized Galileon theories), we can obtain scale-invariant curvature perturbations $\mathcal{R}$. For example, a constant scale factor combined with $\mathcal{G}_S \sim \tau^2$ produces nearly scale invariant perturbations. This is in contrast to the

case of a single scalar field minimally coupled to gravity. This is just one example of the new possibilities which arise in scalar-tensor theories. A very interesting model in this context is the so-called anamorphic cosmology [167].

During the contracting anamorphic smoothing phase (similar to ekpyrosis), nearly scale-invariant curvature perturbations $\mathcal{R}$ are created, which are similar to those produced during inflation. Anamorphic cosmology is described by a scalar-tensor theory, which makes such a construction possible. It has been shown in [167] that one can write (13.1) in the case of a scalar-tensor theory in a frame-invariant way

$$S = \frac{1}{2}\int \mathrm{d}\tau \mathrm{d}^3x \alpha_{PL}\epsilon_{PL}\left(\mathcal{R}'^2 - c_s^2(\vec{\nabla}\mathcal{R})^2\right), \tag{13.5}$$

where α_{PL} and ϵ_{PL} are frame-invariant quantities. The comoving curvature perturbations $\mathcal{R}$ are frame independent.

This very fact was one motivation for the construction of the conflationary model, which we proposed in [10]. The basic idea of the model of conflation is to conflate ideas of inflation and ekpyrosis combining features of both models. Conflation can be thought of as being complementary to the anamorphic phase described above.

During conflation, the universe expands exponentially like during inflation, but perturbations behave like during ekpyrosis. Hence eternal inflation does not occur during conflation since there are no large adiabatic fluctuations.

The starting point of the construction of conflation is an ekpyrotic model described by a scalar field minimally coupled to gravity in a steep negative potential. Then we transform the ekpyrotic model in Einstein frame into a scalar-tensor theory in Jordan frame via a conformal transformation. In this frame, we will construct an accelerated phase.
Remarkably, in this model, the non-minimally coupled scalar field has a kinetic energy term of the wrong sign, and it rolls up a negative potential. Nevertheless, the theory is ghost-free.
Subsequently, the model will be extended allowing for a graceful exit of the phase. This extension is necessary: In Einstein frame, the universe would end up in a big crunch after the ekpyrotic contracting phase. Thus we add a non-singular bounce in Einstein frame and investigate the consequence of such an implementation for the model in Jordan frame.

Chapter 13 D 1 contains the analysis of scalar and tensor fluctuations up to first order in perturbation theory in the two frames. We will demonstrate that their spectra in both frames are indeed the same.

The model of conflation describes a phase of accelerated expansion, where adiabatic fluctuations stay quantum – with no run-away behavior like in eternal inflation – and where entropy perturbations are amplified as during ekpyrosis. The following chapters are based on our paper [10].

B. The Conflationary Phase

1. *Ekpyrotic Phase in Einstein Frame*

We review briefly the ekpyrotic phase described in Chapter (3 B). During the slowly contracting phase the pressure p is very high with an equation of state $w = p/\rho > 1$. Ekpyrosis is modeled by a scalar field minimally coupled to gravity in a steep negative potential. Thus the action in Einstein frame is

$$S = \int \mathrm{d}^4x\sqrt{-g}\left[\frac{R}{2} - \frac{1}{2}g^{\mu\nu}\partial_\mu\phi\partial_\nu\phi - V(\phi)\right], \tag{13.6}$$

where a typical ekpyrotic potential is given by a negative exponential,

$$V(\phi) = -V_0 e^{-c\phi}. \tag{13.7}$$

Considering the flat Friedmann-Lemaître-Robertson-Walker (FLRW) universe, we obtain the equations of motion for the scalar field ϕ

$$\ddot{\phi} + 3H\dot{\phi} + V_{,\phi} = 0, \tag{13.8}$$

which admits the scaling solution [14]

$$a(t) = a_0\left(\frac{t}{t_0}\right)^{1/\epsilon}, \quad \phi = \sqrt{\frac{2}{\epsilon}}\ln\left(\frac{t}{t_0}\right), \quad \text{where } t_0 = -\sqrt{\frac{\epsilon-3}{V_0\epsilon^2}} \quad \text{and } c = \sqrt{2\epsilon}. \tag{13.9}$$

Here the Einstein frame time coordinate t is negative and runs from large negative values towards small negative values. The equation of state is $w = \frac{2}{3}\epsilon - 1$, where $\epsilon = \frac{\dot{\phi}^2}{2H^2}$ is the fast-roll parameter. We require $\epsilon > 3$, since the ekpyrotic phase has to satisfly $w > 1$.

2. *Specific Conformal Transformation*

We will now change from the Einstein frame to the Jordan frame via the conformal transformation

$$g_{\mu\nu} = F(\phi) g_{J\mu\nu}. \tag{13.10}$$

As discussed in Chapter 12 B the corresponding Jordan frame action will be of the form (12.13):

$$S_J = \int \mathrm{d}^4x\sqrt{-g_J}\left[\frac{1}{2}F(\Phi)R_J - \frac{1}{2}K(\Phi)g_J^{\mu\nu}\partial_\mu\Phi\partial_\nu\Phi - V_J(\Phi)\right] + S_J^{(m)}. \tag{13.11}$$

The conformal factor $F(\phi)$ can in principle be chosen arbitrarily. Each choice will correspond to a different frame – each frame is physically equivalent to every other frame. A common choice is a polynomial of the form $F(\Phi) = \xi\Phi^n$, e.g. $n = 1$ in the specific Brans-Dicke model discussed before or non-minimal couplings inspired by dilaton couplings in string theory, e.g. [165, 166, 170].
We will chose the following ansatz in the Einstein frame:

$$F(\phi) = e^{c\gamma\phi}. \tag{13.12}$$

As we will see this ansatz corresponds to a non-minimal coupling in Jordan frame (after field-redefinition) of the form

$$F(\Phi) = \xi\Phi^2, \tag{13.13}$$

which is also known as induced gravity [171]; see e.g. [172] for related studies.
This choice is convenient, since it allows for analytic solutions in the Jordan frame. We will further simplify the initial model by setting the non-canonical kinetic term $K(\Phi) = k = const.$
Using the scaling solution (13.9) in Einstein frame we can find the relations between the times in both frames by integrating $\mathrm{d}t = \sqrt{F}\mathrm{d}t_J$

$$\frac{t_J}{t_{J,0}} = \left(\frac{t}{t_0}\right)^{1-\gamma}, \tag{13.14}$$

where

$$t_{J,0} = \frac{t_0}{1-\gamma}. \tag{13.15}$$

By using this relation we find for the scale factor in Jordan frame $a_J = a/\sqrt{F}$

$$a_J = a_0\left(\frac{t}{t_0}\right)^{\frac{1-\epsilon\gamma}{\epsilon}} = a_0\left(\frac{t_J}{t_{J,0}}\right)^{\frac{1-\epsilon\gamma}{\epsilon(1-\gamma)}}. \tag{13.16}$$

It is important to note, that the ansatz $F(\phi) = e^{c\gamma\phi}$ leads to a power-law relationship between both time coordinates since the scaling solution for the scalar field $\phi \sim ln(-t)$.

The purpose of this conformal transformation into the Jordan frame was the construction of an accelerated phase. The condition for accelerated expansion in the Jordan frame is that the t_J-exponent in equation (13.16) has to be larger than 1,

$$\frac{1-\epsilon\gamma}{\epsilon(1-\gamma)} > 1. \tag{13.17}$$

Keeping in mind that during ekpyrosis $\epsilon > 3$, we can see from (13.17) that γ has to be larger than 1 in order to obtain accelerated expansion.
The non-linear scalar-field redefinition (12.28) with $K(\Phi) = k$

$$\frac{\mathrm{d}\Phi}{\mathrm{d}\phi} = \sqrt{\frac{F}{k}\left(1 - \frac{3}{2}\frac{F_{,\phi}^2}{F^2}\right)} \tag{13.18}$$

can now be integrated by using $F(\phi) = e^{c\gamma\phi}$. We obtain

$$\Phi = \frac{1}{\sqrt{\xi}} e^{c\gamma\phi/2}, \tag{13.19}$$

where the parameter ξ is given terms of the parameters ϵ, γ and k:

$$\xi = \frac{c^2\gamma^2 k}{4 - 6c^2\gamma^2} = \frac{\epsilon\gamma^2 k}{2 - 6\epsilon\gamma^2}\,, \tag{13.20}$$

or in terms of ϵ

$$\epsilon = \frac{2\xi}{\gamma(6\xi + k)}\,. \tag{13.21}$$

We indeed obtain the non-minimal coupling (13.13) by using (13.19) in (13.12). The requirement $\xi > 0$ is fulfilled if $k < 0$, since $\gamma > 1$ and $\epsilon > 3$. Thus the sign of the kinetic term has to be negative and we choose $k = -1$. This "wrong" sign does not lead to ghosts, because of the scalar-tensor coupling as we will see in Chapter 13 D. From (13.20) we obtain the lower bound on $\xi > 1/6$ due to the choice $k = -1$.

Let us summarize the above results: we have constructed an accelerated expansion in Jordan frame via the conformal transformation (13.12). The starting point was an ekpyrotic phase with a negative exponential potential and an equation of state $w > 1$. The acceleration condition led to

$$\gamma > 1\,, \tag{13.22}$$

the positivity of the gravitation coupling resulted in

$$k = -1\,, \tag{13.23}$$

and the choice of k yielded

$$\xi > \frac{1}{6}\,. \tag{13.24}$$

Using equations (13.9) and (13.14) we can write Φ as a function of the Jordan frame time:

$$\Phi(t_J) = \frac{1}{\sqrt{\xi}}\left(\frac{t_J}{t_{J,0}}\right)^{\frac{\gamma}{1-\gamma}}. \tag{13.25}$$

The Jordan frame potential can be written in terms of Φ as

$$V_J(\Phi) = F^2(\phi)V(\phi) = -V_0 e^{(2\gamma-1)c\phi} = -V_{J,0}\Phi^{4-2/\gamma}, \tag{13.26}$$

where we have defined $V_{J,0} \equiv V_0\xi^{2-1/\gamma}$. The negative exponential potential in Einstein frame is transformed into a negative power-law potential in the Jordan frame. This is an important result: Accelerated expansion can be obtained in the presence of a negative potential in Jordan frame. The final Jordan frame action is given by:

$$S_J = \int \mathrm{d}^4x\sqrt{-g_J}\left[\frac{1}{2}\xi\Phi^2 R_J + \frac{1}{2}g_J^{\mu\nu}\partial_\mu\Phi\partial_\nu\Phi + V_{J,0}\Phi^{4-2/\gamma}\right] + S_J^{(m)}. \tag{13.27}$$

3. Equations of Motion in Jordan Frame

The equations of motion derived in (12.9) for the action (13.27) are given by

$$3H_J^2F + 3H_JF_{,t_J} = \frac{1}{2}k\Phi_{,t_J}^2 + V_J, \tag{13.28}$$

$$2FH_{J,t_J} + k\Phi_{,t_J}^2 - H_JF_{,t_J} + F_{,t_Jt_J} = 0, \tag{13.29}$$

$$\Phi_{,t_Jt_J} + 3H_J\Phi_{,t_J} - \frac{3F_{,\Phi}}{k}\left(H_{J,t_J} + 2H_J^2\right) + \frac{V_{J,\Phi}}{k} = 0, \tag{13.30}$$

where the subscript $_{,t_J}$ is the time derivative with respect to the Jordan frame time t_J and where we have not yet specified the potential V_J and the sign of the kinetic term k. We can solve the first Friedmann equation (13.28) for the Hubble parameter H_J,

$$H_J = -\frac{F_{,t_J}}{2F} \pm \sqrt{\frac{F_{,t_J}^2}{4F^2} + \frac{k}{6F}\Phi_{,t_J}^2 + \frac{1}{3F}V_J}. \tag{13.31}$$

The solution for H_J will always be positive, since the square root is always less than $-\frac{F_{,t_J}}{2F} > 0$, because $k, V_J < 0$. We can find the solution corresponding to contraction in Einstein frame via the relation between the Hubble parameter in both frames:

$$H = \frac{1}{\sqrt{F}}\left(H_J + \frac{F_{t_J}}{2F}\right), \tag{13.32}$$

where we have used $\mathrm{d}t = \sqrt{F}\mathrm{d}t_J$ and $a = \sqrt{F}a_J$. Since $H < 0$ in the Einstein frame, the solution H_J has to satisfy

$$H_J < -\frac{F_{,t_J}}{2F}. \tag{13.33}$$

This is exactly the first term in equation (13.31), which means we have to chose the negative solution:

$$H_J = -\frac{F_{,t_J}}{2F} - \sqrt{\frac{F_{,t_J}^2}{4F^2} + \frac{k}{6F}\Phi_{,t_J}^2 + \frac{1}{3F}V_J}. \tag{13.34}$$

The quantity $V_J/\Phi_{,t_J}$ using (13.25) and (13.26) is given by

$$\frac{V_J}{\Phi_{,t_J}} = \frac{\epsilon - 3}{\epsilon(2 - 6\epsilon\gamma^2)} \tag{13.35}$$

This term is time-independent. This will be useful when setting the initial conditions for specific values of the parameters.

4. Initial Conditions and Graceful Exit

In this chapter, we will construct a specific example of the conflationary model. We choose the ekpyrotic fast roll parameter $\epsilon = 10$ and the parameter $\gamma = 2$, which defines the conformal transformation. $\gamma = 2$ leads to a Jordan frame potential of the form:

$$V_J(\Phi) = -V_{J,0}\Phi^3\,. \tag{13.36}$$

We chose the following initial conditions:

$$\Phi(t_{beg}) = 10 \quad , \quad a_J(t_{beg}) = 1 \quad , \quad V_{J,0} = 10^{-10}\,. \tag{13.37}$$

Using (13.26) and (13.35) we find for the initial field velocity $|\Phi_{t_J}| \approx 5.83 \cdot 10^{-3}$. The numerical solution for the potential $V_J(\Phi)$ is shown in blue in Fig. 26, while the scale factor $a(t_J)$ and the scalar field $\Phi(t_J)$ are shown in blue in Fig. 27. The numerical solution indeed reproduces the conflationary solution, which was obtained by the conformal transformation of the ekpyrotic scaling solution. From the solution of the scalar field Φ and the scale factor a_J we see, that there is a space-time singularity at $t_J = 0$, $a_J = 0$, $\Phi = \infty$. This is reminiscent of the inflationary singularity. An extension of the model into, e.g. a cyclic model could resolve this singularity. The effective description might also break down at a certain point since the gravitational coupling $F(\Phi)$ becomes infinite.

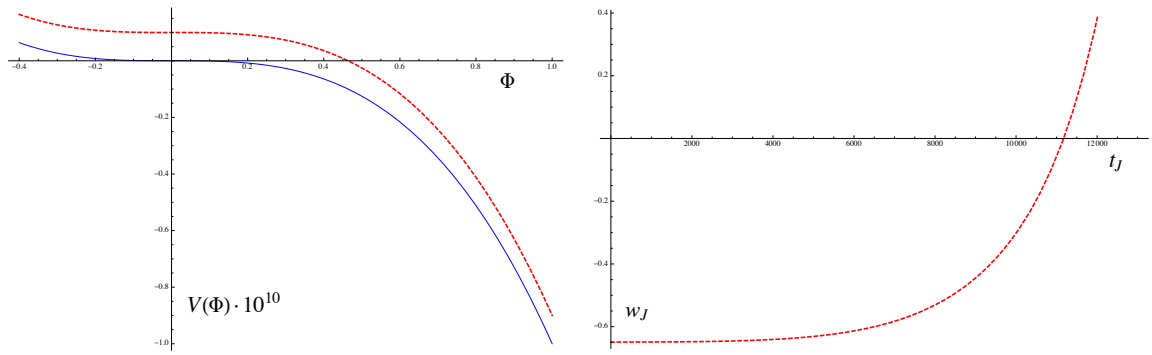

FIG. 26. *Left:* The original Jordan frame potential V_J is shown in blue, the shifted potential U_J in dashed red. *Right:* The equation of state in Jordan frame, for the shifted potential. Figure taken from [10].

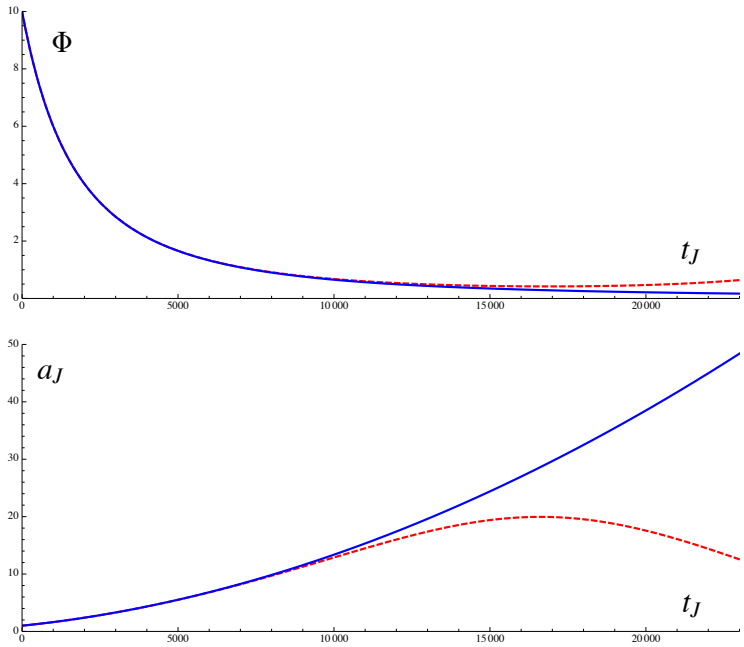

FIG. 27. Scalar field and scale factor in Jordan frame: the blue curves show the transformed ekpyrotic scaling solution and the red dashed curves correspond to the field evolutions in the shifted potential. Figure taken from [10].

The conflationary phase has to end eventually – likewise in Einstein frame the ekpyrotic phase has to end eventually. As a first modification we introduce a small shift in the Jordan frame potential:

$$U_J(\Phi) = V_J(\Phi) + V_1, \tag{13.38}$$

where $V_1 = \frac{V_{J_i}}{10}$. In Einstein frame this shift leads to a change of the ekpyrotic potential in the

form of:

$$U(\phi) = F^{-2}U_J(\phi) = -V_0 e^{-c\phi} + V_1 e^{-2c\gamma\phi}. \tag{13.39}$$

The equation of state in Jordan frame is shown on the right of Fig. 26. Indeed the conflationary phase ends at around $t_J \approx 10\,000$, when the equation of state becomes $\omega_J > -\frac{1}{3}$ the accelerated phase ends. The evolution of the scalar field Φ and the scale factor a_J are shown as red dashed curves in Fig. 27. The scalar field reaches a maximum point on the potential at around $\Phi \approx 0.4$ and then starts to roll back down the potential. The scale factor also reaches a maximum value and starts to re-contract.

The re-contraction is unavoidable in Jordan frame in this model. From

$$H_J = -\frac{F_{,t_J}}{2F} - \sqrt{\frac{F_{,t_J}^2}{4F^2} + \frac{k}{6F}\Phi_{,t_J}^2 + \frac{1}{3F}V_J} = -\frac{F_{,t_J}}{2F} - \sqrt{\frac{F_{,t_J}^2}{4F^2} + \frac{1}{3F}\rho_J}. \tag{13.40}$$

we see that whenever $\rho_J = \frac{k}{2}\Phi_{,t_J}^2 + V_J = 0$ the Hubble parameter $H_J = 0$, since $F_{,t_J} < 0$. The shift in the potential leads to such a behavior. During conflation the potential is negative and the kinetic terms is also negative with $k = -1$, which leads to $\rho_J < 0$. The scalar field slows down, such that at a certain point the positive potential and the negative kinetic term are equal leading to $\rho = 0$ and consequently $H_J = 0$.

While this simple modification stopped the accelerated expansion. It is not enough in order to obtain a graceful exit. In the current model, the scalar field Φ rolls back down the potential. In the following, we want to construct a model, where the scalar field is stabilized on top of the positive potential. The scalar field could then decay, such that reheating would take place or it would stay on top of the potential acting as dark energy.
If the scalar field stabilizes on top of the potential, both Jordan and Einstein frame become essentially equivalent. However, in Einstein frame, the universe still contracts leading to a big crunch. In the following, we will incorporate a non-singular bounce in the Einstein frame and calculate the resulting dynamics in the Jordan frame.

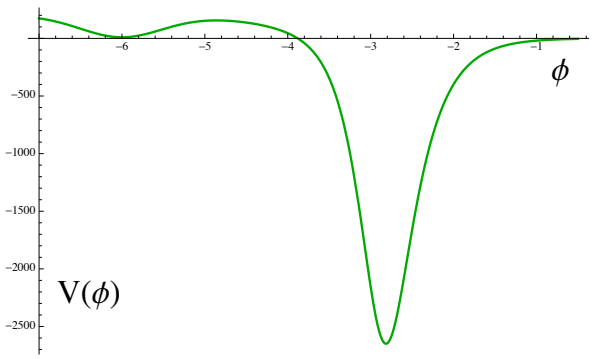

FIG. 28. The Einstein frame scalar potential used in the bounce model (13.41). Figure taken from [10].

C. Einstein Frame Bounce Transformed to Jordan Frame

We have already discussed non-singular bounces in Chapter 10. We have reviewed the general properties, the problems, and differences between various non-singular bounce models. The construction of a non-singular bounce via a ghost condensate phase has the advantage of being technically fairly simple and constituting a healthy effective field theory description. The action takes the form

$$S = \int \mathrm{d}^4x\sqrt{-g}\left[\frac{R}{2} + P(X,\phi)\right] \tag{13.41}$$

with

$$P(X,\phi) = K(\phi)X + Q(\phi)X^2 - V(\phi), \tag{13.42}$$

where $X \equiv -\frac{1}{2}g^{\mu\nu}\partial_\mu\phi\partial_\nu\phi$ denotes the ordinary kinetic term.

The functions $K(\phi)$ and $Q(\phi)$ can be chosen in various ways. At a certain time the sign of $K(\phi)$ has to change, while $Q(\phi)$ has to turn on. We also add a local minimum to the potential, as shown in Fig. 28. After the bounce, the scalar field rolls into the local minimum and stabilizes. At this point reheating can occur.

Here we use the specific functions used in [173]:

$$K(\phi) = 1 - \frac{2}{\left(1+\frac{1}{2}(\phi+4)^2\right)^2}, \tag{13.43}$$

$$Q(\phi) = \frac{V_0}{\left(1+\frac{1}{2}(\phi+4)^2\right)^2}, \tag{13.44}$$

$$V(\phi) = -\frac{1}{e^{3\phi}+e^{-4(\phi+5)}} + 100\left[(1-\tanh(\phi+4))\left(1-0.95e^{-2(\phi+6)^2}\right)\right], \tag{13.45}$$

where compared to [173] the theory has been rescaled according to $g_{\mu\nu} \to V_0^{1/2} g_{\mu\nu}$. This implies $K \to K$, $Q \to V_0 Q$ and $V \to V_0^{-1} V$. The equations of motions are given by

$$\nabla_\mu \left(P_X \nabla^\mu \phi\right) - P_{,\phi} = 0, \tag{13.46}$$

$$3H^2 = \rho, \tag{13.47}$$

$$\dot{H} = -\frac{1}{2}(\rho + p), \tag{13.48}$$

where $p = P$ is the pressure and $\rho = 2XP_X - P$ energy density.

The bounce can occur when the kinetic term changes sign, which can be seen from $\dot{H} = -XP_X$. The higher order term X^2 allows that the kinetic term can pass through zero and also contributes to the fluctuations avoiding ghosts. The Einstein frame bounce solution is shown in Fig. 29. The initial conditions are chosen to be $\phi_0 = 0$, $\dot{\phi}_0 = -2.4555$, $a_0 = 100$ and we have set $V_0 = 10^{-6}$ and $c = 3$. The scalar field first rolls down the potential during the ekpyrotic phase. The bounce occurs at around $\phi = -4$, and afterwards, the universe starts expanding. The scalar field rolls into the dip of the positive potential and oscillates there with a decaying amplitude shown in Fig. 29.

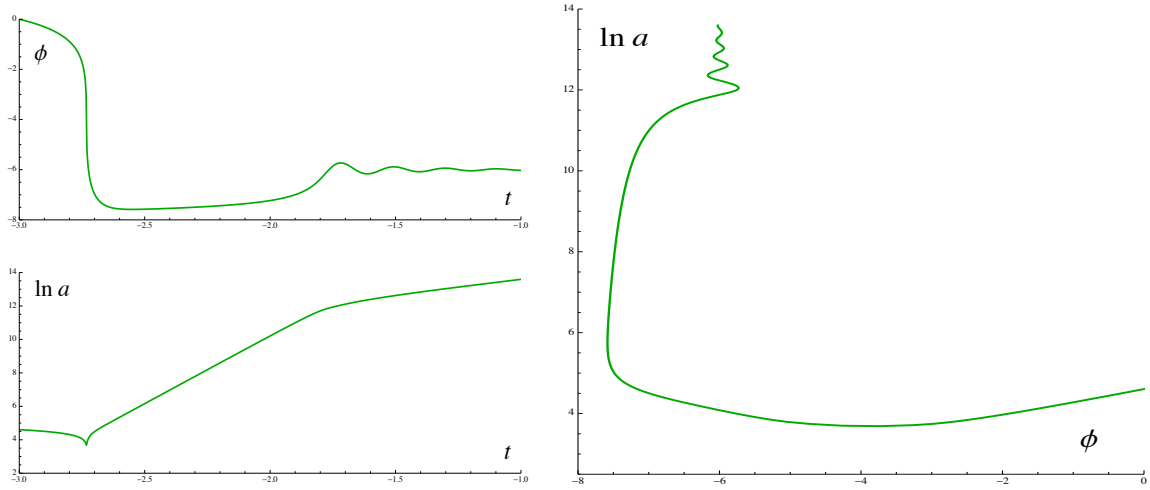

FIG. 29. *Left:* Scalar field and scale factor for the bounce solution in Einstein frame. *Right:* Parametric plot of the scalar field and scale factor in Einstein frame. This plot nicely illustrates the smoothness of the bounce. Figure taken from [10].

We will transform this Einstein frame bounce into Jordan frame. We have discussed the conformal transformation of a scalar field with a standard kinetic term in Chapter (12 B). Here we have added a generalized scalar field $P(X, \phi)$ with higher derivatives and will now calculate the transformation properties of such a term.

The action in Einstein frame is given by

$$S = \int \mathrm{d}^4x\sqrt{-g}\left[\frac{R}{2} + P(X,\phi)\right]. \tag{13.49}$$

The Ricci scalar transforms under the conformal transformation as cf. (12.20)

$$R = \frac{1}{F}\left(R_J - 6\Box_J \ln\sqrt{F} - 6g_J^{\mu\nu}\partial_\mu\left(\ln\sqrt{F}\right)\partial_\nu\left(\ln\sqrt{F}\right)\right), \tag{13.50}$$

while the kinetic term transforms as

$$X \equiv -\frac{1}{2}g^{\mu\nu}\partial_\mu\phi\partial_\nu\phi = -\frac{1}{2F}g_J^{\mu\nu}\partial_\mu\phi\partial_\nu\phi = -\frac{1}{2F}\left(\frac{\partial\phi}{\partial\Phi}\right)^2 g_J^{\mu\nu}\partial_\mu\Phi\partial_\nu\Phi \equiv \frac{1}{F}\left(\frac{\partial\phi}{\partial\Phi}\right)^2 X_J. \tag{13.51}$$

This leads to the following action in Jordan frame

$$S_J = \int \mathrm{d}^4x\sqrt{-g_J}\left[F(\Phi)\frac{R_J}{2} + P_J(X_J,\Phi)\right], \tag{13.52}$$

where the Jordan frame functions are defined as

$$P_J \equiv K_J X_J + Q_J X_J^2 - V_J, \tag{13.53}$$

$$K_J \equiv F\left(K - \frac{3}{2}\frac{F_{,\phi}^2}{F^2}\right)\left(\frac{\partial\phi}{\partial\Phi}\right)^2 = 4\xi\left(\frac{K}{c^2\gamma^2} - \frac{3}{2}\right), \tag{13.54}$$

$$Q_J \equiv Q\left(\frac{\partial\phi}{\partial\Phi}\right)^4 = \frac{16}{c^4\gamma^4\Phi^4}Q, \tag{13.55}$$

$$V_J \equiv F^2V = \xi^2\Phi^2V, \tag{13.56}$$

here we have used the specific transformation used in Chapter 13 B 2:

$$\frac{\partial\phi}{\partial\Phi} = \frac{2}{c\gamma\Phi} \quad \text{and} \quad F(\Phi) = \xi\Phi^2. \tag{13.57}$$

The full evolution of the scale factor is shown in Fig. 30. The scale factor increases by many orders of magnitude, while the scalar field Φ rolls up the negative potential with decreasing velocity. It starts at $\Phi_0 = 2.4267$ and very quickly decreases to a field value $\Phi \sim 10^{-9}$, where it stays for a very long time. It is important to note that during that time, the non-singular bounce in Einstein frame already took place. This Einstein frame bounce leads to no drastic changes in the Jordan frame dynamics – the universe just keeps expanding.

The dynamics in Jordan frame change as soon as $\rho_J = 0$. As already discussed, the universe re-contracts at this point. The potential becomes positive while the kinetic energy decreases leading to the re-contraction at around $t_J \approx 4.05 \cdot 10^9$, see Fig. 31 and Fig. 32. Since $H_J < 0$, the anti-friction term leads to an increased scalar field velocity allowing the scalar field to roll over the

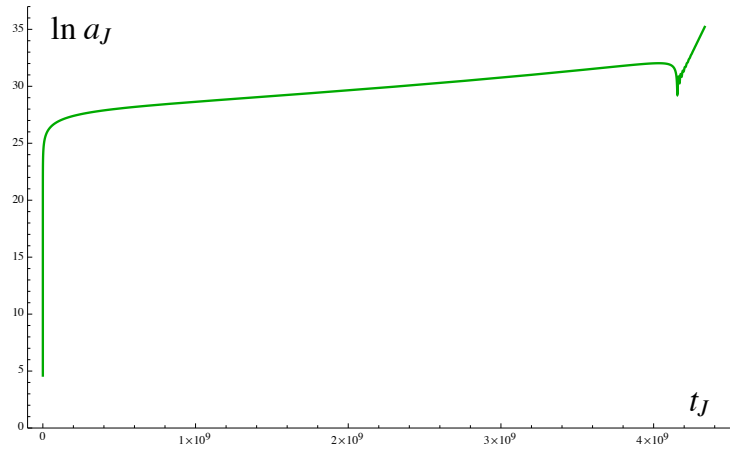

FIG. 30. Full evolution of the scale factor for the transformed solution in Jordan frame. During the conflationary phase, the scale factor increases by many orders of magnitude until the scalar field rolls up the potential towards $\Phi \sim 10^{-9}$. While the scalar field almost rests on the positive potential, the universe keeps expanding. During the exit of the conflationary phase, the scale factor and scalar field undergo non-trivial evolution which is hard to see in the present figure and is shown in detail in Fig. 31 and Fig. 32. Figure taken from [10].

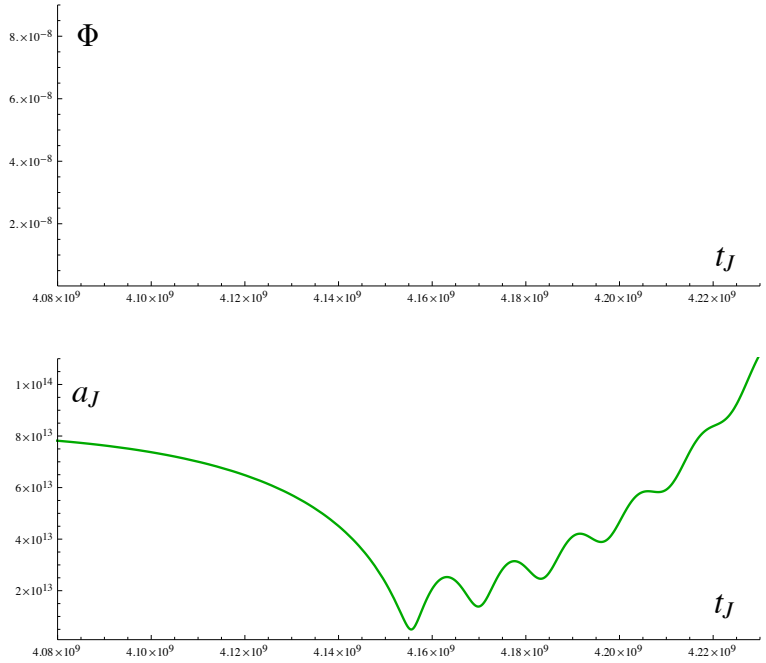

FIG. 31. Scalar field and scale factor for the transformed solution in Jordan frame towards the end of the evolution. The scalar field rolls into the dip of the potential and oscillates. Due to the non-minimal coupling to gravity, the scale factor also oscillates. The universe expands monotonically once the scalar field has stabilized. Figure taken from [10].

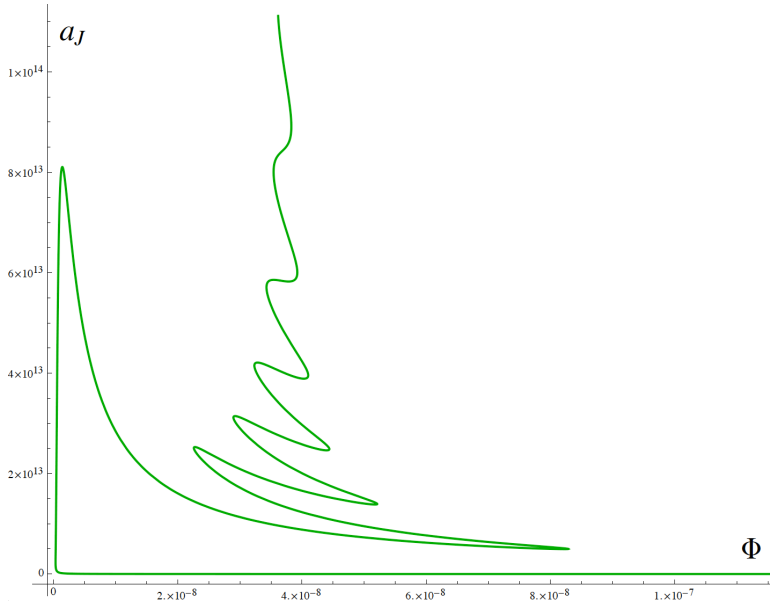

FIG. 32. Parametric plot of the scalar field and scale factor in Jordan frame. Note that initially, the scalar field decreases its value very rapidly. Later on, as the scalar field stabilizes, the scale factor goes through oscillations but eventually increases monotonically. Figure taken from [10].

potential barrier. The scalar field starts to oscillate in the local minimum with decreasing velocity. Whenever $\rho_J = 0$ the Hubble rate H_J changes sign, such that the scale factor oscillates similar to the scalar field. Once the scalar field stabilizes, continuous expansion occurs. The oscillations of the scale factor do not violate the null energy condition. These oscillations occur because of the non-minimal coupling of the scalar field to gravity.

Let us summarize the results: We have constructed an accelerated phase in Jordan frame via a conformal transformation of an ekpyrotic phase in Einstein frame. Conflation is driven by a scalar field with a "wrong" kinetic sign in a negative potential. Moreover, we have included an Einstein frame bounce and modified the ekpyrotic potential leading to a graceful exit of the conflationary phase and stabilization of the scalar field in Jordan frame.

D. Perturbations in Jordan Frame

Under a conformal transformation, the physics does not change – it is just a change of frame. Thus, metric perturbations are unaffected by a conformal transformation, as we will see now. Our starting point was an ekpyrotic phase in Einstein frame, and we already know the behavior of the quantum fluctuations during ekpyrosis. The adiabatic scalar perturbations and the tensor fluctuations obtain a blue spectrum and are not amplified, c.f. Chapter 4 F.
Nearly scale-invariant entropy perturbations can be produced via an introduction of a second scalar field. We have discussed the entropic mechanism in Chapter 5 C and the non-minimal entropic mechanism in Chapter 8.

Thus the conflationary phase, which was constructed in the previous chapter, has unique properties. During the accelerated expansion large adiabatic quantum fluctuations are absent. This is very different compared to inflation, where large quantum fluctuations lead to slow-roll eternal inflation – questioning the predictability of inflation, see Chapter 7.
In the following, we will calculate the adiabatic scalar perturbations and tensor perturbations in the Jordan frame directly. Furthermore, we will add a second scalar field with a non-minimal kinetic coupling. The entropy perturbations produced via the non-minimal entropic mechanism will be calculated afterward.

1. Perturbations for a Single Scalar Field

In Chapter 9 we have calculated the first order perturbations of the Galileon scalar field. The second order action of the comoving curvature perturbation $\mathcal{R}$ in Jordan frame is given by [165]:

$$S_J^{(2)} = \frac{1}{2}\int \mathrm{d}^4x \frac{a_J^2\Phi'^2}{\left(H_J+\frac{\Phi'}{\Phi}\right)^2}(6\xi-1)\left(\mathcal{R}_J'^2-(\partial_i\mathcal{R}_J)^2\right), \tag{13.58}$$

where we have assumed $F(\Phi)=\xi\Phi^2$ and $'$ denotes the derivative w.r.t to conformal time τ, which is equal in both frames as $\mathrm{d}t/a = \mathrm{d}t_J/a_J$. From (13.58) the ghost-free condition is given by

$$\xi > \frac{1}{6}, \tag{13.59}$$

which is the same condition on ξ calculated in Eq. (13.24). As usual we define

$$z_J^2 = \frac{a_J^2\Phi'^2}{\left(H_J+\frac{\Phi'}{\Phi}\right)^2}(6\xi-1)\,, \tag{13.60}$$

in order to canonically normalize the scalar perturbations via $v_{Jk} = z_J \mathcal{R}_J$. The equations of motion for the mode functions in Fourier space has the usual form:

$$v''_{Jk} + (k^2 - \frac{z''_J}{z_J}) v_{Jk} = 0\,. \tag{13.61}$$

The function z_J is however different compared to the standard single scalar field case containing contributions of the scalar field in the denominator. This term is present due to the non-minimal coupling to gravity and thus differs from the standard inflationary solution. Using the background solutions obtained in Chapter 13 B 2, we can calculate the various terms in the equations of motions (13.61). The ekpyrotic scaling solution transformed to Jordan frame is given by

$$a_J(t_J) = a_0 \left(\frac{t_J}{t_{J,0}}\right)^{\frac{1-\epsilon\gamma}{\epsilon(1-\gamma)}}, \quad \Phi(t_J) = \frac{1}{\sqrt{\xi}} \left(\frac{t_J}{t_{J,0}}\right)^{\frac{\gamma}{1-\gamma}}. \tag{13.62}$$

Integrating $\mathrm{d}\tau = \mathrm{d}t_J/a_J$ yields the relationship between physical Jordan frame time and conformal time:

$$t_J \sim (-\tau)^{\frac{\epsilon(1-\gamma)}{\epsilon-1}}. \tag{13.63}$$

Thus we obtain $z_J(\tau) \sim (-\tau)^{1/(\epsilon-1)}$, which leads to

$$\frac{z''_J}{z_J} = \frac{2-\epsilon}{(\epsilon-1)^2} \frac{1}{\tau^2}. \tag{13.64}$$

In the far past the modes are deep in the horizon and thus we impose Bunch-Davies boundary conditions. The solution (up to a phase) reads

$$v_J = \sqrt{-\frac{\pi}{4}\tau} H_\nu^{(1)}(-k\tau)\,, \tag{13.65}$$

where $H_\nu^{(1)}$ is a Hankel function of the first kind with index ν. The resulting spectral index is given by

$$n_s - 1 = 3 - 2\nu = 2 - \left|\frac{\epsilon-3}{\epsilon-1}\right|, \tag{13.66}$$

where ϵ corresponds to the Einstein frame equation of state parameter during ekpyrosis. Since $\epsilon > 3$, the (blue) spectrum is always between $3 < n_s < 4$,. The spectrum is identical to the adiabatic perturbations during ekpyrosis, cf. Eq. (4.114).

This is an expected result: the adiabatic perturbations have the same spectrum in both frames. The adiabatic fluctuations during conflation stay quantum and the run-away behavior of slow-roll eternal inflation is absent in this model.

The second order action of the tensor pertubations γ_{Jij} is given by (9.27) :

$$S_J = -\frac{1}{8}\int \mathrm{d}^4x F(\Phi)\sqrt{g_J}g_J^{\mu\nu}\partial_\mu\gamma_{Jij}\partial_\nu\gamma_{Jij}\,. \tag{13.67}$$

Introducing $z_T^2 = F(\Phi)a_J^2$, we obtain the canonically normalized perturbations $h\,\epsilon_{ij} \equiv z_T\gamma_{ij}$, where ϵ_{ij} is the polarization tensor. The mode equation in Fourier space reads:

$$h_k'' + \left(k^2 - \frac{z_T''}{z_T}\right)h_k = 0\,. \tag{13.68}$$

Again the non-minimal coupling to gravity leads to a different z_T compared to a usual inflationary model in Einstein frame. From $z_T \propto \Phi a_J \propto (-\tau)^{1/(\epsilon-1)}$ we find $z_T \propto z_J$. This leads to a spectral index of

$$n_T = 3 - \left|\frac{\epsilon-3}{\epsilon-1}\right|\,, \tag{13.69}$$

which again coincides with the ekpyrotic model in Einstein frame in Eq. (4.116). In the limit where $|k\tau| \ll 1$, which corresponds to the late-time/large-scale limit, the adiabatic scalar and tensor mode functions behave as [19, 174]

$$v\,,\, h \propto \frac{\pi}{2^{2\nu}\Gamma(\nu)\Gamma(\nu+1)}(-k\tau)^{1-1/\epsilon} - i(-k\tau)^{1/\epsilon}\,. \tag{13.70}$$

Given that $\epsilon > 3$, this implies that as $(-k\tau) \to 0$ neither the scalar nor the tensor perturbations are amplified. There are no primordial gravitational waves during conflation. Moreover, the fact that the adiabatic scalar perturbations stay quantum results in the absence of eternal inflation. There are no large curvature perturbations, which would prolong the conflationary phase creating an infinite amount of pocket universes. We have indeed constructed an early universe model, which incorporates an accelerated phase without the runaway behavior of eternal inflation.

2. Non-Minimal Entropic Mechanism in Jordan Frame

A second scalar field has to be added in order to produce nearly scale-invariant entropy perturbations during ekpyrosis. In the following, we will discuss the transformation of the non-minimal entropic mechanism cf. Chapter 8 in the Jordan frame. The Einstein frame action takes the following form:

$$S = \int \mathrm{d}^4x\sqrt{-g}\left[\frac{1}{2}R - \frac{1}{2}g^{\mu\nu}\partial_\mu\phi\partial_\nu\phi - \frac{1}{2}g^{\mu\nu}e^{-b\phi}\partial_\mu\chi\partial_\nu\chi + V_0e^{-c\phi}\right]. \tag{13.71}$$

The scalar field follows the scaling solution ϕ, while the second scalar field χ is constant. The transformation to Jordan frame is analogous to the calculations in Chapter 13 B 2 with the addition of the non-minimally coupled kinetic term. The action is Jordan frame yields:

$$S_J = \int \mathrm{d}^4x\sqrt{-g_J}\left[\xi\Phi^2\frac{R_J}{2} + \frac{1}{2}g_J^{\mu\nu}\partial_\mu\Phi\partial_\nu\Phi - \frac{1}{2}g_J^{\mu\nu}\xi^{\frac{\gamma c-b}{\gamma c}}\Phi^{\frac{2\gamma c-2b}{\gamma c}}\partial_\mu\chi\partial_\nu\chi + V_{J,0}\Phi^{4-\frac{2}{\gamma}}\right]. \tag{13.72}$$

Note that the non-minimal kinetic coupling $e^{-b\phi}$ in the Einstein frame becomes a power-law coupling in Jordan frame – analogous to the transformation of the potential. The equations of motion for the two fields in Jordan frame are given by

$$\Box\Phi + \frac{\gamma c-b}{\gamma c}\xi^{\frac{\gamma c-b}{\gamma c}}\Phi^{\frac{\gamma c-2b}{\gamma c}}g_J^{\mu\nu}\partial_\mu\chi\partial_\nu\chi - \frac{1}{2}F(\Phi)_{,\Phi}R_J + V(\phi)_{J,\Phi} = 0, \tag{13.73}$$

$$\Box\chi - \frac{2\gamma c-2b}{\gamma c}\frac{\Phi'}{\Phi}\chi' - 2a_J^2\xi^{\frac{b-\gamma c}{\gamma c}}\Phi^{\frac{2b-2\gamma c}{\gamma c}}V(\Phi)_{J,\chi} = 0. \tag{13.74}$$

The potential is again χ-independent leading to a background solution $\chi = const.$ from Eq. (13.74). Thus the equation of motion for Φ coincides with the single scalar field case. The equations of motion for the linear entropy perturbations $\delta\chi$ in Fourier space are

$$\delta\chi'' + \left(2\frac{a_J'}{a_J} + n\frac{\Phi'}{\Phi}\right)\delta\chi' + k^2\delta\chi = 0\,, \tag{13.75}$$

where $n = \frac{2\gamma c-2b}{\gamma c}$. We again introduce the canonically normalized variable

$$v_{Js} = a_J\Phi^{\frac{n}{2}}\delta\chi\,. \tag{13.76}$$

Using the background equation of motion,

$$\Phi'' + 2\frac{a'}{a}\Phi' + 6\xi\frac{a''}{a}\Phi - a^2V_{J,\Phi} = 0, \tag{13.77}$$

we obtain the mode equation in Fourier space:

$$v_{Js}'' + \left[k^2 + \frac{n}{2}\frac{\Phi'^2}{\Phi^2} - \frac{n^2}{4}\frac{\Phi'^2}{\Phi^2} + \frac{a_J''}{a_J}(3n\xi-1) - a_J^2\frac{n}{2}\frac{V_{J,\Phi}}{\Phi}\right]v_{Js} = 0\,. \tag{13.78}$$

We can now plug in the background solution (13.62) into the mode equation leading to

$$v_{Js}'' + \left(k^2 - \frac{1}{(\epsilon-1)^2\tau^2}\left[2-(4+3\Delta)\epsilon+(2+3\Delta+\Delta^2)\epsilon^2\right]\right)v_{Js} = 0, \tag{13.79}$$

where $\Delta = \frac{b}{c} - 1$, such that $n = 2\frac{\gamma-\Delta-1}{\gamma}$. The solution is given in form of a Hankel function with

$$\nu = \frac{3}{2} + \frac{\Delta\epsilon}{\epsilon-1}\,, \tag{13.80}$$

which translates into a spectral index

$$n_s - 1 = 3 - 2\nu = -2\Delta\frac{\epsilon}{(\epsilon-1)}\,. \tag{13.81}$$

The mode equation is independent of γ. Moreover, the spectral index coincides with the spectral index in Einstein frame (8.21), [31]. This confirms that the spectrum of the entropy perturbations is indeed frame-independent.

E. Summary

We have introduced the idea of conflation based on a scalar-tensor theory of gravity, which conflates ideas of inflation and ekpyrosis. An accelerated expanding phase was constructed in Jordan frame via a conformal transformation of an ekpyrotic model in Einstein frame. During conflation, the universe is driven towards homogeneity and flatness due to the accelerated expansion, like in inflation. However, adiabatic and tensor perturbations are not amplified, just as in ekpyrotic models. Conflation may be seen as being complementary to anamorphic models, in which nearly scale-invariant curvature perturbations are created in a contracting universe.

Since adiabatic fluctuations are not amplified, conflation does not lead to eternal inflation and a multiverse. This also remains true in a two-field model: The nearly scale-invariant entropy perturbations have no impact on the background dynamics – even a large entropy perturbation cannot prolong the conflationary phase. Consequently, there is no multiverse and the associated problems are absent.

Another important feature is the construction of accelerated expanding backgrounds via a negative potential. It will be interesting to see if a conflationary model can arise from supergravity or string theory, where negative potentials and non-minimal couplings to gravity arise naturally.

A modification to the conflationary model had to be made in order to obtain a graceful exit – in analogy to the ekpyrotic phase which naturally leads to a big crunch. Moreover, the scalar field should stabilize eventually, such that the non-minimal coupling to gravity becomes minimal leading to essentially equivalent frames. We have implemented a non-singular bounce in Einstein frame and added a dip in the shifted potential, which led to a graceful exit and stabilization of the scalar field.

It would be interesting to see if a graceful exit can be obtained by means of other mechanisms. In further studies, one could investigate the space-time singularity (where the effective gravitational constant also becomes infinite), the initial conditions of conflation and the requirements on the conflationary phase in order to solve the big bang puzzles. An interesting avenue is the implementation of a cyclic model in Einstein frame and the properties of the corresponding model in Jordan frame. Such a cyclic embedding could address some of the above open questions.

14. DISCUSSION

Models of the early universe have to explain the initial conditions which led to the universe we observe today. In particular, we would like to understand the spatial flatness, isotropy, and homogeneity on large scales as well as the existence of small temperature anisotropies in the Cosmic Microwave Background, which led to the structure formation in the universe.

The Planck satellite measured cosmological parameters to very high precision which deepened our understanding of the universe. However, the Planck data also challenges the viability of various early universe models. While the simplest inflationary models – namely $m^2\phi^2$–potentials and exponential potentials – are basically ruled out, the ekpyrotic scenario typically predicts sizable non-Gaussian corrections.

In this thesis, we have reviewed the development of ekpyrotic models, non-singular bounce models, the evolution of adiabatic and entropy perturbations to first and second order, and the conversion process.

The entropic mechanism produces nearly scale-invariant entropy perturbations due to the presence of an unstable transverse direction in the potential. Entropy perturbations source curvature perturbations already during ekpyrosis at second order in perturbations and the intrinsic non-Gaussian corrections depend on the steepness and symmetry of the two-field potential. The final non-Gaussianities after a kinetic conversion from entropy to curvature perturbations before the bounce can be parametrized by the phenomenological formula [35]

$$f_{NL} \approx \frac{3}{2}\sqrt{\epsilon}\kappa_3 + 5, \tag{14.1}$$

where κ_3 is $\mathcal{O}(1)$ and zero for a symmetric potential.

In this thesis, we have proposed two different approaches in order to explain the production of small non-Gaussian correction in the ekpyrotic scenario.

- The non-minimal entropic mechanism
- A kinetic conversion after a non-singular bounce

In the non-minimal entropic mechanism, a non-minimal coupling in the kinetic term of the second scalar field is introduced. This model is stable and does not suffer from initial condition problems. Due to the non-minimal coupling, nearly scale-invariant entropy perturbations are produced. We have shown in [31], that the intrinsic non-Gaussian corrections are precisely zero in this model leading to overall small non-Gaussian corrections, which are in agreement with the Planck data. The non-minimal entropic mechanism was also generalized including more general kinetic couplings. Moreover, an analysis of the non-minimal entropic mechanism to third order in perturbations also confirmed vanishing intrinsic contributions, and the final amplitude of the trispectrum was calculated [104].

Any early universe model with a contracting phase needs to incorporate a viable bounce phase. The difficulty of tracing the evolution of the background and the perturbations during a singular bounce led to the development of various non-singular bounce models. A non-singular bounce can be achieved by a violation of the null energy condition, which usually introduced a variety of pathologies. Most of the pathologies are under control due to the development of non-singular bounce models like the ghost condensate and Galileon bounces. New non-singular bounce models have been proposed due to the recent no-go theorems for Cubic Galileon theories. We have to see if these new theories can produce completely stable bouncing cosmologies.

It has been shown in [8] that the small scale perturbations causing the gradient instabilities during the ghost condensate phase lie outside of the validity of the effective field theoretical description. Thus the non-singular bounce model is healthy in the effective field theoretical description, and we can calculate the evolution of curvature and entropy perturbations through the bounce.

The presence of a potential during the non-singular ghost condensate bounce increases the difference in scale between the cut-off of the effective field theoretical description and the background. This was the motivation for the analysis of a conversion phase after the bounce. In [9] we have calculated the evolution of entropy perturbations through the non-singular bounce and the subsequent evolution during the kinetic conversion phase. The first and second order entropy perturbations can grow substantially during the bounce, especially in the presence of an unstable potential. Moreover, during the kinetic phase after (and maybe before) the bounce the entropy perturbations grow logarithmically. This growth was previously often ignored, but it can be significant if the kinetic phase lasts long enough.

The analysis of a kinetic conversion after the bounce led to very interesting new insights. Due to the growth of the first and second order entropy perturbations during the bounce, the main contribution to the final non-Gaussian corrections is the conversion phase. The intrinsic non-Gaussianities are suppressed due to the evolution of the entropy perturbations during the bounce and kinetic phase. The phenomenological formula (14.1) does not apply in the case of a kinetic conversion after the bounce, and thus the entropic mechanism can produce small non-Gaussian correction in agreement with observations. The growth of the entropy perturbations also has the consequence that the ekpyrotic potential does not have to become as deep. The energy scale can be up to two orders of magnitude below the GUT scale, which implies a healthier effective field theoretical description.

The final non-Gaussian corrections depend highly on the conversion phase and are thus model-dependent. In the cyclic ekpyrotic model, there is a natural explanation for the existence of a repulsive potential. However, it is not clear how such a potential arises in the context of non-singular bounce models. It has to be seen if a non-singular bounce model with a subsequent conversion can be obtained from a fundamental theory. Nevertheless, we can deduce general properties of the conversion phase: the kinetic conversion phase has to be smooth and effective.
During a smooth and effective conversion, a large amount of entropy perturbations are converted to curvature perturbations, which leads to more structure formation and generally small non-Gaussian corrections. Non-smooth, rapid and ineffective conversions lead to less structure formation and large non-Gaussianities, which are incompatible with observations.

Slow-roll eternal inflation challenges the inflationary paradigm. Eternal inflation creates an infinite amount of pocket universes with different physical properties. However, without a probability measure, one should not trust the "predictions" of inflation. In this thesis, we have proposed a model of the early universe, which is accelerating while creating the initial conditions of the universe without the runaway behavior of eternal inflation [10]. This scalar-tensor theory conflates/combines ideas of inflation and ekpyrosis. The perturbations behave like during ekpyrosis: there are no large adiabatic fluctuations, and the entropy perturbations are nearly scale-invariant and nearly Gaussian.

An interesting aspect of this model is the existence of a negative potential. The embedding of inflationary models in a string theory setting is challenged by a variety of problems. A hard task is the construction of a stable de Sitter vacuum. A variety of mechanisms have been proposed in order to obtain a positive potential. In the conflationary model, we have found an accelerating solution incorporating a negative potential. It has to be seen if such a model can arise in supergravity or string theory, where negative potentials and non-minimal couplings to gravity arise naturally.
We would like to note, that a modification to the conflationary model had to be made in order to allow for a graceful exit. The shift in the potential was introduced to obtain a positive value of the potential at the end of conflation. Moreover, we have added a non-singular bounce in Einstein frame, such that both frames become essentially the same after the stabilization of the field. However, there are possibly other mechanisms allowing for a graceful exit, which have to be explored in the future.

It is (nearly) impossible to falsify the inflationary paradigm. The vast amount of inflationary models allow for almost any prediction or feature compatible with observations. The supposed measurement of primordial gravitational waves by the BICEP2 team led to the development of dozens of inflationary models within weeks, which "explained" the tension between the BICEP2 and Planck data. The question if a model fitting the data is natural within the inflationary paradigm has to be asked. We have covered challenges for the plateau-models of inflations, which belong to the class of inflationary models in agreement with observations. One has to see if these problems can be solved and if future experiments can measure primordial gravitational waves.

The question of naturalness or simplicity also has to be addressed in the context of ekpyrotic models. In the new ekpyrotic scenario, the presence of an unstable transverse direction leads to restrictions on the initial conditions of ekpyrosis. The phoenix universe, where the new ekpyrotic model is embedded into a cyclic description, suggests a natural selection principle. Only certain regions with the right initial conditions successfully continue the cycle, while other regions do not. In this thesis, we have incorporated a non-singular bouncing cosmology in order to track the evolution of the background and the perturbations through the bounce. We hope to find a cyclic embedding of such a non-singular bounce model in future work in order to resolve the initial conditions problem in the new ekpyrotic scenario. We have also argued that the naturally large intrinsic non-Gaussian corrections in the new ekpyrotic model are actually suppressed if the conversion phase occurs after a non-singular bounce.

The non-minimal entropic mechanism is at the moment the best ekpyrotic model. The non-minimal kinetic coupling between the two scalar fields can be seen as a drawback of the model. However, non-minimally kinetic couplings appear naturally in string theory, and it would be exciting if the non-minimal entropic mechanism could be obtained from a fundamental theory. The non-minimal entropic mechanism produces small, but non-zero non-Gaussian correction. The predictions of the non-minimal entropic mechanism are:

$$-5 \lesssim f_{NL} \lesssim +5\,, \tag{14.2}$$

$$g_{NL} \sim \mathcal{O}(-10^2) \text{ or } \mathcal{O}(-10^3)\,, \tag{14.3}$$

$$r \approx 0\,, \tag{14.4}$$

$$\alpha_s \sim \mathcal{O}(-10^3)\,. \tag{14.5}$$

These predictions are fairly distinct from single-field inflationary models. The absence of primordial gravitational waves, the non-zero non-Gaussian corrections, the negative trispectrum parameter g_{NL} and the generally larger running α_s are features which can be tested in the not too distant future. The search for primordial gravitational waves via ground- and space-based experiments could reduce the bounds on the tensor-to-scalar ratio to $r \sim \mathcal{O}(10^{-3})$ [175]. A detection of primordial gravitational waves would definitely rule out current ekpyrotic models.

The most exciting upcoming surveys, which will measure the Large Scale Structure in the universe are EUCLID [176] and SKA [156]. The Square Kilometer Array (SKA) will measure the Large Scale Structure for very large volumes and redshifts up to $z \sim 3$. The measurement of the redshifted $21cm$ line of neutral hydrogen allows for a precise redshift determination leading to a 3D mapping of the Large Scale Structure (note that the CMB is a 2D mapping on the sky). It is expected that the SKA survey will operate in 2025, which will help to understand, e.g., the evolution of the Large Scale Structure and the evolution of Dark Energy. Moreover, measurements of the galaxy power spectrum and the dark matter power spectrum will further constrain primordial non-Gaussianity [155, 156]. This means within the next ten to twenty years the errors on f_{NL} will reduce to $\sigma(f_{NL}) \approx 1$. Measurements of non-Gaussian signatures together with tighter bounds on g_{NL} with indications for negative values could favor the non-minimal entropic mechanism as a possible model of the early universe.

In conclusion, the development of fairly healthy non-singular bounce models in the effective field theoretical description and the understanding of general properties of the conversion phase improved the ekpyrotic scenario. In this thesis, we have resolved the tension between ekpyrotic predictions and observations by demonstrating how nearly Gaussian curvature perturbations can be created in ekpyrotic cosmologies. The ekpyrotic scenario is thus a viable model of the early universe.

---

[1] Matthew Colless *et al.* (2DFGRS), "The 2dF Galaxy Redshift Survey: Spectra and redshifts," Mon. Not. Roy. Astron. Soc. **328**, 1039 (2001), arXiv:astro-ph/0106498 [astro-ph].

[2] Daniel Baumann, "Inflation," in *Physics of the large and the small, TASI 09, proceedings of the Theoretical Advanced Study Institute in Elementary Particle Physics, Boulder, Colorado, USA, 1-26 June 2009* (2011) pp. 523–686, arXiv:0907.5424 [hep-th].

[3] R. Adam *et al.* (Planck), "Planck 2015 results. I. Overview of products and scientific results," Astron. Astrophys. **594**, A1 (2016), arXiv:1502.01582 [astro-ph.CO].

[4] Paul J. Steinhardt, Neil Turok, and N. Turok, "A Cyclic model of the universe," Science **296**, 1436–1439 (2002), arXiv:hep-th/0111030 [hep-th].

[5] Christopher Gordon, David Wands, Bruce A Bassett, and Roy Maartens, "Adiabatic and entropy perturbations from inflation," Phys.Rev. **D63**, 23506 (2001), arXiv:astro-ph/0009131 [astro-ph].

[6] Y. Akrami *et al.* (Planck), "Planck 2018 results. X. Constraints on inflation," (2018), arXiv:1807.06211 [astro-ph.CO].

[7] Lorenzo Battarra, Michael Koehn, Jean-Luc Lehners, and Burt A Ovrut, "Cosmological Perturbations Through a Non-Singular Ghost-Condensate/Galileon Bounce," JCAP **1407**, 7 (2014), arXiv:1404.5067 [hep-th].

[8] Michael Koehn, Jean-Luc Lehners, and Burt Ovrut, "Nonsingular bouncing cosmology: Consistency of the effective description," Phys. Rev. **D93**, 103501 (2016), arXiv:1512.03807 [hep-th].

[9] Angelika Fertig, Jean-Luc Lehners, Enno Mallwitz, and Edward Wilson-Ewing, "Converting entropy to curvature perturbations after a cosmic bounce," JCAP **1610**, 005 (2016), arXiv:1607.05663 [hep-th].

[10] Angelika Fertig, Jean-Luc Lehners, and Enno Mallwitz, "Conflation: a new type of accelerated expansion," JCAP **1608**, 073 (2016), arXiv:1507.04742 [hep-th].

[11] Alan H Guth, "The Inflationary Universe: A Possible Solution to the Horizon and Flatness Problems," Phys.Rev. **D23**, 347–356 (1981).

[12] Andreas Albrecht and Paul J Steinhardt, "Cosmology for Grand Unified Theories with Radiatively Induced Symmetry Breaking," Phys.Rev.Lett. **48**, 1220–1223 (1982).

[13] Andrei D Linde, "A New Inflationary Universe Scenario: A Possible Solution of the Horizon, Flatness, Homogeneity, Isotropy and Primordial Monopole Problems," Phys.Lett. **B108**, 389–393 (1982).

[14] Justin Khoury, Burt A Ovrut, Paul J Steinhardt, and Neil Turok, "The Ekpyrotic universe: Colliding branes and the origin of the hot big bang," Phys.Rev. **D64**, 123522 (2001), arXiv:hep-th/0103239 [hep-th].

[15] Paul J Steinhardt and Neil Turok, "Cosmic evolution in a cyclic universe," Phys.Rev. **D65**, 126003 (2002), arXiv:hep-th/0111098 [hep-th].

[16] Justin Khoury, Burt A. Ovrut, Nathan Seiberg, Paul J. Steinhardt, and Neil Turok, "From big crunch to big bang," Phys. Rev. **D65**, 086007 (2002), arXiv:hep-th/0108187 [hep-th].

[17] Robert Brandenberger and Fabio Finelli, "On the spectrum of fluctuations in an effective field theory of the Ekpyrotic universe," JHEP **0111**, 056 (2001), arXiv:hep-th/0109004 [hep-th].

[18] David H Lyth, "The Primordial curvature perturbation in the ekpyrotic universe," Phys.Lett. **B524**, 1–4 (2002), arXiv:hep-ph/0106153 [hep-ph].

[19] Lorenzo Battarra and Jean-Luc Lehners, "Quantum-to-classical transition for ekpyrotic perturbations," Phys.Rev. **D89**, 63516 (2014), arXiv:1309.2281 [hep-th].

[20] Evgeny I Buchbinder, Justin Khoury, and Burt A Ovrut, "New Ekpyrotic cosmology," Phys.Rev. **D76**, 123503 (2007), arXiv:hep-th/0702154 [hep-th].

[21] Evgeny I Buchbinder, Justin Khoury, and Burt A Ovrut, "On the initial conditions in new ekpyrotic cosmology," JHEP **11**, 76 (2007), arXiv:0706.3903 [hep-th].

[22] Jean-Luc Lehners, Paul McFadden, Neil Turok, and Paul J. Steinhardt, "Generating ekpyrotic curvature perturbations before the big bang," Phys. Rev. **D76**, 103501 (2007), arXiv:hep-th/0702153 [HEP-TH].

[23] A. Notari and A. Riotto, "Isocurvature perturbations in the ekpyrotic universe," Nucl. Phys. **B644**, 371–382 (2002), arXiv:hep-th/0205019 [hep-th].

[24] Paolo Creminelli and Leonardo Senatore, "A Smooth bouncing cosmology with scale invariant spectrum," JCAP **0711**, 10 (2007), arXiv:hep-th/0702165 [hep-th].

[25] Jean-Luc Lehners and Paul J Steinhardt, "Dark Energy and the Return of the Phoenix Universe," Phys.Rev. **D79**, 63503 (2009), arXiv:0812.3388 [hep-th].

[26] Jean-Luc Lehners, Paul J. Steinhardt, and Neil Turok, "The Return of the Phoenix Universe," Int. J. Mod. Phys. **D18**, 2231–2235 (2009), arXiv:0910.0834 [hep-th].

[27] Jean-Luc Lehners, "Diversity in the Phoenix Universe," Phys.Rev. **D84**, 103518 (2011), arXiv:1107.4551 [hep-th].

[28] Kazuya Koyama, Shuntaro Mizuno, Filippo Vernizzi, and David Wands, "Non-Gaussianities from ekpyrotic collapse with multiple fields," JCAP **0711**, 24 (2007), arXiv:0708.4321 [hep-th].

[29] Taotao Qiu, Xian Gao, and Emmanuel N Saridakis, "Towards Anisotropy-Free and Non-Singular Bounce Cosmology with Scale-invariant Perturbations," Phys.Rev. **D88**, 43525 (2013), arXiv:1303.2372 [astro-ph.CO].

[30] Mingzhe Li, "Note on the production of scale-invariant entropy perturbation in the Ekpyrotic universe," Phys.Lett. **B724**, 192–197 (2013), arXiv:1306.0191 [hep-th].

[31] Angelika Fertig, Jean-Luc Lehners, and Enno Mallwitz, "Ekpyrotic Perturbations With Small Non-Gaussian Corrections," Phys.Rev. **D89**, 103537 (2014), arXiv:1310.8133 [hep-th].

[32] Anna Ijjas, Jean-Luc Lehners, and Paul J Steinhardt, "General mechanism for producing scale-invariant perturbations and small non-Gaussianity in ekpyrotic models," Phys.Rev. **D89**, 123520 (2014), arXiv:1404.1265 [astro-ph.CO].

[33] Nima Arkani-Hamed, Hsin-Chia Cheng, Markus A Luty, and Shinji Mukohyama, "Ghost condensation and a consistent infrared modification of gravity," JHEP **05**, 74 (2004), arXiv:hep-th/0312099 [hep-th].

[34] Kazuya Koyama and David Wands, "Ekpyrotic collapse with multiple fields," JCAP **0704**, 8 (2007), arXiv:hep-th/0703040 [HEP-TH].

[35] Jean-Luc Lehners, "Ekpyrotic Non-Gaussianity: A Review," Adv.Astron. **2010**, 903907 (2010), arXiv:1001.3125 [hep-th].

[36] Jerome Martin, Christophe Ringeval, and Vincent Vennin, "Encyclopdia Inflationaris," Phys. Dark Univ. **5-6**, 75–235 (2014), arXiv:1303.3787 [astro-ph.CO].

[37] Albert Einstein, "The Foundation of the General Theory of Relativity," Annalen Phys. **49**, 769–822 (1916), [,65(1916)].

[38] A. Friedman, "On the Curvature of space," Z. Phys. **10**, 377–386 (1922), [Gen. Rel. Grav.31,1991(1999)].

[39] A. Friedmann, "On the Possibility of a world with constant negative curvature of space," Z. Phys. **21**, 326–332 (1924), [Gen. Rel. Grav.31,2001(1999)].

[40] Georges Lemaitre, "A Homogeneous Universe of Constant Mass and Growing Radius Accounting for the Radial Velocity of Extragalactic Nebulae," Annales Soc. Sci. Bruxelles A **47**, 49–59 (1927), [Gen. Rel. Grav.45,no.8,1635(2013)].

[41] Georges Lemaitre, "Republication of: The beginning of the world from the point of view of quantum theory," Nature **127**, 706 (1931), [Gen. Rel. Grav.43,2929(2011)].

[42] Edwin Hubble, "A relation between distance and radial velocity among extra-galactic nebulae," Proc. Nat. Acad. Sci. **15**, 168–173 (1929).

[43] Arno A. Penzias and Robert Woodrow Wilson, "A Measurement of excess antenna temperature at 4080-Mc/s," Astrophys. J. **142**, 419–421 (1965).

[44] P. A. R. Ade *et al.* (Planck), "Planck 2015 results. XIII. Cosmological parameters," Astron. Astrophys. **594**, A13 (2016), arXiv:1502.01589 [astro-ph.CO].

[45] P. A. R. Ade *et al.* (Planck), "Planck 2015 results. XVII. Constraints on primordial non-Gaussianity," Astron. Astrophys. **594**, A17 (2016), arXiv:1502.01592 [astro-ph.CO].

[46] Wayne Hu and Scott Dodelson, "Cosmic microwave background anisotropies," Ann. Rev. Astron. Astrophys. **40**, 171–216 (2002), arXiv:astro-ph/0110414 [astro-ph].

[47] Wayne Hu and Martin J. White, "A CMB polarization primer," New Astron. **2**, 323 (1997), arXiv:astro-ph/9706147 [astro-ph].

[48] Roger Penrose, "Gravitational collapse and space-time singularities," Phys. Rev. Lett. **14**, 57–59 (1965).

[49] S. W. Hawking and R. Penrose, "The Singularities of gravitational collapse and cosmology," Proc. Roy. Soc. Lond. **A314**, 529–548 (1970).

[50] V A Belinsky, I M Khalatnikov, and E M Lifshitz, "Oscillatory approach to a singular point in the relativistic cosmology," Adv.Phys. **19**, 525–573 (1970).

[51] Charles W. Misner, "Mixmaster universe," Phys. Rev. Lett. **22**, 1071–1074 (1969).

[52] Imogen P. C. Heard and David Wands, "Cosmology with positive and negative exponential potentials," Class. Quant. Grav. **19**, 5435–5448 (2002), arXiv:gr-qc/0206085 [gr-qc].

[53] Antonio Riotto, "Inflation and the theory of cosmological perturbations," *Astroparticle physics and cosmology. Proceedings: Summer School, Trieste, Italy, Jun 17-Jul 5 2002*, ICTP Lect. Notes Ser. **14**, 317–413 (2003), arXiv:hep-ph/0210162 [hep-ph].

[54] D. Langlois, "Lectures on inflation and cosmological perturbations," Lect. Notes Phys. **800**, 1–57 (2010), arXiv:1001.5259 [astro-ph.CO].

[55] V. Mukhanov, *Physical Foundations of Cosmology* (Cambridge University Press, Oxford, 2005).

[56] James M Bardeen, Paul J Steinhardt, and Michael S Turner, "Spontaneous Creation of Almost Scale - Free Density Perturbations in an Inflationary Universe," Phys. Rev. **D28**, 679 (1983).

[57] Richard L. Arnowitt, Stanley Deser, and Charles W. Misner, "The Dynamics of general relativity," Gen. Rel. Grav. **40**, 1997–2027 (2008), arXiv:gr-qc/0405109 [gr-qc].

[58] Alan H Guth and S Y Pi, "Fluctuations in the New Inflationary Universe," Phys. Rev. Lett. **49**, 1110–1113 (1982).

[59] Alexander Vilenkin, "Quantum Fluctuations in the New Inflationary Universe," Nucl. Phys. **B226**, 527–546 (1983).

[60] Viatcheslav F Mukhanov and G V Chibisov, "Quantum Fluctuation and Nonsingular Universe. (In Russian)," JETP Lett. **33**, 532–535 (1981).

[61] Viatcheslav F. Mukhanov, H. A. Feldman, and Robert H. Brandenberger, "Theory of cosmological perturbations. Part 1. Classical perturbations. Part 2. Quantum theory of perturbations. Part 3. Extensions," Phys. Rept. **215**, 203–333 (1992).

[62] Hideo Kodama and Misao Sasaki, "Cosmological Perturbation Theory," Prog. Theor. Phys. Suppl. **78**, 1–166 (1984).

[63] P. A. R. Ade *et al.* (BICEP2), "Detection of B-Mode Polarization at Degree Angular Scales by BICEP2," Phys. Rev. Lett. **112**, 241101 (2014), arXiv:1403.3985 [astro-ph.CO].

[64] Daniel Baumann, Paul J Steinhardt, Keitaro Takahashi, and Kiyotomo Ichiki, "Gravitational Wave Spectrum Induced by Primordial Scalar Perturbations," Phys.Rev. **D76**, 84019 (2007), arXiv:hep-th/0703290 [hep-th].

[65] S Groot Nibbelink and B J W van Tent, "Density perturbations arising from multiple field slow roll inflation," (2000), arXiv:hep-ph/0011325 [hep-ph].

[66] G I Rigopoulos, E P S Shellard, and B J W van Tent, "Non-linear perturbations in multiple-field inflation," Phys. Rev. **D73**, 83521 (2006), arXiv:astro-ph/0504508 [astro-ph].

[67] David Langlois and Filippo Vernizzi, "Nonlinear perturbations of cosmological scalar fields," JCAP **0702**, 17 (2007), arXiv:astro-ph/0610064 [astro-ph].

[68] Jean-Luc Lehners and Paul J Steinhardt, "Planck 2013 results support the cyclic universe," Phys.Rev. **D87**, 123533 (2013), arXiv:1304.3122 [astro-ph.CO].

[69] Jean-Luc Lehners and Paul J. Steinhardt, "Non-Gaussianity Generated by the Entropic Mechanism in Bouncing Cosmologies Made Simple," Phys. Rev. **D80**, 103520 (2009), arXiv:0909.2558 [hep-th].

[70] Juan Martin Maldacena, "Non-Gaussian features of primordial fluctuations in single field inflationary models," JHEP **05**, 013 (2003), arXiv:astro-ph/0210603 [astro-ph].

[71] Xingang Chen, "Primordial Non-Gaussianities from Inflation Models," Adv. Astron. **2010**, 638979 (2010), arXiv:1002.1416 [astro-ph.CO].

[72] Jean-Luc Lehners and Sebastien Renaux-Petel, "Multifield Cosmological Perturbations at Third Order and the Ekpyrotic Trispectrum," Phys.Rev. **D80**, 063503 (2009), arXiv:0906.0530 [hep-th].

[73] Evgeny I. Buchbinder, Justin Khoury, and Burt A. Ovrut, "Non-Gaussianities in new ekpyrotic cosmology," Phys. Rev. Lett. **100**, 171302 (2008), arXiv:0710.5172 [hep-th].

[74] Kazuya Koyama, Shuntaro Mizuno, and David Wands, "Curvature perturbations from ekpyrotic collapse with multiple fields," Class.Quant.Grav. **24**, 3919–3932 (2007), arXiv:0704.1152 [hep-th].

[75] Thorsten Battefeld, "Modulated Perturbations from Instant Preheating after new Ekpyrosis," Phys.Rev. **D77**, 63503 (2008), arXiv:0710.2540 [hep-th].

[76] David H Lyth, Karim A Malik, and Misao Sasaki, "A General proof of the conservation of the curvature perturbation," JCAP **0505**, 4 (2005), arXiv:astro-ph/0411220 [astro-ph].

[77] Jean-Luc Lehners, "Ekpyrotic and Cyclic Cosmology," Phys.Rept. **465**, 223–263 (2008), arXiv:0806.1245 [astro-ph].

[78] Jean-Luc Lehners and Paul J Steinhardt, "Intuitive understanding of non-gaussianity in ekpyrotic and cyclic models," Phys.Rev. **D78**, 23506 (2008), arXiv:0804.1293 [hep-th].

[79] Anna Ijjas, Paul J Steinhardt, and Abraham Loeb, "Inflationary paradigm in trouble after Planck2013," Phys.Lett. **B723**, 261–266 (2013), arXiv:1304.2785 [astro-ph.CO].

[80] R. Penrose, "Difficulties with inflationary cosmology," *Relativistic astrophysics. Proceedings, 14th Texas Symposium, Dallas, USA, December 11-16, 1988*, Annals N. Y. Acad. Sci. **571**, 249–264 (1989).

[81] Lasha Berezhiani and Mark Trodden, "How Likely are Constituent Quanta to Initiate Inflation?" Phys. Lett. **B749**, 425–430 (2015), arXiv:1504.01730 [hep-th].

[82] Alexei A Starobinsky, "A New Type of Isotropic Cosmological Models Without Singularity," Phys. Lett. **B91**, 99–102 (1980).

[83] A. A. Starobinsky, "The Perturbation Spectrum Evolving from a Nonsingular Initially De-Sitter Cosmology and the Microwave Background Anisotropy," Sov. Astron. Lett. **9**, 302 (1983).

[84] Andrei D. Linde, "Inflationary Cosmology," *22nd IAP Colloquium on Inflation + 25: The First 25 Years of Inflationary Cosmology Paris, France, June 26-30, 2006*, Lect. Notes Phys. **738**, 1–54 (2008), arXiv:0705.0164 [hep-th].

[85] Arvind Borde, Alan H. Guth, and Alexander Vilenkin, "Inflationary space-times are incompletein past directions," Phys. Rev. Lett. **90**, 151301 (2003), arXiv:gr-qc/0110012 [gr-qc].

[86] Robert H. Brandenberger, "TransPlanckian physics and inflationary cosmology," in *Proceedings, 1st International Symposium on Cosmology and particle astrophysics (CosPA 2002): Taipei, Taiwan, May 31-June 2, 2002* (2002) pp. 101–113, arXiv:hep-th/0210186 [hep-th].

[87] Robert Brandenberger and Patrick Peter, "Bouncing Cosmologies: Progress and Problems," Found. Phys. **47**, 797–850 (2017), arXiv:1603.05834 [hep-th].

[88] G. W. Gibbons and Neil Turok, "The Measure Problem in Cosmology," Phys. Rev. **D77**, 063516 (2008), arXiv:hep-th/0609095 [hep-th].

[89] Alan H. Guth, "Inflation and eternal inflation," Phys. Rept. **333**, 555–574 (2000), arXiv:astro-ph/0002156 [astro-ph].

[90] Alan H Guth, "Eternal inflation and its implications," J.Phys. **A40**, 6811–6826 (2007), arXiv:hep-th/0702178 [HEP-TH].

[91] Andrei D. Linde, Dmitri A. Linde, and Arthur Mezhlumian, "From the Big Bang theory to the theory of a stationary universe," Phys. Rev. **D49**, 1783–1826 (1994), arXiv:gr-qc/9306035 [gr-qc].

[92] Raphael Bousso, Ben Freivogel, and I-Sheng Yang, "Boltzmann babies in the proper time measure," Phys. Rev. **D77**, 103514 (2008), arXiv:0712.3324 [hep-th].

[93] Jaume Garriga, Delia Schwartz-Perlov, Alexander Vilenkin, and Sergei Winitzki, "Probabilities in the inflationary multiverse," JCAP **0601**, 017 (2006), arXiv:hep-th/0509184 [hep-th].

[94] Andrea De Simone, Alan H. Guth, Michael P. Salem, and Alexander Vilenkin, "Predicting the cosmological constant with the scale-factor cutoff measure," Phys. Rev. **D78**, 063520 (2008), arXiv:0805.2173 [hep-th].

[95] Raphael Bousso, "Holographic probabilities in eternal inflation," Phys. Rev. Lett. **97**, 191302 (2006), arXiv:hep-th/0605263 [hep-th].

[96] Aaron M. Levy, Anna Ijjas, and Paul J. Steinhardt, "Scale-invariant perturbations in ekpyrotic cosmologies without fine-tuning of initial conditions," Phys. Rev. **D92**, 063524 (2015), arXiv:1506.01011 [astro-ph.CO].

[97] V A Rubakov, "Harrison-Zeldovich spectrum from conformal invariance," JCAP **0909**, 30 (2009), arXiv:0906.3693 [hep-th].

[98] Kurt Hinterbichler and Justin Khoury, "The Pseudo-Conformal Universe: Scale Invariance from Spontaneous Breaking of Conformal Symmetry," JCAP **1204**, 23 (2012), arXiv:1106.1428 [hep-th].

[99] Paolo Creminelli, Alberto Nicolis, and Enrico Trincherini, "Galilean Genesis: An Alternative to inflation," JCAP **1011**, 21 (2010), arXiv:1007.0027 [hep-th].

[100] Fabrizio Di Marco, Fabio Finelli, and Robert Brandenberger, "Adiabatic and isocurvature perturbations for multifield generalized Einstein models," Phys.Rev. **D67**, 63512 (2003), arXiv:astro-ph/0211276 [astro-ph].

[101] Sebastien Renaux-Petel and Gianmassimo Tasinato, "Nonlinear perturbations of cosmological scalar fields with non-standard kinetic terms," JCAP **0901**, 12 (2009), arXiv:0810.2405 [hep-th].

[102] David Langlois and Sebastien Renaux-Petel, "Perturbations in generalized multi-field inflation," JCAP **0804**, 017 (2008), arXiv:0801.1085 [hep-th].

[103] Jean-Luc Lehners and Edward Wilson-Ewing, "Running of the scalar spectral index in bouncing cosmologies," JCAP **1510**, 038 (2015), arXiv:1507.08112 [astro-ph.CO].

[104] Angelika Fertig and Jean-Luc Lehners, "The Non-Minimal Ekpyrotic Trispectrum," JCAP **1601**, 26 (2016), arXiv:1510.03439 [hep-th].

[105] Cumrun Vafa, "The String landscape and the swampland," (2005), arXiv:hep-th/0509212 [hep-th].

[106] T. Daniel Brennan, Federico Carta, and Cumrun Vafa, "The String Landscape, the Swampland, and the Missing Corner," (2017), arXiv:1711.00864 [hep-th].

[107] Prateek Agrawal, Georges Obied, Paul J. Steinhardt, and Cumrun Vafa, "On the Cosmological Implications of the String Swampland," Phys. Lett. **B784**, 271–276 (2018), arXiv:1806.09718 [hep-th].

[108] Jean-Luc Lehners, "Small-Field and Scale-Free: Inflation and Ekpyrosis at their Extremes," (2018), arXiv:1807.05240 [hep-th].

[109] Alberto Nicolis, Riccardo Rattazzi, and Enrico Trincherini, "The Galileon as a local modification of gravity," Phys. Rev. **D79**, 064036 (2009), arXiv:0811.2197 [hep-th].

[110] C. Deffayet, Gilles Esposito-Farese, and A. Vikman, "Covariant Galileon," Phys. Rev. **D79**, 084003 (2009), arXiv:0901.1314 [hep-th].

[111] C. Deffayet, S. Deser, and G. Esposito-Farese, "Generalized Galileons: All scalar models whose curved background extensions maintain second-order field equations and stress-tensors," Phys. Rev. **D80**, 064015 (2009), arXiv:0906.1967 [gr-qc].

[112] Tsutomu Kobayashi, Masahide Yamaguchi, and Jun'ichi Yokoyama, "Generalized G-inflation: Inflation with the most general second-order field equations," Prog. Theor. Phys. **126**, 511–529 (2011), arXiv:1105.5723 [hep-th].

[113] Gregory Walter Horndeski, "Second-order scalar-tensor field equations in a four-dimensional space," Int. J. Theor. Phys. **10**, 363–384 (1974).

[114] C. Armendariz-Picon, Viatcheslav F. Mukhanov, and Paul J. Steinhardt, "A Dynamical solution to the problem of a small cosmological constant and late time cosmic acceleration," Phys. Rev. Lett. **85**, 4438–4441 (2000), arXiv:astro-ph/0004134 [astro-ph].

[115] Eva Silverstein and David Tong, "Scalar speed limits and cosmology: Acceleration from D-cceleration," Phys. Rev. **D70**, 103505 (2004), arXiv:hep-th/0310221 [hep-th].

[116] Paolo Creminelli, Markus A Luty, Alberto Nicolis, and Leonardo Senatore, "Starting the Universe: Stable Violation of the Null Energy Condition and Non-standard Cosmologies," JHEP **12**, 80 (2006), arXiv:hep-th/0606090 [hep-th].

[117] Michael Koehn, Jean-Luc Lehners, and Burt Ovrut, "Nonsingular bouncing cosmology: Consistency of the effective description," Phys. Rev. **D93**, 103501 (2016), arXiv:1512.03807 [hep-th].

[118] Yi-Fu Cai, Damien A Easson, and Robert Brandenberger, "Towards a Nonsingular Bouncing Cosmology," JCAP **1208**, 20 (2012), arXiv:1206.2382 [hep-th].

[119] C. Brans and R. H. Dicke, "Mach's principle and a relativistic theory of gravitation," Phys. Rev. **124**, 925–935 (1961), [,142(1961)].

[120] G. R. Dvali, Gregory Gabadadze, and Massimo Porrati, "4-D gravity on a brane in 5-D Minkowski space," Phys. Lett. **B485**, 208–214 (2000), arXiv:hep-th/0005016 [hep-th].

[121] Karel Van Acoleyen and Jos Van Doorsselaere, "Galileons from Lovelock actions," Phys. Rev. **D83**, 084025 (2011), arXiv:1102.0487 [gr-qc].

[122] Richard P. Woodard, "Avoiding dark energy with 1/r modifications of gravity," *The invisible universe: Dark matter and dark energy. Proceedings, 3rd Aegean School, Karfas, Greece, September 26-October 1, 2005*, Lect. Notes Phys. **720**, 403–433 (2007), arXiv:astro-ph/0601672 [astro-ph].

[123] B. P. Abbott *et al.* (Virgo, LIGO Scientific), "Observation of Gravitational Waves from a Binary Black Hole Merger," Phys. Rev. Lett. **116**, 061102 (2016), arXiv:1602.03837 [gr-qc].

[124] M. Libanov, S. Mironov, and V. Rubakov, "Generalized Galileons: instabilities of bouncing and Genesis cosmologies and modified Genesis," JCAP **1608**, 037 (2016), arXiv:1605.05992 [hep-th].

[125] Tsutomu Kobayashi, "Generic instabilities of nonsingular cosmologies in Horndeski theory: A no-go theorem," Phys. Rev. **D94**, 043511 (2016), arXiv:1606.05831 [hep-th].

[126] Anna Ijjas and Paul J. Steinhardt, "Classically stable nonsingular cosmological bounces," Phys. Rev. Lett. **117**, 121304 (2016), arXiv:1606.08880 [gr-qc].

[127] Anna Ijjas and Paul J. Steinhardt, "Fully stable cosmological solutions with a non-singular classical bounce," Phys. Lett. **B764**, 289–294 (2017), arXiv:1609.01253 [gr-qc].

[128] Jrme Gleyzes, David Langlois, Federico Piazza, and Filippo Vernizzi, "Healthy theories beyond Horndeski," Phys. Rev. Lett. **114**, 211101 (2015), arXiv:1404.6495 [hep-th].

[129] Yong Cai, Youping Wan, Hai-Guang Li, Taotao Qiu, and Yun-Song Piao, "The Effective Field Theory of nonsingular cosmology," JHEP **01**, 090 (2017), arXiv:1610.03400 [gr-qc].

[130] Yong Cai, Hai-Guang Li, Taotao Qiu, and Yun-Song Piao, "The Effective Field Theory of nonsingular cosmology: II," Eur. Phys. J. **C77**, 369 (2017), arXiv:1701.04330 [gr-qc].

[131] Paolo Creminelli, Alberto Nicolis, and Matias Zaldarriaga, "Perturbations in bouncing cosmologies: Dynamical attractor versus scale invariance," Phys.Rev. **D71**, 63505 (2005), arXiv:hep-th/0411270 [hep-th].

[132] Itzhak Bars, Shih-Hung Chen, Paul J. Steinhardt, and Neil Turok, "Complete Set of Homogeneous Isotropic Analytic Solutions in Scalar-Tensor Cosmology with Radiation and Curvature," Phys. Rev. **D86**, 083542 (2012), arXiv:1207.1940 [hep-th].

[133] Itzhak Bars, Paul Steinhardt, and Neil Turok, "Sailing through the big crunch-big bang transition," Phys. Rev. **D89**, 061302 (2014), arXiv:1312.0739 [hep-th].

[134] Renata Kallosh and Andrei Linde, "Hidden Superconformal Symmetry of the Cosmological Evolution," JCAP **1401**, 020 (2014), arXiv:1311.3326 [hep-th].

[135] D. Battefeld and Patrick Peter, "A Critical Review of Classical Bouncing Cosmologies," Phys.Rept. **571**, 1–66 (2015), arXiv:1406.2790 [astro-ph.CO].

[136] Taotao Qiu, Jarah Evslin, Yi-Fu Cai, Mingzhe Li, and Xinmin Zhang, "Bouncing Galileon Cosmologies," JCAP **1110**, 036 (2011), arXiv:1108.0593 [hep-th].

[137] Damien A Easson, Ignacy Sawicki, and Alexander Vikman, "G-Bounce," JCAP **1111**, 21 (2011), arXiv:1109.1047 [hep-th].

[138] Robert H. Brandenberger, "The Matter Bounce Alternative to Inflationary Cosmology," (2012), arXiv:1206.4196 [astro-ph.CO].

[139] Taotao Qiu and Yu-Tong Wang, "G-Bounce Inflation: Towards Nonsingular Inflation Cosmology with Galileon Field," JHEP **04**, 130 (2015), arXiv:1501.03568 [astro-ph.CO].

[140] Robert Brandenberger, "Matter Bounce in Horava-Lifshitz Cosmology," Phys. Rev. **D80**, 043516 (2009), arXiv:0904.2835 [hep-th].

[141] Shinji Mukohyama, Kazunori Nakayama, Fuminobu Takahashi, and Shuichiro Yokoyama, "Phenomenological Aspects of Horava-Lifshitz Cosmology," Phys. Lett. **B679**, 6–9 (2009), arXiv:0905.0055 [hep-th].

[142] Kazuharu Bamba, Andrey N. Makarenko, Alexandr N. Myagky, Shin'ichi Nojiri, and Sergei D. Odintsov, "Bounce cosmology from $F(R)$ gravity and $F(R)$ bigravity," JCAP **1401**, 008 (2014), arXiv:1309.3748 [hep-th].

[143] Kazuharu Bamba, Andrey N. Makarenko, Alexandr N. Myagky, and Sergei D. Odintsov, "Bouncing cosmology in modified Gauss-Bonnet gravity," Phys. Lett. **B732**, 349–355 (2014), arXiv:1403.3242 [hep-th].

[144] Costas Kounnas, Herve Partouche, and Nicolaos Toumbas, "Thermal duality and non-singular cosmology in d-dimensional superstrings," Nucl. Phys. **B855**, 280–307 (2012), arXiv:1106.0946 [hep-th].

[145] Robert H. Brandenberger, Costas Kounnas, Herv Partouche, Subodh P. Patil, and N. Toumbas, "Cosmological Perturbations Across an S-brane," JCAP **1403**, 015 (2014), arXiv:1312.2524 [hep-th].

[146] Abhay Ashtekar, Tomasz Pawlowski, and Parampreet Singh, "Quantum Nature of the Big Bang: Improved dynamics," Phys. Rev. **D74**, 84003 (2006), arXiv:gr-qc/0607039 [gr-qc].

[147] Parampreet Singh, "Are loop quantum cosmos never singular?" Class. Quant. Grav. **26**, 125005 (2009), arXiv:0901.2750 [gr-qc].

[148] Yi-Fu Cai and Edward Wilson-Ewing, "Non-singular bounce scenarios in loop quantum cosmology and the effective field description," JCAP **1403**, 26 (2014), arXiv:1402.3009 [gr-qc].

[149] Michael Koehn, Jean-Luc Lehners, and Burt A. Ovrut, "Cosmological super-bounce," Phys.Rev. **D90**, 025005 (2014), arXiv:1310.7577 [hep-th].

[150] D Krotov, C Rebbi, V A Rubakov, and V Zakharov, "Holes in the ghost condensate," Phys. Rev. **D71**, 45014 (2005), arXiv:hep-ph/0407081 [hep-ph].

[151] Yi-Fu Cai, Evan McDonough, Francis Duplessis, and Robert H. Brandenberger, "Two Field Matter Bounce Cosmology," JCAP **1310**, 024 (2013), arXiv:1305.5259 [hep-th].

[152] Edward Wilson-Ewing, "Ekpyrotic loop quantum cosmology," JCAP **1308**, 15 (2013), arXiv:1306.6582 [gr-qc].

[153] Jean-Luc Lehners and Neil Turok, "Bouncing Negative-Tension Branes," Phys.Rev. **D77**, 23516 (2008), arXiv:0708.0743 [hep-th].

[154] Jean-Luc Lehners and Paul J Steinhardt, "Non-Gaussian density fluctuations from entropically generated curvature perturbations in Ekpyrotic models," Phys.Rev. **D77**, 63533 (2008), arXiv:0712.3779 [hep-th].

[155] Stefano Camera, Mario G. Santos, and Roy Maartens, "Probing primordial non-Gaussianity with SKA galaxy redshift surveys: a fully relativistic analysis," Mon. Not. Roy. Astron. Soc. **448**, 1035–1043 (2015), [Erratum: Mon. Not. Roy. Astron. Soc.467,no.2,1505(2017)], arXiv:1409.8286 [astro-ph.CO].

[156] Roy Maartens, Filipe B. Abdalla, Matt Jarvis, and Mario G. Santos (SKA Cosmology SWG), "Overview of Cosmology with the SKA," *Proceedings, Advancing Astrophysics with the Square Kilometre Array (AASKA14): Giardini Naxos, Italy, June 9-13, 2014*, PoS **AASKA14**, 016 (2015), arXiv:1501.04076 [astro-ph.CO].

[157] Justin Alsing, Emanuele Berti, Clifford M. Will, and Helmut Zaglauer, "Gravitational radiation from compact binary systems in the massive Brans-Dicke theory of gravity," Phys. Rev. **D85**, 064041 (2012), arXiv:1112.4903 [gr-qc].

[158] A. I. Vainshtein, "To the problem of nonvanishing gravitation mass," Phys. Lett. **39B**, 393–394 (1972).

[159] Eugeny Babichev and Cdric Deffayet, "An introduction to the Vainshtein mechanism," Class. Quant. Grav. **30**, 184001 (2013), arXiv:1304.7240 [gr-qc].

[160] Philippe Brax, C. van de Bruck, A. C. Davis, J. Khoury, and A. Weltman, "Chameleon dark energy," *Phi in the sky: The quest for cosmological scalar fields. Proceedings, Workshop, Porto, Portugal, July 8-10, 2004*, AIP Conf. Proc. **736**, 105–110 (2005), [,105(2004)], arXiv:astro-ph/0410103 [astro-ph].

[161] Y. Fujii and K. Maeda, *The scalar-tensor theory of gravitation*, Cambridge Monographs on Mathematical Physics (Cambridge University Press, 2007).

[162] Valerio Faraoni and Salvatore Capozziello, *Beyond Einstein Gravity*, Vol. 170 (Springer, Dordrecht, 2011).

[163] Robert M. Wald, *General Relativity* (Chicago Univ. Pr., Chicago, USA, 1984).

[164] C Wetterich, "Hot big bang or slow freeze?" Phys.Lett. **B736**, 506–514 (2014), arXiv:1401.5313 [astro-ph.CO].

[165] M Li, "Generating scale-invariant tensor perturbations in the non-inflationary universe," Physics Letters B **736**, 488–493 (2014), arXiv:1405.0211 [hep-th].

[166] Guillem Domenech and Misao Sasaki, "Conformal Frame Dependence of Inflation," JCAP **1504**, 22 (2015), arXiv:1501.07699 [gr-qc].

[167] Anna Ijjas and Paul J. Steinhardt, "The anamorphic universe," JCAP **1510**, 001 (2015), arXiv:1507.03875 [astro-ph.CO].

[168] David Wands, "Duality invariance of cosmological perturbation spectra," Phys. Rev. **D60**, 23507 (1999), arXiv:gr-qc/9809062 [gr-qc].

[169] Fabio Finelli and Robert Brandenberger, "On the generation of a scale invariant spectrum of adiabatic fluctuations in cosmological models with a contracting phase," Phys. Rev. **D65**, 103522 (2002), arXiv:hep-th/0112249 [hep-th].

[170] Ralph Blumenhagen, Dieter Lust, and Stefan Theisen, "Basic concepts of string theory," *Basic concepts of string theory*, Springer Verlag (2013), 10.1007/978-3-642-29496-9.

[171] F Finelli, A Tronconi, and Giovanni Venturi, "Dark Energy, Induced Gravity and Broken Scale Invariance," Phys. Lett. **B659**, 466–470 (2008), arXiv:0710.2741 [astro-ph].

[172] Alexander Y Kamenshchik, Alessandro Tronconi, and Giovanni Venturi, "Reconstruction of Scalar Potentials in Induced Gravity and Cosmology," Phys. Lett. **B702**, 191–196 (2011), arXiv:1104.2125 [gr-qc].

[173] Jean-Luc Lehners, "New Ekpyrotic Quantum Cosmology," Phys. Lett. **B750**, 242–246 (2015), arXiv:1504.02467 [hep-th].

[174] Chien-Yao Tseng, "Decoherence problem in an ekpyrotic phase," Phys.Rev. **D87**, 23518 (2013), arXiv:1210.0581 [hep-th].

[175] Howard Hui *et al.*, "BICEP Array: a multi-frequency degree-scale CMB polarimeter," *Proceedings, SPIE Astronomical Telescopes + Instrumentation 2018: Modeling, Systems Engineering, and Project Management for Astronomy VIII: Austin, USA, June 10-15, 2018*, Proc. SPIE Int. Soc. Opt. Eng. **10708**, 1070807 (2018), [Astronomy9,1070807(2018)], arXiv:1808.00568 [astro-ph.IM].

[176] Luca Amendola *et al.*, "Cosmology and fundamental physics with the Euclid satellite," Living Rev. Rel. **21**, 2 (2018), arXiv:1606.00180 [astro-ph.CO].